

**Defining the bio-energetic limits of**  
***Symbiodinium* sp's host-symbiont**  
**relationship under future climate**  
**scenarios**

**Verena Schrameyer**

Dipl. Biol. University of Bremen

Submitted in fulfilment of the requirements for the degree of Doctor  
of Philosophy, School of the Environment, University of Technology,

Sydney March 2013

## CERTIFICATE OF AUTHORSHIP/ORIGINALITY

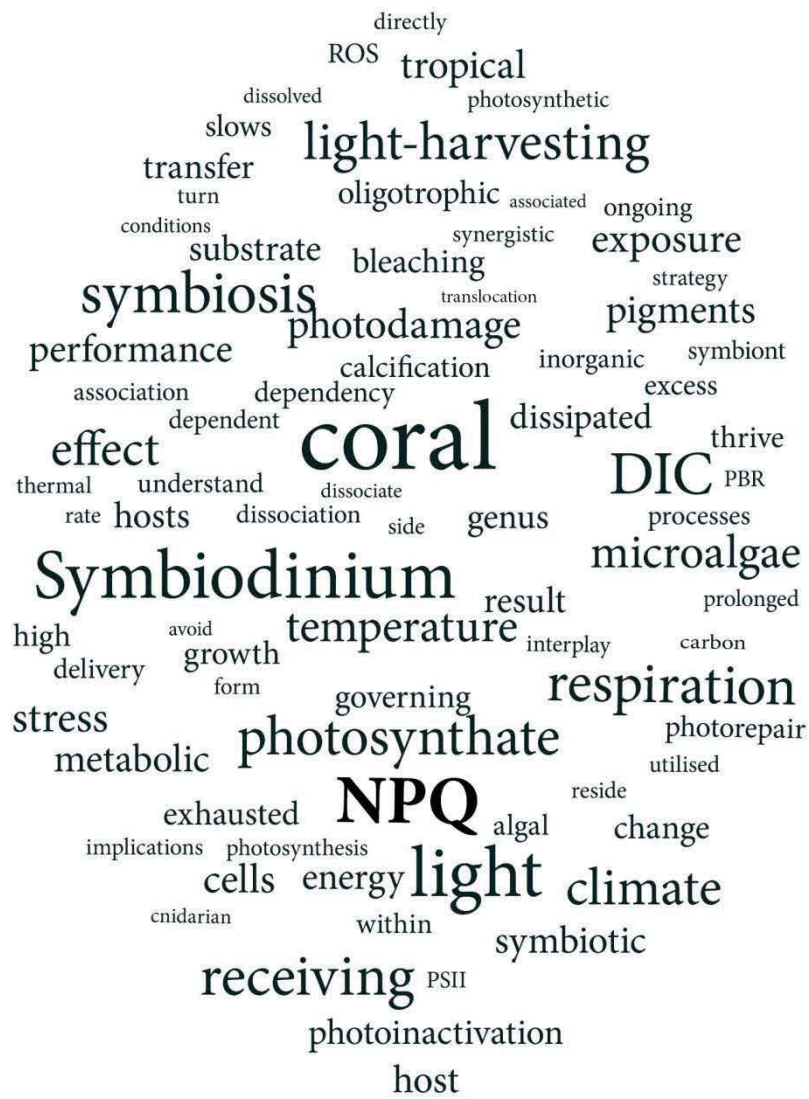
I certify that the work in this thesis has not previously been submitted for a degree nor has it been submitted as part of requirements for a degree except as fully acknowledged within the text.

I also certify that the thesis has been written by me. Any help that I have received in my research work and the preparation of the thesis itself has been acknowledged. In addition, I certify that all information sources and literature used are indicated in the thesis.

Signature of Student

---





# Acknowledgements-Danksagung

Ich moechte mich von tiefstem Herzen bei meinen Eltern Rita und Bernhard Schrameyer und meiner Schwester Uta fuer ihre unsagbare Unterstuetzung bedanken. Ihr habt immer an mich geglaubt und mich immer wieder von neuem motiviert und habt mich dadurch an ein lang ertraeumtes Ziel gebracht. Ausserdem moechte ich mich bei meinen lieben Grosseltern Bork bedanken, meiner Oma, die mir immer die neuesten Zeitungsberichte ueber meeresbiologische Themen zugesandt hat und mein Opa, der mich als Kleinkind fuer die Natur begeistert hat und damit fuers Leben.

A special 'thank you' goes to Kasper Elgetti Brodersen who greatly supported me and always made me laugh in the last and especially hectic phase. I also thank Bruce D. Wilkie for supporting me to pursue my dream and take on this 'PhD journey' despite having to give up a lot to accompany me and my dream. I am very grateful for the support and friendship I received from people around me in the past and present during my 'PhD journey'. People who have been great friends and mentors cheering me up during not so bright times, as well as celebrating the good times during the past 4 years: Daniel and Daniel, Thilde, Radka, Andre, Louisa, Nicole, Daniela, Ingo, Mathieu, Ute, Davey, Linda, Wiebke, Julia, Beatrix, Tanja, Kirsten, Nina, Sandra, Nathalie and everyone I forgot.

Very special thanks goes to my dear friend Wiebke Kraemer for all the invaluable discussions and her inspiring mind; thank you for the the great time, partially supported by portwine (thanks Paul), on Heron island, despite the lack of sleep and experiment craziness. Also I would like to thank my eager honours student Mitch Duley for assistance with data collection and being an A\* student, Malin Gustafsson for great fieldwork assistance and Deniz for volunteering for me in the lab.

It was a great pleasure to be part of the Aquatic processes group (APG) at UTS and I thank the team and other UTS people for the last 4 years with all its ups and downs for your support, enthusiasm and joy; Noni, Malin, Sutinee, Olivia, Katherina, Ernesto, Vinod, Marlene, Charlie, Jessica, Ball, Kieran, Louisa, Joh, Stacey, John and all the rest.

I especially thank my primary supervisor Professor Peter Ralph for allowing me to pursue the path of my PhD project the way I did and to support my decisions and ideas. It has been a journey with various complexities, where Peter was always a great mentor, even though I sometimes didn't accept suggestions in the first place, I am very grateful for the way I was guided. I also thank Ross Hill and Anthony W.D Larkum for their support and guidance; the manuscripts wouldn't have improved the way they did through their thoughtful and very honest feedback, which certainly broadened my perspective and way of thinking.

Prototype testing of the developed photobioreactor during my PhD, partly took place at the laboratories of the Marine Biological Laboratory of the University of Copenhagen in Helsingør, Denmark, where I would like to thank Michael Kühl to allow me to use his facilities and hosting me during that time. Thanks to Lars Behrendt for his great algae culturing for those testruns and bringing kilos of *Piratos* to the lab for support. I would like to thank the UTS technicians Greg Evans, Greg Dalsanto and Geoff McCredie for technical support and the inspiring chats in the Science workshop. Also I have to thank Daniel Nielsen for constructive discussions during the development of the data analysis.

This study was partially funded by UTS Plant Functional Biology and Climate Change Cluster, ARC DP110105200 (PR). Corals were collected under GBRMPA permit No. G09/30854.1. I thank UTS to provide me with a living allowance scholarship as well as supporting me to obtain a tuition fee scholarship.

# Table of Contents

<b>List of Figures</b> .....	<b>xiii</b>
<b>List of Tables</b> .....	<b>xxii</b>
<b>Abbreviations</b> .....	<b>xxv</b>
<b>Abstract</b> .....	<b>xxviii</b>
<b>Chapter 1</b> .....	<b>1</b>
1.1 Coral reef ecosystems .....	2
1.2 Coral Symbiosis .....	5
1.2.1 Calcification and photosynthesis interdependency.....	6
1.2.2 DIC uptake and symbiotic dependencies .....	9
1.3 Climate change and El Niño-Southern Oscillation.....	11
1.3.2 Climate change and coral bleaching events .....	12
1.4 Mechanistic understanding of coral bleaching .....	14
1.4.1 Coral bleaching during non-stressful environmental conditions .....	15
1.4.2 Algal-stress response towards extreme environmental conditions.....	15
1.5 Photophysiology of <i>Symbiodinium</i> .....	16
1.5.1 Photosynthetic light harvesting in <i>Symbiodinium</i> .....	16
1.5.2 Photosynthetic machinery of <i>Symbiodinium</i> .....	17
1.5.3 Energy quenching within the photosynthetic apparatus.....	18
1.5.4 Photoprotection.....	21
1.5.4.1 Xanthophyll cycle.....	22
1.5.5 Photodamage .....	22
1.6 Research Objectives and Thesis Outline.....	25
1.7 Declaration of author contribution .....	28

<b>Chapter 2.1 .....</b>	<b>30</b>
2.1.1 Introduction.....	32
2.1.2 Materials and Methods.....	35
2.1.2.1 <i>Sample preparation</i> .....	35
2.1.2.2 <i>Experimental set-up</i> .....	36
2.1.2.3 <i>Experimental conditions</i> .....	37
2.1.2.4 <i>Data analysis</i> .....	40
2.1.3 Results and Discussion .....	47
2.1.3.1 <i>Quenching in Symbiodinium cells under stress conditions</i> .....	47
2.1.3.2 <i>Kinetic target modeling</i> .....	49
2.1.3.3 <i>Effects of light stress</i> .....	53
2.1.3.4 <i>Temperature stress and bleaching conditions</i> .....	54
2.1.3.5 <i>Molecular model for thylakoid reorganization</i> .....	55
2.1.3.6 <i>Breakdown of lateral segregation and linear electron flow</i> .....	58
2.1.4 References.....	61
<b>Chapter 2.2 .....</b>	<b>66</b>
2.2.1 Introduction.....	67
2.2.2 Materials and Methods.....	70
2.2.2.1 <i>Experimental design</i> .....	70
2.2.2.2 <i>PAM fluorometry</i> .....	72
2.2.2.3 <i>Chlorophyll emission spectra at 77K</i> .....	73
2.2.2.4 <i>Pigment analyses</i> .....	74
2.2.2.5 <i>Statistical analyses</i> .....	75
2.2.3 Results.....	76
2.2.3.1 <i>Chlorophyll fluorescence</i> .....	76

2.2.3.2	<i>77K fluorescence emissions</i>	78
2.2.3.3	<i>Pigment analyses</i>	86
2.2.3.4	<i>Cell counts</i>	89
2.2.4	Discussion	90
2.2.4.1	<i>Stressor triggered LHC movement</i>	91
2.2.4.2	<i>Regulation and mechanisms of LHC movement</i>	93
2.2.4.3	<i>Chl a fluorescence and absorption cross section</i>	94
2.2.4.5	<i>Conclusion</i>	95
2.2.5	References	97
<b>Chapter 3</b>		<b>105</b>
3.1	Introduction	106
3.2	Materials and Methods	111
3.2.1	<i>Coral collection and preparation</i>	111
3.2.2	<i>Treatment and sampling regime</i>	112
3.2.3	<i>Chlorophyll a fluorescence</i>	113
3.2.3.1	<i>Chl a fluorescence-based photorepair requirement</i>	115
3.2.4	<i>Post-measurement sample processing</i>	116
3.2.5	<i>Photosynthetic and photoprotective pigment analyses</i>	116
3.2.6	<i>D1 protein concentrations</i>	118
3.2.6.1	<i>Protein Extraction and Assay</i>	118
3.2.6.2	<i>Quantitative Immunoblotting</i>	119
3.2.6.3	<i>D1 concentration-based photorepair requirement</i>	119
3.2.7	<i>Abiotic parameters</i>	120
3.2.8	<i>Statistical analyses</i>	122
3.3	Results	122
3.3.1	<i>Maximum quantum yield at midday and at night time</i>	122



3.3.2 <i>psbA</i> protein concentrations .....	125
3.3.3 Results of the two independent photorepair estimates.....	128
3.3.4 Chlorophyll <i>a</i> fluorescence quenching analysis .....	129
3.3.5 Photosynthetic productivity.....	131
3.3.6 Pigment analyses .....	133
3.3.7 Cell density.....	135
3.4 Discussion .....	137
3.4.1 Dissipative energy quenching .....	137
3.4.2 Differential photorepair in the two species examined .....	138
3.4.3 Inference about photorepair .....	139
3.4.4 Energy expenditure for photorepair .....	141
3.4.5 Conclusion .....	143
3.5 References .....	144
3.6 Supplementary information .....	152
<b>Chapter 4 .....</b>	<b>154</b>
4.1 Introduction.....	155
4.2 Materials and Procedures .....	159
4.2.1 Instrumental setup.....	159
4.2.2 Gaseous DIC and O <sub>2</sub> exchange measurements.....	161
4.2.3 Measurement protocol .....	162
4.2.4 PBR application for coral holobiont/symbioses assessment .....	163
4.3 Assessment.....	164
4.3.1 Light source capacity and resolution.....	164
4.3.2 Gas circuit volume .....	165
4.3.3 Gaseous exchange in the PBR and total alkalinity of incubation seawater .....	166
4.3.3.1 Dissolved inorganic carbon speciation at different light intensities .....	166

4.3.3.2	<i>Dissolved inorganic carbon speciation at different salinity regimes</i>	168
4.3.4	<i>Gas- and liquid-phase equilibration times</i>	170
4.3.5	<i>O<sub>2</sub> concentration measurement</i>	173
4.3.6	<i>Coral holobiont gaseous exchange and photosynthetic efficiency</i>	174
4.4	Discussion	181
4.4.1	<i>Benefits of the photobioreactor setup</i>	181
4.4.2	<i>Dissolved inorganic carbon exchange</i>	182
4.4.3	<i>Gas-phase of the photobioreactor</i>	182
4.5	Comments and recommendations	183
4.5.1	<i>Shortfalls of utilised specimen and data analysis</i>	184
4.5.2	<i>Alternative electron pathways</i>	185
4.5.3	<i>Demonstration of stoichiometric analysis of theoretical electron flow</i>	185
4.6	References	188
<b>Chapter 5</b>		<b>196</b>
5.1	Introduction	197
5.2	Materials and Methods	201
5.2.1	<i>Coral collection and preparation</i>	201
5.2.2	<i>Experimental setup</i>	201
5.2.3	<i>Experimental protocol</i>	202
5.2.4	<i>Chlorophyll fluorescence</i>	203
5.2.5	<i>Curve fitting</i>	204
5.2.6	<i>CO<sub>2</sub> light compensation point (CO<sub>2</sub>E<sub>c</sub>)</i>	205
5.2.7	<i>Oxygen microsensor measurements</i>	205
5.2.8	<i>Metabolic gas exchange analyses</i>	207
5.2.9	<i>Biometric measures</i>	208
5.2.10	<i>Statistical analyses</i>	209

5.3 Results.....	210
5.3.1 Biometric measures.....	210
5.3.2 Photosynthetic measurements.....	211
5.3.3 Gross primary production and gross photosynthesis rates.....	213
5.3.4 Light and dark respiration.....	216
5.3.5 CO <sub>2</sub> compensation point ( $E_c$ ) irradiance.....	218
5.3.6 P/R ratios.....	219
5.4 Discussion.....	221
5.4.1 Light utilisation and gross primary productivity.....	221
5.4.2 Gross photosynthesis and light respiratory activity.....	223
5.4.3 Light-driven mitochondrial processes.....	225
5.4.3.1 Oxygen consuming pathways.....	225
5.4.3.2 Dissolved inorganic carbon as a substrate for light-driven processes.....	226
5.4.4 Measuring gross photosynthesis rates.....	227
5.4.5 Photosynthetic energy dissipation.....	229
5.4.6 Conclusion.....	230
5.5 References.....	232
<b>Chapter 6.....</b>	<b>242</b>
6.1 Assessing <i>Symbiodinium</i> 's photoprotective capacity and bio-energetic limits.....	243
6.2 NPQ capacity of cultured <i>Symbiodinium</i> .....	243
6.3 High light stress impact upon <i>in hospite Symbiodinium</i> .....	245
6.4 Symbiotic interdependencies within the coral holobiont.....	246
6.5 Ecological significance.....	249
6.6 Conclusion.....	251
6.7 Remarks about instruments and methodologies used.....	252

6.7.1 77K and ultrafast fluorescence .....	252
6.7.2 Application of the photobioreactor .....	253
6.8 Key findings .....	255
6.9 Future research objectives .....	256
General References .....	257

# List of Figures

**Figure 1.1:** Four cell layer model of a coral; simplified view of coral host cell harboring algal symbionts (indicated as zoox) in the upper cell layer of the coelenteron and calcifying cell layers below the gastrodermis in the calicodermis (adopted from Jokiel 2011)..... 7

**Figure 1.2:** The linear electron transport (LET) through the "Z" scheme indicating energetic redox potential on the left side; LET from water (H<sub>2</sub>O) to ultimate electron acceptor NADP<sup>+</sup>; three major protein complexes are involved in running the "Z" scheme: (1) **Photosystem II**; (2) **Cytochrome bf complex** (containing Cytb<sub>6</sub>; FeS; and Cytf ) and (3) **Photosystem I**. Abbreviations and explanation: **Mn**-manganese complex containing 4 Mn atoms, bound to Photosystem II (PSII) reaction center; **Tyr** for a particular tyrosine in PSII; **O<sub>2</sub>** for oxygen evolved through oxidation of water; **H<sup>+</sup>** for protons (proton gradient inducing ATP synthesis is not indicated but needs to be considered as a product of LET); **P<sub>680</sub>** for the reaction center chlorophyll (Chl) in PSII: it is the primary electron donor of PSII; Excited (Chl) **P<sub>680</sub>\*** light energy charged through harvested photon of light; **Pheo** for pheophytin molecule (the primary electron acceptor of PSII); **Q<sub>A</sub>** for a plastoquinone molecule tightly bound to PSII; **Q<sub>B</sub>** for another plastoquinone molecule that is loosely bound to PSII; **FeS** for Rieske Iron Sulfur protein; **Cyt. f** for Cytochrome f; **Cytb<sub>6</sub>** (L and H) for Cytochrome b<sub>6</sub> (of Low and High Energy); **PC** for copper protein plastocyanin; **P<sub>700</sub>** for the reaction center chlorophyll (Chl) of PSI; it is the primary electron donor of PSI; Excited (Chl) **P<sub>700</sub>\*** light energy charged through harvested photon of light; **A<sub>0</sub>** for a special chlorophyll a molecule (primary electron acceptor of PSI); **A<sub>1</sub>** for a phylloquinone (Vitamin K) molecule; **F<sub>X</sub>**, **F<sub>A</sub>**, and **F<sub>B</sub>** are three separate Iron Sulfur Centers; **FD** for ferredoxin; and **FNR** for Ferredoxin NADP oxido Reductase (FNR); (adapted from Veit and Govindje 2000). ..... 20

**Figure 2.1.1:** A - schematic of the experimental setup; B - schematic representation of the four different conditions applied to the *Symbiodinium* cells. ....39

**Figure 2.1.2:** Principles of kinetic models used for describing the primary reactions in the photosynthetic apparatus of *Symbiodinium* cells under the different treatments. A) kinetic chain describing PSII that is not involved in spillover with PSI; B) kinetic compartment describing peripheral antenna complexes that are associated neither with PSII nor with PSI; C) kinetic chains describing PSI and PSII involved in spillover. Model compartments: i) PSII/RC compartment – a combined antenna-RC compartment representing the PSII complexes together with their peripheral antenna, this compartment could either be involved in spillover with PSI or not; ii) PSI/RC compartment – a combined antenna-RC compartment accounting for PSI and its peripheral antenna; iii) radical pair (RP) compartments – accounting for the electron transfer reaction in each of the photosystems. *Note that several kinetic models reflecting previous knowledge about different structural and functional aspects of the studied samples were tested for compatibility with the retrieved experimental data before arriving at the proposed models.* .....41

**Figure 2.1.3:** Decay- (DAS) and Species-associated emission spectra (SAES) resulting from the kinetic modeling of the time resolved fluorescence data from *Symbiodinium* cells under the four treatments: A, E)  $F_C$  condition; B, F)  $F_{HL}$  condition; C, G)  $F_B$  condition; D, H)  $F_{HT}$  condition. ....48

**Figure 2.1.4:** Molecular model for thylakoid organization and their reorganization induced under elevated thermal stress. **A)** Under optimal growth temperature conditions, there exist two PSII pools: one that is involved in excitation spillover with PSI and another that is not; **B)** When cells are exposed to elevated temperature (with or without high light) a major

reorganization of the peripheral antenna of PSII occurs. In this state there is a homogeneous PSII-PSI distribution in the thylakoid membrane, causing strong spillover and the increase in the effective antenna size of PSI. There is also some (8%) dissociation of light harvesting antenna, previously attached to PSII. The model allows for the full relaxation of the heat-induced state if the exposure to elevated temperatures is mild and not very prolonged. Under long term heat stress permanent damage to the cells may be induced.....56

**Figure 2.2.1:** Overview of the 3 treatment incubations applied. Treatment 1: ( $F_{\text{Heat+NPQ}}$ ) 11.5 h of combined thermal and high light stress; treatment 2: ( $F_{\text{Heat}}$ ) 8 h of incubation in the dark with thermal stress exposure and 3.5 h of high light stress at the end of treatment incubation; treatment 3 ( $F_{\text{NPQ}}$ ) high light stress exposure for 3.5 h.....72

**Figure 2.2.2:** Variable chlorophyll *a* fluorescence parameters at sampling times throughout treatment incubation; ramping time for thermal stress treatments is indicated as -2 and 0 h on the x-axis, where  $F_{\text{NPQ}}$  is displayed from 0; panel A: Maximum quantum yield ( $F_V/F_M$ ) of all treatments, panel B: relative electron transport rate (rETR);  $F_{\text{Heat+NPQ}}$ : closed circles,  $F_{\text{Heat}}$ : closed triangles,  $F_{\text{NPQ}}$ : open triangles; Tukey-HSD grouping results are indicated in lower case letters ( $F_{\text{NPQ}}$  post-hoc analyses results are indicated as greek letters);  $n=4$ , mean  $\pm$  SEM are displayed. ....77

**Figure 2.2.3:** Difference spectra of 77K fluorescence emission amplitudes between wavelengths of 620 – 750 nm are displayed, panel A:  $F_{\text{Heat}}$  treatment; difference spectrum (dotted line) of  $T_{-2h}$  and  $T_0$ , original  $T_{-2h}$  (dashed line) and  $T_0$  (straight line) fluorescence emission spectra, panel B:  $F_{\text{Heat+NPQ}}$  treatment; difference spectrum (dotted line) of  $T_{-2h}$  and  $T_0$ ,  $T_{-2h}$  (dashed line) and  $T_0$  (straight line) fluorescence emission spectra, panel C:  $F_{\text{Heat}}$  treatment; difference spectrum (dotted line) of  $T_0$  and  $T_{11.5h}$ ,  $T_0$  (dashed line) and  $T_{11.5h}$

(straight line) fluorescence emission spectra, panel D:  $F_{\text{Heat+NPQ}}$  treatment; difference spectra (dotted line) of  $T_0$  and  $T_{11.5h}$ ,  $T_0$  (dashed line) and  $T_{11.5h}$  (straight line) fluorescence emission spectra. ....85

**Figure 2.2.4:** Xanthophyll pigment concentrations as a function of sampling time (h). Diatoxanthin ( $\text{pg cell}^{-1}$ ) for  $F_{\text{Heat}}$  and  $F_{\text{Heat+NPQ}}$  (A), and  $F_{\text{NPQ}}$  (B), De-epoxidation status for  $F_{\text{Heat}}$  and  $F_{\text{Heat+NPQ}}$  (C), and  $F_{\text{NPQ}}$  (D), xanthophyll pool concentration for  $F_{\text{Heat}}$  and  $F_{\text{Heat+NPQ}}$  (E), and  $F_{\text{NPQ}}$  (F); ramping time for thermal stress treatments is indicated between  $T_{.2h}$  and  $T_{0h}$  on the x-axis, where  $F_{\text{NPQ}}$  sampling is displayed from  $T_{0h}$ ; Tukey HSD results are indicated in lower case letters; mean  $\pm$  SEM,  $n = 4$  are displayed. ....88

**Figure 3.1:** Sampling location Heron Island, Capricorn Bunker Group, Great Barrier Reef, in Australia ( $23^{\circ}26'31.20''\text{S } 151^{\circ}54'50.40''\text{E}$ ) and a close-up of sampling site indicated as (1) (adapted from Krämer et al., 2012). Map was produced using Ocean Data View (Schlitzer, 2011, <http://odv.awi.de>) with data from ‘Coral reef distribution of the World (2010)’ provided by UNEP-WCMC..... 111

**Figure 3.2:** Photosynthetic active radiation (PAR) intensities, as well as incubating temperature throughout the experimental time. PAR is indicated through grey solid line and incubating temperature indicated with black dotted line. .... 121

**Figure 3.3:**  $F_V/F_M$  of midday dark-adapted specimens with (+LM) and without lincomycin (-LM) treatment (panel A: *P. damicornis*, panel B: *P. decussata*) and night measurements of with (+LM) and without lincomycin (-LM) treatment (panel C: *P. damicornis*, panel D: *P. decussata*). Tukey HSD results are indicated; mean  $\pm$  SEM;  $n = 4$ ..... 124



**Figure 3.4:** Intact psbA concentrations A) *P. damicornis*, C) *P. decussata*; fragmented psbA to intact psbA ratios B) *P. damicornis*, D) *P. decussata* as well as are displayed for all experimental sampling events (days) for treatments of high light exposure without lincomycin at midday (midday – LM) and night time (night – LM), as well as high light exposure with lincomycin at midday (midday + LM) and night time (night + LM). T0 measurements were taken n=4 at midday and night representative for both treatment conditions. Tukey HSD results are indicated; mean ± SEM; n = 4. .... 127

**Figure 3.5:** Photorepair (%) derived through Chl *a* fluorescence ( $F_V/F_M$  levels) and from intact psbA concentration changes for *P. damicornis* (black) and *P. decussata* (grey) Between species differences are indicated with an asterisk; mean ± SEM; n = 4. .... 128

**Figure 3.6:** Quenching parameters of *P. damicornis* and *P. decussata* for all experimental sampling times (h) for midday high light exposure without lincomycin A) *P. damicornis*, b) *P. decussata* and for midday high light exposure with lincomycin treatment C) *P. damicornis*, D) *P. decussata*; Tukey HSD results are indicated; mean ± SEM; n = 4. .... 130

**Figure 3.7:** Gross (black circles) and net photosynthesis (black triangles) and respiration (clear circles) of for midday high light exposure without lincomycin; A) *P. damicornis* and B) *P. decussata*; as well as high light exposure with lincomycin treatment C) *P. damicornis* and B) *P. decussata* for all sampling times (h); zero is indicated as dashed grey line; Tukey HSD results are indicated; mean ± SEM; n = 4. .... 132

**Figure 3.8:** Xanthophyll pigments Dt and Dd normalised to Chl *a* for midday and night time of high light exposure without lincomycin (A) *P. damicornis* and (B) *P. decussata* (legend indicated in A), and for midday and night time of high light exposure with lincomycin (C) *P.*

*damicornis* and (D) *P. decussata* (legend indicated in C); and the resulting de-epoxidation status (DPS) for both species of high light exposure without lincomycin (E) and with lincomycin treatment (F) (species legend indicated in E). Tukey HSD results are indicated; mean  $\pm$  SEM; n = 4. .... 135

**Figure S 3.6.1:** Representative immunoblot for psbA immunoblots. The presented blot shows samples of the final sampling event. .... 152

**Figure 4.1:** Schematic of the photosynthesis bioreactor (PBR); the system consists of a laptop for data management and device operation, an Algae-Growth-PAM computer interface as an optional controlling device, a temperature controlled water-bath and a pump, which feeds into the water jacket of the sample chamber. Within the sample chamber 4 sensor slots (indicated as circled symbols: pH, temperature, O<sub>2</sub> optode, 4 $\pi$  PAR sensor) and a PAM fiber optic (45° angle to the specimen) are recording measurements within the liquid-phase at or near the specimen surface; the mounting spots for the front-mounted LED panel are indicated as white circles on the sample chamber; the gas-phase was a closed circuit connecting a cold-trap, a drying column, an IRGA for CO<sub>2</sub> detection, flowmeter, 3-way luer-lock valve for N<sub>2</sub> purging and/or calibration. The gas flow direction is indicated by the arrows (measures are not to size). .... 160

**Figure 4.2:** Relative changes (%) of CO<sub>2</sub> concentrations upon equilibration with gas- and liquid-phase (here indicated with a dashed vertical line) to initial CO<sub>2</sub> concentrations. Dark incubations of *Pocillopora damicornis* while incubating in FSW with two salinity regimes, salinity of 35 and 25 and resulting DIC species concentrations. The DIC species concentrations (HCO<sub>3</sub><sup>-</sup>, CO<sub>3</sub><sup>-2</sup>, CO<sub>2</sub>  $\mu$ mol kg SW<sup>-1</sup>) and total DIC ( $\mu$ mol kg SW<sup>-1</sup>) of salinity 35 and salinity 25, as well as the % loss in DIC species concentrations and total DIC from

salinity of 35 to salinity of 25 are indicated in the table above the graph. Displayed are mean  $\pm$  SEM (n = 3). ..... 169

**Figure 4.3:** Results of gas- and liquid-phase equilibration times for CO<sub>2</sub> concentrations (ppm) as a function of incubation time for *Pocillopora damicornis* (n=4, standard errors are indicated) incubated at irradiances above and below O<sub>2</sub> compensation point (E<sub>c</sub>), (a) 350  $\mu\text{mol photons m}^{-2} \text{s}^{-1}$  and (b) 40  $\mu\text{mol photons m}^{-2} \text{s}^{-1}$ , respectively and post-illumination incubation of above and below E<sub>c</sub> irradiances (c), (d) are displayed. N<sub>2</sub> purged and closed system CO<sub>2</sub> readings without biological specimen and FSW (liquid-phase) are inserted in panel a) for comparison; each panel includes information about equilibration phase time indicated with a circled arrow and equilibration time (t) next to it; pre- and post-equilibration phase are additionally indicated by separation with a dotted line in each panel. Displayed are mean  $\pm$  SEM (n = 3). To highlight gas exchange variation of light incubations below E<sub>c</sub>, replicates were plotted individually (b). ..... 172

**Figure 4.4:** Gas exchange rates of O<sub>2</sub> (open circles) and DIC (P<sub>gDIC</sub> and P<sub>netDIC</sub>/R<sub>CO2</sub> exchange (closed circles) as a function of irradiance (78 – 1100  $\mu\text{mol photons m}^{-2} \text{s}^{-1}$ ) are displayed; (a) gross photosynthetic rates (P<sub>gO2</sub> and P<sub>gDIC</sub>), (b) net photosynthetic rates (P<sub>netO2</sub> and P<sub>netDIC</sub>), (c) post-illumination respiration rates (R<sub>O2</sub> and R<sub>CO2</sub>); mean  $\pm$  SEM (n = 3), standard errors are indicated, dotted line indicates zero (in panel b and c). Tukey HSD results are indicated. .... 175

**Figure 4.5:**  $\Delta F/F_M'$  (closed circles), relative electron transport rate (rETR) (open stars) and NPQ (open circles) displayed as a function of irradiance (78 – 1100  $\mu\text{mol photons m}^{-2} \text{s}^{-1}$ ); n=4, standard errors are indicated; legends are included in the axis labelling to not complicate the display of the data symbols in the graph panel. .... 178

**Figure 4.6:** Replicate estimates of metabolic quotients are displayed as a function of irradiance ( $78 - 1100 \mu\text{mol photons m}^{-2} \text{s}^{-1}$ ) with exponential trend lines for (a) respiratory quotient considering the holobiont (RQc), (b) photosynthetic quotient considering the holobiont (PQnet), (c) photosynthetic quotient considering the algal symbiont (PQz); replicates are indicated (n=4).....180

**Figure 4.7:** Conceptual display of a theoretical stoichiometric analysis of electron equivalents estimated from metabolic gas exchange rates and Chl fluorometry derived electron transport rates to describe light utilisation of aquatic phototrophs in terms of alternative electron pathways and C fixation as a function of irradiance (adapted from Wilhelm and Selmar, 2011). .....186

**Figure 5.1:** Dissipative energy quenching pathways displayed as the combined total light energy input of 1, at nine irradiances for (A) *P. damicornis* and (B) *P. decussata*. Photosynthetic efficiency of photosystem II indicated from bottom to top Y(II) (black bars), non-regulated non-photochemical quenching Y(NO) (light grey bars), regulated non-photochemical quenching Y(NPQ) (dark grey bars); (mean  $\pm$  SEM; *P. decussata*: n=3 and *P. damicornis*: n=4); Tukey HSD results are indicated ( $p < 0.05$ ).....212

**Figure 5.3:** A)  $R_{\text{light O}_2}$  rates as a function of light intensity at 6 irradiances, *P. damicornis* (clear circle) and *P. decussata* (clear triangle); B) respiratory rate changes of  $R_{\text{light O}_2}$  (white symbols) and  $R_{\text{EPIR O}_2}$  (black symbols) relative to pre-illumination rates ( $R_{\text{dark}}$ ) for *P. damicornis* (circles) and *P. decussata* (triangles) are displayed for 6 irradiances;(mean  $\pm$  SEM;  $R_{\text{light O}_2}$ : n=2,  $R_{\text{EPIR O}_2}$ : n=4); Tukey HSD results are indicated ( $p < 0.05$ ).....217

**Figure 5.4:** Photosynthesis to respiration ratios (P/R ratios) of microsensor derived gross photosynthesis ( $GP_{\text{micro}}$ ) to light respiration rates ( $R_{\text{light O}_2}$ ); *P. decussata* (streaked bars) and *P. damicornis* (clear bars) at nine irradiances; dotted line indicates  $P = R$  level where ratios  $> 1$  indicate autotrophy was efficient to meet coral holobiont respiratory demand and  $< 1$  indicate that respiratory demand of the holobiont was greater than autotrophic output; (mean  $\pm$  SEM; n=2); Tukey HSD results are indicated for *P. decussata* ( $p < 0.05$ ), no significant differences were found for *P. damicornis*.....220

# List of Tables

**Table 2.1.1:** Kinetic parameters obtained from the kinetic modeling of the experimental data recorded from *Symbiodinium* cells under control condition,  $F_C$ ; A, kinetic rates; B weighted eigenvector matrix; C, lifetimes (ps) attributed to different model compartments.....43

**Tables 2.1.2:** Kinetic parameters obtained from the kinetic modeling of the experimental data recorded from *Symbiodinium* cells under high light stress,  $F_{HL}$ ; A, kinetic rates; B weighted eigenvector matrix; C, lifetimes (ps) attributed to different model compartments.....44

**Tables 2.1.3:** Kinetic parameters obtained from the kinetic modeling of the experimental data recorded from *Symbiodinium* cells under elevated temperature stress,  $F_{HT}$ ; A, kinetic rates; B weighted eigenvector matrix; C, lifetimes (ps) attributed to different model compartments..45

**Tables 2.1.4:** Kinetic parameters obtained from the kinetic modeling of the experimental data recorded from *Symbiodinium* cells under coral bleaching condition,  $F_B$ .....46

**Table 2.1.2:** Relative excitation vectors (excitation probability for the different compartments), spillover rate, NPQ rate and average lifetimes in each of the four treatments; for all four treatment conditions;  $F_C$  – control condition,  $F_{HL}$  – high light stress,  $F_{HT}$  – thermal stress,  $F_B$  – bleaching conditions (combined thermal and high light stress).....51

**Table 2.2.1.1:** Amplitude (relative units; 0-1) and area (%) of component bands (675, 688, 701 and 721 nm) of fluorescence emission spectra at 77K. Means ( $\pm$  S.E.) shown. *P* values show difference over time for each component in each treatment. Significant differences indicated by \*, with superscript letters indicating Tukey HSD results ( $\alpha = 0.05$ )..... 79

**Table 2.2.1.2:** Amplitude (relative units; 0-1) and area (%) of component bands (675, 688, 701 and 721 nm) of fluorescence emission spectra at 77K. Means ( $\pm$  S.E.) shown. *P* values show difference over time for each component in each treatment. Significant differences indicated by \*, with superscript letters indicating Tukey HSD results ( $\alpha = 0.05$ )..... 80

**Table 2.2.3:** T-test statistical analyses ( $\alpha = 0.05$ ) results for 77K fluorescence emission spectra amplitude differences at critical wavelengths 672, 683, 701 and 721 nm, comparing  $F_{\text{Heat}}$  and  $F_{\text{Heat+NPQ}}$  at the start of the experiment ( $T_{-2h}$ ), after 2 h of ramping to experimental temperature at 30.5 °C ( $T_{0h}$ ;  $F_{\text{Heat}}$ : in the dark,  $F_{\text{Heat+NPQ}}$ : at ambient light) and at conclusion of experimental incubation ( $T_{11.5h}$ ; total of 9.5 h in treatment conditions;  $F_{\text{Heat}}$ : 6 h dark + thermal stress and 3.5 h of high light at the end of treatment incubation;  $F_{\text{Heat+NPQ}}$ : 9.5 h of combination of high light + thermal stress). ..... 84

**Table 2.2.4:** Density of *Symbiodinium* cells per mL ( $\times 10^5$ ) at the start and end of each of the three treatments. .... 89

**Table 4.1:** Parameters of the carbonate system each of 4 sampled light intensity incubations; pH, total dissolved inorganic carbon (DIC), total inorganic carbon speciations ( $\text{CO}_2$ ,  $\text{CO}_3^{-2}$ ,  $\text{HCO}_3^-$ ), total alkalinity (TA) (n=3; mean  $\pm$  SEM). ..... 167

**Table 4.2:** Quantitative parameters derived from fitted net photosynthetic DIC uptake rates as a function of irradiances applied during P – E curves (n=3; mean  $\pm$  SEM). ..... 177

**Table 5.1:** Biometric measures of the two hard coral species examined (n=4; mean  $\pm$  SEM) displaying total chlorophyll (Chl *a* + Chl *c*<sub>2</sub>), algal cell densities per coral surface area and total Chl per cell (significant differences are indicated with an asterisk). ..... 210

**Table 5.2:** Quantitative curve parameters of variable Chl fluorescence derived from fitted relative electron transport rates (rETR) and microsensor measurement derived gross photosynthesis (GP) rates as a function of incident irradiance.  $rETR_{max}$  (a.u.),  $GP_{max}$  (nmol  $O_2\ cm^{-3}\ s^{-1}$ ),  $E_{k\ rETR}$  and  $E_{k\ GP}$  ( $\mu\text{mol photons m}^{-2}\ s^{-1}$ ) as well as  $\alpha_{rETR}$  and  $\alpha_{GP}$  are presented; n=4 for *P. damicornis* and n=3 for *P. decussata* mean  $\pm$  SEM.....215

**Table 5.3:** Algal symbiont characteristics at  $CO_2$  light compensation point ( $E_c$ ), metabolic gas exchange characteristics for  $< CO_2E_c$ : gross photosynthetic (GP) activity (mmol  $O_2$  mg Chl  $a^{-1}\ cm^{-2}$ ), respiratory activity measured as  $CO_2$  exchange during light ( $R_{light\ CO_2}$ ) and during dark ( $R_{EPIR\ CO_2}$ ) (mmol C mg Chl  $a^{-1}\ cm^{-2}$ ) (significant differences are indicated with an asterisk); n=4, mean  $\pm$  SEM.....218



# Abbreviations

acpPC	Chl <i>a/c</i> <sub>2</sub> – Peridinin-binding protein complex
AEPS	Alternative electron pathways
ATP	Adenosin triphosphate
CCM	Carbon concentrating mechanism
CET	Cyclic electron transport
Chl	Chlorophyll
CO <sub>2</sub> E <sub>c</sub>	CO <sub>2</sub> light compensation point
DCMU	3-(3,4-Dichlorophenyl)-1,1-dimethylurea
Dd	Diadinoxanthin
Dt	Diatoxanthin
DIC	Dissolved inorganic carbon
DO	Dissolved oxygen
E <sub>c</sub>	Light compensation point
ENSO	El Niño-Southern Oscillation
ETR	Electron transport rate
FSW	Filtered seawater
GFP	Green fluorescent protein

GHG	Greenhouse Gas
GP	Gross photosynthesis
GPP	Gross primary productivity
HPLC	High performance liquid chromatography
IRGA	Infrared gas analyser
LET	Linear electron transport
MAA	Mycosporine-like amino acid
MAP	Mehler-Ascorbate-Peroxidase cycle
NADPH	Nicotinamide adenine dinucleotide phosphate hydrogen
NPQ	Non-photochemical-quenching
OEC	Oxygen evolving complex
PAM	Pulse- amplitude- modulate fluorometry
PBR	Photobioreactor
PCP	Peridinin-Chl <i>a</i> -binding protein complex
PPR	Photoprotective pigment ratio
PSP	Photosynthetic pigment pool
PQP	Plastoquinone pool
PSI	Photosystem I
PSII	Photosystem II

PSU	Photosynthetic unit
RC	Reaction center
ROS	Reactive oxygen species
SOD	Superoxide dismutase
SOI	Southern Oscillation Index
XC	Xanthophyll cycling
XP	Xanthophyll pool

# Abstract

Hard corals are a living association of a cnidarian and microalgae of the genus *Symbiodinium*. This symbiosis is critical for corals to survive in oligotrophic tropical waters. The algal symbionts reside within the host cells receiving photosynthetic substrate in form of dissolved inorganic carbon (DIC) and in turn transfer photosynthate to their coral host. The photosynthetic performance of the algal symbionts is directly dependent on the DIC substrate delivery, which in turn can have implications on the photosynthate translocation to their coral hosts.

Under thermal and or high light stress, the algal symbiont's photosynthetic substrate can become limited, so that the photosynthetic rate slows down and excess light energy, not utilised for photosynthesis, is dissipated to avoid photodamage. Upon prolonged exposure under these stress conditions, the symbiotic association can dissociate and result in coral bleaching. It was of interest to understand ongoing processes governing the dissociation of a coral symbiosis, focussing on cultured algal symbionts as well as when associated with a coral host.

The photosynthetic apparatus of *Symbiodinium* has different pathways for dissipating excess energy to alleviate the impact of high light stress. Here a novel non-photochemical quenching mechanism was described through the application of picosecond chlorophyll fluorescence measurements on *Symbiodinium* clade C cells suggesting a heterogeneously organized photosystem II (PSII) pool. A model was developed, revealing the re-organization of the alga's photosynthetic apparatus under normal and photoprotective modes, during thermal and high light stress. We propose a new "super-quenching" mechanism, triggered when quenching at the peripheral antennas is insufficient to protect PSII from photodamage. PSII

then transfers its excited state energy to PSI, transforming a non-spillover PSII pool into a spillover pool. The inherently higher stability of PSI and high quenching efficiency of  $P_{700}^+$  allows dumping excess energy to heat, and resulting in an almost complete cessation of photosynthetic electron transport. A similar breakdown of *Symbiodinium*'s photosynthesis could occur when living *in hospite* associated with corals and this could provide a trigger for coral bleaching.

*Symbiodinium* is equipped with light-harvesting and reaction centre components in the thylakoid membrane including a water-soluble peridinin-chlorophyll (chl) *a*-protein complex (PCP), and a membrane-bound chl *a*-chl *c*<sub>2</sub>-peridinin- protein complex (acpPC), along with typical photosynthetic electron transport systems such as the PSII reaction centre and the chl *a*- $P_{700}$  reaction centre complex of PSI. Recent findings suggest that structural changes to PSII associated light harvesting pigment-protein antenna complexes (LHC), membrane intrinsic acpPC and peripherally associated PCP, in *Symbiodinium* are a mean of photoprotection, in addition to xanthophyll cycling. How LHC movement and xanthophyll cycling possibly complement each other under thermal and high light conditions, corresponding to coral bleaching conditions (the expulsion of algal symbionts from the coral host) has been addressed in this thesis. Here it could be revealed that thermal stress is the main precursor for movement of light harvesting complexes in order to shunt excess energy away from PSII. The findings presented here demonstrate the substantial non-photochemical quenching capacity of cultured *Symbiodinium*.

Coral bleaching resilience has been found to be species-specific, with differential impairment of *Symbiodinium*'s photobiology. Whilst much is known about the importance of considering *Symbiodinium* clades and resulting differential photophysiological characteristics affecting the overall coral physiology, the influence of the host upon autotrophic/photophysiological performance of their symbionts is largely unstudied. With the application of an inhibitor

preventing the *de novo* synthesis of the PSII core protein D1, coral species were incubated in natural high light stress conditions for 4 days. Gross photoinhibitory conditions of *Symbiodinium* clade C1 were examined when harboured in two distinct coral host organisms. Algal symbionts harboured in *Pavona decussata*, a bleaching resilient coral species displayed lower photodamage, compared to algal symbionts harboured in *Pocillopora damicornis*, a bleaching sensitive coral species, which was found to exhibit different photoprotective strategies. Despite differences in photodamage and resulting photorepair requirements (re-synthesis of D1 and incorporation in the PSII to create a functional reaction centre), both species displayed constant maximum quantum yields throughout exposure to high light conditions. Results clearly suggest that the photophysiological viability of *Symbiodinium* can be influenced depending on the harbouring coral host species.

In order to understand intricate physiological processes occurring in a coral holobiont and to further assess interdependencies of a *Symbiodinium*-coral host symbiosis, a closed metabolic chamber system (photobioreactor; PBR) was developed for the simultaneous assessment of three key integrated parameters of aquatic oxygenic phototrophs; chlorophyll fluorometry, oxygen and dissolved inorganic carbon (DIC) exchange. The performance of the PBR was evaluated for *in hospite Symbiodinium* associated with the scleractinian coral *Pocillopora damicornis*. The 'two-phase' PBR utilised circulation of a gas-phase through a liquid-phase (seawater) along with continuous stirring to reach equilibrium and allowed for determination of CO<sub>2</sub> as an indirect measure of changes in DIC concentration within the liquid-phase. Simultaneous measures of photosynthetic efficiency (using pulse amplitude modulated fluorometry) and metabolic gas exchange (using state-of-the art dissolved oxygen sensor technology and an infra-red gas analyser for CO<sub>2</sub> detection) were performed. The developed instrumental setup can be used to examine any aquatic phototroph, where the preliminary results presented, show the great capacity of this application.

Further, the novel PBR and additional O<sub>2</sub> microsensors were used to examine the photophysiology and metabolic gas exchange of the symbiont subclade (C1) harboured in two morphologically different coral species; *Pocillopora damicornis* and *Pavona decussata*. Here light respiratory dynamics were described through the application of O<sub>2</sub> microsensors under photosynthesis – irradiance (P – E) curve measurements. Comparable light respiratory dynamics but differing gross primary production, as well as light utilisation were found between the two species examined. *P. decussata*, displayed a much lower CO<sub>2</sub> light compensation point at only half the photon flux density compared to *P. damicornis*, indicating differing DIC supply to its algal symbionts. It was therefore concluded that *P. damicornis* has a comparable respiratory activity per symbiont to *P. decussata*, but as *P. damicornis* harbours less than half the symbionts per unit area compared to *P. decussata*, the holobiont exhibits a higher CO<sub>2</sub> compensation point (CO<sub>2</sub>E<sub>c</sub>) irradiance. Dissipative energy pathways also differed during photosynthesis-irradiance (P – E) curve measurements, where *P. decussata* displayed an increase of non-light induced energy quenching (Y(NO)) and *P. damicornis* increased active energy quenching (Y(NPQ)). O<sub>2</sub> microsensor derived light respiration rates were demonstrated for the first time from P – E curve measurements for coral holobionts. This is a significant contribution to the field as respiration increased with irradiance ~ 20 times compared to steady-state dark respiration for both species. Light respiration rate results demonstrated here clearly highlight that enhanced post-illumination rates, which have commonly been used to infer about light respiratory activity, are not reflecting the much greater actual light respiratory activity.

In concert, this thesis has revealed that *Symbiodinium* is equipped with a broad capacity of non-photochemical quenching pathways, where the species-specific pairing of *Symbiodinium* and its coral host can mediate photoprotective capacity. The importance of sufficient DIC as

photosynthetic substrate available to the algal symbionts has been identified as a possible key role governing bleaching resilience in hard coral species.



# **Chapter 1**

## **Introduction**

## 1.1 Coral reef ecosystems

Coral reefs are diverse and productive ecosystems which thrive in shallow tropical marine waters (Muscatine and Porter 1977). They occupy over 280,000 km<sup>2</sup> of the Earth's surface making up less than 1% of the world's oceans, yet hosting 25% of the world's fish species and are rich in biodiversity, harbouring a range of different animal and plant phyla (Berkelmans and Van Oppen 2006; Spalding et al. 2001). A common analogy is drawn that coral reefs represent the 'rainforests under the sea' (Goreau 1994). But in fact coral reefs sustain representatives from 32 of the 34 animal phyla compared to only 9 phyla which reside in rainforests (Coral 2006). Furthermore, the income of over 500 million people depends on these biodiversity hotspots (Wilkinson 2002) and the ecosystem service is valued at ~ \$375 billion (Costanza et al. 1997); therefore the protection of coral reef ecosystems is of global importance.

Scleractinian corals thrive in oligotrophic waters and the key to their success is their mutualistic association with unicellular dinoflagellates (*Symbiodinium* sp. Freudenthal), originally called zooxanthellae, a term given by Karl Brandt in 1883 (Gr. zoo = animal, xanth = yellow, ella = diminutive) (Baker 2011; Loeblich and Sherley 1979). However, as the term zooxanthellae does not contain any characteristics upon taxonomic traits, and because not all dinoflagellates are yellow or brown in color (Dawson 2007), the algal symbiont genus was called *Symbiodinium* (Freudenthal 1962). *Symbiodinium* is not just exclusively associated with scleractinian corals, also other coral reef dwelling invertebrate and protists such as foraminiferans, porifera, mollusca and platyhelminthes are commonly found to be symbiotically associated with *Symbiodinium* (Stat et al. 2006).

Exposure to high light and/or increased seawater temperatures have been shown to cause a dysfunction and in some cases a disruption of the coral-algal symbiosis (Hoegh-Guldberg 1999; Hoegh-Guldberg 2009; Lesser et al. 1990). This phenomenon is widely described as ‘coral bleaching’ and is one of the major threats to coral reef ecosystems worldwide (Brown et al. 1997; Dunn et al. 2004; Hoegh-Guldberg 1999; Strychar et al. 2005). Coral bleaching is the result of a decrease in *Symbiodinium* density and/or a reduction in photosynthetic pigments from within the symbiont (Lesser et al. 1990). Mass coral bleaching has been reported, where large areas of coral reef undergo bleaching for extended time periods and mortality is usually the end result (Hoegh-Guldberg 1999).

Scleractinian corals are the foundation for coral reef ecosystems and threats to these species will subsequently cause a threat to a whole ecosystem. Indeed scleractinian corals meet the characteristics of a keystone species, which is defined as a species that has a tremendous effect on its environment relative to its abundance (Mills et al. 1993; Paine 1969). Coral reef ecosystems are based on the calcifying properties of scleractinian corals with a net calcification rate of 5 to 126 mol CaCO<sub>3</sub> cm<sup>-2</sup> y<sup>-1</sup> (Gattuso et al. 1999). The abundance and diversity of scleractinian corals control the diversity and association of the reef community, they are exceptionally important as fish nursery grounds, as well as providing food and shelter for numerous coral reef inhabitants (e.g. coral reef fish, crustaceans, poriferans etc.) (Cole et al. 2009; McClanahan 2002; Nagelkerken et al. 2002). The biodiversity of specialised life forms surviving in oligotrophic tropical waters, such as several symbiotic associations, filter feeders or growth-substrate serving encrusting algae types create these coral reef ecosystems. In the past decades these extraordinary ecosystems have been found to be vulnerable to changing environmental conditions caused by climate change (Hoegh-Guldberg 2009).

Worldwide tropical coral reefs are suffering the loss of keystone species, which ultimately leads to a decline in ecosystem biodiversity (Bellwood et al. 2004; Done 1992; Roff and Mumby 2012). This loss can be a consequence of the impact of changing climatic conditions (Hoegh-Guldberg 2009). Differences among coral species in their susceptibility towards disturbances and stressful conditions such as high light and/or thermal stress exposure have been reported (Hughes and Connell 1999). Physiologically distinct *Symbiodinium* genotypes have been identified and are suspected to influence the bleaching tolerance and susceptibility of their coral host (Berkelmans and Van Oppen 2006; Hennige et al. 2011; Lajeunesse et al. 2004; Ulstrup et al. 2006a). Different features of a coral symbiosis have been examined in order to explain these species-specific stress responses, where metabolic gas exchange processes (Gates and Edmunds 1999), differential symbiont densities (Cunning and Baker 2013; Loya et al. 2001) and release of degraded algal symbionts (Ralph et al. 2005a), as well as photosynthetic competency of the algal symbionts (Hill et al. 2005; Hill et al. 2004a) have all been considered; but also differential tolerance of genetically distinct *Symbiodinium* subclades have been suggested to explain bleaching responses of different species (Berkelmans and Van Oppen 2006; Lajeunesse et al. 2010; Putnam et al. 2012).

To be able to define and manage these changes, the underlying mechanisms of a bleaching response of a coral symbiosis needs to be understood. The function and regulation of the photophysiology of *Symbiodinium* and its impact upon the coral host requires a much more detailed understanding in order to describe responses of the coral symbiosis to environmental stress conditions.

## 1.2 Coral Symbiosis

In scleractinian corals, the algal symbionts reside endosymbiotically within the gastroderm in vacuole-like cells surrounded by host-derived membranes called perialgal membranes or symbiosomes (Barnes et al. 2003; Roth et al. 1988; Trench 1979; Wakefield and Kempf 2001). The symbiosome separates the endosymbiont from host cytoplasm and external seawater; therefore creating a host controlled microenvironment for the algal symbionts (Seibt and Schlichter 2001; Wakefield and Kempf 2001).

The osmotic conditions in the host cell's cytosol are changing constantly as they are dependent upon the metabolic activity of the host which alters the concentration of osmolytes by means of catabolic products (Timasheff 1992). The breakdown of macromolecules produces amino acids, monosaccharides and fatty acids which are either metabolised to waste products or conveyed to further catabolic processes such as glycolysis or the citric acid cycle (Campbell and Reece 2011). Catabolic products such as CO<sub>2</sub> and water, the main substrates for photosynthesis, as well as ammonium, phosphorus and urea are transferred from the host to the endosymbiont (Venn et al. 2008).

Scleractinian corals are essentially mixotrophic, thriving from the photosynthetically fixed carbon of their endosymbionts, but they are also active suspension feeders and gatherers of dissolved organic material and particulate matter (Anthony and Fabricius 2000; Fabricius et al. 1995). The coral host derives almost 95% of its energetic needs through the delivery of photosynthate (glucose, glycerol, succinate, fumarate, various amino acids, free amino acids) from its algal symbionts (Burriesci et al. 2012; Muscatine and Cernichiaro 1969; Wang and Douglas 1997). The coral host uses these

compounds to support metabolic processes (i.e. growth and organic carbon for calcification processes) (Gattuso et al. 1999; Tremblay et al. 2012a). The algal symbionts benefit from this symbiosis as they reside in a sheltered high light environment and receive essential nutrients for photosynthesis (Tremblay et al. 2012b).

In scleractinian corals, *Symbiodinium* is residing within the coral tissue at densities reported to be  $\sim 1$  and 5 million  $\text{cm}^{-2}$ , varying with species and habitat (Buxton et al. 2009). The symbiont density was found to decrease with depth of habitat (Fitt et al. 2001), as a decrease in the symbiont density avoids self-shading of the symbionts and can lead to increased light fields reaching the photosynthetic machinery (McCloskey and Muscatine 1984). Also seasonal changes in symbiont density have been observed in long-term studies (Ulstrup et al. 2008).

### ***1.2.1 Calcification and photosynthesis interdependency***

Scleractinian corals are diploblastic animals, which tissues are consisting of an epidermis (surface epithelium), gastrodermis and calicoblastic layer (calicoblastic epithelium) with the latter facing the skeleton (Figure 1.1).

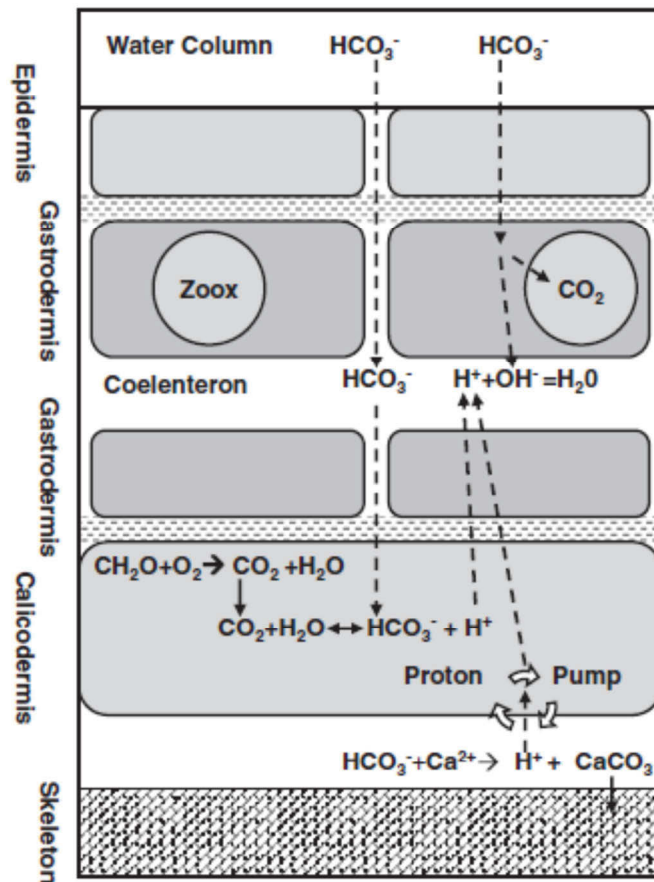


**Figure 1.1:** Four cell layer model of a coral; simplified view of coral host cell harboring algal symbionts (indicated as zoox) in the upper cell layer of the coelenteron and calcifying cell layers below the gastrodermis in the calicodermis (adopted from Jokiel 2011).

Between oral and aboral tissue is the coelenteron, which is filled with interstitial fluid. The calciblastic layer underlying the aboral ectoderm, overlays the skeleton where  $\text{CaCO}_3$  is deposited (Goreau 1959). The calciblastic layer has been described to be a ‘fluid pocket’ rich in mitochondria, underneath which the  $\text{CaCO}_3$  secretion takes place, where skeletal growth is controlled by the host tissue (Cohen and McConnaughey 2003; Johnston 1980). Passive and active transport systems like  $\text{Ca}^{2+}$ ATPase ‘pumps’ are involved in the calcification process, which have been found to be light-induced (Al-Horani et al. 2003a; Cohen and McConnaughey 2003).

Kawaguti and Sakomoto (1948) showed that calcification processes are light enhanced and dark suppressed and later Gattuso et al. (1999) reviewed findings of 109 data sets confirming this trend. Different methodological approaches have been explored to elucidate this interdependency. In order to disentangle these two major processes, Yamashiro (1995) inhibited the skeletal mineral deposition of *Stylophora pistillata* by 99% using a specific inhibitor (1-hydroxyethylidene-1, 1-bisphosphonate, HEBP), however, the diminished calcification was not found to influence the photosynthetic rate of *Stylophora pistillata* (Yamashiro 1995). In another study, the inhibition of protein-synthesis decreased the calcification processes by 60-85%, but did not influence the photosynthetic efficiency (Allemand et al. 1998). Equally incubations of *S. pistillata* in a low calcium medium did not correlate with reduction in photosynthetic efficiency and lowered calcification rate by 2 – 2.4 times (Gattuso et al. 2000). It was therefore concluded that calcification does not stimulate photosynthesis, but whether or not photosynthesis stimulates calcification, remains unresolved. Herfort et al. (2008) examined the influence of increased external  $\text{HCO}_3^-$  concentrations on two coral species (*Porites porites* and *Acropora* sp.), which resulted in an enhanced calcification rate in the dark for both species. Furla et al. (2000) found that calcification processes are saturated through the internal supply of metabolically derived dissolved inorganic carbon (DIC). Also, calcification activity is the highest at the branch tips, that part of a branching coral where algal symbionts are not present (Pearse and Muscatine 1971). The deposition of  $\text{CaCO}_3$  at the calcicoblastic layer is therefore most likely coupled to the DIC uptake (Herfort et al. 2008). As photosynthesis, as well as calcification are both fundamental processes ongoing in a coral symbiosis, but are also both relying on DIC substrate it is of interest to solve their interdependency and possible resulting rate limitations.



### ***1.2.2 DIC uptake and symbiotic dependencies***

Photosynthesis of the algal symbionts requires carbon as substrate to produce photosynthate, which is supplied by the host (Goiran et al. 1996; Venn et al. 2008). However, the high photosynthetic rate of the symbionts would suggest the need for a greater DIC pool than host respiration could offer (Weis et al. 1989). Carbonic anhydrases (CA) and  $\text{HCO}_3^-$  exchanger ( $\text{Na}^+$ -independent  $\text{Cl}^-/\text{HCO}_3^-$  exchanger and a  $\text{Na}^+/\text{HCO}_3^-$  co-transporter) are located in the host membrane adjacent to the symbiosome and are constantly taking up DIC from the external seawater (Al-Moghrabi et al. 1996; Venn et al. 2008; Weis 1993). A high  $\text{CO}_2$  partial pressure is maintained via CA's by the host to favour the carboxylase function for C fixation of the algal symbiont's enzyme ribulose-1,5-bisphosphate carboxylase/oxygenase (RUBISCO; see 1.5.3) (Giordano et al. 2005); the host is activating carbon concentrating mechanisms (CCM) to supply DIC to its algal symbionts (Leggat et al. 2002). Effective C fixation yields the synthesis of photosynthate, which is then translocated to the host (Muscatine 1991).

Studies using radio-labelling techniques have shown that corals incubated in  $\text{C}^{13}$ -enriched seawater resulted in differing carbon ratios in their skeleton compared to ambient seawater concentrations (for review, see Gattuso et al. 1999). C taken up from the external seawater is distributed within the holobiont between the host for calcification and the symbiont as photosynthetic substrate. Feeding experiments using  $\text{C}^{14}$  labelled *Artemia salina* as a food source showed that skeletal carbon ratios differed from food intake, which demonstrated that 40% of the C was derived from external sources and 60% from recycled metabolic products (Goreau 1977b). Outcomes of radio carbon labelled food or seawater experiment suggest that an alternative DIC pool other

than the surrounding seawater and heterotrophic food source was in place (Goreau 1977b). Furla et al. (2000) used a double labelling technique with  $^{45}\text{Ca}$  and  $\text{H}^{14}\text{CO}_3$  in order to clarify inorganic carbon transport for calcification. Results showed that the coral holobiont is taking up DIC during the light to assist photosynthesis and calcification, but also during the dark uptake was detected, although the uptake rate was much less (Furla et al. 2000). The difference in C uptake of dark and light incubations indicates that the host-driven CCMs are light-induced and might be closely related to incident irradiances.

Increased  $\text{O}_2$  evolution and  $\text{CaCO}_3$  accretion at external DIC concentrations up to 6 mM were found for a massive coral *Porites porites* and a branching coral *Acropora* sp. (Herfort et al. 2008). Examining *Pocillopora damicornis* and cultured *Symbiodinium* incubated in external DIC concentrations up to 4 mM revealed similar enhancement of photosynthetic efficiency ( $\text{O}_2$  evolution and relative electron transport rates) through increased external DIC concentrations (Buxton et al. 2009). Also, photoprotective energy dissipation known as non-photochemical quenching (NPQ) was lowered with increasing DIC concentrations suggesting that photoprotective mechanisms of the algal symbionts are also dependent on the overall DIC pool availability (Buxton et al. 2009). Reduced net  $\text{O}_2$  evolution was found at  $< 2$  mM DIC concentrations, along with increased NPQ values indicating a downregulation of photosynthetic efficiency under decreased DIC availability (Buxton et al. 2009). This study clearly showed that efficiency of photophysiological processes of the algal symbionts are intricately related to DIC availability. The DIC sources of a coral are either metabolically derived or it is taken up through CCMs from the external environment, for the latter the energy supply by the algal symbiont through fixed carbon products is essential to assist the coral host in activating its uptake mechanisms. All internal processes of a coral holobiont,

presented above, are creating a physiologically complex living arrangement, making the coral symbiosis vulnerable to changes in the natural environment.

### **1.3 Climate change and El Niño-Southern Oscillation**

Increasing temperatures, irregular rainfall patterns, as well as enriched atmospheric CO<sub>2</sub> levels, just to name a few, have been associated with rapidly changing climate (IPCC, 2007). Earliest predictions for global warming were given by Svante Arrhenius who was one of the first scientists to draft a “greenhouse effect theory” (Arrhenius 1896). He hypothesised that *“if the quantity of carbonic acid increases in geometric progression, the augmentation of the temperature will increase nearly in arithmetic progression”* and based his hypothesis on the impact of burning fossil fuels and other ignition processes. His theory was a matter of fervent discussion amongst physicists at the time. Even though Arrhenius could predict the continuous warming of the biosphere, he did not see any harm in the warming effect; he rather pointed out that it would be a “positive change” and would prevent another predicted ice-age. Over 100 years have passed and detrimental effects of the once so called “positive change” are now being faced by ecosystems all over the world (IPCC, 2007). The natural greenhouse effect is based on ‘greenhouse gases’ (GHG) which act like a shield trapping the heat of the sun.

However, since the Industrial Revolution of the late 18<sup>th</sup> century large amounts of CO<sub>2</sub> and other so called GHG (such as methane and nitrous oxide) have been released into the atmosphere, mainly as a result of burning fossil fuels, concrete production and land use changes (Buddemeier et al. 2004; Sabine et al. 2004). The increase of GHG’s has led to global warming as more heat is trapped in the atmosphere (Lough 2007).

Increased CO<sub>2</sub> results in a greater dissolution into the oceans and shifting the natural carbonate buffer system towards more acidic conditions (Hoegh-Guldberg 2010).

### ***1.3.2 Climate change and coral bleaching events***

The ‘El Niño-Southern Oscillation’ (ENSO) climate phenomenon is periodically changing between extreme climate phenomena called ‘El Niño’ and ‘La Niña’. Every 3-8 years El Niño periods arise, and is characterised in Australia by elevated sea surface temperatures and elongated drought phases (Glynn 1993; Lough 2007). La Niña events in turn are responsible for extended rainfall and flooding events as experienced in the western Pacific region. An increase in frequency and intensity of these climate events is predicted for upcoming decades (Lough 2004; Woodger et al. 2005).

Global climate change has been attributed to be one of the main causative agents for the increased occurrence of coral bleaching. The impact of increased seawater temperatures during El Niño phases, but also changes in salinity regimes have been observed to result in coral bleaching episodes (Coles and Brown 2003; Hoegh-Guldberg et al. 2005; Jones et al. 1998; Kerswell and Jones 2003). At least 7 major bleaching events have taken place in the past two decades (i.e. 1979-1980, 1982-1983, 1986-1987, 1991, 1995-1996, 1997-1998, 2002) (Berkelmans et al. 2004; Glynn 1993). The 1998 event being one of the most severe, reporting affected coral reefs in over 42 countries and causing 80% loss of reef-building species on inshore reefs on the Great Barrier Reef (GBR) (Berkelmans and Oliver 1999; Wilkinson et al. 1999). ENSO is the primary driving force for the reportedly highly variable Australian climate (Bom and Government 2005). During El Niño and La Niña events the Great Barrier Reef experiences elevated sea surface temperatures and lowered salinity regimes, respectively, where both phenomena can

have large scale negative effects upon coral reefs (Timmermann et al. 1999). Changing seawater temperatures have been found to be detrimental and result in significant impact upon coral reefs. Most hard corals live near their upper thermal tolerance limits making them highly susceptible towards small thermal fluctuations (Glynn 1993); however, thermal sensitivity has been found to be highly species specific (Baghooli and Hidaka 2003; Beltran et al. 2012). Amongst other factors, the differences in heat fluxes at the coral surface due to high pigmentation (Fabricius 2006) as well as the coral growth form (Jimenez et al. 2008) can be the reason for observing coral species specific thermal tolerances.

Increases of 1-2°C in seawater surface temperature have been found to cause widespread coral bleaching events (Hoegh-Guldberg 1999). Interestingly, massive coral species such as *Porites* spp. often show a higher thermal tolerance  $\sim + 1-2^\circ\text{C}$  (Goulet et al. 2008; Hoegh-Guldberg 2009) and are frequently more resilient towards external abiotic stress such as thermal stress (Hill et al. 2012; Jimenez et al. 2008). It has been shown that tissue thickness and biomass was lower in bleached corals as compared to unbleached ones (Loya et al. 2001; Mendes and Woodley 2002). Also the lipid and protein content was found to be diminished compared to intact corals (Glynn et al. 1985; Szmant and Gassman 1990). It has been argued that the host corals are catabolising their tissue storages when the translocation of photosynthate is altered (Mendes and Woodley 2002). Nutrient enrichment experiments showed that fed corals were less likely to show a bleaching response compared to starved corals (Borell et al. 2008).

#### 1.4 Mechanistic understanding of coral bleaching

The earliest publication about coral bleaching on the Great Barrier Reef was recorded by Yonge and Nichols (1931) from a Great Barrier Reef expedition which took place in 1928. To date, the process of bleaching of anthozoan-dinoflagellate symbioses has been widely examined and only partially described (Baird et al. 2009a). A lot of attempts were made to understand which part of the symbiosis, the animal or the algal symbionts, is the weakest link i.e. the trigger to initiate coral bleaching (e.g. Baird et al. 2009a; Dove et al. 2006; Franklin et al. 2004; Hennige et al. 2011; Hill et al. 2005; Hill and Ralph 2007; Jones et al. 1998; Weis 2008).

Many studies have focussed on the most commonly observed environmental factors to result in coral bleaching, namely increased temperature and high light (Berkelmans 2002; Coles and Jokiel 1977; Hill et al. 2004b; Warner et al. 1996). A decrease in chlorophyll (Chl) concentration per alga by 52% was detected for *Acropora digitifera* (branching coral) subjected to 32°C although no expulsion of algal symbionts was found (Takahashi et al. 2004). Previous studies also observed the loss of Chl prior to bleaching or under extreme thermal stress (Dove et al. 2006; Hoegh-Guldberg and Smith 1989; Lesser 1996; Lesser et al. 1990).

However, coral bleaching can be caused by a variety of environmental factors such as elevated seatemperature (Hoegh-Guldberg 1999), high light and/or enhanced UV exposure (Gleason and Wellington 1993), salinity changes (Kerswell and Jones 2003), sedimentation (Acevedo and Goenaga 1986), but also low temperature regimes (Hoegh-Guldberg et al. 2005). One of the primary impacts of coral bleaching results in a downregulation of photosynthetic efficiency of the algal symbiont, this is possibly

caused through excessive photodamage exceeding photorepair rate (Takahashi et al. 2004) (see below). However, the downregulation of the photosynthetic efficiency of the algal symbiont, regardless which part of the photosynthetic apparatus causes the loss in functionality, leads to enhanced oxidative stress within the symbiotic system (for review Lesser 2011).

#### ***1.4.1 Coral bleaching during non-stressful environmental conditions***

A natural disruption of the symbiosis can occur as a result of adjustments based on the concept that host tissue has a limited carrying capacity, where endosymbiont density is generally directly correlated to the biomass of the coral host (Fitt et al. 2001; Jones et al. 1998). The symbiont density naturally fluctuates as a result of changing environmental parameters; the host can lose up to 50% of their symbiont density between seasons which parallels with changes in host-tissue biomass (Brown et al. 1999b; Fitt et al. 2000; Ulstrup et al. 2008; Warner et al. 2002), where the richest host tissue biomass (high concentration of lipids) and the highest symbiont density can be found at the end of a winter season (Brown et al. 1999b; Fitt et al. 2001). This has been attributed to lowered respiration rates during winter season, due to lowered irradiance and temperature, leading to increased tissue biomass from lipid and protein storage (Anthony et al. 2002).

#### ***1.4.2 Algal-stress response towards extreme environmental conditions***

A great number of studies have attributed bleaching to damage to the algal symbionts photosynthetic apparatus (Hill et al. 2011; Hill et al. 2012; Jones et al. 1998; Takahashi et al. 2004; Tchernov et al. 2004b; Warner et al. 1999). The ‘algal-stress’ bleaching model (Fitt et al. 2001) considers a decline in photosynthetic efficiency in algal

symbionts and/or reduction of pigments, as the primary reason for symbiosis dissociation (Dove et al. 2006; Fitt et al. 2001; Kleppel et al. 1989). The connectivity of light-harvesting complexes and photosystem II (PSII) (Dove et al. 2006; Hill et al. 2012), as well as PSII itself are sensitive to temperature, irradiance and/or UV exposure (Lesser 1996). Damage to PSII through external stressors can be a result of elevated sea surface temperatures in conjunction with high irradiances leading to the shutdown of PSII in terms of electron transport (generally referred to as photoinhibition) (Baird et al. 2009a; Takahashi et al. 2004; Warner et al. 1999).

The algal-stress bleaching model was the focus of this doctorate thesis as the energetic dependency of the coral host (Muscatine 1990) is directly dependent on the photosynthetic efficiency of the algal symbiont. It has been demonstrated in various situations that a drop in photosynthetic competence of *Symbiodinium* can be a precursor to the breakdown of the coral-algal symbiosis under thermal and/or high light stress (Buxton et al. 2012; Gorbunov et al. 2001; Hill et al. 2011; Hill et al. 2005; Hill et al. 2004a; Hill et al. 2012; Hill and Ralph 2006; Jones and Hoegh-Guldberg 2001; Tchernov et al. 2004a; Warner and Berry-Lowe 2006).

## **1.5 Photophysiology of *Symbiodinium***

### ***1.5.1 Photosynthetic light harvesting in Symbiodinium***

Phototrophic organisms are equipped with antenna pigment-protein complexes to harvest light energy and to transfer this energy to reaction centers, where conversion to chemical energy occurs. The dinoflagellate microalgae *Symbiodinium* spp. (Dinophyceae), are equipped with Chl *a* and additional accessory pigments Chl *c*<sub>2</sub> and peridinin. Dinoflagellates contain two characteristic types of light harvesting complexes



(LHCs), where one is a membrane associated water soluble fraction Peridinin-Chl *a*-Protein complex (PCP) (Hofmann et al. 1996; Larkum and Barrett 1983) and one that is a membrane-intrinsic Chl *a*-Chl *c*<sub>2</sub>-Peridinin-Protein complex (acpPC) (Hiller et al. 1993; Iglesias-Prieto et al. 1993). The dominance of peridinin within the LHCs of dinoflagellates allows efficient light harvesting within the blue-green spectral region (470-550 nm), allowing for extra wavelength absorption outside of the Chl *a* characteristic absorption spectra, which peaks at 430 nm and at 680 nm. Where acpPC resembles the membrane-intrinsic LHCs of higher plants (Hofmann et al. 1996; Kühlbrandt and Wang 1991), PCP does not possess any genetic homology to other pigment proteins (Norris and Miller 1994), but is related to fucoxanthin-Chl *a/c* proteins described in other chromophytes (Green and Durnford 1996). Peridinin as well as Chl *c*<sub>2</sub> are able to pass excitation energy to Chl *a* and therefore function as accessory pigments with 100% energy transfer efficiency (Govindje et al. 1979). The photosynthetic apparatus of *Symbiodinium* along with typical photosynthetic electron transport systems such as the photosystem II reaction centre (P<sub>680</sub>) and the photosystem I (P<sub>700</sub>) reaction centre complex resembles other oxygenic phototrophs (Iglesias-Prieto et al. 1991; Iglesias-Prieto et al. 1993).

### ***1.5.2 Photosynthetic machinery of Symbiodinium***

Chloroplasts consist of an outer and inner membrane, an inter-membrane space and contain in their stroma, stacks of thylakoids, where photosynthesis is taking place. Dinoflagellate chloroplasts are of secondary endosymbiotic origin indicated by its characteristic 3 envelope membranes (Larkum et al. 2007). Thylakoid membranes of dinoflagellates are known to be loosely stacked in groups of three (Taylor 1990). This thylakoid membrane organisation is in stark contrast to higher plants, where grana and

stroma-exposed membrane regions are housing PSII and PSI, which are therefore spatially separated and prevent energetic interaction between the two photosystems. The thylakoid organisation in dinoflagellates therefore allows for energetic interaction between PSII and PSI, indicating that a very different light energy utilisation is possible. Also associated with the thylakoids are xanthophyll pigments from a specialist group of dinoxanthins called diadinoxanthin and diatoxanthin (see 1.5.4.1) and the carotenoid  $\beta$ -carotene (Ambarsari et al. 1997).

### ***1.5.3 Energy quenching within the photosynthetic apparatus***

When pigments absorb light energy as photons, the pigment molecules are raised to a higher energetic state. The subsequent decay of energy can occur in one of three pathways: (1) photochemical quenching (qP), when charge separation has occurred and electrons are passed to the primary quinone acceptor of PSII ( $Q_A$ ) initiating a photosynthetic light reaction; (2) Non-photochemical quenching (NPQ) where excess energy is dissipated (see below); (3) Fluorescence quenching (qF), where absorbed light energy is re-emitted at a longer wavelength, as chlorophyll fluorescence (Baker 2008).

Photochemical quenching is the result of a sequence of redox reactions initiating at the site of the reaction center of PSII  $P_{680}^+$ , which receives its electrons from the oxidation of water at the  $O_2$  evolving complex (Figure 1.2). Electrons are being passed to  $P_{680}^+$  due its strong oxidation potential of +1.2V, making it an extremely responsive reaction center, which can also be a disadvantage (see below) (Wydrzynski 2008). It takes a total of 4 electrons to be ejected from  $P_{680}$  before water is oxidised and  $O_2$  and  $4 H^+$  are liberated into the lumen. During the light reaction, these electrons are traversing a series of reducing reactions, being passed on to pheophytin (primary electron acceptor),  $Q_A$

(first quinone electron acceptor of PSII),  $Q_B$  (secondary quinone electron acceptor of PSII) and plastoquinone (PQ) as part of the linear electron transport intersystem between PSII and PSI to eventually reach the reaction center at PSI  $P_{700}^+$  (Aro et al. 1993). From there electrons travel to a one-electron carrier ferredoxin, which has a lower reduction potential than NADPH, wherefore it can reduce  $NADP^+$  to NADPH propelling the ferredoxin- $NADP^+$  reductase. Along with initiating the transport of electrons from the oxidation of water, the released  $H^+$  cause the acidification of the thylakoid lumen resulting in a pH gradient, which activates ATP-synthases and hence the production of ATP (Falkowski and Raven 2007). ATP and NADPH are synthesised as energy to fuel the dark reactions.

During the 'dark reactions', also termed the Calvin Cycle, ATP and NADPH derived from the light-reactions are used for C fixation. The pyrenoids within the chloroplast contain the nuclear-encoded enzyme RUBISCO (Rowan et al. 1996). RUBISCO is the key enzyme for C fixation, which catalyses the assimilation of  $CO_2$  (or  $O_2$  in case of oxygenase operation/ photorespiration) (Raven 1992). *Symbiodinium* is equipped with the prokaryotic-type form II RUBISCO, differing from higher plant eukaryotic form I by lacking the small subunit characteristic (Morse 1995; Rowan et al. 1996). Further, type II RUBISCO is known to have a low  $CO_2$  affinity, wherefore high  $CO_2$  concentrations are needed to prevent oxygenase activity (photorespiration) of RUBISCO, which would alter the efficiency of the primary production. This is especially important for a coral symbiosis, where synthesised C products are crucial for delivery of energetic nutrition to the coral host (Muscatine et al. 1989).

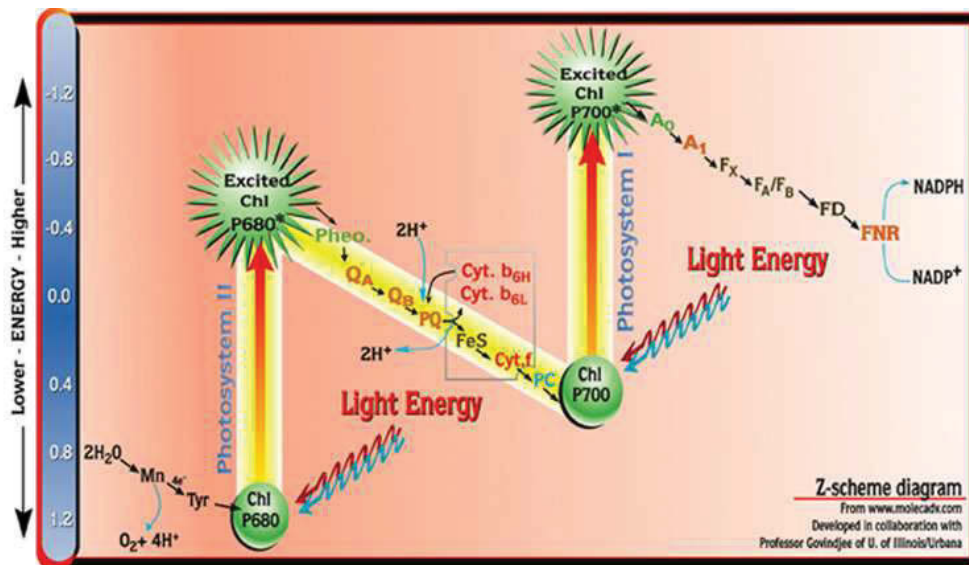


**Figure 1.2:** The linear electron transport (LET) through the "Z" scheme indicating energetic redox potential on the left side; LET from water ( $\text{H}_2\text{O}$ ) to ultimate electron acceptor  $\text{NADP}^+$ ; three major protein complexes are involved in running the "Z" scheme: (1) **Photosystem II**; (2) **Cytochrome bf complex** (containing  $\text{Cytb}_6$ ;  $\text{FeS}$ ; and  $\text{Cyt f}$ ) and (3) **Photosystem I**. Abbreviations and explanation: **Mn**-manganese complex containing 4 Mn atoms, bound to Photosystem II (PSII) reaction center; **Tyr** for a particular tyrosine in PSII;  **$\text{O}_2$**  for oxygen evolved through oxidation of water;  **$\text{H}^+$**  for protons (proton gradient inducing ATP synthesis is not indicated but needs to be considered as a product of LET);  **$\text{P}_{680}$**  for the reaction center chlorophyll (Chl) in PSII: it is the primary electron donor of PSII; Excited (Chl)  **$\text{P}_{680}^*$**  light energy charged through harvested photon of light; **Pheo** for pheophytin molecule (the primary electron acceptor of PSII);  **$\text{Q}_A$**  for a plastoquinone molecule tightly bound to PSII;  **$\text{Q}_B$**  for another plastoquinone molecule that is loosely bound to PSII;  **$\text{FeS}$**  for Rieske Iron Sulfur protein; **Cyt. f** for Cytochrome f;  **$\text{Cytb}_6$**  (L and H) for Cytochrome  $\text{b}_6$  (of Low and High Energy); **PC** for copper protein plastocyanin;  **$\text{P}_{700}$**  for the reaction center chlorophyll (Chl) of PSI; it is the primary electron donor of PSI; Excited (Chl)  **$\text{P}_{700}^*$**  light energy charged through harvested photon of light;  **$\text{A}_0$**  for a special chlorophyll a molecule (primary electron acceptor of PSI);  **$\text{A}_1$**  for a phylloquinone (Vitamin K) molecule;  **$\text{F}_X$ ,  $\text{F}_A$ , and  $\text{F}_B$**  are three separate Iron Sulfur Centers; **FD** for ferredoxin; and **FNR** for Ferredoxin NADP oxidoreductase (FNR); (adapted from Veit and Govindje 2000).

### **1.5.4 Photoprotection**

High light conditions can cause an over-reduction of components in the linear electron transport chain, which ultimately saturates both PSII and PSI reaction centers with excess electrons. Under conditions where both high light and thermal stress are prevailing the thermal threshold for photoinactivation is lower and this can result in oxidative stress (see 1.5.5) (Robison and Warner 2006; Suggett et al. 2008). Photoprotective mechanisms are primarily in place to dissipate excess energy away from PSII to avoid over-reduction and saturation of PSII. Different mechanisms have been described to date, but the intricate relation to specific metabolic reactions makes it at times difficult to differentiate trigger and function. For example, when the Calvin-Cycle becomes rate limited in macroalgae, chloroplasts increase the rate of N-assimilation, as oppose to utilising free electrons coming from photosystem II (PSII) in order to protect photosynthetic membranes from reduction (Geider et al. 1985). *Symbiodinium* photobiology has been clearly understudied, specifically when it comes to photoprotective pathways and mechanisms that are in place to deal with excess energy dissipation at PSII and to sustain its overall photosynthetic efficiency. Recent studies have suggested the activity of LHC movement as a photoprotective mechanism acting in *Symbiodinium* (Hill et al. 2012; Hoogenboom et al. 2012; Reynolds et al. 2008). But besides structural changes within the thylakoid organisation, the excess energy dissipation through carotenoids can be very efficient (Demmig-Adams 1990). Carotenoids have the ability to quench excess radical O<sub>2</sub> arising from the reaction of excited Chl with O<sub>2</sub> (Niyogi 1999; Shick and Lesser 1996). The highly conjugated double bonds of  $\beta$ -carotene are able to quench <sup>1</sup>O<sub>2</sub> as well as excited triplet state Chl (Lesser 2006).

#### ***1.5.4.1 Xanthophyll cycle***

The xanthophyll cycle provides an important photoprotective mechanism which is able to quench excess energy via conversion of diadinoxanthin (Dd) to diatoxanthin (Dt), a process first described by Jeffrey and Haxo (1968). Cycle-dependent thermal energy dissipation of excess light occurs within the light-harvesting complex via the de-epoxidation of Dd to Dt (Ambarsari et al. 1997; Brown et al. 1999a); and limits oxidative damage to the photosynthetic apparatus under bleaching conditions (Long et al. 1994). Studies showed that under thermal stress, the xanthophyll to Chl ratio increased (Dove et al. 2008; Niyogi 1999). It has been suggested that the algal symbiont even liberates Chl in order to accommodate xanthophylls for more effective photoprotection (Anthony and Hoegh-Guldberg 2003). Under high light conditions, microalgae usually show a linear correlation of de-epoxidation status ( $[Dt/(Dt+Dd)]$ ) or Dt formation to NPQ (Brown et al. 1999b). Xanthophyll cycling is considered as an effective antenna-based energy quenching mechanism (Demmig-Adams 1990).

#### ***1.5.5 Photodamage***

Under high light conditions, excited Chl pigments which are unable to shift energy to an immediate neighbouring pigment or carotenoid will cause a rapid build-up of ROS (singlet oxygen ( $^1O_2$ ), superoxide ( $O_2^-$ )) in the light-harvesting complexes around PSII as these react with  $O_2$  originating from the oxidation of water (Telfer et al. 1994). ROS can further damage the antenna pigments, as well as functional units of the photosynthetic apparatus. But also the excitation pressure under high light conditions at PSII can exceed the rate of electrons being passed through the PSII reaction center to the primary electron acceptor (as a result of  $Q_A$  not being relaxed/re-oxidised in time).

Due to the extreme oxidation potential of  $P_{680}^+$ , it can extract electrons from its aqueous surroundings, which also leads to the formation of reactive oxygen species (ROS) (Wydrzynski 2008). As these ROS are being formed in the immediate vicinity to D1 protein, the first electron acceptor, the result is an ‘acceptor-side’ photoinhibition (Allahverdiyeva and Aro 2012). The strong redox potential of PSII is also the reason, why it is often referred to as the ‘weak link’ of the photosynthetic apparatus and PSI considered being energetically more stable under high light conditions (Hill et al. 2012). D1 is a *de novo* synthesised part of PSII, where its degradation as a result of excessive photodamage under high light conditions, can outcompete the capacity for its photorepair (Aro et al. 1993; Hill et al. 2011). The level of photosynthetic reduction is determined by differential rates of photodamage versus protein repair of the *de novo* synthesised D1 reaction centre protein, in order to resume photochemistry (Hill et al. 2011; Takahashi et al. 2004).

Oxidative stress can also occur at the site of PSI e.g. when the Calvin cycle is down-regulated, excess electrons from PSII reduction accumulate around  $P_{700}^+$  and can either cause cyclic electron flow around PSI (Finazzi et al. 2002), or react with oxygen produced at the oxygen evolving complex (OEC) to form ROS (Durchan et al. 2001). High irradiance and temperature cause a disruption of the Calvin cycle which has been linked to bleaching in scleractinian corals (Jones et al. 1998; Lilley et al. 2010). The disruption of downstream processes past ferredoxin can lead to an over—reduction of the electron transport chain between  $P_{700}^+$  and later electron acceptors. The excess electrons being funnelled from PSII to  $P_{700}^+$  are then in excess, wherefore an antioxidative mechanism is in place at PSI; the so called Mehler-Ascorbate-Peroxidase (MAP) cycle (Schreiber et al. 1995a). During the MAP cycle,  $O_2$  evolved at PSII is reduced over two ROS intermediates (superoxide ( $O_2^-$ ) and hydrogen peroxide ( $H_2O_2$ ))

to water (Asada 1999). Under high light conditions ROS formation can exceed the antioxidant mechanisms of the MAP cycle and cause an over-reduction of intermediate components and damage the thylakoid membranes, ultimately causing a decline in the overall photosynthetic efficiency (Lesser 2006).

Light as a trigger for photoinhibition can be exacerbated by other stressors such as increased temperature, which was shown for *in hospite Symbiodinium* of thermally stressed scleractinian corals (Hill and Ralph 2006). Nevertheless, photoinhibition causes a degradation of PSII efficiency as a result of an over-reduction of the PSII electron transport chain (Jones et al. 1998). This in turn causes a decrease in light absorbing capacity for photochemical quenching and a built-up of excess light energy causing an increase in reactive oxygen species (ROS) at the pigment and acceptor-side as well as at  $P_{700}^+$  (Lesser 1997).



## 1.6 Research Objectives and Thesis Outline

High irradiances and thermal stress can impair the photosynthetic efficiency of *Symbiodinium* especially under prolonged exposure; therefore the synergistic effects of these two stressors can impair the corals symbiotic functionality and can lead to dysfunction of the symbiosis. The major objective of this thesis was to provide insight into photoprotective strategies/pathways of the microalgae *Symbiodinium* sp. both *in vitro* and *in vivo*. For the *in vivo* experiments especially the interaction of the host animal and its algal symbiont when exposed to high light irradiances were of interest.

**Chapter 2** is divided into two sections, where the first experimental part utilised ultrafast time-resolved fluorescence measurements, which allowed for the first time the detection of fluorescence quenching pathways acting in *Symbiodinium*. Novel insights into the response of *Symbiodinium*'s photosystems in terms of structural changes are presented for algal cultures subjected to bleaching relevant thermal stress and high light. In the second experimental part, the same stress treatments were applied, but *Symbiodinium* cultures were examined using low temperature (77K) fluorescence measurements, as well as pulse amplitude modulated (PAM) fluorometry and HPLC pigment analyses to verify and partially explain the findings that *Symbiodinium* utilises dynamic energy partitioning between PSII and PSI. The role of LHC movement in *Symbiodinium* under bleaching conditions has been examined during this experiment. The photoprotective strategy of *Symbiodinium* when harboured in different coral hosts and exposed to high light irradiance was the focus of **Chapter 3**. The core of PSII, a heterodimer-protein complex containing the *de novo* synthesised D1 protein, requires continuous photorepair even under optimal irradiances. Prolonged exposure to high irradiances causes increased photodamage to the core of PSII until photorepair rates are exceeded, which leads to photoinactivated conditions. The loss of photosynthetic

activity leads to the loss of autotrophic sustenance for the coral host and can ultimately lead to the loss of algal symbionts and/or pigments. The outcomes of this field experiment demonstrated the differential response of algal symbionts of the two coral species symbioses, *Pocillopora damicornis* and *Pavona decussata*, upon high light exposure. Algal symbionts' photorepair capacity as well as photoprotective pathways differed under the influence of simulated photoinactivated conditions (application of the D1 synthesis inhibitor – lincomycin), as well as under high light exposure.

Thermal and high light stress affecting the coral symbiosis has been studied in various simulation experiments in order to understand coral bleaching. Commonly applied techniques such as PAM fluorometry and O<sub>2</sub> respirometry are used to gain insight into the photosynthetic efficiency of the algal symbiont, as well as the holobiont health and growth. However, the coral organism is tightly bound to and driven by the utilisation of DIC (metabolic/internal and external pool utilisation), which is important for the host animal for calcification and for the algal symbiont as a photosynthetic substrate. **Chapter 4** describes the development and application of a photobioreactor (PBR), which allows the combined measurement of metabolic DIC and O<sub>2</sub> exchange characteristics in conjunction with PAM fluorometry to assess aquatic phototrophs for photosynthetic performance with photosynthesis-irradiance (P - E) curves. **Chapter 5** is a species comparison study of two hard corals, *P. damicornis* and *P. decussata*, which differ in growth form, as well as biometric characteristics, but host the same subclade of *Symbiodinium* (C1). The application of the PBR allowed the detection of differences in light utilisation features and metabolic gas exchange pointing towards host modulated photosynthetic algal symbiont performance. The additional application of O<sub>2</sub> microsensors demonstrated for the first time, light respiration rates derived from photosynthesis – irradiance curves. Light and dark respiration responses upon exposure

to various irradiances yielded comparable rate dynamics in the two coral species examined at saturating light intensities. Light respiration enhancement as a result of applied increasing light intensities was much greater than post-illumination dark respiration rates. Sub-saturating light intensities displayed differing respiratory activity of the two coral species examined and indicated the importance of DIC acquisition for algal symbionts. Respiratory activity and/or DIC demand of the algal symbiont consortia differed in the two coral species examined, where *P. decussata* displayed a more efficient light utilisation possibly because carbon concentrating mechanisms were activated at much lower light intensities.

Finally, in **Chapter 6** the major findings of the thesis are aligned and the general outcomes and implications for future research directions are discussed.

## **1.7 Declaration of author contribution**

### **Chapter 2.1**

As outlined below, laboratory work, data collection and partial data analysis was undertaken by me. Chavdar Slavov coordinated the instrument handling and conducted the modelling of data with Alfred Holzwarth. Alfred Holzwarth and Anthony W. D. Larkum designed the experiment.

### **Chapter 2.2**

Laboratory work and data collection were a joint effort undertaken by Ross Hill and myself. Secondary data analysis was supplied by Milan Szabo, where interpretation and manuscript write-up was solely performed by me.

### **Chapter 3**

Fieldwork, sample and data collection were undertaken by me, where immunoblot analyses was undertaken by Jennifer Jeans and Douglas A. Campbell at the Mount Alison University laboratories, Canada. Wiebke E. Krämer and I designed the experiment in a joint undertaking. Manuscript write-up and data interpretation was solely performed by me.

### **Chapter 4**

Designing the prototype and establishing measurement protocol and data analyses was done by myself and Peter Ralph. Rolf Gademann produced a commercial product from the prototype, where Lars Behrendt and Michael Kühl were supporting and hosting the initial test-runs at the Marine Biology laboratories in Helsingør, Denmark. Manuscript write-up was done by me.

## **Chapter 5**

Data collection for microsensor measurements was done in a joint effort with Daniel Wangpraseurt and myself. All other laboratory work and data collection was performed by myself. Manuscript write-up and data interpretation was done by me.

The write-up for all chapters was greatly supported by my supervisors, Peter J. Ralph, Anthony W.D. Larkum and Ross Hill.

## Chapter 2.1

# New super-quenching mechanism protects *Symbiodinium* from thermal stress – implications for coral bleaching

Chavdar Slavov<sup>1,#</sup>, Verena Schrameyer<sup>2</sup>, Michael Reus<sup>1</sup>, Peter J. Ralph<sup>2</sup>, Ross Hill<sup>2,†</sup>, Anthony W.D. Larkum<sup>2,3,\*</sup>, Alfred R. Holzwarth<sup>1,\*</sup>

<sup>1</sup>*Max-Planck-Institute for Chemical Energy Conversion, Stiftstr. 34-36, D-45470 Mülheim a.d. Ruhr, Germany*

<sup>2</sup>*Plant Functional Biology and Climate Change Cluster (C3), School of the Environment, University of Technology, Sydney, PO Box 123, Broadway, NSW 2007, Australia*

<sup>3</sup>*School of Biological Sciences, University of Sydney, NSW 2006, Australia*

### Keywords:

*Symbiodinium*, dinoflagellate, coral bleaching, photoprotection

### \*Corresponding authors:

Prof. Alfred R. Holzwarth; Phone: +49 208 306 3571; Fax: +49 208 306 3951; e-mail: [alfred.holzwarth@cec.mpg.de](mailto:alfred.holzwarth@cec.mpg.de)

Prof. Anthony W.D. Larkum; Phone: +61 2 9660 7030; Fax: +61 2 9351 4991; e-mail: [a.larkum@sydney.edu.au](mailto:a.larkum@sydney.edu.au)

<sup>#</sup>Current address: *Institute of Physical and Theoretical Chemistry, Goethe-Universität Frankfurt am Main, Max von Laue-Str. 7, Building N120/203, D-60438 Frankfurt am Main, Germany*

<sup>†</sup>Current address: *Centre for Marine Bio-Innovation. School of Biological, Earth and Environmental Sciences, The University of New South Wales, Sydney 2052 NSW, Australia*

Letter of consent

---

Dr. Chavdar Slavov

Institute of Physical and Theoretical  
Chemistry  
Goethe-Universitaet, Frankfurt  
Max von Laue-Str. 7, N120/203  
D-60438 Frankfurt, Germany

[chslavov@theochem.uni-frankfurt.de](mailto:chslavov@theochem.uni-frankfurt.de)

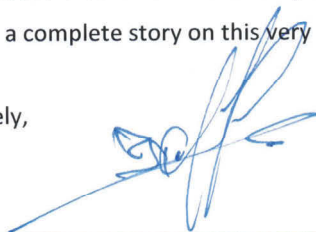
Tel.: +49 69 798 29281

Fax.: +49 69 798 29709

To whom it may concern,

The first part of the following experimental chapter was produced in collaboration with a workgroup at the Max Planck Institute for Chemical Energy Conversion (formerly Max Planck Institute for Bioinorganic Chemistry) in Mülheim an der Ruhr, Germany. The PhD candidate Verena Schrameyer spent 4 weeks at the institute to perform the described experiment in February 2010. Being the first author of this piece of work, I hereby certify that Verena Schrameyer took substantial part in sample preparation, setup preparation, as well as conducted the experiment together with me. The experiment was designed and the collaboration initiated by Professor Alfred Holzwarth and Professor Anthony W.D. Larkum, who were at the institute at the time and supported the experimental progress. The manuscript was created as a group effort of all listed co-authors. This piece of work demonstrates a novel finding revealing a new concept of photoprotective processes in *Symbiodinium* and is currently under review in the journal Science. Important follow-up experiments resulted from our findings (part 2 of this chapter), which were conducted by Verena Schrameyer upon her return at the University of Technology Sydney. I hereby give my consent that Verena Schrameyer can include this manuscript as part of her thesis, to deliver a complete story on this very interesting new finding.

Sincerely,



---

Dr. Chavdar Slavov  
Frankfurt, 11.12.2012

### 2.1.1 Introduction

Coral reefs provide the scaffolding and the habitat for some of the largest and most diverse ecosystems on the planet. Corals consist of a complex and fragile symbiosis between an animal host (phylum Cnidaria) and endosymbiotic microalgae (dinoflagellates from the genus *Symbiodinium*). Dinoflagellate photopigments (chl a and c2) give the coral an overall brown coloration, but a range of host pigments combine to produce the colourful array of species we see across a coral reef. When bleaching triggers the release of the algal symbionts, the coral loses much of its coloration uncovering the white skeleton indicative of bleaching. In this respect, the health of the coral holobiont is critical for the survival of corals and therefore of coral reefs and their denizens. However, the current threats of global climate change (especially rising ocean temperature and ocean acidification) are threatening the health of this symbiotic relationship worldwide (Hoegh-Guldberg 1999; Hoegh-Guldberg et al. 2007).

Studies have shown that the prolonged exposure of corals to high irradiance and an elevated seawater temperature, 1-2°C above the summer average, induces pigment degradation and/or the loss of the symbionts from the host (Lesser and Farrell 2004), which in turn causes visible whitening due to the exposure of the skeleton underlying the animal tissue (*coral bleaching*). Death of the coral often ensues (Fitt et al. 2001; Lesser and Farrell 2004), with recent reports showing a disturbingly increasing trend (Hoegh-Guldberg et al. 2007), and warning that by 2050 coral reefs may face extinction (Hoegh-Guldberg 1999; Hoegh-Guldberg et al. 2007). Therefore, it is critical to understand the fundamental processes in the algal-host association, especially the photosynthetic processes of the algae, which appear to be a crucial trigger point of coral bleaching (Jones et al. 1998; Warner et al. 1999).



At present, there is a general consensus that coral bleaching is linked to the dysfunction of photosynthetic processes in the algal symbiont. It has been suggested that bleaching results from the combined action of elevated temperature and high light stress which triggers a pronounced reduction in photosynthetic activity, in particular of photosystem (PS) II, and in linear electron transport (see Lesser 2011 for recent review). Over the last decade, research has focused on a variety of *Symbiodinium* clades with differing photosynthetic properties and tolerances to elevated water temperatures (Baker 2003; Berkelmans and Van Oppen 2006; Fitt et al. 2001). However, scarce knowledge on the ultrastructure and the light-dependent reaction of the photosynthetic apparatus (PSA) in dinoflagellates has hindered coral bleaching research. It is known that the structure of the thylakoid membrane, that houses the light reactions, differs substantially from that in higher plants (Larkum 2003). In higher plants, the thylakoid membranes form tightly appressed, stacked regions (grana) connected by single stroma thylakoids, due to the inter-membrane interaction of the peripheral light-harvesting complexes (LHCs) that are coupled to the PSII cores. This thylakoid ultrastructure enforces strict lateral separation of PSII and PSI between the grana and the stroma membrane regions respectively, which does not allow for intersystem excitation energy transfer (known as “spillover” in the literature) to occur (Larkum and Howe 1997). In contrast, the thylakoids of dinoflagellates, as in most microalgae (Bertos and Gibbs 1998), are loosely grouped in pairs. This situation allows for mixing of PSII and PSI units and thus for spillover. The LHCs of dinoflagellates are composed of both membrane-bound chlorophyll *a/c*<sub>2</sub>-peridinin-protein complexes (Hiller et al. 1993) and water soluble, membrane-extrinsic peridinin-chlorophyll *a*-protein complexes (Hofmann et al. 1996; Reynolds et al. 2008).

The absorption of light by light-harvesting pigment-protein complexes is essential for photosynthesis, however high levels of irradiance can exceed the utilisation capacity of the PSA. Since excess light can be damaging, conversion of excess harvested light energy into heat, generally known as non-photochemical quenching (NPQ), is a key adaptive feature for all photosynthetic organisms (Li et al. 2009). Many studies have demonstrated that symbiotic algae in corals have also developed adaptive processes to cope with conditions of high solar irradiation (Fitt et al. 2001; Hill et al. 2012) to protect the photosystems (Vass 2012) and ultimately the whole cell against oxidative damage (Lesser 2011). However, the details of NPQ and the mechanisms of redistribution of excitation energy operating in dinoflagellates and especially in *Symbiodinium* sp., are largely unknown.

Over the last two decades, the use of ultrafast time-resolved chlorophyll (Chl) fluorescence, in combination with kinetic modeling (Holzwarth 2004; Holzwarth 2008a; Holzwarth 2008b), has contributed tremendously to our understanding of the light harvesting processes and their regulation in photosynthetic organisms. The combination of these two methods has provided a tool which gives much greater detail and much better reliability on the location and mechanisms of the photoprotective mechanisms in the antennae, than was possible with the widely used steady-state Chl fluorescence methods. Recently, this non-invasive approach has also been successfully applied to study NPQ in diatom algae (Miloslavina et al. 2009), but not yet in dinoflagellates. However, the approach is expected to be very powerful for characterizing the largely unknown structural and functional changes that occur in the PSA of coral symbionts exposed to stress conditions relevant to coral bleaching.

The study on intact cultured *Symbiodinium* cells aims to reveal the changes of the algae's PSA during their transformation from unstressed to the photoprotective mode of operation. It was demonstrated that temperature stress causes a major functional reorganization of the thylakoid membrane that is photoprotective at the early stages but over time has catastrophic consequences for the integrity of the photosynthetic functions despite the presence of formally intact photosystems. This “super-quenched state”, is characterized by a nearly total loss of photosynthetic energy transformation due to the short-circuiting of PSII activity by spillover to PSI. On the one hand it will provide strong photoprotection for PSII and thus enable the survival of the photobiont. On the other hand it could at the same time have severe and adverse consequences for symbiosis in the coral holobiont and may well trigger coral bleaching under extreme stress conditions.

## **2.1.2 Materials and Methods**

### ***2.1.2.1 Sample preparation***

The *Symbiodinium* cultures used in the experiments were from the strain CS-156 (originating from Hawaiian scleractinian coral *Montipora verrucosa*; obtained from the Commonwealth Scientific and Industrial Research Organization (CSIRO), Australia). The algae were grown in f/2 medium at 24 °C under 40  $\mu\text{mol photons m}^{-2} \text{ s}^{-1}$  on a 12:12 h light:dark cycle.

In preparation for the picosecond time-resolved fluorescence measurements, algae were concentrated using a centrifuge at 1000 g for 10 min; the supernatant was discarded and algae were resuspended in 1 L of fresh f/2 medium.

During the experiments, the algae were continuously stirred to keep them in a homogenous suspension and monitored for aggregation on the reservoir walls. To prevent clumping of the algae culture, the sample reservoirs were held for short periods of time in an ultrasound bath at 80W (Sonorex Digitec DT 100/H, Bandelin, Germany) at random intervals during the experimental runs. The determination of the effective quantum yield ( $\Delta F/F_M$ ) using a Water Pulse-Amplitude Modulated (PAM) fluorometer (Walz, Effeltrich, Germany) showed that the ultrasound had no effect on the physiological state of the algae (data not shown).

### ***2.1.2.2 Experimental set-up***

Time-resolved fluorescence measurements were performed to examine the changes in the functional state of the algae and relate these to structural changes in the photosynthetic apparatus. The single-photon timing technique was used to record the picosecond fluorescence decays at 10 different wavelengths in the range 670-750 nm. The set-up consisted of a synchronously-pumped, cavity-dumped, mode-locked dye laser operating at 800 kHz or 4 MHz repetition frequency (Holzwarth et al. 2005). The pulse of the dye laser has a full width at half maximum (FWHM) of ~10 ps and the whole response of the system is about 30 ps FWHM, which after deconvolution results in a time resolution of ~2 ps. The laser intensity at the sample was <0.5 mW, ~0.8 mm spot diameter. The excitation wavelength was 662 nm to selectively excite the bulk antenna Chls. A flow-through cuvette system as described in Miloslavina et al. (2009) was used for the measurements.

### 2.1.2.3 Experimental conditions

The experimental treatments applied to the cultured *Symbiodinium* (Fig. 2.1.1 B) were designed to compare optimal growth conditions and conditions known to cause coral bleaching (Hill and Ralph 2006). Four different treatments were applied to the samples (Fig. 2.1.1 B): 1) control condition ( $F_C$ ) – unquenched cells with closed ( $P_{680}^+$ ) PSII reaction centers (RCs) at growth temperature (24°C, 10  $\mu\text{mol photons m}^{-2} \text{ s}^{-1}$  illumination on the sample reservoir, 10  $\mu\text{M}$  DCMU); 2) high light stress ( $F_{HL}$ ) – quenched light-adapted cells with closed PSII RCs during both incubation and measurement periods (600  $\mu\text{mol photons m}^{-2} \text{ s}^{-1}$  illumination on the sample reservoir); 3) elevated temperature stress ( $F_{HT}$ ) – unquenched cells at high temperature during the incubation period (31°C and 10  $\mu\text{mol photons m}^{-2} \text{ s}^{-1}$  illumination on the sample reservoir), and quenched light-adapted cells with closed PSII RCs during the measurement periods (31°C and 600  $\mu\text{mol photons m}^{-2} \text{ s}^{-1}$  illumination on the sample reservoir); and 4) elevated temperature and high light stress, equivalent to coral bleaching conditions ( $F_B$ ) – heat stressed, quenched light-adapted cells with closed PSII RCs during both incubation and measurement periods (31°C and 600  $\mu\text{mol photons m}^{-2} \text{ s}^{-1}$  illumination on the sample reservoir).

The incubation period was 10 h to ensure the algae were brought to a steady state (tested by fluorescence induction) characteristic for a particular environmental condition. The illumination was performed with royal blue LEDs (Luxeon Star/O LEDs, Philips Lumileds Lighting company; maximum peak wavelength 450 - 455nm). The total duration of the fluorescence measurements at a particular experimental condition was 3 h.

The control sample was designed to ensure that the other treatments could be appropriately compared. Experimental conditions would naturally lead to a heterogeneity in the redox state of the PSII RCs, which would obscure the treatment effects in the recorded time-resolved fluorescence data and make the data analysis extremely difficult (Miloslavina et al. 2009). In this respect we have chosen to reference the results to control samples (no light or heat stress) where all of the PSII RCs are in a closed state. Such a homogeneous state can be achieved either by DCMU incubation or by additional illumination (~200 ms duration) applied right before the samples enter the laser spot (Fig. 2.1.1 A). To ensure consistency in the control treatment the PSII RCs were brought into closed state by adding 10  $\mu\text{M}$  DCMU to the cultures before the start of the measurement and by applying weak additional illumination (10  $\mu\text{mol photons m}^{-2} \text{s}^{-1}$ ). For the rest of the treatment conditions, the closed state of the PSII RCs was induced by applying strong additional illumination (3000  $\mu\text{mol photons m}^{-2} \text{s}^{-1}$ ).

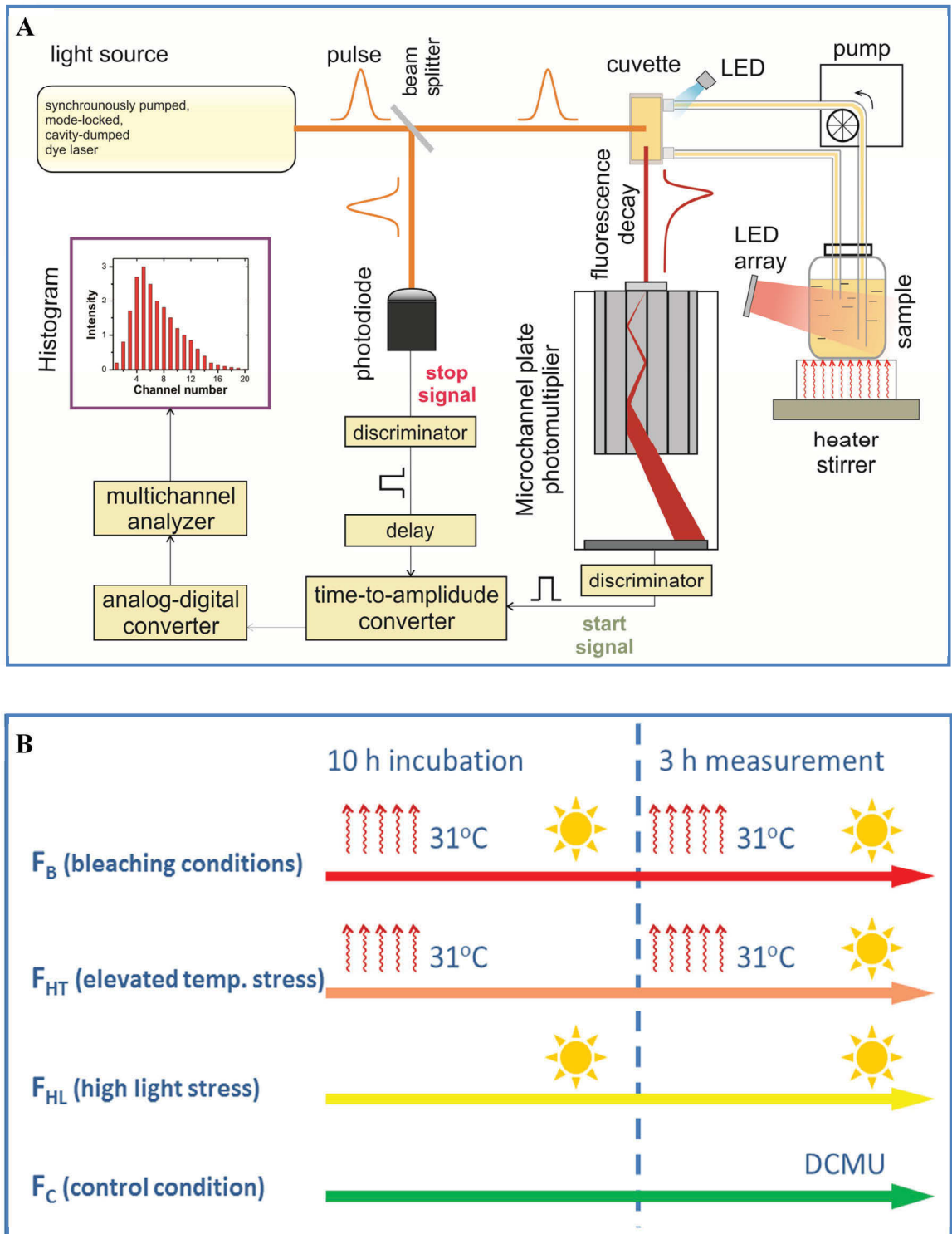


**Figure 2.1.1:** A - schematic of the experimental setup; B - schematic representation of the four different conditions applied to the *Symbiodinium* cells.

#### **2.1.2.4 Data analysis**

The fluorescence decays were analyzed by means of global and target analysis (Holzwarth 1996; Van Stokkum et al. 2004). “Global” refers to simultaneous fitting of the decay curves at different wavelengths. In its basic form, global analysis is a pure mathematical fitting of the data with a sum of exponents function. The analysis results in lifetimes and pre-exponential amplitudes, which yield the so-called decay-associated spectra (DAS). The DAS is a direct and compact way of representing the complete set of original data. In the more elaborate form, called “target” analysis, instead of the sum of exponents function, kinetic models are fitted to the experimental data. Such an approach allows to obtain DAS with detailed information about the rate constants of the different processes taking place in the systems under investigation as well as resolving of the spectra of the different compartments (species-associated emission spectra, SAES) that are involved in those processes (Figure 2.1.2). The SAES are one of the main criteria by which the suitability of a kinetic model can be judged. It should reflect the features projected in the different kinetic components during the construction of the kinetic model, e.g. PSII or PSI (Holzwarth 1996).



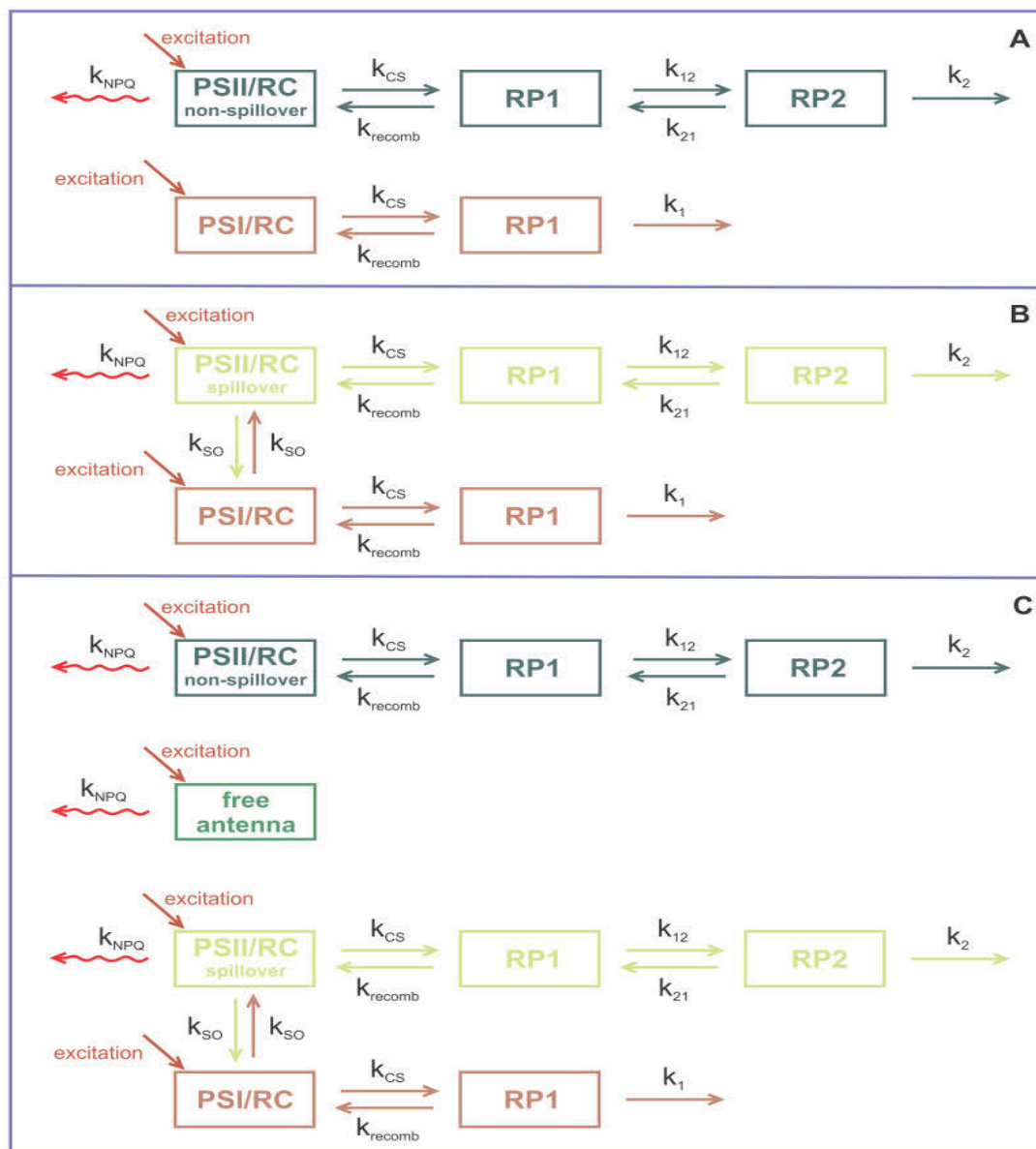


**Figure 2.1.2:** Principles of kinetic models used for describing the primary reactions in the photosynthetic apparatus of *Symbiodinium* cells under the different treatments. A) kinetic chain describing PSII that is not involved in spillover with PSI; B) kinetic compartment describing peripheral antenna complexes that are associated neither with PSII nor with PSI; C) kinetic chains describing PSI and PSII involved in spillover. Model compartments: i) PSII/RC compartment – a combined antenna-RC compartment representing the PSII complexes together with their peripheral antenna, this compartment could either be involved in spillover with PSI or not; ii) PSI/RC compartment – a combined antenna-RC compartment accounting for PSI and its peripheral antenna; iii) radical pair (RP) compartments – accounting for the electron transfer reaction in each of the photosystems. *Note that several kinetic models reflecting previous knowledge about different structural and functional aspects of the studied samples were tested for compatibility with the retrieved experimental data before arriving at the proposed models.*

The kinetic modeling allows also the extraction of another valuable parameter – the so-called excitation vector. The excitation vector represents the initial population of the different model compartments and thus is directly related to the number of pigments and their extinction coefficient. In particular, for photosynthetic complexes, where the extinction coefficient of the studied pigments (here Chls) are the same, the parameter delivers information about the size of the antenna system of the model compartments (PSII or PSI). We have tested several kinetic models reflecting previous knowledge about different structural and functional aspects of the studied samples (Holzwarth et al. 2009; Miloslavina et al. 2009) for compatibility with the retrieved experimental data. The DAS retrieved here through target analysis show higher complexity than the one obtained from the global analysis. This is a result of the higher resolution inherently associated with the kinetic model that was used. However, all of those lifetime components can be traced back to the different kinetic compartments in the model using the weighted eigenvector matrices in Tables 2.1.1 - 4 A-C (see below).

**Table 2.1.1:** Kinetic parameters obtained from the kinetic modeling of the experimental data recorded from *Symbiodinium* cells under control condition,  $F_C$ ; A, kinetic rates; B weighted eigenvector matrix; C, lifetimes (ps) attributed to different model compartments.

**A – Kinetic rates ( $ns^{-1}$ ) matrix – condition  $F_C$ .**

PSII (spillover)			PSII (no spillover)			PSI	
PSII/RC	RP1	RP2	PSII/RC	RP1	RP2	PSI/RC	RP1
0.35	9.83	0.00	0.00	0.00	0.00	0.60	0.00
3.70	0.00	3.05	0.00	0.00	0.00	0.00	0.00
0.00	2.88	1.00	0.00	0.00	0.00	0.00	0.00
0.00	0.00	0.00	0.35	8.72	0.00	0.00	0.00
0.00	0.00	0.00	1.34	0.00	1.60	0.00	0.00
0.00	0.00	0.00	0.00	4.37	1.00	0.00	0.00
0.48	0.00	0.00	0.00	0.00	0.00	0.30	46.50
0.00	0.00	0.00	0.00	0.00	0.00	300.00	9.11

**B – Weighted eigenvector matrix – condition  $F_C$ .**

PSII (spillover)			PSII (no spillover)			PSI	
PSII/RC	RP1	RP2	PSII/RC	RP1	RP2	PSI/RC	RP1
-0.00079	8.76E-06	-7.3E-08	0	0	0	0.45557	-0.46658
0.04976	-0.06038	0.01401	0	0	0	-0.00033	-0.00255
0	0	0	0.01320	-0.01951	0.00712	0	0
-0.00497	-0.00265	0.00194	0	0	0	0.07201	0.45364
0.06116	0.00232	-0.06770	0	0	0	0.00115	0.00669
0	0	0	0.03913	-0.00298	-0.05274	0	0
0.15485	0.06071	0.05176	0	0	0	0.00161	0.00880
0	0	0	0.15768	0.02249	0.04563	0	0

**C – Lifetimes (ps) attributed to different model compartments – condition  $F_C$ .**

<b>PSII (spillover)</b>	60.7	241.2	1488.2
<b>PSII (no spillover)</b>	68.6	425.6	2239.3
<b>PSI</b>	2.9	125.2	

**Tables 2.1.2:** Kinetic parameters obtained from the kinetic modeling of the experimental data recorded from *Symbiodinium* cells under high light stress,  $F_{HL}$ ; A, kinetic rates; B weighted eigenvector matrix; C, lifetimes (ps) attributed to different model compartments.

**A – Kinetic rates ( $ns^{-1}$ ) matrix – condition  $F_{HL}$ .**

PSII (spillover)			PSII (no spillover)			PSI	
PSII/RC	RP1	RP2	PSII/RC	RP1	RP2	PSI/RC	RP1
2.55	14.90	0.00	0.00	0.00	0.00	0.50	0.00
5.38	0.00	3.09	0.00	0.00	0.00	0.00	0.00
0.00	2.37	0.90	0.00	0.00	0.00	0.00	0.00
0.00	0.00	0.00	0.97	11.30	0.00	0.00	0.00
0.00	0.00	0.00	1.50	0.00	3.56	0.00	0.00
0.00	0.00	0.00	0.00	1.34	0.90	0.00	0.00
0.13	0.00	0.00	0.00	0.00	0.00	0.30	68.60
0.00	0.00	0.00	0.00	0.00	0.00	250.00	15.90

**B – Weighted eigenvector matrix – condition  $F_{HL}$ .**

PSII (spillover)			PSII (no spillover)			PSI	
PSII/RC	RP1	RP2	PSII/RC	RP1	RP2	PSI/RC	RP1
-0.00061	1.08E-05	-8E-08	0	0	0	0.38392	-0.40281
0.06894	-0.06918	0.00862	0	0	0	-0.00018	-0.00072
0	0	0	0.02307	-0.0246	0.00328	0	0
-0.00308	-0.00296	0.00082	1E-15	-1E-15	0	0.11553	0.40130
0.07920	0.01808	-0.0641	0	0	0	0.00033	0.00104
0	0	0	0.01708	-0.00261	-0.01338	0	0
0.12556	0.05405	0.05466	0	0	0	0.00039	0.00119
0	0	0	0.18985	0.02721	0.01011	0	0

**C – Lifetimes (ps) attributed to different model compartments – condition  $F_{HL}$ .**

<b>PSII (spillover)</b>	43.4	214.7	607.4
<b>PSII (no spillover)</b>	68.9	238.0	1173.2
<b>PSI</b>	3.1	79.9	

**Tables 2.1.3:** Kinetic parameters obtained from the kinetic modeling of the experimental data recorded from *Symbiodinium* cells under elevated temperature stress,  $F_{HT}$ ; A, kinetic rates; B weighted eigenvector matrix; C, lifetimes (ps) attributed to different model compartments.

**A – Kinetic rates ( $ns^{-1}$ ) matrix – condition  $F_{HT}$ .**

PSII (spillover)			Free	PSI	
PSII/RC	RP1	RP2		PSI/RC	RP1
0.98	30.40	0.00	0.00	1.00	0.00
8.73	0.00	1.80	0.00	0.00	0.00
0.00	2.78	0.90	0.00	0.00	0.00
0.00	0.00	0.00	0.62	0.00	0.00
0.68	0.00	0.00	0.00	0.30	55.90
0.00	0.00	0.00	0.00	300.00	11.20

**B – Weighted eigenvector matrix – condition  $F_{HT}$ .**

PSII (spillover)			Free	PSI	
PSII/RC	RP1	RP2		PSI/RC	RP1
-0.00168	4.5E-05	-3.5E-07	0	0.58437	-0.60101
0.04834	-0.04989	0.00355	0	-8.1E-05	-0.00096
-0.01107	-0.00398	0.00160	0	0.11252	0.58726
0.07123	0.01648	-0.07227	0	0.00138	0.00647
0.12319	0.03735	0.06712	0	0.00181	0.00825
0	0	0	0.073	0	0

**C – Lifetimes (ps) attributed to different model compartments – condition  $F_{HT}$ .**

<b>PSII (spillover)</b>	23.9	299.6	866.9
<b>PSI</b>	2.8	103.9	
<b>Free</b>	1610.0		

**Tables 2.1.4:** Kinetic parameters obtained from the kinetic modeling of the experimental data recorded from *Symbiodinium* cells under coral bleaching condition,  $F_B$ .

**A – Kinetic rates ( $ns^{-1}$ ) matrix – condition  $F_B$ .**

PSII (spillover)			Free	PSI	
PSII/RC	RP1	RP2		PSI/RC	RP1
1.11	33.80	0.00	0.00	0.39	0.00
9.04	0.00	2.61	0.00	0.00	0.00
0.00	1.77	0.90	0.00	0.00	0.00
0.00	0.00	0.00	0.87	0.00	0.00
1.50	0.00	0.00	0.00	0.30	56.00
0.00	0.00	0.00	0.00	300.00	14.00

**B – Weighted eigenvector matrix – condition  $F_B$ .**

PSII (spillover)			Free	PSI	
PSII/RC	RP1	RP2		PSI/RC	RP1
-0.0006	1.7E-05	-8.4E-08	0	0.53176	-0.55228
0.05827	-0.05728	0.00245	0	-0.00021	-0.00253
-0.00313	-0.00117	0.00025	0	0.10184	0.52536
0.06442	0.01448	-0.04826	0	0.00230	0.01048
0.15105	0.04396	0.04556	0	0.00431	0.01897
0	0	0	0.091	0	0

**C – Lifetimes (ps) attributed to different model compartments – condition  $F_B$ .**

<b>PSII (spillover)</b>	22.3	247.4	554.6
<b>PSI</b>	2.8	84.4	
<b>Free</b>	1148.6		

## 2.1.3 Results and Discussion

### 2.1.3.1 Quenching in *Symbiodinium* cells under stress conditions

The kinetic modeling, as applied here, affords a detailed insight into both the site and the molecular mechanisms of the high light stress responses of *Symbiodinium* by testing a wide range of potential kinetic models on the experimental data. As a consequence important, new information is gained on the state of the photosynthetic apparatus (PSA).

The analysis of the time-resolved data indicated that in the control ( $F_C$ ) measurement, the contribution of the long-lived states (originating from PSII) was dominant and thus long average fluorescence lifetimes of 500-700 ps (depending on the emission wavelength) were obtained (Fig. 2.1.3 A, E). As expected, high light stress ( $F_{HL}$ ) caused shortening of the lifetime components (average lifetime ~200-300 ps) due to NPQ (Holzwarth et al. 2009; Miloslavina et al. 2009) (Fig. 2.1.3 B, F). Under temperature stress conditions ( $F_B$  and  $F_{HT}$ ), the average lifetimes were drastically further shortened (to ~100 ps) due to the disappearance of all PSII lifetimes longer than 1 ns (Fig. 2.1.3 C,D and G, H). In fact, the major lifetime amplitude was now associated with a new, very short (3.5 ps) lifetime component (Fig. 2.1.3 G, H). The shortening of the average lifetime indicated that the stress treatments opened additional excited state deactivation (quenching) pathways in the photosynthetic units (PSU) causing a reduction in the overall Chl fluorescence yield and lifetime, as shown in detail by the kinetic target modeling.

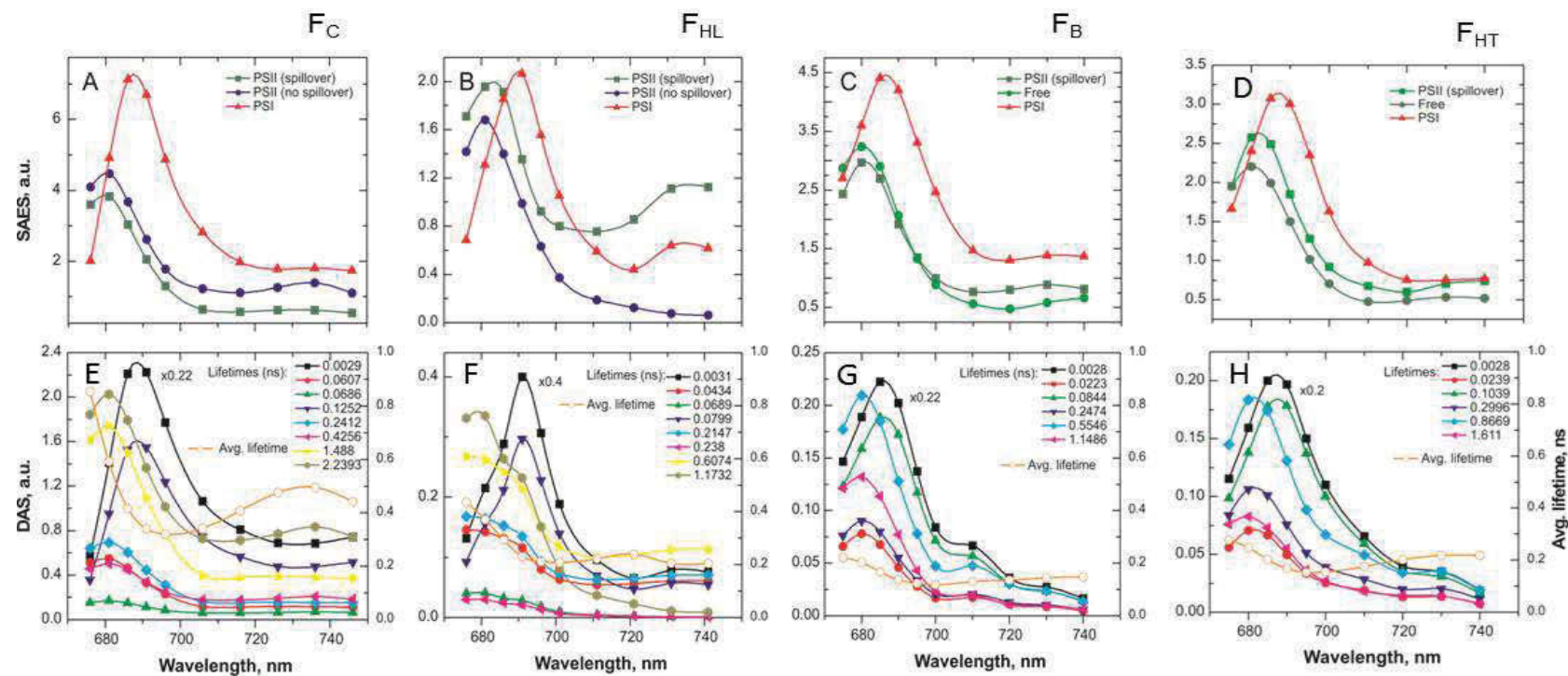


**Figure 2.1.3:** Decay- (DAS) and Species-associated emission spectra (SAES) resulting from the kinetic modeling of the time resolved fluorescence data from *Symbiodinium* cells under the four treatments: A, E)  $F_C$  condition; B, F)  $F_{HL}$  condition; C, G)  $F_B$  condition; D, H)  $F_{HT}$  condition.



### 2.1.3.2 Kinetic target modeling

To reveal the detailed changes introduced into the PSA by the various stress conditions, kinetic target modeling was performed. The major results of the Chl fluorescence kinetics of *Symbiodinium* cells recorded under various stress conditions are summarized in Table 2.1.2. Firstly the usual kinetic scheme of unconnected PSII and PSI primary processes was tested, which turned out to be very successful in describing the kinetics of both control and high light stressed (HL) higher plants (Holzwarth et al. 2009) as well as diatoms (Miloslavina et al. 2009). However, such a kinetic scheme was grossly unsuitable to describe the data of *Symbiodinium* cells under any of the experimental conditions. All modifications of the unconnected PSII and PSI reaction schemes resulted in unsuccessful model fits. The kinetic schemes that were successful for a proper kinetic description are summarized in Fig. 2.1.2 (for full details of rate constants). Consequently, connected schemes were tested by introducing a rate constant  $k_{so}$  accounting for a process – traditionally called “spillover” – by which PSII transfers excitation energy to PSI. Since efficient excited state energy transfer occurs over relatively short distances (typically  $\leq 20\text{-}30\text{\AA}$ ) (Van Amerongen et al. 1996), spillover from PSII to PSI is possible only if direct contact of the two antenna systems within the same membrane exists. Such a direct contact appears feasible in *Symbiodinium* due to the loose packing of the thylakoids (Bertos and Gibbs 1998; Pyszniak and Gibbs 1992), which strongly reduces PSII-PSI segregation as compared to higher plants. Introduction of spillover into the model did indeed allow for an excellent description of the high-temperature conditions with or without additional light stress ( $F_B$  and  $F_{HT}$ , correspondingly). However, the kinetic model was still not suitable for the description of the control ( $F_C$ ) and high-light ( $F_{HL}$ ) conditions. For the latter two cases, a scheme with a heterogeneous PSII population, one part involved in spillover to PSI, and the

other part behaving “normally” (non-spillover PSII), was required (Fig. 2.1.2). Under optimal temperature conditions ( $F_C$  and  $F_{HL}$ ) both PSII populations were present; while under temperature stress conditions ( $F_{HT}$  and  $F_B$ ) the non-spillover population of PSII disappeared. The results are presented in Figure 2.1.3 and Table 2.1.2.

**Table 2.1.2:** Relative excitation vectors (excitation probability for the different compartments), spillover rate, NPQ rate and average lifetimes in each of the four treatments; for all four treatment conditions;  $F_C$  – control condition,  $F_{HL}$  – high light stress,  $F_{HT}$  – thermal stress,  $F_B$  – bleaching conditions (combined thermal and high light stress).

Condition	Relative excitation vectors				Spillover rate ( $\text{ns}^{-1}$ )		
	<i>PSII</i> (spillover)	<i>PSII</i> (no spillover)	<i>Free</i>	<i>PSI</i>	<i>PSII</i> (spillover)		
$F_C$	0.26	0.21	-	0.53	0.48		
$F_{HL}$	0.27	0.23	-	0.50	0.13		
$F_{HT}$	0.27	-	0.09	0.64	0.68		
$F_B$	0.23	-	0.07	0.70	1.50		

Condition	NPQ rate ( $\text{ns}^{-1}$ )			Average lifetime (ps)			
	<i>PSII</i> (spillover)	<i>PSII</i> (no spillover)	<i>PSII</i> (spillover)	<i>PSII</i> (no spillover)	<i>Free</i>	<i>PSI</i>	<i>total</i>
$F_C$	0.35	0.35	940	1765	-	19	500- 700
$F_{HL}$	2.55	1.50	352	993	-	20	200- 300
$F_{HT}$	0.98	-	535	-	1610	18	~100
$F_B$	1.11	-	372	-	1148	15.7	~100

The intrinsic rate constants for PSI and PSII that result from the data fitting to this kinetic model were all within a range that is typical of other oxygen-evolving photosynthetic organisms including diatoms (Holzwarth et al. 2009; Miloslavina et al. 2009) and of isolated PSI and PSII particles (Holzwarth 2008a; Holzwarth 2008b). Importantly, the species-associated emission spectra (SAES) obtained from kinetic modeling have typical shape and spectral positions for PSI and PSII compartments (Fig. 2.1.3 A-D) (Miloslavina et al. 2009) and do allow clear assignment of the respective signals to one of the two photosystems.

The relative excitation probabilities (Table 2.1.2) for the different compartments were proportional to the relative absorption cross-sections of the associated pigment complexes at the excitation wavelength and thus provided good estimates of the relative antenna sizes i.e. the relative amounts of light captured directly by the various PSUs. The similar excitation probability of the spillover and the non-spillover PSII under control conditions ( $F_C$ ), 0.26 and 0.21 respectively, indicated that the two PSII pools were similar in size (Table 2.1.2). In addition, the antenna size of the complete PSII pool (PSII spillover plus PSII non-spillover) and PSI were also almost the same (total excitation probability  $\sim 0.5$ ). The high light ( $F_{HL}$ ) condition did not induce significant changes in the relative excitation probabilities of PSI and PSII, which indicated that photosystems were stable and essentially no antenna movement from one photosystem to the other occurred (Table 2.1.2).

### 2.1.3.3 Effects of light stress

The results of this study (Fig. 2.1.3 and Table 2.1.2) show that under normal temperature conditions ( $F_C$  and  $F_{HL}$ ) indeed two PSII populations – spillover and non-spillover – coexisted in the cells in a ca. 60/40 ratio. The spillover rate was moderate ( $0.48 \text{ ns}^{-1}$ ) under dark-adapted conditions and even decreased substantially under high light stress ( $0.13 \text{ ns}^{-1}$ ) possibly due to light-induced modifications of the peripheral PSII antenna. For both PSII populations, high light stress caused a strong increase in the direct antenna deactivation rate  $k_D$  (from a dark-adapted value of  $0.35 \text{ ns}^{-1}$  to  $2.6 \text{ ns}^{-1}$  and  $1.5 \text{ ns}^{-1}$  respectively, for spillover and non-spillover PSII units). The strong increase in  $k_D$  could be considered as the normal photoprotective NPQ effects occurring in PSII related to the light-induced xanthophyll cycle occurring in the PSII antenna complexes (De Bianchi et al. 2010; Holzwarth et al. 2009; Miloslavina et al. 2009), which also occurs in *Symbiodinium* (Brown et al. 1999a). Evidently, this photoprotection effect was sufficient to avoid damage to PSII at the applied high light intensity since no significant population of photoinhibited PSII centers was observed, which would be detected easily by their long lifetimes in the nanosecond range. Under high high light stress condition ( $F_{HL}$ ), the spillover PSII component did show some enhanced far-red emission (Fig. 2.1.3 B) that was reminiscent of the quenched peripheral LHCII fluorescence in higher plants (Holzwarth et al. 2009). This indicated that a similar quenching process was activated in *Symbiodinium*, but without a pronounced antenna detachment.

#### 2.1.3.4 Temperature stress and bleaching conditions

The observed quenching effects were very different when temperature stress was applied. The population of non-spillover PSII centers disappeared entirely and all PSII units turned into spillover centers (Table 2.1.2). Furthermore, the spillover rate increased strongly (up to a factor of  $\sim 3$ ) as compared to non-heat-stressed conditions (Table 2.1.2). Additionally, the emergence of a small amount of free antenna component showed that part of the peripheral PSII antenna systems, that were associated with the non-spillover PSII units, became functionally disconnected from the PSII core (contributing up to  $\sim 8\%$  of the total absorption cross-section at the excitation wavelength), while some other part of PSII antenna connected to PSI. This explained the increase in the relative absorption cross-section of PSI in comparison to control temperature conditions (from  $\sim 50\%$  to about  $\sim 65-70\%$ , Table 2.1.2). The results presented here are consistent with recent studies of Hoogenboom *et al.* (2012) and Hill *et al.* (2012), which also indicated the presence of a mobile LHC pool moving between PSII and PSI depending on temperature. Under temperature stress conditions the drastically reduced PSII average lifetimes were explained by two effects: i) the very high spillover rates from PSII to PSI; and, ii) the increased antenna deactivation rate,  $k_D$ . The former, however, clearly dominated the PSII deactivation under temperature stress.

On the one hand, spillover is clearly a mechanism that is photoprotective to PSII since it diverts excess excitation energy away from PSII and towards PSI, where it is harmlessly converted to heat due to the high quenching efficiency of  $P_{700}^+$ . Effectively, this protects the most vulnerable component of the PSA – PSII in a similar manner as direct NPQ located in the PSII antenna. Consequently, in moderate amounts it is possible to balance

the light input to PSII and PSI. On the other hand, a very pronounced spillover would have a deleterious effect on the overall photosynthetic electron transport, if not regulated carefully in response to the impinging light intensity and redox state of the electron transport chain. In the extreme case, triggering complete spillover could efficiently shut down electron flow through PSII, without actual modification or damage to the PSII RC units. This would be the case for high temperature stress conditions. Thus, it makes sense that: i) only part of the PSII centers are involved in spillover under normal temperature conditions; and, ii) that the spillover rates for those centers that are undergoing spillover are moderate.

#### ***2.1.3.5 Molecular model for thylakoid reorganization***

Based on the results presented here it was proposed, that a structural/functional model for the heat stress-induced reorganization of the thylakoid membrane in *Symbiodinium* (Fig. 2.1.4). It follows from the kinetic modeling (Fig. 2.1.2) that under normal conditions ( $F_C$ ), there exist two PSII pools: one involved in spillover to PSI (most likely located in the non-appressed membrane regions) and another (located in the appressed regions and thus laterally segregated from PSI) that does not exchange excitation energy with PSI (Fig. 2.1.2). This indicates that the PSII-PSI segregation, typical for higher plant thylakoids, is not even realised in *Symbiodinium* under non-stressed control conditions ( $F_C$ ). The effect can be well-understood considering the thylakoid ultrastructure of dinoflagellates, which shows only a low degree of membrane appression (Hill et al. 2009; Tchernov et al. 2004a) and therefore allows mixing of PSII and PSI units in the non-appressed regions.

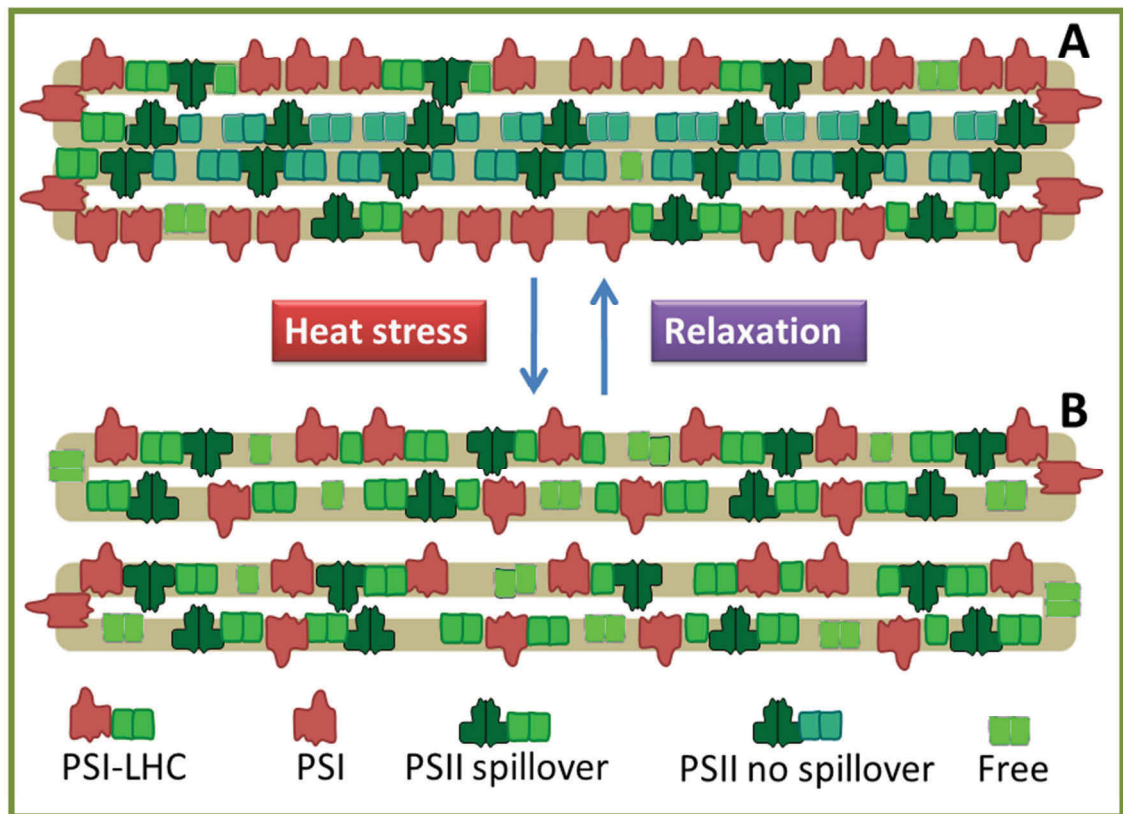


**Figure 2.1.4:** Molecular model for thylakoid organization and their reorganization induced under elevated thermal stress. **A)** Under optimal growth temperature conditions, there exist two PSII pools: one that is involved in excitation spillover with PSI and another that is not; **B)** When cells are exposed to elevated temperature (with or without high light) a major reorganization of the peripheral antenna of PSII occurs. In this state there is a homogeneous PSII-PSI distribution in the thylakoid membrane, causing strong spillover and the increase in the effective antenna size of PSI. There is also some (8%) dissociation of light harvesting antenna, previously attached to PSII. The model allows for the full relaxation of the heat-induced state if the exposure to elevated temperatures is mild and not very prolonged. Under long term heat stress permanent damage to the cells may be induced.



Interestingly, our data did not reveal significant changes in this membrane organization induced by high light stress only ( $F_{HL}$ ). This is in agreement with the work of Reynolds et al. (2008) where the 77 K fluorescence results from *Symbiodinium* clade B and C exposed to similar light conditions did not show dissociation of the peripheral antenna from PSII. However, light-induced dissociation was found in a clade A strain, which might suggest a photoprotective mechanism for this clade similar to the one proposed for diatoms and higher plants (Holzwarth et al. 2009; Miloslavina et al. 2009).

On the other hand the results of the kinetic analysis demonstrate that under temperature stress ( $F_{HT}$  and  $F_B$ ), the thylakoid membrane appression, and thus the lateral segregation of PSII and PSI in *Symbiodinium*, is lost entirely (Fig. 2.1.3 B, D), which can only occur due to a major reorganization of the thylakoid membrane structure. This loss of membrane appression appears to be caused by two factors: i) partial dissociation of the peripheral antenna complexes from the PSII supercomplex; and/or, ii) unfavorable lipid composition that is not adequate to maintain the membrane integrity at the higher temperatures. These findings are consistent with (Tchernov et al. 2004a) in the sense that temperature stress induces loss of membrane integrity, including loss of membrane appression for dinoflagellate strains that are sensitive to temperature-induced bleaching. They now reveal, for the first time, the details of a new “super-quenching mechanism” which forms the basis of the temperature and also high light stress induced breakdown in photosynthetic activity, which occurs in both intact coral and isolated dinoflagellate cells. For strains that are not temperature sensitive, no such heat-induced loss of membrane integrity was observed (Tchernov et al. 2004a) or the loss of photosynthetic activity was shifted to higher temperatures (Díaz-Almeyda et al. 2011; Hill et al. 2009).

### ***2.1.3.6 Breakdown of lateral segregation and linear electron flow***

Clearly, such a reorganization of the thylakoid membranes in dinoflagellates permits significant flexibility of the energy distribution between PSII and PSI. If performed in a controlled manner it can be a powerful regulation mechanism. However, an uncontrolled breakdown of membrane structure – as seems to occur under heat stress conditions – could lead to a catastrophic breakdown of photosynthetic activity.

It has been found earlier that bleaching conditions dramatically reduce the efficiency of PSII and of CO<sub>2</sub> fixation (Hill et al. 2004a; Jones et al. 1998; Warner et al. 1999). However, previously this was attributed primarily to a damage of PSII units (e.g. photoinhibition etc. Hill and Ralph 2006; Takahashi et al. 2009); however the actual occurrence of photoinhibition has been questioned by Tchernov et al. (2004a). The results presented here can explain all these previous data in terms of the functional loss of PSII activity, without actually requiring a real damage of PSII units. Therefore, all the kinetic parameters of the PSII units in the super-quenched state indicate an intact electron transfer capability. Yet, strong spillover has the same effect of strongly reducing the PSII yield, measured as  $F_V/F_M$ , just as a real damage of PSII centers would do. This explains why the two mechanisms cannot be distinguished in the conventional fluorescence analysis. Yet these two entirely different underlying causes cannot be distinguished in usual steady-state fluorescence measurements. The total loss of PSII/PSI segregation under heat stress and the resulting extra spillover with the shift of part of the PSII peripheral antennae (15-20%) to PSI effectively shuts down electron flow through PSII. It follows directly from the rate constants of all the quenching processes (see Tables 2.1.2) that under combined heat and light stress, less than 5% of all the photons being absorbed by PSII caused electron transfer and more than 95% was

converted to heat. Thus linear electron flow in the entire PSA essentially broke down, along with all the subsequently ensuing negative consequences for adenosine-5'-triphosphate (ATP) synthesis and carbon fixation that have been reported as characteristics of the coral symbionts under bleaching conditions (Hill et al. 2012; Jones et al. 1998; Warner et al. 1999). This loss of photosynthetic function will eventually cause death of the algal symbiont. It may, however, be expelled well before that event (Ralph et al. 2001), resulting in a bleached coral. Ironically, modest spillover actually does protect the most vulnerable component of the light harvesting antennae – PSII – in a similar manner as the normal light-induced NPQ of other organisms (Holzwarth et al. 2009; Miloslavina et al. 2009). However, under combined heat and light stress spillover changes from a controlled and limited process to an uncontrolled event causing the photosynthetic apparatus to become super quenched ( $\geq 95\%$  of all the photons exciting PSII are converted to heat). In consequence this leads then to the described breakdown of photosynthetic activity. In this situation, the possibility for deleterious consequences in the holobiont is high.

The results now provide a molecular basis for understanding the mechanisms of the heat-induced loss of thylakoid integrity and the ensuing loss of photosynthetic function due to the total breakdown of linear electron flow. This insight now enables us to examine and correlate differences in bleaching between the various *Symbiodinium* clades and their photoprotective mechanisms suggested by some recent results in the literature (cf. Krämer et al. 2012; Ragni et al. 2010). As bleaching varies between species and habitats, this new understanding is essential for estimating expected climate change effects on coral reefs (Lesser 2011). Future studies need to integrate this super-

quenching state into our understanding of how symbiotic dinoflagellates on tropical coral reefs will respond to a changing climate (Hill et al. 2012; Ragni et al. 2010).

### 2.1.4 References

- Baker, A. C. 2003. Flexibility and specificity in coral-algal symbiosis: diversity, ecology, and biogeography of *Symbiodinium*. *Annual Review of Ecology, Evolution and Systematics* **34**: 661-689.
- Berkelmans, R., and M. J. H. Van Oppen. 2006. The role of zooxanthellae in the thermal tolerance of corals: a 'nugget of hope' for coral reefs in an era of climate change. *Proceedings of the Royal Society B* **273**: 2305-2312.
- Bertos, N. R., and S. P. Gibbs. 1998. Evidence for a lack of photosystem segregation in *Chlamydomonas reinhardtii* (Chlorophyceae). *Journal of Phycology* **34**: 1009-1016.
- Brown, B. E., I. Ambarsari, M. Warner, W. Fitt, R. P. Dunne, S. W. Gibb, and D. G. Cummings. 1999a. Diurnal changes in photochemical efficiency and xanthophyll concentrations in shallow water reef corals: evidence for photoinhibition and photoprotection. *Coral Reefs* **18**: 99-105.
- De Bianchi, S., M. Ballottari, L. Dall'osto, and R. Bassi. 2010. Regulation of plant light harvesting by thermal dissipation of excess energy. *Biochemical Society Transactions* **38**: 651-660.
- Díaz-Almeyda, E., P. E. Thomé, M. E. Hafidi, and R. Iglesias-Prieto. 2011. Differential stability of photosynthetic membranes and fatty acid composition at elevated temperature in *Symbiodinium*. *Coral Reefs* **30**: 217-225.
- Fitt, W. K., B. E. Brown, M. E. Warner, and R. P. Dunne. 2001. Coral bleaching: interpretation of thermal tolerance limits and thermal thresholds in tropical corals. *Coral Reefs* **20**: 51-65.
- Hill, R., A. W. D. Larkum, C. Frankart, M. Kühl, and P. J. Ralph. 2004. Loss of functional photosystem II reaction centers in zooxanthellae of corals exposed to bleaching conditions: using fluorescence rise kinetics. *Photosynthesis Research* **82**: 59-72.
- Hill, R., A. W. D. Larkum, O. Prášil, D. M. Kramer, V. Kumar, and P. J. Ralph. 2012. Light-induced redistribution of antenna complexes in the symbionts of scleractinian corals correlates with sensitivity to coral bleaching. *Coral Reefs* **31**: 963-975.

- Hill, R., and P. J. Ralph. 2006. Photosystem II heterogeneity of *in hospite* zooxanthellae in scleractinian corals exposed to bleaching conditions. *Photochemistry and Photobiology* **82**: 1577-1585.
- Hill, R., K. E. Ulstrup, and P. J. Ralph. 2009. Temperature induced changes in thylakoid membrane thermostability of cultured, freshly isolated, and expelled zooxanthellae from scleractinian corals. *Bulletin of Marine Science* **85**: 223-244.
- Hiller, R. G., P. M. Wrench, A. P. Gooley, G. Shoebridge, and J. Breton. 1993. The major intrinsic light-harvesting protein of *Amphidinium*: characterization and relation to other light-harvesting proteins. *Photochemistry and Photobiology* **57**: 125-131.
- Hoegh-Guldberg, O. 1999. Climate change, coral bleaching and the future of the world's coral reefs. *Marine & Freshwater Research* **50**: 839-866.
- Hoegh-Guldberg, O., P. J. Mumby, H. A.J., R. S. Steneck, P. Greenfield, E. Gomez, C. D. Harvell, P. F. Sale, A. J. Edwards, K. Caldeira, N. Knowlton, C. M. Eakin, R. Iglesias-Prieto, N. Muthiga, R. H. Bradbury, A. Dubi, and M. E. Hatziolos. 2007. Coral reefs under rapid climate change and ocean acidification. *Science* **318**: 1737-1742.
- Hofmann, E., P. M. Wrench, F. P. Sharples, R. G. Hiller, W. Welte, and K. Diederichs. 1996. Structural basis of light harvesting by carotenoids: peridinin-chlorophyll-protein from *Amphidinium carterae*. *Science* **272**: 1788-1791.
- Holzwarth, A. R. 1996. Data analysis of time-resolved measurements, p. 75-92. *In* J. Amez and A. J. Hoff [eds.], *Biophysical Techniques in Photosynthesis. Advances in Photosynthesis Research*. Kluwer Academic Publishers.
- Holzwarth, A. R. 2004. p. 43-115. *In* M. D. Archer and J. Barber [eds.], *Molecular to global photosynthesis*. Imperial college press.
- Holzwarth, A. R. 2008a. Primary reactions-from isolated complexes to intact plants, p. 77-83. *In* J. F. Allen, E. Gantt, J. H. Golbeck and B. Osmond [eds.], *Photosynthesis: Energy from the Sun*.
- Holzwarth, A. R. 2008b. Ultrafast primary reactions in the photosystems of oxygen-evolving organisms, p. 141-164. *In* M. Braun, P. Gilch and W. Zinth [eds.], *Ultrashort laser pulses in biology and medicine*. Springer.
- Holzwarth, A. R., Y. Miloslavina, M. Nilkens, and P. Jahns. 2009. Identification of two quenching sites active in the regulation of photosynthetic light-harvesting studied by time-resolved fluorescence. *Chemical Physics Letters* **483**: 262-267.

- Holzwarth, A. R., M. G. Mueller, J. Niklas, and J. Lubitz. 2005. Charge Recombination Fluorescence in Photosystem I Reaction Centers from *Chlamydomonas reinhardtii*. *Journal of Physical Chemistry* **109**: 5903-5911.
- Hoogenboom, M. O., D. A. Campbell, E. Beraud, K. Dezeew, and C. Ferrier-Pagès. 2012. Effects of light, food availability and temperature stress on the function of photosystem II and photosystem I of coral symbionts. *Plos One* **7**: e30167.
- Jones, R. J., O. Hoegh-Guldberg, A. W. D. Larkum, and U. Schreiber. 1998. Temperature-induced bleaching of corals begins with impairment of the CO<sub>2</sub> fixation mechanism in zooxanthellae. *Plant, Cell & Environment* **21**: 1219-1230.
- Krämer, W., I. Caamaño-Ricken, C. Richter, and K. Bischof. 2012. Dynamic regulation of photoprotection determines thermal tolerance of two phylotypes of *Symbiodinium* clade A at two photon fluence rates. *Photochemistry and Photobiology* **88**: 398-413.
- Larkum, A. W. D. 2003. Light-harvesting systems in algae, p. 277-304. *In* A. W. D. Larkum, Douglas, S.E., Raven, J.A. [ed.], *Photosynthesis in Algae*. Kluwer Academic Publishers.
- Larkum, A. W. D., and C. J. Howe. 1997. Molecular aspects of light-harvesting processes in algae. *Advances in Botanical Research* **27**: 257-330.
- Lesser, M. 2011. Coral Bleaching: causes and mechanisms, p. 405-419. *In* Z. Dubinsky and N. Stambler [eds.], *Coral Reefs: An Ecosystem in Transition*. Springer Netherlands.
- Lesser, M. P., and J. H. Farrell. 2004. Exposure to solar radiation increases damage to both host tissues and algal symbionts of corals during thermal stress. *Coral Reefs* **23**: 367-377.
- Li, Z., S. Wakao, B. B. Fischer, and K. K. Niyogi. 2009. Sensing and responding to excess light. *Annual Review of Plant Biology* **60**: 239-260.
- Miloslavina, Y., I. Grouneva, P. H. Lambrev, B. Lepetit, R. Goss, C. Wilhelm, and A. R. Holzwarth. 2009. Ultrafast fluorescence study on the location and mechanism of non-photochemical quenching in diatoms. *Biochimica et Biophysica Acta* **1787**: 1189-1197.
- Pyszniak, A. M., and S. P. Gibbs. 1992. Immunocytochemical localization of photosystem I and the fucoxanthin-chlorophyll a/c light-harvesting complex in the diatom *Phaeodactylum tricorutum*. *Protoplasma* **166**: 208-217.

- Ragni, M., R. L. Airs, S. J. Hennige, D. J. Suggett, M. E. Warner, and R. J. Geider. 2010. PSII photoinhibition and photorepair in *Symbiodinium* (Pyrrophyta) differs between thermally tolerant sensitive phylotypes. *Marine Ecology Progress Series* **406**: 57-70.
- Ralph, P. J., R. Gademann, and A. W. D. Larkum. 2001. Zooxanthellae expelled from bleached corals at 33°C are photosynthetically competent. *Marine Ecology Progress Series* **220**: 163-168.
- Reynolds, M. J., B. U. Bruns, W. K. Fitt, and G. W. Schmidt. 2008. Enhanced photoprotection pathways in symbiotic dinoflagellates of shallow-water corals and other cnidarians. *Proceedings of the National Academy of Sciences U.S.A.* **105**: 13674-13678.
- Takahashi, S., S. M. Whitney, and M. R. Badger. 2009. Different thermal sensitivity of the repair of photodamaged photosynthetic machinery in cultured *Symbiodinium* species. *Proceedings of the National Academy of Sciences U.S.A.* **106**: 3237-3242.
- Tchernov, D., M. Y. Gorbunov, C. De Vargas, S. N. Yadav, A. J. Milligan, M. Haegblom, and P. G. Falkowski. 2004a. Membrane lipids of symbiotic algae are diagnostic of sensitivity to thermal bleaching in corals. *Proceedings of the National Academy of Sciences U.S.A.* **101**: 13531-13535.
- Van Amerongen, H., L. Valkunas, and R. Van Grondelle. 1996. *Photosynthetic excitons*, p. 1-590. World scientific.
- Van Stokkum, I. H. M., D. S. Larsen, and R. Van Grondelle. 2004. Global and target analysis of time-resolved spectra. *Biochimica et Biophysica Acta* **1657**: 82-104.
- Vass, I. 2012. Molecular mechanisms of photodamage in the photosystem II complex. *Biochimica et Biophysica Acta* **1817**: 209-217.
- Warner, M. E., W. K. Fitt, and G. W. Schmidt. 1999. Damage to photosystem II in symbiotic dinoflagellates: a determinant of coral bleaching. *Proceedings of the National Academy of Sciences U.S.A.* **96**: 8007-8012.



Page intentionally left blank

## Chapter 2.2

# Functional characterisation of the PSII-LHC antenna complex under thermal stress in *Symbiodinium* sp. - implications for coral bleaching

Verena Schrameyer<sup>1</sup>, Ross Hill<sup>1,2</sup>, Milan Szabo<sup>1</sup>, Chavdar Slavov<sup>3</sup>, Alfred R. Holzwarth<sup>3</sup>, Anthony W.D. Larkum<sup>2</sup>, Peter J. Ralph<sup>1</sup>

<sup>1</sup>*Plant Functional Biology and Climate Change Cluster, School of the Environment, University of Technology, Sydney, PO Box 123, Broadway, NSW 2007, Australia*

<sup>2</sup>*Centre for Marine Bio-Innovation, School of Biological, Earth and Environmental Sciences, The University of New South Wales, Sydney 2052 NSW, Australia*

<sup>3</sup>*Max-Planck-Institut für Bioanorganische Chemie, Stiftstr. 34-36, D-45470 Mülheim a.d. Ruhr, Germany*

**Keywords:** Light harvesting, *Symbiodinium*, PCP, acpPC, photoprotective pathways, thylakoid membrane organisation, xanthophyll cycle

### 2.2.1 Introduction

Coral reefs are under threat from climate change with coral bleaching events becoming more frequent and widespread (Hoegh-Guldberg 1999). Increases in sea-surface temperature as well as downwelling irradiance during periods of calmer seas present increasing stress to the symbiosis of hard corals and their microalga symbionts (genus *Symbiodinium*, class Dinophyceae) (Hoegh-Guldberg 2010). This successful symbiotic relationship has allowed corals to thrive in tropical oligotrophic waters over millennia and is heavily based on the photosynthetic contribution of the algal symbiont (Muscatine and Porter 1977). However, under stressful conditions this symbiosis is disrupted as the photosynthetic efficiency of *Symbiodinium* declines (Hill et al. 2004a; Jones and Hoegh-Guldberg 2001; Middlebrook et al. 2010; Warner and Berry-Lowe 2006). The dysfunction of the photosynthetic apparatus of *Symbiodinium* has been identified as one of the main triggers leading to a bleaching response, but there is an ongoing debate as to where the site of damage to photosynthesis is located. Damaged PSII (Hill and Ralph 2006; Warner et al. 1999), Calvin-cycle inefficiency (Jones et al. 1998; Lilley et al. 2010) as well as thylakoid membrane dysfunction (Tchernov et al. 2004a) have been examined as potential primary triggers to initiate coral bleaching from the side of the algal symbiont.

During the light reactions of photosynthesis, photosynthetic active radiation (PAR; 400-700 nm) is channelled through the light harvesting complexes (LHC) into photosystem (PS) II and I; in brief, water is oxidised at the oxygen evolving complex (OEC), which liberates excited electrons, which are then channelled from the excited reaction center at PSII ( $P_{680}^*$ ) through pheophytin into a series of redox reactions upon which electrons are being passed through an intersystem electron carrier, the plastoquinone pool (PQP), towards Nicotinamide adenine dinucleotide phosphate ( $NADP^+$ ) (through ferredoxin) at

PSI. The protonation of  $\text{NADP}^+$  to NADPH is one of the energy supplies for carbon fixation during the dark reactions (as well as ATP, which is produced through protonation of  $\text{ADP}^+$  through ATP synthase, but not directly related to linear electron transport) (Falkowski and Raven 2007). Down-regulation as a result of over-reduction due to excess light energy at either of the PSs could therefore alter the overall photosynthetic efficiency. PSII is generally more sensitive to over-reduction than PSI as PSII has a higher redox potential ( $\sim 1.3$  V; Rappaport et al. (2002)) compared to PSI ( $-0.54$  V; Munge et al. (2003)), which is needed for oxidation of water at the OEC.

Structural changes to the antenna complex can result in a decrease in absorption cross section of PSII which in turn helps to alleviate excess light energy at PSII and is therefore a strategy of photoprotection (Chapter 2.1 , Wollman 2001). This type of photoprotection has been well described in higher plants and some types of algae, as well as cyanobacteria (Campbell et al. 1998; Lunde et al. 2000). High light exposure to PSII reduces the plastoquinone pool, and upon full reduction activates a regulatory kinase, which phosphorylates LHCs associated with PSII (state 1) and initiates the movement of these phosphorylated LHCs towards PSI (state 2), a mechanism that is called 'state-transition', although the exact process regulation has been a matter of debate (Larkum 2003; Tikkanen et al. 2011).

Photosynthetic efficiency in *Symbiodinium* has been well documented for various 'living states' (*in hospite*, *in vitro*, freshly isolated), as well as stress conditions (high light, thermal stress) (Brown et al. 1999a; Hill et al. 2009; Iglesias-Prieto and Trench 1997; Warner et al. 1996). However, functional aspects of the photosynthetic apparatus of *Symbiodinium* have only been rudimentarily resolved (Jiang et al. 2012). *Symbiodinium* is equipped with two unique LHCs; a membrane associated (peripheral) water-soluble fraction the Peridinin-chlorophyll-protein complex (PCP) and the

membrane-integrated chlorophyll *a*-chlorophyll *c*<sub>2</sub>-peridinin-protein complex (acpPC) (Hiller et al. 1993; Iglesias-Prieto and Trench 1997). PCPs in *Symbiodinium* can be highly diverse in terms of length (i.e. homodimer ~ 15 kDa or monomer ~32-34 kDa), pigment content, genetic coding and spectroscopic properties, where a recent study demonstrated for PCPs of *Symbiodinium* (strain CS-156) a pigment concentration ratio of peridinin to Chl *a* of 4 (Jiang et al. 2012). A unique feature of dinoflagellates is the carotenoid (peridinin) which they contain as a functional light-absorbing pigment (Green and Durnford 1996). As peridinin is the primary pigment of PCP it absorbs in the blue-green region (470-550 nm) and emits at around 675 nm (Hiller et al. 1995; Iglesias-Prieto et al. 1993). Recent studies, based on low temperature (77 K) fluorescence emission spectra of PSII and PSI, brought forward the notion that the movement of PCP and/or acpPC, as in flexible adjustments within the photosynthetic apparatus, could indeed be involved in light energy distribution between PSII and PSI in *Symbiodinium* (Hill et al. 2012; Reynolds et al. 2008). How photoprotective mechanisms function in *Symbiodinium* under coral bleaching conditions is of fundamental interest in order to define stress limits and understand bleaching physiology.

*In hospite Symbiodinium* are exposed to variable light regimes in their natural habitat (Wangpraseurt et al. 2012), due to fluctuations as a result of tidal changes, turbidity, wave action and depth (Veal et al. 2010). Host pigmentation (green fluorescence protein (GFP), mycosporine-like amino acids (MAAs) (Dove et al. 2008)), as well as photosynthetic pigment concentrations and cell density of *Symbiodinium* (inducing self-shading) can change and influence light utilisation and photoprotection (Cunning and Baker 2013; Venn et al. 2006). Under high light conditions, excess energy is alleviated through the activity of non-photochemical quenching (NPQ) pathways where energy is

dissipated as 'heat' (energy-dependent quenching; qE) or by means of conformational changes during de-epoxidation of xanthophyll pigments (de-epoxidation of diadinoxanthin (Dd) to diatoxanthin (Dt) in dinoflagellates) (Ambarsari et al. 1997; Garcia-Mendoza et al. 2002; Warner and Berry-Lowe 2006). Dissipation of excess energy can prevent damage to the natural photorepair cycle of *de novo* synthesised PSII core proteins D1 (Hill et al. 2011; Takahashi and Badger 2011). If excess energy results in photodamage of the PSII core proteins (D1) that exceeds the photorepair rate, then photoinactivation (photoinhibition) is the result (Takahashi et al. 2004). Photoinactivated PSII antenna systems are thought to be still capable of dissipating harvested light energy and therefore can prevent damage to oxidised and active PSII reaction centers (Matsubara and Chow 2004).

Here we examined the utilisation and activity of NPQ pathways in *Symbiodinium* strain CS-156 under different coral bleaching relevant scenarios. We asked the following questions i) do structural changes of thylakoid membrane associated LHCs occur under high light and thermal stress treatments?, ii) how flexible are NPQ pathways under thermal and high light stress?, iii) if structural changes in LHC occur, are these stressor specific? and iv) do they complement other NPQ pathways?

## **2.2.2 Materials and Methods**

### ***2.2.2.1 Experimental design***

*Symbiodinium* culture CS-156 (originating from the Hawaiian scleractinian coral *Montipora verrucosa*) was obtained from the Commonwealth Scientific and Industrial Research Organization (CSIRO) (Australia) and grown at 26 °C and 40  $\mu\text{mol photons m}^{-2} \text{ s}^{-1}$  on a 12:12 light:dark cycle. The algal culture suspension (400 mL) was put into a

re-circulating system powered with a peristaltic pump at  $200 \text{ mL min}^{-1}$ , to avoid settlement of the algae. The main culture vessel was held in a temperature controlled water jacket with side mounted green (peak emission wavelengths 530 nm) and red (peak emission wavelengths 625 nm) light-emitting diode panels (LEDs, 12 per panel; Luxeon Star/O, Philips Lumileds Lighting company) as actinic light source. A total of 4 treatments was applied and examined on consecutive days (Fig 2.2.1). During treatment 1 ( $F_{\text{Heat}}$ ) the algal cells were exposed to thermal stress ( $30.5^\circ \text{C}$ ) for the first 8 h of treatment incubation and then additionally exposed to high light stress ( $600 \mu\text{mol photons m}^{-2} \text{ s}^{-1}$ ) for the last 3.5 h of the treatment incubation time. Treatment 2 ( $F_{\text{Heat+NPQ}}$ ) simulated exposure to thermal stress ( $30.5^\circ \text{C}$ ) and high light stress ( $600 \mu\text{mol photons m}^{-2} \text{ s}^{-1}$ ) relevant to bleaching scenarios (Hill and Ralph 2006) for a total of 11.5 h in treatment incubation. Treatment 3 ( $F_{\text{NPQ}}$ ) served as a treatment to measure light induced quenched cells with closed RCs, here the algae were incubated at rearing temperature  $26^\circ \text{C}$  and incubated under high light ( $600 \mu\text{mol photons m}^{-2} \text{ s}^{-1}$ ). Treatment 3 was incubated for 3.5 h; algae of thermal stress exposure treatments (treatment 1 and 2) were incubated for a total of 11.5 h. Algae of treatments 1 and 2 were ramped in ambient light ( $\sim 40 \mu\text{mol photons m}^{-2} \text{ s}^{-1}$ ) ( $F_{\text{Heat+NPQ}}$ ) or in the dark ( $F_{\text{Heat}}$ ) from  $26^\circ \text{C}$  to experimental  $30.5^\circ \text{C}$  in  $0.5^\circ \text{C}$  steps every 10 min at the beginning of experimental incubation (indicated  $T_{-2\text{h}}$  to  $T_{0\text{h}}$ ) in data presenting figures. Experimental algae culture was sampled for Chl fluorescence and pigment analyses at initiation of the experiment, after heat ramping for treatment 1 and 2 and further every 2h throughout the treatment incubation, with the last sampling interval 1.5h ( $n=4$ ; 8 sampling points for  $F_{\text{Heat}}$  and  $F_{\text{Heat+NPQ}}$  and 3 sampling points for  $F_{\text{NPQ}}$ ). Cell densities were determined at the start and end of each treatment.

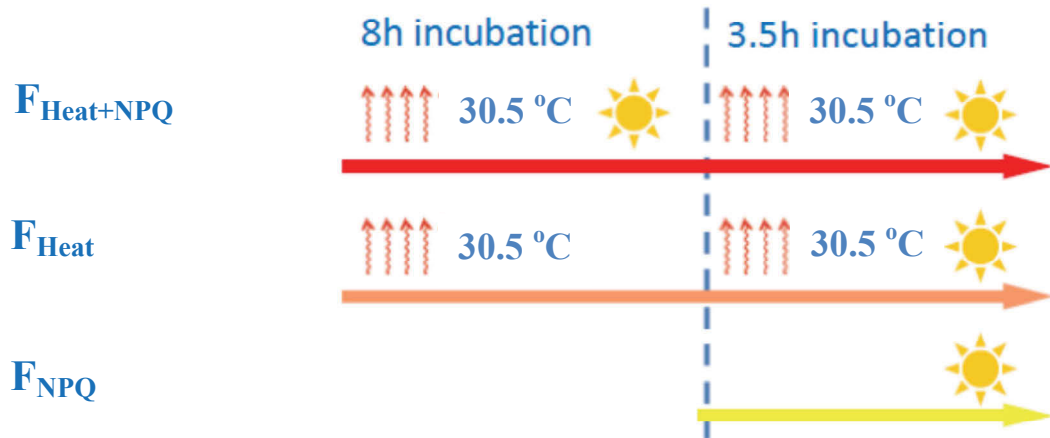


**Figure 2.2.1:** Overview of the 3 treatment incubations applied. Treatment 1: ( $F_{\text{Heat+NPQ}}$ ) 11.5 h of combined thermal and high light stress; treatment 2: ( $F_{\text{Heat}}$ ) 8 h of incubation in the dark with thermal stress exposure and 3.5 h of high light stress at the end of treatment incubation; treatment 3 ( $F_{\text{NPQ}}$ ) high light stress exposure for 3.5 h.

### 2.2.2.2 PAM fluorometry

Algal suspension subsamples were examined for variable Chl *a* fluorescence using a Water pulse amplitude modulated (PAM) fluorometer (settings: measuring light frequency= 6, photomultiplier gain= 7, out gain = 1, actinic light = 600  $\mu\text{mol photons m}^{-2} \text{ s}^{-1}$ , saturating pulse intensity = 10 ( $\sim 8000 \mu\text{mol photons m}^{-2} \text{ s}^{-1}$ ) saturating pulse width = 0.8 s). The algal suspensions were measured on two Water PAM units to allow for simultaneous and fast sample processing. Subsamples of the algal suspension were taken directly from the incubation vessel and measured in a 1:6 dilution in f/2 media (Guillard and Ryther 1962). Ten min dark-adaptation ( $F_0$ ) was applied to reach steady-state, a saturation pulse ( $F_M$ ) was applied and used to calculate the maximum quantum yield of PSII ( $F_V/F_M$ );  $F_V/F_M$  (a.u.) =  $(F_M - F_0) / F_M$  (Schreiber 2004). The relative



electron transport rate (rETR) was calculated according to Genty et al. (1989) without accounting for the absorption cross section of PSII;  $rETR (\mu\text{mol e}^- \text{m}^{-2} \text{s}^{-1}) = \Delta F / F_M' \times E$ , where  $\Delta F$  is the variable Chl *a* fluorescence between transient Chl *a* fluorescence during light incubation ( $F$ ) and maximum fluorescence after application of a saturating pulse ( $F_M'$ ) and  $E$  is the incident irradiance.

### ***2.2.2.3 Chlorophyll emission spectra at 77K***

For the 77K fluorescence measurements, 5 mL of algal suspension was filtered on a GF/F filter, where an oval disk was cut out of the middle of the filter to be examined with a custom-build low temperature (77K) fluorescence detection device. Detailed description is given elsewhere about the device (Hill et al. 2012). Briefly, blue excitation was applied with a peak wavelength at 470 nm. Fluorescence intensity (photon counts; in arbitrary units) was detected every 0.3 nm, while the sample was held in liquid nitrogen, at wavelengths > 600 nm using a long-pass filter in front of the internal spectrometer fiber optic. The spectra were normalised to emission at 688 nm, and then de-convoluted into component bands at 675, 688, 701 and 721 nm using PeakFit software (SeaSolve Software Inc., Framingham, Massachusetts, USA). Here 688 nm is characteristic for PSII fluorescence emission, 675 nm is the characteristic fluorescence emission for PCP as well as acpPC and 701, as well as 721 nm are indicating fluorescence emission of PSI (Hill et al. 2012). Amplitude and area for each component band (wavelengths) at each sampling time were calculated and used for statistical treatment comparison.

In a more detailed analysis attempt, algae of the two thermal stress treatments were analysed for their specific fluorescence emission characteristics for PCP (672 nm) and acpPC (683 nm). Wavelengths previously characterised to indicate monomeric PCP

(672 nm; Carbonera et al. (1996)) and acpPC (683 nm; Iglesias-Prieto and Trench (1996) and Reynolds et al. (2008)), as well as PSI associated emission wavelengths at 701 and 721 nm (Hill et al. 2012) were chosen for sampling time comparison within each of these treatments, as well as spectral comparison between thermal stress treatments ( $F_{\text{Heat}}$  and  $F_{\text{Heat+NPQ}}$ ). Gaussian fitting results for the thermal treatment comparison was obtained using Origin software (fitting quality was set to  $r^2 > 0.9$ ); emission peak area, center, width and height can be found in the supplementary information (S 2.2.1). The 77K fluorescence emission difference spectra of the two treatments where algae were exposed to thermal stress ( $F_{\text{Heat}}$  and  $F_{\text{Heat+NPQ}}$ ) were analysed via spectral differences in emission amplitude at wavelengths from 650 – 720 nm relative to 688 nm at  $T_{-2h}$ ,  $T_{0h}$  and at  $T_{11.5h}$ .

#### **2.2.2.4 Pigment analyses**

Samples were snap frozen in liquid nitrogen and analysed for pigment concentration using the method of van Heukelem and Thomas (2001) with slight modifications as described in detail in Hill et al. (2012). A Waters HPLC system was used to separate pigments, which was achieved by using Eclipse XDB C<sub>8</sub> HPLC 4.6 mm x 150 mm column and guard column (Agilent Technologies, Australia) using a linear elution gradient from 5 – 95 % of solvent B (100 % Methanol, HPLC grade, Lomb Scientific (AUST) Pty Ltd., Part no. C2517-4L). Empower Pro 2 software was used to quantify chlorophyll *a* at 665 nm and all other pigments at 450 nm through peak integration.

As Chl *a* can degrade during exposure to high light i.e. during treatment exposure (Flores-Ramírez and Liñán-Cabello 2007) it was decided to normalise pigment concentrations to cell density. Diadinoxanthin (Dd), diatoxanthin (Dt), total xanthophyll

pool ( $\sum XP = Dd + Dt$ ) as well as de-epoxidation status (DPS;  $DPS = Dt / \sum XP$ ) were calculated for treatment comparison.

#### **2.2.2.5 Statistical analyses**

Data were analysed using one-way ANOVA and post-hoc Tukey HSD (Statistica version 10, Stat Soft Inc., Tulsa, USA). ANOVA assumptions for homogeneity and normality were tested using Levene's test and Shapiro Wilk test. If assumptions were not met, data were  $\log_{10}$  transformed or analysed using non-parametric Kruskal-Wallis H-test (non-parametric ANOVA by ranks; ranks are indicated). 77 K fluorescence emission spectra of the two thermal stress treatments ( $F_{Heat}$  and  $F_{Heat+NPQ}$ ) were compared using Student's t-test; where each treatment was analysed for within treatment differences between  $T_{2h}$  and  $T_{11.5h}$  results, which were compared for their fluorescence emission spectra amplitude at 4 critical wavelengths (672, 683, 701 and 721nm); further, a comparison between the two treatments was drawn using their emission spectra amplitude at the 4 critical wavelengths (672, 683, 701 and 721 nm) at 3 critical time points ( $T_{-2h}$ ,  $T_{0h}$ ,  $T_{11.5h}$ ).

## 2.2.3 Results

### 2.2.3.1 Chlorophyll fluorescence

Maximum quantum yield of PSII ( $F_V/F_M$ ) significantly declined for algae in all three treatments over the length of the incubation (Fig. 2.2.2 a;  $F_{Heat}$ , Kruskal Wallis test,  $H(7) = 24.886$ ,  $p < 0.001$ ;  $F_{NPQ}$ , one-way ANOVA,  $F(2,9) = 44.065$ ,  $p < 0.001$ ;  $F_{Heat+NPQ}$ , Kruskal Wallis test,  $H(7) = 17.057$ ,  $p = 0.017$ ). Once exposed to  $600 \mu\text{mol photons m}^{-2} \text{s}^{-1}$ ,  $F_V/F_M$  of algae from the  $F_{Heat}$  treatment declined significantly during the final 3.5 h of this treatment (Tukey HSD,  $p < 0.05$ ; Fig. 2.2.2 a). Algae of  $F_{Heat+NPQ}$  and  $F_{NPQ}$  treatment displayed a gradual decrease throughout the experimental incubation. Relative electron transport rates (rETR; Fig. 2.2.2 b) significantly declined for algae of the  $F_{Heat+NPQ}$  treatment ( $H(7) = 21.932$ ,  $p = 0.003$ ), where no significant changes were found for rETR of algae from the  $F_{NPQ}$  and  $F_{Heat}$  treatment (Fig 2.2.2 b).

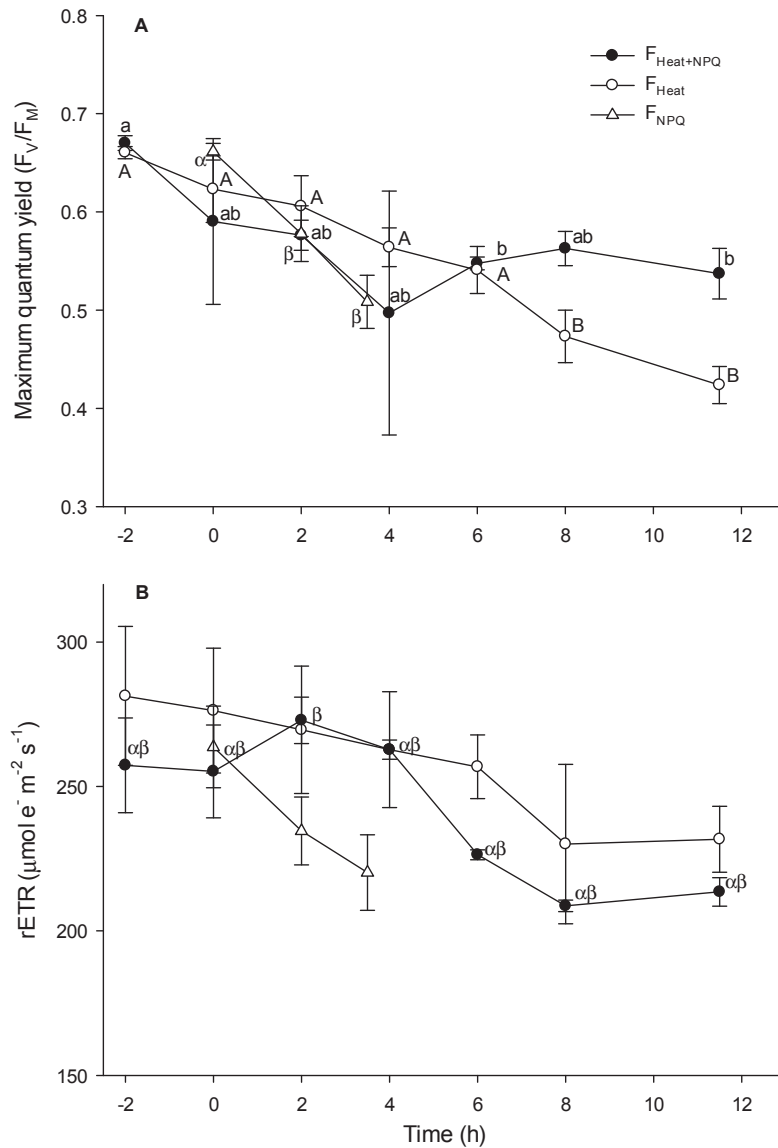


**Figure 2.2.2:** Variable chlorophyll *a* fluorescence parameters at sampling times throughout treatment incubation; ramping time for thermal stress treatments is indicated as -2 and 0 h on the x-axis, where  $F_{\text{NPQ}}$  is displayed from 0; panel A: Maximum quantum yield ( $F_v/F_m$ ) of all treatments, panel B: relative electron transport rate (rETR);  $F_{\text{Heat+N PQ}}$ : closed circles,  $F_{\text{Heat}}$ : closed triangles,  $F_{\text{NPQ}}$ : open triangles; Tukey-HSD grouping results are indicated in lower case letters ( $F_{\text{NPQ}}$  post-hoc analyses results are indicated as greek letters);  $n=4$ , mean  $\pm$  SEM are displayed.

### 2.2.3.2 77K fluorescence emissions

The amplitude (0-1) and area (%) as well as the descriptive statistics are indicated for each identified peak and sampling time for all treatments in Table 2.2.1. Algae exposed to  $F_{\text{Heat}}$  treatment conditions displayed a moderate increase in emission at 675, 701 and 721 nm following 3.5 h of high light applied at the end of the treatment (Tukey HSD,  $p < 0.001$  for all wavelengths), while the area under the 688 nm peak decreased at the end of the treatment (Tukey HSD,  $p < 0.001$ ; Table 2.2.1). Interestingly, upon illumination at  $T_{8h}$  algae of  $F_{\text{Heat}}$  treatment displayed a significant decrease in the amplitude of the 721 nm emission (Tukey HSD,  $p < 0.001$ ), which then increased again towards the end of the experiment. Algae from the  $F_{\text{Heat+NPQ}}$  treatment showed a sharp increase in emission at 675 nm at  $T_{2h}$  and then gradually decreased towards the end of the treatment (Tukey HSD,  $p < 0.001$ ). Simultaneous increases in emission area and amplitude occurred at 701 and 721 nm paralleled with a decrease in 688 nm amplitude area for algae of the  $F_{\text{Heat+NPQ}}$  treatment (Tukey HSD,  $p < 0.05$  for all wavelengths). Algae from the  $F_{\text{Heat}}$  treatment displayed the greatest areal increase in the emission peak at 721 nm at the end of the treatment incubation compared to all other treatments (one-way ANOVA,  $F(3,12) = 51.012$ ;  $p < 0.001$ ). Algae from the  $F_{\text{NPQ}}$  treatment increased area and amplitude at 675 nm throughout treatment incubation (one-way ANOVA,  $F(2,9) = 52.641$ ;  $p < 0.01$ ), while all other component band emissions remained unchanged (Table 2.2.1). However, the changes in 675 nm emission amplitude were 4.19 times higher in algae from the  $F_{\text{Heat}}$  treatment.

**Table 2.2.1.1:** Amplitude (relative units; 0-1) and area (%) of component bands (675, 688, 701 and 721 nm) of fluorescence emission spectra at 77K. Means ( $\pm$  S.E.) shown. *P* values show difference over time for each component in each treatment. Significant differences indicated by \*, with superscript letters indicating Tukey HSD results ( $\alpha = 0.05$ )

Light ( $\mu\text{mol photons m}^{-2} \text{ s}^{-1}$ )	Temp. ( $^{\circ}\text{C}$ )	Time (h)	Wavelength (nm)								
			675		688		701		721		
			Amplitude	Area	Amplitude	Area	Amplitude	Area	Amplitude	Area	
$F_{\text{heat}}$	0	26	-2	0.056 $\pm$ 0.015 <sup>a</sup>	3.6 $\pm$ 0.6 <sup>a</sup>	0.954 $\pm$ 0.008	61.8 $\pm$ 0.8 <sup>b</sup>	0.349 $\pm$ 0.008 <sup>ab</sup>	23.7 $\pm$ 0.9 <sup>a</sup>	0.185 $\pm$ 0.008 <sup>ab</sup>	10.8 $\pm$ 0.8 <sup>a</sup>
		30.5	0	0.061 $\pm$ 0.012 <sup>a</sup>	3.8 $\pm$ 0.7 <sup>a</sup>	0.974 $\pm$ 0.014	61.1 $\pm$ 1.4 <sup>b</sup>	0.383 $\pm$ 0.022 <sup>ab</sup>	24.0 $\pm$ 0.9 <sup>a</sup>	0.177 $\pm$ 0.009 <sup>ab</sup>	11.1 $\pm$ 0.5 <sup>a</sup>
			2	0.076 $\pm$ 0.010 <sup>a</sup>	4.0 $\pm$ 0.6 <sup>a</sup>	0.957 $\pm$ 0.012	61.5 $\pm$ 1.5 <sup>b</sup>	0.333 $\pm$ 0.008 <sup>a</sup>	23.8 $\pm$ 2.0 <sup>a</sup>	0.157 $\pm$ 0.007 <sup>a</sup>	10.8 $\pm$ 0.7 <sup>a</sup>
			4	0.070 $\pm$ 0.002 <sup>a</sup>	4.1 $\pm$ 0.3 <sup>a</sup>	0.980 $\pm$ 0.012	58.0 $\pm$ 2.1 <sup>b</sup>	0.433 $\pm$ 0.040 <sup>b</sup>	25.4 $\pm$ 1.4 <sup>ab</sup>	0.213 $\pm$ 0.026 <sup>ab</sup>	12.4 $\pm$ 1.1 <sup>a</sup>
			6	0.078 $\pm$ 0.010 <sup>a</sup>	4.6 $\pm$ 0.6 <sup>a</sup>	0.977 $\pm$ 0.012	56.9 $\pm$ 0.6 <sup>b</sup>	0.427 $\pm$ 0.007 <sup>b</sup>	24.9 $\pm$ 0.5 <sup>a</sup>	0.233 $\pm$ 0.009 <sup>b</sup>	13.6 $\pm$ 0.6 <sup>ab</sup>
			8	0.082 $\pm$ 0.014 <sup>a</sup>	5.0 $\pm$ 0.8 <sup>a</sup>	0.945 $\pm$ 0.019	58.4 $\pm$ 0.5 <sup>b</sup>	0.393 $\pm$ 0.015 <sup>ab</sup>	24.3 $\pm$ 0.5 <sup>a</sup>	0.199 $\pm$ 0.009 <sup>ab</sup>	12.3 $\pm$ 0.5 <sup>a</sup>
		10	0.093 $\pm$ 0.005 <sup>a</sup>	4.8 $\pm$ 0.8 <sup>a</sup>	0.944 $\pm$ 0.010	55.8 $\pm$ 1.9 <sup>b</sup>	0.430 $\pm$ 0.010 <sup>b</sup>	25.8 $\pm$ 0.5 <sup>ab</sup>	0.222 $\pm$ 0.011 <sup>b</sup>	13.6 $\pm$ 0.7 <sup>ab</sup>	
11.5	0.172 $\pm$ 0.010 <sup>b</sup>	9.1 $\pm$ 0.7 <sup>b</sup>	0.927 $\pm$ 0.007	44.9 $\pm$ 1.0 <sup>a</sup>	0.583 $\pm$ 0.007 <sup>c</sup>	29.8 $\pm$ 0.4 <sup>b</sup>	0.323 $\pm$ 0.012 <sup>c</sup>	16.3 $\pm$ 0.5 <sup>b</sup>			
<i>P</i> value			< 0.001 *	< 0.001 *	0.057	< 0.001 *	< 0.001 *	0.007 *	< 0.001 *	< 0.001 *	
$F_{\text{heat+NPQ}}$	0	26	-2	0.051 $\pm$ 0.007 <sup>a</sup>	2.3 $\pm$ 0.3 <sup>a</sup>	0.954 $\pm$ 0.015	65.4 $\pm$ 1.5 <sup>c</sup>	0.341 $\pm$ 0.006 <sup>a</sup>	21.6 $\pm$ 0.5 <sup>a</sup>	0.175 $\pm$ 0.003 <sup>a</sup>	10.8 $\pm$ 0.7 <sup>a</sup>
		30.5	0	0.072 $\pm$ 0.008 <sup>ab</sup>	4.3 $\pm$ 0.3 <sup>abc</sup>	0.928 $\pm$ 0.004	53.3 $\pm$ 0.5 <sup>b</sup>	0.487 $\pm$ 0.030 <sup>b</sup>	28.9 $\pm$ 0.4 <sup>b</sup>	0.250 $\pm$ 0.005 <sup>b</sup>	13.4 $\pm$ 0.2 <sup>ab</sup>
			2	0.141 $\pm$ 0.019 <sup>c</sup>	7.5 $\pm$ 1.0 <sup>c</sup>	0.952 $\pm$ 0.014	46.6 $\pm$ 1.1 <sup>a</sup>	0.589 $\pm$ 0.007 <sup>c</sup>	31.3 $\pm$ 0.5 <sup>bc</sup>	0.269 $\pm$ 0.010 <sup>b</sup>	14.6 $\pm$ 0.6 <sup>b</sup>
			4	0.104 $\pm$ 0.006 <sup>bc</sup>	6.1 $\pm$ 1.1 <sup>bc</sup>	0.912 $\pm$ 0.023	46.8 $\pm$ 1.3 <sup>a</sup>	0.591 $\pm$ 0.018 <sup>c</sup>	31.6 $\pm$ 0.9 <sup>bc</sup>	0.281 $\pm$ 0.012 <sup>b</sup>	15.5 $\pm$ 0.8 <sup>b</sup>
			6	0.059 $\pm$ 0.010 <sup>ab</sup>	3.9 $\pm$ 0.6 <sup>ab</sup>	0.940 $\pm$ 0.007	47.7 $\pm$ 0.5 <sup>a</sup>	0.593 $\pm$ 0.005 <sup>c</sup>	32.2 $\pm$ 0.2 <sup>bc</sup>	0.289 $\pm$ 0.002 <sup>b</sup>	16.3 $\pm$ 0.3 <sup>b</sup>
			8	0.063 $\pm$ 0.005 <sup>ab</sup>	4.1 $\pm$ 0.4 <sup>ab</sup>	0.948 $\pm$ 0.012	45.9 $\pm$ 1.5 <sup>a</sup>	0.629 $\pm$ 0.022 <sup>c</sup>	34.0 $\pm$ 1.2 <sup>c</sup>	0.289 $\pm$ 0.013 <sup>b</sup>	16.0 $\pm$ 0.8 <sup>b</sup>
			10	0.047 $\pm$ 0.012 <sup>a</sup>	3.2 $\pm$ 0.8 <sup>ab</sup>	0.946 $\pm$ 0.005	48.7 $\pm$ 0.4 <sup>ab</sup>	0.604 $\pm$ 0.011 <sup>c</sup>	33.2 $\pm$ 0.8 <sup>c</sup>	0.268 $\pm$ 0.012 <sup>b</sup>	14.9 $\pm$ 0.8 <sup>b</sup>
11.5	0.051 $\pm$ 0.011 <sup>a</sup>	3.3 $\pm$ 0.7 <sup>ab</sup>	0.957 $\pm$ 0.016	48.5 $\pm$ 0.9 <sup>ab</sup>	0.598 $\pm$ 0.020 <sup>c</sup>	32.4 $\pm$ 0.9 <sup>bc</sup>	0.284 $\pm$ 0.007 <sup>b</sup>	15.9 $\pm$ 0.5 <sup>b</sup>			
<i>P</i> value			< 0.001 *	< 0.001 *	0.294	< 0.001 *	< 0.001 *	< 0.001 *	< 0.001 *	< 0.001 *	

**Table 2.2.1.2:** Amplitude (relative units; 0-1) and area (%) of component bands (675, 688, 701 and 721 nm) of fluorescence emission spectra at 77K. Means ( $\pm$  S.E.) shown. *P* values show difference over time for each component in each treatment. Significant differences indicated by \*, with superscript letters indicating Tukey HSD results ( $\alpha = 0.05$ )

Light ( $\mu\text{mol photons m}^{-2} \text{ s}^{-1}$ )	Temp. ( $^{\circ}\text{C}$ )	Time (h)	Wavelength (nm)							
			675		688		701		721	
			Amplitude	Area	Amplitude	Area	Amplitude	Area	Amplitude	Area
F <sub>NPQ</sub> 600	26	0	0.018 $\pm$ 0.006 <sup>a</sup>	1.2 $\pm$ 0.4 <sup>a</sup>	0.958 $\pm$ 0.016	63.0 $\pm$ 0.9	0.381 $\pm$ 0.008	23.8 $\pm$ 0.1	0.195 $\pm$ 0.002	12.1 $\pm$ 0.3
		2	0.044 $\pm$ 0.006 <sup>b</sup>	2.8 $\pm$ 0.3 <sup>b</sup>	0.946 $\pm$ 0.018	60.8 $\pm$ 0.6	0.380 $\pm$ 0.019	24.4 $\pm$ 0.6	0.187 $\pm$ 0.005	12.0 $\pm$ 0.4
		3.5	0.041 $\pm$ 0.002 <sup>b</sup>	2.6 $\pm$ 0.1 <sup>b</sup>	0.961 $\pm$ 0.021	60.9 $\pm$ 0.4	0.389 $\pm$ 0.022	24.6 $\pm$ 0.7	0.187 $\pm$ 0.002	11.9 $\pm$ 0.4
<i>P</i> value			0.009 *	0.006 *	0.844	0.065	0.921	0.545	0.286	0.920



Emission amplitudes at 672 and 683 nm were compared between  $T_{0h}$  and  $T_{11.5h}$  for the two thermal stress treatments after heat ramping at  $T_{0h}$  and at conclusion of the experiment at  $T_{11.5h}$  (Table 2.2.2). Algae exposed to  $F_{Heat}$  treatment displayed significantly increased emission amplitudes at 672 nm (t-test;  $t(6) = 3.46$ ;  $p = 0.013$ ), where emission at 683nm did not change throughout the treatment (Table 2.2.2). In contrast, algae of the  $F_{Heat+NPQ}$  treatment showed a significant decrease in amplitude at the 683nm band (t-test;  $t(6) = 34.523$ ;  $p < 0.001$ , Table 2.2.2), while emission amplitudes at 672 nm band remained unchanged (Table 2.2.2). Both treatments displayed significant increases at 701 nm (t-test;  $F_{Heat}$ :  $t(6) = 8.64$ ;  $p < 0.001$ ;  $F_{Heat+NPQ}$ :  $t(6) = 3.10$ ;  $p < 0.021$ ) as well as at 721 nm (t-test;  $F_{Heat}$ :  $t(6) = 9.92$ ;  $p < 0.001$ ;  $F_{Heat+NPQ}$ :  $t(6) = 3.71$ ;  $p = 0.001$ ; Table 2.2.2).

**Table 2.2.2:** T-test statistical analyses ( $\alpha = 0.05$ ) comparing  $T_{2h}$  and  $T_{end}$  results of 77K fluorescence emission spectra amplitude differences at critical wavelengths 672, 683, 701 and 721 nm for algae of the  $F_{Heat}$  and  $F_{Heat+NPQ}$  treatment. Spectra of  $T_{2h}$ ; after ramping to experimental temperature to 30.5 °C ( $F_{Heat}$ : in the dark,  $F_{Heat+NPQ}$ : at ambient light) were compared to  $T_{end}$  (mean  $\pm$  SEM are displayed); after experimental incubation (total of 9.5 h;  $F_{Heat}$ : 6 h dark + thermal stress and 3.5 h of high light at the end of experimental incubation;  $F_{Heat+NPQ}$ : 9.5 h of combination of high light + thermal stress).

	$F_{Heat}$	$F_{Heat + NPQ}$
<b>672 nm</b>		
$T_{0h}$	0.085 $\pm$ 0.012	0.095 $\pm$ 0.007
$T_{11.5h}$	0.138 $\pm$ 0.008	0.075 $\pm$ 0.011
t-value (df); p-value	t(6) = 3.462; p = 0.013	n.s.
<b>683 nm</b>		
$T_{0h}$	0.534 $\pm$ 0.006	0.549 $\pm$ 0.010
$T_{11.5h}$	0.548 $\pm$ 0.005	0.552 $\pm$ 0.019
t-value (df); p-value	n.s.	n.s.
<b>701 nm</b>		
$T_{0h}$	0.383 $\pm$ 0.022	0.487 $\pm$ 0.030
$T_{11.5h}$	0.583 $\pm$ 0.007	0.598 $\pm$ 0.020
t-value (df); p-value	t(6) = 8.638; p < 0.001	t(6) = 3.101; p = 0.021
<b>721 nm</b>		
$T_{0h}$	0.177 $\pm$ 0.009	0.250 $\pm$ 0.005
$T_{11.5h}$	0.323 $\pm$ 0.012	0.284 $\pm$ 0.007
t-value (df); p-value	t(6) = 9.922; p < 0.001	t(6) = 3.710; p = 0.001

Further, the spectral emission amplitudes of algae in  $F_{\text{Heat}}$  and  $F_{\text{Heat+NPQ}}$  treatments were examined for between-treatment differences at 675, 688, 701 and 721 nm at sampling point  $T_{-2h}$ ,  $T_{0h}$  and  $T_{11.5h}$  (Table 2.2.3).

No significant differences in spectral emission were found between the treatments at the beginning of the experiment. After ramping to 30.5°C ( $T_{0h}$ ) no significant fluorescence emission differences were found at 672 nm, where the emission amplitude at 683 nm was higher for algae of the  $F_{\text{Heat+NPQ}}$  treatment compared to algae of the  $F_{\text{Heat}}$  treatment (t-test;  $t(6) = 3.09$ ;  $p = 0.021$ ; Table 2.2.3 and Fig 2.2.3 a, b). Further, algae of the  $F_{\text{Heat+NPQ}}$  treatment displayed significantly greater emission amplitudes at 701 and 721 nm compared to algae of the  $F_{\text{Heat}}$  treatment at  $T_{0h}$  (t-test;  $t(6) = 2.79$ ;  $p = 0.032$  and  $t(6) = 7.34$ ;  $p < 0.001$ , respectively; Table 2.2.3). Upon conclusion of the experiment at  $T_{11.5h}$  algae of the  $F_{\text{Heat}}$  treatment displayed greater fluorescence emission amplitude at 672 nm and 721 nm (t-test;  $t(6) = 8.13$ ;  $p < 0.001$  and  $t(6) = 2.80$ ;  $p = 0.031$ , respectively; Table 2.2.3 and Fig 2.2.3 c). Algae of both thermal stress treatments showed comparable emission amplitude increases at 701nm at conclusion of the experiment (Table 2.2.3 and Fig 2.2.3 c, d).

**Table 2.2.3:** T-test statistical analyses ( $\alpha = 0.05$ ) results for 77K fluorescence emission spectra amplitude differences at critical wavelengths 672, 683, 701 and 721 nm, comparing  $F_{\text{Heat}}$  and  $F_{\text{Heat+NPQ}}$  at the start of the experiment ( $T_{-2\text{h}}$ ), after 2 h of ramping to experimental temperature at  $30.5^\circ\text{C}$  ( $T_{0\text{h}}$ ;  $F_{\text{Heat}}$ : in the dark,  $F_{\text{Heat+NPQ}}$ : at ambient light) and at conclusion of experimental incubation ( $T_{11.5\text{h}}$ ; total of 9.5 h in treatment conditions;  $F_{\text{Heat}}$ : 6 h dark + thermal stress and 3.5 h of high light at the end of treatment incubation;  $F_{\text{Heat+NPQ}}$ : 9.5 h of combination of high light + thermal stress).

Emission spectra ( $\lambda$ nm)	Sampling time	$F_{\text{Heat}}$ (mean $\pm$ stde)	$F_{\text{Heat+NPQ}}$ (mean $\pm$ stde)	Statistical values
<b>672 nm</b>	$T_{-2\text{h}}$	0.052 $\pm$ 0.004	0.050 $\pm$ 0.006	n.s.
	$T_{0\text{h}}$	0.085 $\pm$ 0.012	0.095 $\pm$ 0.007	n.s.
	$T_{11.5\text{h}}$	0.138 $\pm$ 0.008	0.075 $\pm$ 0.011	t(6) = 8.13; p < 0.001
<b>683 nm</b>	$T_{-2\text{h}}$	0.497 $\pm$ 0.003	0.514 $\pm$ 0.014	n.s.
	$T_{0\text{h}}$	0.534 $\pm$ 0.006	0.549 $\pm$ 0.010	t(6) = 3.09; p = 0.021
	$T_{11.5\text{h}}$	0.548 $\pm$ 0.005	0.552 $\pm$ 0.019	n.s.
<b>701 nm</b>	$T_{-2\text{h}}$	0.349 $\pm$ 0.008	0.341 $\pm$ 0.006	n.s.
	$T_{0\text{h}}$	0.383 $\pm$ 0.022	0.487 $\pm$ 0.030	t(6) = 2.79; p = 0.032
	$T_{11.5\text{h}}$	0.583 $\pm$ 0.007	0.598 $\pm$ 0.020	n.s.
<b>721 nm</b>	$T_{-2\text{h}}$	0.185 $\pm$ 0.008	0.175 $\pm$ 0.003	n.s.
	$T_{0\text{h}}$	0.177 $\pm$ 0.009	0.250 $\pm$ 0.005	t(6) = 7.34; p < 0.001
	$T_{11.5\text{h}}$	0.323 $\pm$ 0.012	0.284 $\pm$ 0.007	t(6) = 2.80; p = 0.031

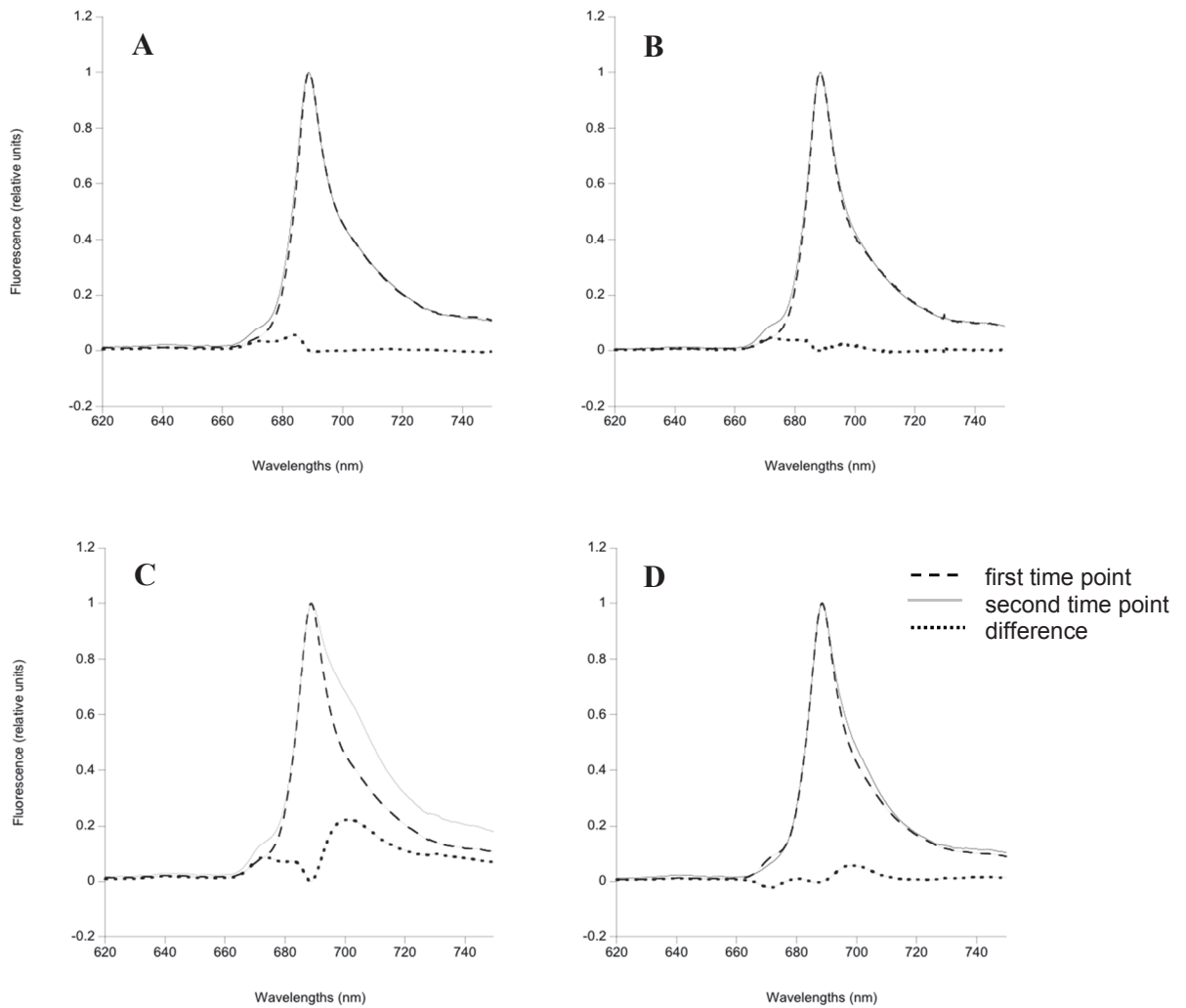


**Figure 2.2.3:** Difference spectra of 77K fluorescence emission amplitudes between wavelengths of 620 – 750 nm are displayed, panel A:  $F_{\text{Heat}}$  treatment; difference spectrum (dotted line) of  $T_{-2\text{h}}$  and  $T_0$ , original  $T_{-2\text{h}}$  (dashed line) and  $T_0$  (straight line) fluorescence emission spectra, panel B:  $F_{\text{Heat+NPQ}}$  treatment; difference spectrum (dotted line) of  $T_{-2\text{h}}$  and  $T_0$ ,  $T_{-2\text{h}}$  (dashed line) and  $T_0$  (straight line) fluorescence emission spectra, panel C:  $F_{\text{Heat}}$  treatment; difference spectrum (dotted line) of  $T_0$  and  $T_{11.5\text{h}}$ ,  $T_0$  (dashed line) and  $T_{11.5\text{h}}$  (straight line) fluorescence emission spectra, panel D:  $F_{\text{Heat+NPQ}}$  treatment; difference spectra (dotted line) of  $T_0$  and  $T_{11.5\text{h}}$ ,  $T_0$  (dashed line) and  $T_{11.5\text{h}}$  (straight line) fluorescence emission spectra.

Difference spectra for algae of the  $F_{\text{Heat}}$  and  $F_{\text{Heat+NPQ}}$  treatment are presented in Figure 2.2.3. Fluorescence emission spectral changes of dark ( $F_{\text{Heat}}$ ) and light ( $F_{\text{Heat+NPQ}}$ ) ramping to experimental temperature (30.5° C) were visualised through difference spectra of  $T_{-2\text{h}}$  and  $T_{0\text{h}}$  (Fig 2.2.3 a, b). Treatment related fluorescence spectral differences were presented by difference spectra of  $T_{0\text{h}}$  and  $T_{11.5\text{h}}$  for both thermal stress treatments  $F_{\text{Heat}}$  and  $F_{\text{Heat+NPQ}}$  (Fig 2.2.3 c, d) (identified peak area, center, width and height from Gaussian fitting are tabulated in S 2.2.1).

### 2.2.3.3 Pigment analyses

Total diadinoxanthin concentration (Dd) significantly decreased for algae in the  $F_{\text{Heat+NPQ}}$  treatment (one-way ANOVA,  $F(7,24) = 4.20$ ,  $p = 0.004$ ; data not displayed) and for algae in the  $F_{\text{NPQ}}$  treatment ( $F(2,9) = 13.042$ ,  $p = 0.002$ ; data not displayed) where Dd remained unchanged in algae of the  $F_{\text{Heat}}$  treatment (one-way ANOVA,  $p > 0.05$ ; data not displayed). Dt concentrations significantly increased in algae of all treatments ( $F_{\text{Heat}}$ :  $H(7) = 18.27$ ,  $p = 0.011$ ;  $F_{\text{Heat+NPQ}}$ :  $H(7) = 25.01$ ,  $p = 0.001$ ;  $F_{\text{NPQ}}$ : one-way ANOVA,  $F(2,9) = 27.23$ ,  $p < 0.001$ ; Fig 2.2.4 a, b).

In agreement with these findings, the de-epoxidation status (DPS;  $\text{DPS} = \text{Dt} / \sum \text{XP}$ ) increased significantly in algae of all treatments, where algae from the  $F_{\text{Heat}}$  treatment ( $H(2) = 16.31$ ,  $p = 0.022$ ) displayed a distinct peak at  $T_{8\text{h}}$  (mean rank = 27.50) relative to  $T_{0\text{h}}$  (mean rank = 4.13) (Fig 2.2.4 c). DPS for algae of  $F_{\text{NPQ}}$  treatment increased over time of incubation (one-way ANOVA,  $F(2,9) = 133.97$ ,  $p < 0.001$ ; Fig 2.2.4 d), where levels peaked at  $T_{2\text{h}}$  (Tukey HSD,  $p < 0.05$ ). DPS of  $F_{\text{Heat+NPQ}}$  did not increase for the first 3 sampling events ( $T_{0\text{h}}$ ,  $T_{2\text{h}}$ ,  $T_{3.5\text{h}}$ ; Tukey HSD,  $p < 0.05$ ; Fig 2.2.4 c), but then increased for the remaining treatment incubation (one-way ANOVA,  $F(7,24) = 16.89$ ,  $p < 0.001$ ).

$\Sigma$  XP concentrations changed significantly during the time of experimental incubation in algae of the  $F_{\text{Heat+NPQ}}$  treatment, with a significant drop at  $T_{0h}$  after heat ramping (Tukey HSD,  $p < 0.05$ ) and at  $T_{6h}$  (Tukey HSD,  $p < 0.05$ ) (one-way ANOVA,  $F(7, 24) = 4.06$ ,  $p = 0.005$ ; Fig 2.2.4 e).  $\Sigma$  XP concentrations in algae of the  $F_{\text{Heat}}$  remained unchanged during experimental treatment incubation. Algae in the  $F_{\text{NPQ}}$  treatment displayed a significant decline in their  $\Sigma$  XP at the end of treatment incubation  $T_{3.5h}$  (Tukey HSD,  $p < 0.05$ ; one-way ANOVA,  $F(2, 9) = 11.10$ ,  $p = 0.004$ ; Fig 2.2.4 f).

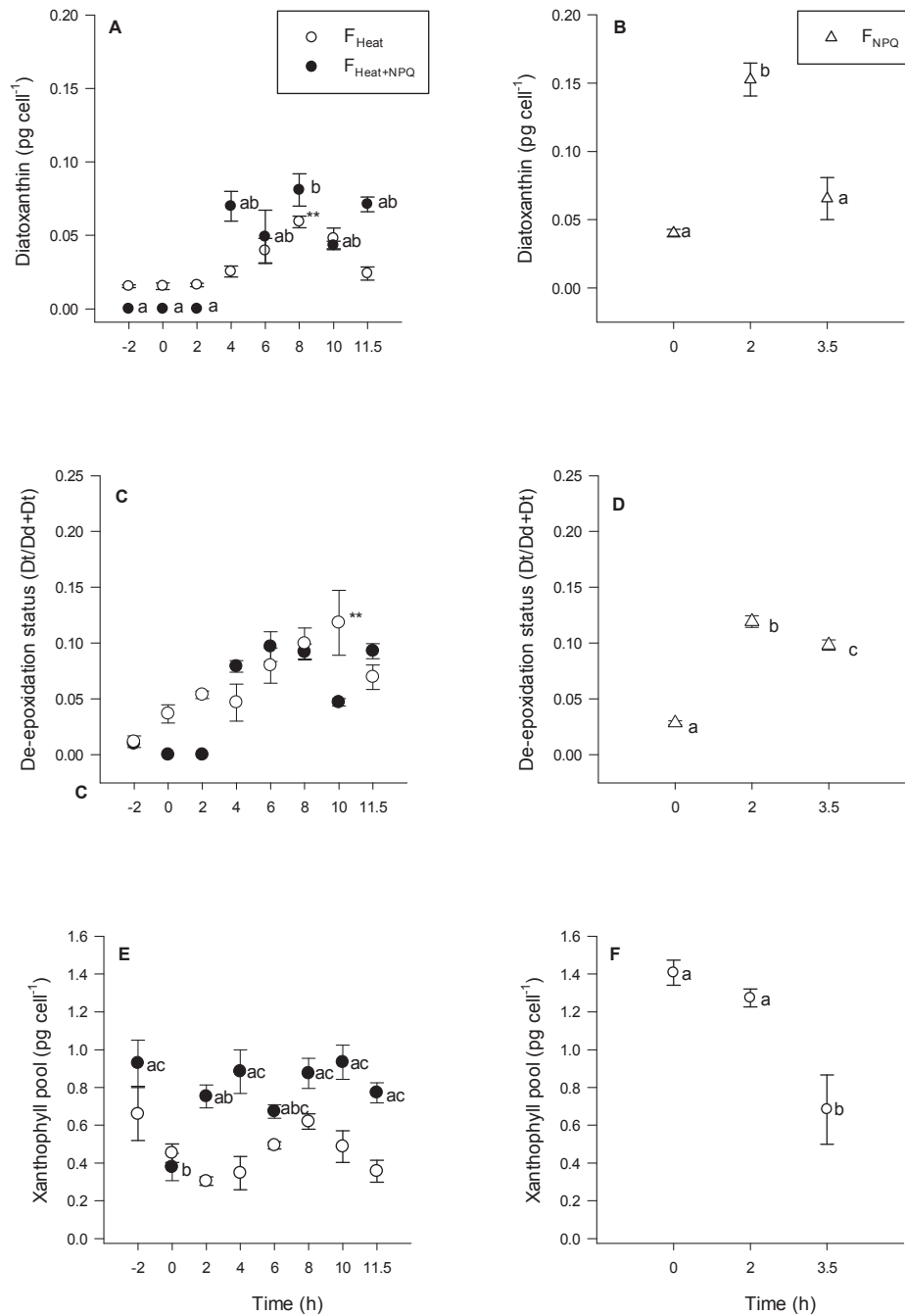


**Figure 2.2.4:** Xanthophyll pigment concentrations as a function of sampling time (h). Diatoxanthin (pg cell<sup>-1</sup>) for F<sub>Heat</sub> and F<sub>Heat+NPQ</sub> (A), and F<sub>NPQ</sub> (B), De-epoxidation status for F<sub>Heat</sub> and F<sub>Heat+NPQ</sub> (C), and F<sub>NPQ</sub> (D), xanthophyll pool concentration for F<sub>Heat</sub> and F<sub>Heat+NPQ</sub> (E), and F<sub>NPQ</sub> (F); ramping time for thermal stress treatments is indicated between T<sub>-2h</sub> and T<sub>0h</sub> on the x-axis, where F<sub>NPQ</sub> sampling is displayed from T<sub>0h</sub>; Tukey HSD results are indicated in lower case letters; mean ± SEM, n = 4 are displayed.



### 2.2.3.4 Cell counts

The density of *Symbiodinium* cells (cells x 10<sup>5</sup> cells mL<sup>-1</sup>) remained unchanged over the length of the experiment in all treatments in all treatments (Table 2.2.4).

**Table 2.2.4:** Density of *Symbiodinium* cells per mL (x 10<sup>5</sup>) at the start and end of each of the three treatments.

Treatment	Cell density (x 10 <sup>5</sup> cells mL <sup>-1</sup> )		<i>p</i> - value
	Start	End	
F <sub>Heat</sub>	4.67 ± 0.22	4.38 ± 0.99	0.226
F <sub>Heat + NPQ</sub>	2.19 ± 0.06	1.57 ± 0.46	0.781
F <sub>NPQ</sub>	4.29 ± 0.55	2.99 ± 0.48	0.125

### 2.2.4 Discussion

During light reactions of photosynthesis, light energy is converted into organic compounds, but this process can only function efficiently if no limitation in electron turnover occurs at PSI (Bailey et al. 2008). Structural changes of pigment-protein complexes (antenna system) associated with the thylakoid membrane can balance the quantity of incoming light between the photosystems and therefore enhance photosynthetic efficiency (Wollman 2001). These structural changes to the antenna system have been described in great detail for higher plants (Tikkanen et al. 2011), but also for macro- (Satoh and Fork 1983a) and micro-algae (Satoh and Fork 1983b), as well as cyanobacteria (Campbell et al. 1998; Lemeille and Rochaix 2010). Recent studies have proposed, that besides the xanthophyll cycle (Ambarsari et al. 1997), structural changes of the antenna system could indeed be another important photoprotective mechanism acting in *Symbiodinium*'s photosynthetic apparatus either through shifts of LHCs (Hill et al. 2012; Reynolds et al. 2008) or reaction center adjustments of PSII and/or PSI (Hennige et al. 2009; Hoogenboom et al. 2012). Photoprotective mechanisms are primarily in place to prevent photoinhibition and are most efficiently operating when they dissipate excess light energy away from PSII (Takahashi and Badger 2011). By shunting excess energy away from PSII, over-excitation and photoinactivation can be prevented, as well as the formation of reactive oxygen species (ROS) (Alexandre et al. 2007). What influence thermal stress can have upon dynamics of photoprotective mechanisms in *Symbiodinium* (strain CS156, clade C) commonly associated with corals, was focus of this study.

#### **2.2.4.1 Stressor triggered LHC movement**

Here it could be demonstrated that thermal stress alone can affect the organisation of thylakoid membrane associated LHCs of *Symbiodinium* (see also Chapter 2.1). The results therefore indicate that thermal stress could be a precursor initiating LHC movement as a means of photoprotection. Re-distribution of membrane intrinsic and peripheral LHCs could be observed through differences in fluorescence emissions of 77 K derived fluorescence emission spectra at different sampling time points (Fig 2.2.3). Shifts in spectra maxima can be used to identify characteristic locations within the photosynthetic apparatus (Iglesias-Prieto and Trench 1996). Algae pre-incubated in the dark and exposed to thermal stress for 8 h ( $F_{\text{Heat}}$ ) displayed enhanced emission at 701 and 721 nm wavelength bands indicating PSI associated energy distribution, and this was further increased upon high light exposure during the last 3.5 h of the treatment (Table 2.2.1; Fig 2.2.3 a). Further, algae from the  $F_{\text{Heat}}$  treatment displayed increasing detachment of the water-soluble peripheral antenna complexes, PCP, as shown by an increase of the 672 nm band as well as at 675 nm fluorescence emission (Carbonera et al. 1996; Iglesias-Prieto and Trench 1996) (Table 2.2.1 and 2.2.3) after being exposed to 3.5 h of high light. At the conclusion of the experiment, algae from the  $F_{\text{Heat}}$  treatment displayed the greatest emission peak area increase at the 721 nm component band compared to the other two treatments (Table 2.2.1). Results of picosecond resolved fluorescence spectra were comparable (Chapter 2.1). This suggests that once thermal and/or high light stress conditions becomes excessive, a transformation of the PSII associated LHCs results in an increase of the absorption cross section of PSI to shunt energy away from PSII (Chapter 2.1). Also, peripheral as well as intrinsic thylakoid associated LHCs in *Symbiodinium* are fully connected to PSII during dark incubation under culturing temperatures (Hill et al. 2012; Reynolds et al. 2008). In concert with the

findings presented here, LHC movement as a photoprotective mechanism is operating in *Symbiodinium* under combined high light and thermal stress conditions, where thermal stress seems to be the precursor.

Results of  $F_{\text{Heat}}$  treatment suggest that a greater absorption cross section of PSI resulted from the treatment along with increased PCP detachment. Algae in both thermal stress treatments increased the peak area associated with PSI (701 and 721 nm), which was found to be accompanied by a decrease in PSII associated 688 nm peak area (Table 2.2.1). These findings clearly indicate that structural changes in thylakoid organisation occurred and resulted in differing absorption cross sections of PSII and PSI. In contrast, algae of the  $F_{\text{NPQ}}$  treatment, displaying quenched RCs, showed increased detachment of PCP, although only a fraction of the enhancement compared to algae of the  $F_{\text{Heat}}$  treatment. No structural changes in thylakoid membrane organisation was found in previous investigations of algae exposed only to high light, although increased spillover was suggested to occur under these conditions (Chapter 2.1).

The results presented here are different to findings reported by Reynolds et al. (2008), who found that *Symbiodinium* of clade C did not show any re-distribution of LHCs within the thylakoid membrane. However, the light conditions applied in Reynolds et al. (2008) ( $250 \mu\text{mol photons m}^{-2} \text{s}^{-1}$ ) were 2.4 times lower compared to the high light conditions applied in our study ( $600 \mu\text{mol photons m}^{-2} \text{s}^{-1}$ ), which might explain this discrepancy in the results. Also, the changes observed here are highlighting the precursory role of thermal stress for LHC dissociation/movement.

#### 2.2.4.2 Regulation and mechanisms of LHC movement

The regulatory mechanisms of LHC movement is so far unknown for *Symbiodinium*, where in higher plants, a regulatory kinase is in place to initiate re-distribution of LHCs by activating the synthesis of phosphorylated LHCs upon reduction of the plastoquinone pool under saturating light intensities (Allen 1992; Larkum 2003). Some evidence has been presented that similar mechanisms exist in dinoflagellates with reported light regulated gene expression of distinct LHCs (Ten Lohuis and Miller 1998). Yet the reduction of the plastoquinone pool in *Symbiodinium* is known to be not exclusively light driven, as chlororespiration has been suggested to reduce the plastoquinone pool in the dark (Hill and Ralph 2008a). According to this one could speculate that the activity of chlororespiration acting in *Symbiodinium* can initiate LHC movement in the dark. However, the mechanisms behind LHC movement in *Symbiodinium* require further investigation.

Changes in fatty acid composition have been described for *Symbiodinium* as a result of thermal stress exposure (for 7 days at 31° C) and were interpreted to be in place to counteract increasing thylakoid membrane fluidity with increasing incubation temperature (Díaz-Almeyda et al. 2011). Therefore, thermal stress exposure could support structural re-organisation as a result of increased thylakoid membrane fluidity, of LHCs to re-distribute energy away from PSII and/or towards PSI. Algae of both thermally exposed treatments  $F_{\text{Heat}}$  and  $F_{\text{Heat+NPQ}}$  treatment displayed increasing detachment of PCP and/or acpPC (77K emission amplitude at 675 nm), which was further enhanced by high light incubation when algae were pre-incubated under thermal stress only ( $F_{\text{Heat}}$  treatment). As algae of the  $F_{\text{Heat}}$  treatment were exposed to 3.5 h of high light, LHCs re-distributed increasingly away from PSII to alleviate

disproportionate excitation pressure (Table 2.2.1). Changes in thylakoid membrane organisation due to thermal stress exposure have previously been discussed to be a precursor for loss in photosynthetic capacity (Díaz-Almeyda et al. 2011; Iglesias-Prieto et al. 1992; Tchernov et al. 2004a).

#### **2.2.4.3 Chl *a* fluorescence and absorption cross section**

$F_V/F_M$  decreased throughout treatment incubation in algae of all applied experimental conditions. Thermal stress-induced decreases of  $F_V/F_M$  have been described previously (Hill et al. 2005; Hill et al. 2004a; Iglesias-Prieto et al. 1992; Jones and Hoegh-Guldberg 2001; Middlebrook et al. 2010; Takahashi et al. 2009; Warner et al. 1996) and have been explained as downregulated PSII and/or photodamage being a result of exposure to thermal stress. A new super-quenching mechanism was described in Chapter 2.1 and hypothesises that light energy shifts away from PSII through structural thylakoid adjustments and would influence the Chl *a* fluorescence induction results. Therefore, the decreased  $F_V/F_M$  found for algae of the  $F_{Heat}$  and  $F_{Heat+NPQ}$  treatments could possibly be a result of LHC dissociating from PSII and thereby decreasing PSII absorption cross-section which leads to a lowered Chl *a* fluorescence signal as reported previously (Campbell and Öquist 1996; Ochoa De Alda et al. 1996; Silva et al. 2001). Algae in the  $F_{Heat+NPQ}$  treatment displayed a significant loss in rETR, which supports the suggestion that light energy has been re-distributed to PSI possibly through structural adjustments of the thylakoid membrane. In contrast, algae in the  $F_{NPQ}$  and  $F_{Heat}$  treatment displayed a loss in  $F_V/F_M$  of PSII, but no loss of rETR capacity was detected in algae of either of the two treatments. Hence the increased detachment of PCPs and/or acpPCs found in algae of  $F_{NPQ}$  and  $F_{Heat}$  treatment could be a result of dissipative photoprotection acting in *Symbiodinium* to primarily shunt excess energy away from

PSII. This could be accomplished through detachment of LHCs rather than redistribution of LHCs towards PSI. Here, decreases of  $F_V/F_M$  found in algae from the  $F_{NPQ}$  treatment could possibly be a result of increasing photodamage as  $D_d$  was also found to decrease, indicating that the capacity of the xanthophyll cycle was exhausted. All other treatments displayed light triggered xanthophyll activity as previously reported (Krämer et al. 2012; Warner and Berry-Lowe 2006).

#### **2.2.4.5 Conclusion**

The presence of state transition-like processes as a photoprotective pathway acting in *Symbiodinium* has far reaching implications for coral photobiology. Our results suggest that the characteristic of the stressor is the regulator of initiating the appropriate photoprotective mechanisms in *Symbiodinium*, which raises the question if this is the same when living *in hospite* associated with a coral host. The findings presented here resemble the stressor impact of a coral symbioses under bleaching conditions in the coral reef environment (bleaching scenarios as defined in Hoegh-Guldberg (1999)). If *Symbiodinium* is able to actively 'balance' the two photosystems, it would mean that *Symbiodinium* has indeed the capacity for a sustained photosynthetic efficiency even under bleaching conditions. State transition-like processes have been reported as a possible strategy to sustain ATP production under sub-optimal abiotic conditions, as these processes can activate cyclic electron transport (CET) around PSI (Finazzi et al. 2002). This would be particularly relevant to *Symbiodinium* under bleaching conditions where sustained ATP production is crucial for activating antioxidant pathways (Weis 2008).

Overall, the results imply that NPQ pathways in *Symbiodinium* are indeed flexible depending on the acting stressor (thermal and/or high light stress). Thermal stress was identified to be the precursor to allow for LHC re-distribution between PSII and PSI or away from PSII. Although thermal stress is a mediator for initiating LHC movement, high light stress seems to initiate the dissipation of excess light energy *via* xanthophyll cycle activity. The combined stressor impact initiates the two photoprotective mechanisms of xanthophyll cycling and LHC movement to complement each other. These findings introduce a new concept about photoprotective strategies acting in *Symbiodinium* (here clade C; strain CS-156), which opens a new understanding about stress susceptibility and coral resilience to bleaching.



### 2.2.5 References

- Alexandre, M. T. A., D. C. Lührs, I. H. M. Van Stokkum, R. G. Hiller, M.-L. Groot, J. T. M. Kennis, and R. Van Grondelle. 2007. Triplet state dynamics in peridinin-chlorophyll-*a*-protein: a new pathway of photoprotection in LHCs? *Biophysical Journal* **93**: 2118-2128.
- Allen, J. F. 1992. Chloroplast protein phosphorylation couples plastoquinone redox state to distribution of excitation energy between photosystems. *Nature* **291**: 25-29.
- Ambarsari, I., B. E. Brown, R. G. Barlow, G. Britton, and D. Cummings. 1997. Fluctuations in algal chlorophyll and carotenoid pigments during solar bleaching in the coral *Goniastrea aspera* at Phuket, Thailand. *Marine Ecology Progress Series* **159**: 303-307.
- Bailey, S., A. Melis, K. R. M. Mackey, P. Cardol, G. Finazzi, G. Van Dijken, G. M. Berg, K. Arrigo, J. Shrager, and A. Grossman. 2008. Alternative photosynthetic electron flow to oxygen in marine *Synechococcus*. *Biochimica et Biophysica Acta* **1777**: 269-276.
- Brown, B. E., I. Ambarsari, M. Warner, W. Fitt, R. P. Dunne, S. W. Gibb, and D. G. Cummings. 1999a. Diurnal changes in photochemical efficiency and xanthophyll concentrations in shallow water reef corals: evidence for photoinhibition and photoprotection. *Coral Reefs* **18**: 99-105.
- Campbell, D. A., V. Hurry, A. K. Clarke, P. Gustafsson, and G. Öquist. 1998. Chlorophyll fluorescence analysis of cyanobacterial photosynthesis and acclimation. *Microbiology and Molecular Biology Reviews* **6**: 667-683.
- Campbell, D. A., and G. Öquist. 1996. Predicting light acclimation in cyanobacteria from non-photochemical quenching of photosystem II fluorescence, which reflects state transitions in these organisms. *Plant Physiology* **111**: 1293-1298.
- Carbonera, D., G. Giacometti, and U. Segre. 1996. Carotenoid interactions in peridinin chlorophyll *a* proteins from dinoflagellates. *Journal of Chemistry Society, Faraday Transactions* **92**: 989-993.
- Cunning, R., and A. C. Baker. 2013. Excess algal symbionts increase the susceptibility of reef corals to bleaching. *Nature Climate Change* **3**: 259-262.

- Díaz-Almeyda, E., P. E. Thomé, M. E. Hafidi, and R. Iglesias-Prieto. 2011. Differential stability of photosynthetic membranes and fatty acid composition at elevated temperature in *Symbiodinium*. *Coral Reefs* **30**: 217-225.
- Dove, S. G., C. Lovell, M. Fine, J. Deckenback, O. Hoegh-Guldberg, R. Iglesias-Prieto, and K. R. N. Anthony. 2008. Host pigments: potential facilitators of photosynthesis in coral symbioses. *Plant, Cell & Environment* **31**: 1532-1533.
- Falkowski, P. G., and J. A. Raven. 2007. *Aquatic Photosynthesis*, 2nd ed. Princeton University Press.
- Finazzi, G., F. Rappaport, A. Furia, M. Fleischmann, J.-D. Rochaix, F. Zito, and G. Forti. 2002. Involvement of state transitions in the switch between linear and cyclic electron flow in *Chlamydomonas reinhardtii*. *EMBO reports* **3**: 280-285.
- Flores-Ramírez, L. A., and M. A. Liñán-Cabello. 2007. Relationships among thermal stress, bleaching and oxidative damage in the hermatypic coral, *Pocillopora capitata*. *Comparative Biochemistry and Physiology - Part C: Toxicology and Endocrinology* **146**: 194-202.
- Garcia-Mendoza, E., H. C. P. Matthijs, H. Schubert, and L. R. Mur. 2002. Non-photochemical quenching of chlorophyll fluorescence in *Chlorella fusca* acclimated to constant and dynamic light conditions. *Photosynthesis Research* **74**: 303-315.
- Genty, B., J.-M. Briantais, and N. R. Baker. 1989. The relationship between the quantum yield of photosynthetic electron transport and quenching of chlorophyll fluorescence. *Biochimica et Biophysica Acta* **990**: 87-92.
- Green, E. P., and D. G. Durnford. 1996. The chlorophyll-carotenoid proteins of oxygenic photosynthesis. *Annual Review in Plant Physiology and Plant Molecular Biology* **47**: 685-714.
- Guillard, R. R. L., and J. H. Ryther. 1962. Studies of marine planktonic diatoms. I. *Cyclotella nana* Hustedt, and *Detonula confervacea* (Cleve) Gran. *Canadian Journal for Microbiology* **8**: 229-239.
- Hennige, S. J., D. J. Suggett, M. E. Warner, K. E. McDougall, and D. J. Smith. 2009. Photobiology of *Symbiodinium* revisited: bio-physical and bio-optical signatures. *Coral Reefs* **28**: 179-195.
- Hill, R., C. M. Brown, K. Dezeew, D. A. Campbell, and P. J. Ralph. 2011. Increased rate of D1 repair in coral symbionts during bleaching is insufficient to counter accelerated photoinactivation. *Limnology and Oceanography* **56**: 139-146.

- Hill, R., C. Frankart, and P. J. Ralph. 2005. Impact of bleaching conditions on the components of non-photochemical quenching in the zooxanthellae of a coral. *Journal of Experimental Marine Biology and Ecology* **322**: 83-92.
- Hill, R., A. W. D. Larkum, C. Frankart, M. Kühl, and P. J. Ralph. 2004. Loss of functional photosystem II reaction centers in zooxanthellae of corals exposed to bleaching conditions: using fluorescence rise kinetics. *Photosynthesis Research* **82**: 59-72.
- Hill, R., A. W. D. Larkum, O. Prášil, D. M. Kramer, V. Kumar, and P. J. Ralph. 2012. Light-induced redistribution of antenna complexes in the symbionts of scleractinian corals correlates with sensitivity to coral bleaching. *Coral Reefs* **31**: 963-975.
- Hill, R., and P. J. Ralph. 2006. Photosystem II heterogeneity of *in hospite* zooxanthellae in scleractinian corals exposed to bleaching conditions. *Photochemistry and Photobiology* **82**: 1577-1585.
- Hill, R., and P. J. Ralph. 2008. Dark-induced reduction of the plastoquinone pool in zooxanthellae of scleractinian corals and implications for measurements of chlorophyll a fluorescence. *Symbiosis* **46**: 45-56.
- Hill, R., K. E. Ulstrup, and P. J. Ralph. 2009. Temperature induced changes in thylakoid membrane thermostability of cultured, freshly isolated, and expelled zooxanthellae from scleractinian corals. *Bulletin of Marine Science* **85**: 223-244.
- Hiller, R. G., P. M. Wrench, A. P. Gooley, G. Shoebridge, and J. Breton. 1993. The major intrinsic light-harvesting protein of *Amphidinium*: characterization and relation to other light-harvesting proteins. *Photochemistry and Photobiology* **57**: 125-131.
- Hiller, R. G., P. M. Wrench, and F. P. Sharples. 1995. The light-harvesting chlorophyll *a-c* binding protein of dinoflagellates: a putative polyprotein. *FEBS Letters* **363**: 175-178.
- Hoegh-Guldberg, O. 1999. Climate change, coral bleaching and the future of the world's coral reefs. *Marine & Freshwater Research* **50**: 839-866.
- Hoegh-Guldberg, O. 2010. The impact of climate change on the world's marine ecosystems. *Science* **328**: 1523-1528.
- Hoogenboom, M. O., D. A. Campbell, E. Beraud, K. Dezeew, and C. Ferrier-Pagès. 2012. Effects of light, food availability and temperature stress on the function of photosystem II and photosystem I of coral symbionts. *Plos One* **7**: e30167.

- Iglesias-Prieto, R., N. S. Govind, and R. K. Trench. 1993. Isolation and characterization of three membrane-bound chlorophyll-protein complexes from four dinoflagellate species. *Philosophical Transactions of the Royal Society B* **340**: 381-392.
- Iglesias-Prieto, R., J. L. Matta, W. A. Robins, and R. K. Trench. 1992. Photosynthetic response to elevated temperature in the symbiotic dinoflagellate *Symbiodinium microadriaticum* in culture. *Proceedings of the National Academy of Sciences U.S.A.* **89**: 10302-10305.
- Iglesias-Prieto, R., and R. K. Trench. 1996. Spectroscopic properties of chlorophyll *a* in the water-soluble peridinin-chlorophyll *a*-protein complexes (PCP) from the symbiotic dinoflagellate *Symbiodinium microadriaticum*. *Journal of Plant Physiology* **149**: 510-516.
- Iglesias-Prieto, R., and R. K. Trench. 1997. Acclimation and adaptation to irradiance in symbiotic dinoflagellates. II. Response of chlorophyll-protein complexes to different photon flux densities. *Marine Biology* **130**: 23-30.
- Jiang, J., H. Zhang, Y. Kang, D. Bina, C. S. Lo, and R. E. Blankenship. 2012. Characterization of the peridinin-chlorophyll *a*-protein complex in the dinoflagellate *Symbiodinium*. *Biochimica et Biophysica Acta (BBA)* **1817**: 983-989.
- Jones, R. J., and O. Hoegh-Guldberg. 2001. Diurnal changes in the photochemical efficiency of the symbiotic dinoflagellates (Dinophyceae) of corals: photoprotection, photoinactivation and the relationship to coral bleaching. *Plant Cell & Environment* **24**: 89-99.
- Jones, R. J., O. Hoegh-Guldberg, A. W. D. Larkum, and U. Schreiber. 1998. Temperature-induced bleaching of corals begins with impairment of the CO<sub>2</sub> fixation mechanism in zooxanthellae. *Plant, Cell & Environment* **21**: 1219-1230.
- Krämer, W., I. Caamaño-Ricken, C. Richter, and K. Bischof. 2012. Dynamic regulation of photoprotection determines thermal tolerance of two phylotypes of *Symbiodinium* clade A at two photon fluence rates. *Photochemistry and Photobiology* **88**: 398-413.
- Larkum, A. W. D. 2003. Light-harvesting systems in algae, p. 277-304. *In* A. W. D. Larkum, Douglas, S.E., Raven, J.A. [ed.], *Photosynthesis in Algae*. Kluwer Academic Publishers.

- Lemeille, S., and J.-D. Rochaix. 2010. State transitions at the crossroad of thylakoid signalling pathways. *Photosynthesis Research* **106**: 33-46.
- Lilley, R. M., P. J. Ralph, and A. W. D. Larkum. 2010. The determination of activity of the enzyme Rubisco in cell extracts of the dinoflagellate alga *Symbiodinium* sp. by manganese chemiluminescence and its response to short-term stress of the alga. *Plant, Cell & Environment* **33**: 995-1004.
- Lunde, C., P. E. Jensen, A. Haldrup, J. Knoetzel, and H. V. Scheller. 2000. The PSI-H subunit of photosystem I is essential for state transitions in plant photosynthesis. *Nature* **408**: 613-615.
- Matsubara, S., and W. S. Chow. 2004. Populations of photoinactivated photosystem II reaction centers characterized by chlorophyll *a* fluorescence lifetime *in vivo*. *PNAS* **101**: 18234-18239.
- Middlebrook, R., K. R. N. Anthony, O. Hoegh-Guldberg, and S. Dove. 2010. Heating rate and symbiont productivity are key factors determining thermal stress in the reef-building coral *Acropora formosa*. *The Journal of Experimental Biology* **213**: 1026-1034.
- Munge, B., S. K. Das, R. Ilagan, Z. Pendon, J. Yang, H. A. Frank, and J. F. Rusling. 2003. Electron transfer reactions of redox cofactors in spinach photosystem I reaction center protein in lipid films on electrodes. *Journal of the American Chemical Society* **125**: 12457-12463.
- Muscattine, L., and J. W. Porter. 1977. Reef Corals: mutualistic symbioses adapted to nutrient-poor environments. *Bioscience* **27**: 454-460.
- Ochoa De Alda, J. a. G., M. I. Tapia, F. Franck, M. J. Llama, and J. L. Serra. 1996. Changes in nitrogen source modify distribution of excitation energy in the cyanobacterium *Phormidium laminosum*. *Physiologia plantarum* **97**: 69-78.
- Rappaport, F., M. Guergova-Kuras, P. J. Nixon, B. A. Diner, and J. Lavergne. 2002. Kinetics and pathways of charge recombination in Photosystem II. *Biochemistry* **41**: 8518-8527.
- Reynolds, M. J., B. U. Bruns, W. K. Fitt, and G. W. Schmidt. 2008. Enhanced photoprotection pathways in symbiotic dinoflagellates of shallow-water corals and other cnidarians. *Proceedings of the National Academy of Sciences U.S.A.* **105**: 13674-13678.
- Satoh, K., and D. C. Fork. 1983a. A new mechanism for adaptation to changes in light intensity and quality in the red alga, *Porphyra perforata*. I. relation to state 1 -

- state 2 transitions. *Biochimica et Biophysica Acta (BBA) - Bioenergetics* **722**: 190-196.
- Satoh, K., and D. C. Fork. 1983b. State I - state II transitions in the green alga *Scenedesmus obliquus* *Photochemistry and Photobiology* **37**: 429-434.
- Schreiber, U. 2004. Pulse-amplitude-modulation (PAM) fluorometry and saturation pulse method: an overview, p. 279-319. *In* G. C. Papageorgiou and Govindjee [eds.], *Chlorophyll a fluorescence: a signature of photosynthesis*. *Advances in Photosynthesis and Respiration*. Springer.
- Silva, L. M. T., C. P. Dos Santos, and R. M. Chaloub. 2001. Effect of the respiratory activity on photoinhibition of the cyanobacterium *Synechocystis* sp. *Photosynthesis Research* **68**: 61-69.
- Takahashi, S., and M. R. Badger. 2011. Photoprotection in plants: a new light on photosystem II damage. *Trends in Plant Science* **16**: 53-60.
- Takahashi, S., T. Nakamura, M. Sakamizu, R. Van Woesik, and H. Yamasaki. 2004. Repair machinery of symbiotic photosynthesis as the primary target of heat stress for reef-building corals. *Plant Cell Physiology* **45**: 231-235.
- Takahashi, S., S. M. Whitney, and M. R. Badger. 2009. Different thermal sensitivity of the repair of photodamaged photosynthetic machinery in cultured *Symbiodinium* species. *Proceedings of the National Academy of Sciences U.S.A.* **106**: 3237-3242.
- Tchernov, D., M. Y. Gorbunov, C. De Vargas, S. N. Yadav, A. J. Milligan, M. Haeggbloom, and P. G. Falkowski. 2004a. Membrane lipids of symbiotic algae are diagnostic of sensitivity to thermal bleaching in corals. *Proceedings of the National Academy of Sciences U.S.A.* **101**: 13531-13535.
- Ten Lohuis, M. R., and D. J. Miller. 1998. Light-regulated transcription of genes encoding peridinin chlorophyll a proteins and the major intrinsic light-harvesting complex proteins in the dinoflagellate *Amphidinium carterae* Hulbert (Dinophyceae) - changes in cytosine methylation accompany photoadaptation. *Plant Physiology* **117**: 189-196.
- Tikkanen, M., M. Grieco, and E.-M. Aro. 2011. Novel insights into plant light-harvesting complex II phosphorylation and 'state transitions'. *Trends in Plant Science* **16**: 126-131.

- Van Heukelem, L., and C. Thomas. 2001. Computer-assisted high-performance liquid chromatography method development with applications to the isolation and analysis of phytoplankton pigments. *Journal of Chromatography A* **910**: 31-49.
- Veal, C., M. Carmi, G. Dishon, Y. Sharon, K. Michael, D. Tchernov, O. Hoegh-Guldberg, and M. Fine. 2010. Shallow-water wave lensing in coral reefs: a physical and biological case study. *The Journal of Experimental Biology* **213**: 4303-4312.
- Venn, A. A., M. A. Wilson, H. G. Trapido-Rosenthal, B. J. Keely, and A. E. Douglas. 2006. The impact of coral bleaching on the pigment profile of the symbiotic alga, *Symbiodinium*. *Plant, Cell & Environment* **29**: 2133-2142.
- Wangpraseurt, D., A. W. D. Larkum, P. J. Ralph, and M. Kühl. 2012. Light gradients and optical microniches in coral tissues. *Frontiers in Microbiology* **3**: 316.
- Warner, M. E., and S. Berry-Lowe. 2006. Differential xanthophyll cycling and photochemical activity in symbiotic dinoflagellates in multiple locations of three species of caribbean coral. *Journal of Experimental Marine Biology and Ecology* **339**: 86-95.
- Warner, M. E., W. K. Fitt, and G. W. Schmidt. 1996. The effects of elevated temperature on the photosynthetic efficiency of zooxanthellae *in hospite* from four different species of reef coral: a novel approach. *Plant, Cell & Environment* **19**: 291-299.
- Warner, M. E., W. K. Fitt, and G. W. Schmidt. 1999. Damage to photosystem II in symbiotic dinoflagellates: a determinant of coral bleaching. *Proceedings of the National Academy of Sciences U.S.A.* **96**: 8007-8012.
- Weis, V. M. 2008. Cellular mechanisms of cnidarian bleaching: stress causes the collapse of symbiosis. *The Journal of Experimental Biology* **211**: 3059-3066.
- Wollman, F.-A. 2001. State transitions reveal the dynamics and flexibility of the photosynthetic apparatus. *The EMBO Journal* **20**: 3623-3630.

Page intentionally left blank



## Chapter 3

# *Symbiodinium* in morphologically distinct corals show differences in photodamage and -repair under high light exposure

Verena Schrammeyer<sup>a</sup>, Wiebke Krämer<sup>b#</sup>, Ross Hill<sup>ac</sup> Jennifer Jeans<sup>d</sup>, Douglas A. Campbell<sup>d</sup>, Anthony W.D. Larkum<sup>a</sup>, Kai Bischof<sup>b</sup>, Peter J. Ralph<sup>a\*</sup>

<sup>a</sup> Plant Functional Biology and Climate Change Cluster (C3), University of Technology, Broadway, NSW, Australia

<sup>b</sup> Department of Marine Botany, University of Bremen, Bremen, Germany

<sup>c</sup> Centre for Marine Bio-Innovation, School of Biological, Earth and Environmental Sciences, The University of New South Wales, Sydney 2052 NSW, Australia

<sup>d</sup> Biology Department, Mount Allison University, Sackville, New Brunswick, Canada

# Current address: Laboratorio de Fotobiología, Unidad Académica de Sistemas Arrecifales (Puerto Morelos), Instituto de Ciencias del Mar y Limnología, Universidad Nacional Autónoma de México, Cancún, Quintana Roo, México

**Keywords:** Coral symbioses, high light stress, non-photochemical quenching, photo-protection, photorepair

### 3.1 Introduction

Hermatypic corals form a symbiotic relationship between a cnidarian host and a dinoflagellate symbiont (genus: *Symbiodinium* Freudenthal). Light is the obligatory driving force of a functional relationship between the host cnidarian and their algal symbionts, commonly called ‘zooxanthellae’. Algal symbiont photosynthesis produces organic compounds through carbon fixation, such as glycerol, glucose, amino acids and lipids (Wang and Douglas 1997; Whitehead and Douglas 2003), although a recent study demonstrated that glucose seems to be the main compound being transferred to the coral host (Burriesci et al. 2012). It is assumed that up to 95% of the photosynthate is translocated from the algal-harboursing host cells into the host tissue and serves as an autotrophic food source to the host (Muscatine 1990). The algal symbiont receives host metabolic waste-products, inorganic nutrients, and dissolved inorganic carbon to sustain photosynthetic processes (Wang and Douglas 1999; Yellowlees et al. 2008).

Coral reef ecosystems can be found in most of the world’s oceans, residing from shallow tropical waters (<30 m) to deep reefs (> 30 m) (Bongaerts et al. 2010), in the latitude belt of 30° north and 30° south (Wilkinson et al. 1999). Tropical and subtropical waters are characterised by near particle-free seawater. The full spectra of photosynthetic active radiation (PAR: 400-700 nm) can almost penetrate down to 2 m in these ocean regions due to the minimal attenuation of light from scattering and absorption by particulate matter (Richardson et al. 1993). The photosynthate input to the host is dependent on the light reaching the algal symbiont. Light quantity, as well as quality, in combination with elevated temperatures, has an impact on the coral symbioses, where oversaturating light intensities can harm the photosynthetic apparatus of the algal symbionts and combined with high seawater temperatures can ultimately

disrupt the symbiotic relationship, a phenomenon commonly referred to as coral bleaching (Hoegh-Guldberg 1999). Coral bleaching is characterised by a dysfunction of the symbiosis, formed between the cnidarian host and the dinoflagellate, which leads to loss of photosynthetic pigmentation and/or a loss of algal symbionts (Baird et al. 2009a; Takahashi et al. 2004).

The absorption of excessive (i.e. above saturation) irradiance by photosynthetic organisms can result in excessive formation of reactive oxygen species (ROS), either caused by the formation of triplet chlorophyll reacting with triplet oxygen originating through the oxidation of water at the oxygen evolving complex (OEC) and resulting in the production of singlet oxygen ( $^1\text{O}_2$ ) (Vass 2011); or other ROS formed as intermediate products of the Mehler-ascorbate peroxidase (MAP) cycle following the Mehler reaction (Nishiyama et al. 2004; Schreiber et al. 1995a). ROS can also cause oxidative stress in the coral host tissue, as ROS leak through cell membranes from their algal symbionts (Lesser 1997; Weis 2008). ROS are harmful for the coral symbiosis as they can oxidise lipids, proteins and DNA, resulting e.g. in lipid peroxidation in the mitochondria, site-specific amino acid modifications and mutations respectively (Lesser 2006). Hence, the formation of ROS can impact on the overall functionality of the photosynthetic apparatus.

The photosystem (PS) II core protein, D1, is encoded by the *psbA* gene, located within the chloroplast genome and the *de novo* synthesis is described as being light induced (Mattoo et al. 1984). Photoprotective pathways which dissipate excess excitation energy are important in preventing photodamage exceeding the photorepair rate, can lead to photoinhibition (Hill et al. 2011; Takahashi et al. 2004; Warner et al. 1999). Photorepair processes are in place to *de novo* synthesise D1, but also for proteolysis and deletion of

damaged PSII core protein (Six et al. 2007). Photorepair reported for *Symbiodinium* has been estimated through chlorophyll (Chl) *a* fluorometry parameters, where changes in maximum quantum yield were used to infer the rate of D1 photorepair (Hennige et al. 2011; Hill et al. 2011; Krämer et al. 2013; Ragni et al. 2010). Once PSII degrades, the linear electron transport between PSII and PSI becomes less efficient, which has consequences for several processes e.g. the rate efficiency of carbon fixation. As a result, photosynthetic output such as production of carbon products for the coral host is diminished, which could trigger a dysfunction of the coral symbiosis (Lesser and Farrell 2004).

Photodamage of D1 occurs even under low light intensities (Edelman and Mattoo 2008) and *de novo* synthesis and turnover of D1 occurs as a regular process within the photosynthetic apparatus, where the magnitude of photorepair is dependent on incident irradiance (Aro et al. 1993). Once high light causes photodamage which exceeds the photorepair rate through *de novo* synthesis of D1, PSII efficiency progressively deteriorates (Takahashi et al. 2009). Indeed, the impact of excessive solar irradiance on the *de novo* synthesis of the D1 protein has been suggested to be a critical link in coral bleaching (Brown et al. 1999a; Hill et al. 2011; Takahashi et al. 2004), where the production of  $^1\text{O}_2$  can cause D1 proteolysis (Vass et al. 1992).

*Symbiodinium's* PSII efficiency is therefore a result of the interplay between photodamage, photorepair and photo-protection, where high irradiance levels can easily imbalance these processes (Hill et al. 2011; Levy et al. 2004; Ragni et al. 2010; Takahashi et al. 2004). The over-reduction of intersystem linear electron transport between PSII and PSI can ultimately impact upon carbon fixation rates, as these are dependent on reducing agents synthesised as a product of linear electron transport

(Jones 2004; Suggett et al. 2010a). In order to prevent photodamage, *Symbiodinium*, like other phototrophic organisms (Demmig-Adams et al. 2012), utilises non-photochemical quenching (NPQ) to dissipate excess excitation energy (Demmig-Adams and Adams 2006; Hill et al. 2005; Warner and Berry-Lowe 2006). An efficient photosynthetic apparatus utilises NPQ pathways to ensure the highest quantum efficiency of PSII for carbon fixation (Hoogenboom et al. 2012).

Carotenoids such as xanthophylls (Demmig-Adams and Adams 1996) and betaines (Hill et al. 2010) can dissipate excess light energy as heat, but carotenoids can also directly quench  $^1\text{O}_2$  or triplet chlorophyll (Burton 1990; Edge and Truscott 1999). Dinoflagellates such as *Symbiodinium* utilise the de-epoxidation of diadinoxanthin (Dd) to diatoxanthin (Dt) during the xanthophyll cycle to thermally dissipate excess energy away from PSII (Frank et al. 1996; Warner and Berry-Lowe 2006). Further, redistribution of thylakoid membrane associated light harvesting complexes (LHCs), as well as modifications of active photosynthetic units (PSU) have been discussed as a strategy of *Symbiodinium* to distribute energy between PSII and PSI (Chapter 2.2, Hill et al. 2005; Hill et al. 2012; Hoogenboom et al. 2009; Reynolds et al. 2008). High light stress can result in reversible down-regulation (Brown et al. 1999a; Hill et al. 2012; Hoegh-Guldberg and Jones 1999; Jones and Hoegh-Guldberg 2001) as well as permanent photoinhibition (Gorbunov et al. 2001) of PSII. Under bleaching scenarios, thermal stress can exacerbate the sensitivity towards high light and result in permanent PSII damage ultimately causing a dysfunction of the coral symbiosis (e.g. Hill et al. 2004a; Hill et al. 2012; Jones and Hoegh-Guldberg 2001).

This study examined the influence of high light stress on the photosynthetic efficiency of *Symbiodinium* harboured in two morphologically distinct hard coral species and

focus was given to *Symbiodinium's* photorepair capacity under high light stress. Here we report photorepair requirements based on changes in D1 concentrations as a result of high light exposure and compared these to Chl *a* fluorescence-based photorepair requirements. The inhibitor lincomycin was applied to specifically inhibit the *de novo* protein synthesis of the PSII core protein D1 (Ragni et al. 2010) thereby simulating photoinhibitory conditions.

It was hypothesised that under high light stress, *Pavona decussata* (Dana), a bleaching resilient coral species, can support its photorepair cycle more efficiently compared to *Pocillopora damicornis* (Linnaeus), a bleaching sensitive coral species. This was assessed by measuring the photosynthetic productivity in terms of photosynthetic O<sub>2</sub> production, intact and fragmented D1 protein concentrations and excess energy dissipation pathways when specimens were exposed to natural midday high light conditions for 4 days.

## 3.2 Materials and Methods

### 3.2.1 Coral collection and preparation

Two hard coral species, *Pocillopora damicornis* (Linnaeus) and *Pavona decussata* (Dana), were chosen for this experiment, as they are known to differ in tissue properties, symbiont densities and bleaching susceptibility (Glynn et al. 2001; Grimsditch et al. 2008; Hill et al. 2012; Krämer et al. 2013). Specimens of *P. damicornis* and *P. decussata* were sampled from lowest astronomical tide of 1-2 m depth on Heron Island reef flat, in the southern Great Barrier Reef, Australia (Fig 3.1).



**Figure 3.1:** Sampling location Heron Island, Capricorn Bunker Group, Great Barrier Reef, in Australia ( $23^{\circ}26'31.20''\text{S}$   $151^{\circ}54'50.40''\text{E}$ ) and a close-up of sampling site indicated as (1) (adapted from Krämer et al., 2012). Map was produced using Ocean Data View (Schlitzer, 2011, <http://odv.awi.de>) with data from ‘Coral reef distribution of the World (2010)’ provided by UNEP-WCMC.

The corals were cut into experimental size pieces ( $\sim \varnothing = 4$  cm) to fit the sample chamber of the Algae-Growth Pulse Amplitude Modulated (PAM) fluorometer (Gademann Instruments GmbH, Germany; see chapter 4). Corals were left to recover in shaded ( $< 100 \mu\text{mol photons m}^{-2} \text{s}^{-1}$ ) flow-through aquaria for 3 days to recover from handling-stress and then hung with nylon strings in 150 mL of 0.2  $\mu\text{m}$  filtered seawater (FSW), in continuously aerated glass vessels. Three sampling events took place every 48 h over a 96 h (4 day) experimental incubation ( $T_{0 \text{ h}}$ ,  $T_{48 \text{ h}}$ ,  $T_{96 \text{ h}}$ ).

### ***3.2.2 Treatment and sampling regime***

Corals were kept in individual glass vessels throughout the experiment, where water changes were done every night after sampling. All glass vessels in the experimental setup were immersed in a flow-through aquarium table, which was fully sun-exposed during day time. For each sampling event two treatments were defined for each species, where one was treated with lincomycin ( $500 \mu\text{g mL}^{-1}$ ) (a total of  $n = 7$  was incubated) and one set remained untreated ( $0 \mu\text{g mL}^{-1}$ ) (a total of  $n = 7$  was put into the experimental setup). Corals were sampled at solar noon (between 12:00 and 14:00) ( $n = 4$ ) for Algae-Growth PAM measurements (see below), and at night time ( $\sim 3$  h after sunset) corals were sampled ( $n = 3$ ) for analyses of photosynthetic and photoprotective pigment. Prior to specimen processing at night time, maximum quantum yield of PSII ( $F_V/F_M$ ) was measured with a Diving-PAM (Walz GmbH, Germany) (see next section 3.3.3). All measured corals midday and night time were detrimentally processed.



### 3.2.3 Chlorophyll *a* fluorescence

To assess the utilisation of absorbed light at midday, photochemical quenching pathways as defined by Kramer et al. (2004) were determined from steady-state light curves (SSLC) measured in the Algae-Growth-PAM (for detailed instrument description see Chapter 4). Actinic light was applied through a mounted LED panel in front of the sample chamber, where incubation light intensity was matched with prevailing irradiances at the time of sampling which was on average  $1464 \pm 22 \mu\text{mol photons m}^{-2} \text{s}^{-1}$  (mean  $\pm$  SEM). Coral specimens were placed in the incubation chamber and left in the dark for 5 min prior to 5 min light incubation and 2 min post-illumination dark incubation.

To estimate fluorescence quenching pathways, three dissipation processes were considered, which describe the fate of harvested light energy in PSII (Kramer et al. 2004). This fluorescence quenching analysis distinguished between photochemical use of light energy (Y(II)), regulated heat dissipation by PSII downregulation (Y(NPQ)) and non-light induced quenching also described as non-regulated heat dissipation (Y(NO)), see equations 1 - 3 (Kramer et al. 2004).

$$1) Y(\text{II}) = (F_{M'} - F) / F_{M'}$$

$$2) Y(\text{NPQ}) = 1 - \Phi_{\text{PSII}} - (1 / (\text{NPQ} + 1 + q_L (F_M / F_0 - 1)))$$

$$3) Y(\text{NO}) = 1 / (\text{NPQ} + 1 + q_L (F_M / F_0 - 1))$$

Where Y(II) is calculated through light-adapted fluorescence parameters,  $F$  is the transient Chl *a* fluorescence signal before and  $F_{M'}$  is the Chl *a* fluorescence signal after a saturation flash (Gorbunov et al. 2001). Y(NPQ) is calculated through parameters,

which describe the differential Chl *a* fluorescence signal during the light and during the dark; where  $\Phi_{\text{PSII}}$  is the effective quantum yield and is equivalent to  $Y(\text{II})$  and NPQ defines non-photochemical quenching processes as the difference between maximum Chl *a* fluorescence signal derived after the application of a saturation flash after dark adaption ( $F_M$ ) and during light incubation ( $F_M'$ ); NPQ was calculated as follows in equation 4:

$$4) \text{ NPQ} = (F_M - F_M') / F_M'$$

Further,  $Y(\text{NPQ})$  is estimated considering  $q_L$ , which is a parameter to estimate the fraction of open PSII centers (see Kramer et al. 2004 for detailed description) assuming a lake model for LHCs of PSII reaction centers (high connectivity) and  $F_0$  the dark adapted Chl *a* fluorescence signal.  $Y(\text{NO})$  indicates the combined radiative and non-radiative energy dissipative pathways not leading to a photochemical reaction and are independent of NPQ (Klughammer and Schreiber 2008).

Coral specimens were measured with a Diving-PAM to determine the maximum quantum yield of PSII ( $F_V/F_M$ ) prior to pigment harvest during night sampling, which was calculated as follows (Genty et al. 1989).

$$5) F_V/F_M = (F_M - F_0) / F_M$$

In this study, the influence of high light stress upon photorepair has been assessed using two different methods, one was based on Chl *a* fluorescence (3.2.3.1; equation 7) and one was based on psbA (D1 protein) concentration changes (3.2.6.3; equation 10). This approach was chosen in order to assess the viability of utilising Chl *a* fluorescence to

infer about the integrity of PSII reaction centers as previously presented (e.g. Hennige et al. 2011; Ragni et al. 2010).

### 3.2.3.1 *Chl a fluorescence–based photorepair requirement*

The decline in  $F_V/F_M$  of algal symbionts exposed to high light conditions and treated with lincomycin is a result of the accumulation of photoinactivated PSII, as *de novo* synthesis of the D1 protein is inhibited (Krämer et al. 2013).  $F_V/F_M$  values of algal symbionts exposed to high light conditions alone (i.e. in the absence of lincomycin) are a result of photodamaged PSII through high light exposure, but in the presence of active repair processes (Hill et al. 2011; Six et al. 2007). The difference in  $F_V/F_M$  lost between the lincomycin treatments can therefore give information about ongoing photorepair. The percent loss in  $F_V/F_M$  of lincomycin treated, as well as the loss of  $F_V/F_M$  through high light exposure was calculated relative to T0h levels at midday for each sampling event (T48h and T96h) as described in equation 6:

$$6) \text{ Loss (\%)} = - (100 - ((F_V/F_M \text{ treatment} / F_V/F_M \text{ T0h}) * 100))$$

Where “ $F_V/F_M$  treatment” either stands for  $F_V/F_M$  of  $\pm$  lincomycin treated corals and “ $F_V/F_M \text{ T0h}$ ” was  $F_V/F_M$  at T0h. Loss in  $F_V/F_M$  of  $\pm$  lincomycin treated corals (equation 6) was used to define Chl *a* fluorescence based photorepair. The percent photorepair was then calculated according to equation 7 (Krämer et al. 2013):

$$7) \text{ Photorepair}_{\text{Chl } a} (\%) = \left| (\% \text{ LOSS}_{\text{lincomycin treated}}) - (\% \text{ LOSS}_{\text{high light exposed}}) \right|$$

### ***3.2.4 Post-measurement sample processing***

Coral specimens were air-brushed in 5 mL of chilled (~ 4 °C) FSW and the resulting slurry was centrifuged at 4 °C and 500 g for 10 min after midday sampling. At night time coral specimens were snap-frozen prior to being air-brushed under dim light conditions to account for fast inter-conversion of xanthophyll pigments (Macintyre et al. 2000). The resulting supernatant (host fraction) was discarded and the algal symbiont pellet was re-suspended in 4 mL of chilled (~ 4 °C) FSW, 2 mL of the suspension was filtered on 0.25 mm diameter GF/F filters (Whatman) and immediately snap-frozen in liquid nitrogen and stored at – 80 °C until pigment analyses. The remaining 2 mL subsample was used to determine symbiont density which was done using a haemocytometer (Edmunds and Gates 2002). Coral surface area was determined with the single dip wax technique (Stimson and Kinzie 1991).

### ***3.2.5 Photosynthetic and photoprotective pigment analyses***

High performance liquid chromatography (HPLC) was used to quantify photosynthetic (Chl *a* and *c*<sub>2</sub>) and photoprotective (diadinoxanthin and diatoxanthin) pigment concentrations. Glass fibre filters paper was placed in 15 mL falcon tubes which contained 5 mL chilled acetone (~ 4 °C; 100% HPLC grade Lomb Scientific (AUST) Pty Ltd., Part no. C2501-4L). Extraction was carried out in darkness and falcon tubes were placed on ice to prevent any pigment degradation. Each filter paper was then individually disrupted using an ultrasonic probe (Sonic and Material Inc. USA Model-VC50T; 50W, 20 KHz) for approximately 30 s on an output of 40W, while keeping the tube in ice to prevent any heating. Sample slurry was then passed through another GF/C filter paper (Whatman<sup>®</sup> Part no. 1822-025). Finally, the filtrate was passed through 0.2 µm PTFE 13 mm syringe filters (Micro-Analytix Pty Ltd; Part no. 13HP020AN) and

stored in amber HPLC glass vials (Waters 15x45 amber glass, screw neck vials with cap and preslit PTFE/silicon septa (LectraBond; Part no. 186001134C). Samples were extracted overnight at  $-80\text{ }^{\circ}\text{C}$  in the dark and analysed by HPLC.

Pigments were analysed as per UTS laboratory standard protocol as follows. A Waters HPLC system equipped with pump system and in-line degasser, as well as programmable autoinjector, temperature controlled autosampler, temperature controlled column oven compartment, a photodiode array detector and Empower Pro software (All from Waters Australia Pty. Ltd) was used for spectral detection and logging. For sample injections a unique program called 'Sandwich injection' was developed where vials of buffer and sample/standard were placed alternately in autosampler (maintained at  $4 \pm 1\text{ }^{\circ}\text{C}$ ) and alternate volumes of buffer and sample/standard (150-75-75-75-150 mL) were drawn into 900  $\mu\text{L}$  sample loop. The entire volume was then injected into the column. Separation of pigments was achieved by using Eclipse XDB C<sub>8</sub> HPLC 4.6 mm x 150 mm column and guard column (Agilent Technologies, Australia) using a linear elution gradient from 5 - 95% of solvent B (100 % Methanol, HPLC grade, Lomb Scientific (AUST) Pty Ltd., Part no. C2517-4L) up to 22 min, isocratic hold on 95% solvent B from 22 - 29 min, and returned to initial conditions in 31 min, allowing the column to equilibrate for 9 min before starting the next injection cycle. Solvent A was mixture of (30:70) Tetrabutyl Ammonium Acetate (TBAA; 28 mM): Methanol (100%, pH 6.5). The column temperature was maintained at  $55 \pm 2\text{ }^{\circ}\text{C}$  with a flow rate of  $1.1\text{ mL min}^{-1}$ . A complete pigment spectrum from 270 to 700 nm was recorded using the photodiode array detector with 3.4 nm band width. The software was programmed to extract the wavelengths from 450 to 665 nm. The signal at 665 nm was used to quantify monovinyl and divinyl Chl *a*, whereas the signal at 450 nm was used to quantify all other pigments. Calibration and quality assurance was performed by using external calibration

Standards (DHI, Hørsholm Denmark) of each pigment which were stored at -80 °C. Peaks were integrated using the software Empower Pro. All peaks were manually inspected to confirm that software had drawn correct peak baselines and integrations according to the pigment standards.

Pigment analysis of *Symbiodinium* focussed on xanthophyll-based photoprotective strategies of the coral species examined. Diadinoxanthin (Dd) and diatoxanthin (Dt) concentrations, total xanthophyll pool ( $\sum XP = Dd + Dt$ ), as well as de-epoxidation status ( $DPS = Dt / \sum XP$ ) were considered for analysis.

### ***3.2.6 D1 protein concentrations***

#### ***3.2.6.1 Protein Extraction and Assay***

Protein was extracted from the cells on the frozen filters using an MPBio FastPrep® - 24 with the 24 x 2 rotor. Each frozen filter was transferred to a 2 mL tube containing bead lysing matrix D (SKU 116913050) and 1 X extraction buffer. The extraction buffer was prepared from 4 X protein solubilization buffer and 50 X Pefabloc (modified from Brown et al. 2008). The 4 X protein solubilization buffer contained 0.55 M TRIS buffer (pH 7.5), 0.3 M LDS, 4.3 M glycerol and 2 mM EDTA. The FastPrep was set to run at  $6.5 \text{ m s}^{-1}$  for three 1 min cycles with the specified 24 x 2 rotor. The samples were held on ice for 1 min between each cycle. Following cell lysis, the samples were centrifuged for 3 min at 10 000 x g and the supernatant was assayed for total protein concentration using the BioRad DC protein assay kit with Bovine Gamma Globulin standards of known concentration.

### 3.2.6.2 *Quantitative Immunoblotting*

Protein blot results were matched with known molecular weight standards and loaded with a known volume, which allowed for quantification of psbA in  $\text{fmol } \mu\text{g protein}^{-1}$ . To measure protein concentrations of the algal cells, immunoblotting techniques were performed, as detailed in Six et al. (2007) and Brown et al. (2007; 2008) and has previously been applied on coral samples as detailed in Hill et al. (2011). Quantitative psbA protein standards (Agriseria) were loaded on SDS-PAGE gels in parallel with extracted total protein samples of known total protein content, to quantify the amount of each target protein present in the sample. The anti-psbA primary antibody used in detection was diluted to 1: 50 000 (AS05 084 lot 0905). The secondary antibody goat anti-rabbit IgG was used in a dilution of 1: 50 000 (ImmunoReagents Inc, lot 14-122-042810). Intact psbA protein was identified with given protein standards at  $\sim 30$  kDa. All samples displayed an additional 2 bands with lower molecular weight than psbA standards, which were interpreted as fragmented psbA (for representative immunoblot see Hill et al. 2011). Breakdown products of psbA resulting from high light exposure have been described to follow characteristic defragmentation (Shipton and Barber 1991), so that ratios of fragmented psbA ( $\text{psbA}_{\text{frag}}$ ) to intact psbA ( $\text{psbA}_{\text{intact}}$ ) concentrations ( $\text{psbA}_{\text{frag}}/\text{psbA}_{\text{intact}}$ ) were computed for analysis to indicate the magnitude of photodamage (see representative blot in the supplementary section at the end of this chapter, Figure S3.6.1).

### 3.2.6.3 *D1 concentration-based photorepair requirement*

With the application of lincomycin, the *de novo* synthesis of D1 is inhibited, so that the percent loss of intact D1 in algal symbionts treated with lincomycin can be interpreted as the amount of gross photodamage. Accordingly, algal symbionts exposed to high

light, balance photodamage with active photorepair through *de novo* synthesis of D1, so that the percent loss of intact D1 in algal symbionts exposed to high light can be interpreted as photodamage countered through photorepair. The percent loss of intact D1 at the end of the experiment relative to T0h was calculated as follows (equation 9).

$$9) \text{ Loss (\%)} = - (100 - ((\text{D1 loss treatment} / \text{psbA}_{\text{T0h}}) * 100))$$

Where the term “psbA loss treatment” describes intact psbA of  $\pm$  lincomycin treated corals and “psbA<sub>T0h</sub>” was the initial intact psbA concentration at T0h.

The difference in percent loss of intact psbA in lincomycin treated and high light exposed algal symbionts was used to quantify the photorepair requirements for midday sampled coral species and were calculated as follows (equation 10).

$$10) \text{ Photorepair}_{\text{D1}} (\%) = | (\% \text{ intact psbA loss}_{\text{lincomycin treated}}) - (\% \text{ intact psbA loss}_{\text{high light exposed}}) |$$

These parameters are based on D1 concentrations and are similar to those calculated from chl *a* fluorescence values (3.2.3.1; equation 7, see above). Two independent measures of photorepair were applied in this study, which enabled to estimate the viability of chl *a* fluorescence based photorepair estimates.

### 3.2.7 Abiotic parameters

Irradiance was logged in 10 min intervals throughout the experiment as an integrated spectral intensity (400-700 nm) using a logger (LI-COR 1400). Maximum photon flux density at midday was  $\sim 1464 \pm 22 \mu\text{mol photons m}^{-2} \text{ s}^{-1}$  (mean  $\pm$  SEM), which corresponds with previously defined ‘high light’ conditions at the depth where corals were harvested for this study (Davies 1991). Temperature was logged (Progress Plus



Thermobuttons) in 10 min intervals ( $20.5 \pm 0.8^\circ\text{C}$ ), which were kept in specimen-free glass vessels filled with the same volume of FSW and added to the experimental glass vessels on the flow-through aquarium table (see Fig 3.2 for abiotic parameters throughout the experimental time).

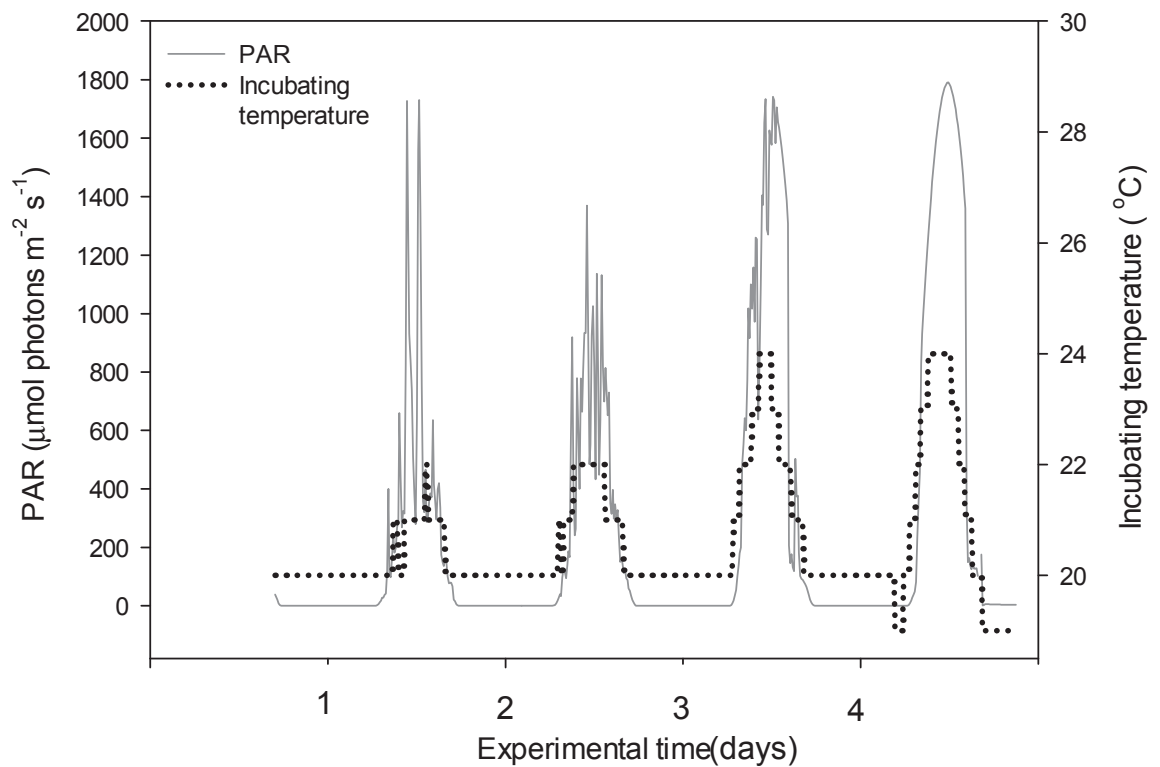


**Figure 3.2:** Photosynthetic active radiation (PAR) intensities, as well as incubating temperature throughout the experimental time. PAR is indicated through grey solid line and incubating temperature indicated with black dotted line.

### 3.2.8 Statistical analyses

Data were tested for equal variance using the Levene's test and for normal distribution using the Shapiro-Wilk test. In cases where the ANOVA assumptions were not met Kruskal Wallis H-tests (H-values are indicated) were performed. One- way ANOVA was applied to test for differences throughout the experimental incubation (T<sub>0h</sub> to T<sub>96h</sub>) and two-way ANOVAs were used to test for influences of inhibitor treatment, and the sampling times (midday or night) and sampling events (T<sub>0h</sub>, T<sub>48h</sub>, T<sub>96h</sub>) in the measured parameters. Tukey HSD post-hoc analyses were performed to define differences between group means at a significance level of  $\alpha = 0.05$ . Student's t-test was used to identify any differences at given sampling events (midday and night). All data were analysed using Statistica (Statsoft).

## 3.3 Results

### 3.3.1 Maximum quantum yield at midday and at night time

Midday  $F_V/F_M$  levels did not change for algal symbionts from *P. damicornis* without lincomycin application throughout their experimental incubation. Only with the application of lincomycin,  $F_V/F_M$  in algal symbionts of *P. damicornis* were found to decrease at midday at T<sub>48h</sub> and T<sub>96h</sub> compared to initial T<sub>0h</sub> levels (Tukey HSD; one-way ANOVA,  $F(2,9) = 354.51$ ,  $p < 0.001$ ; Fig 3.3 A).  $F_V/F_M$  levels increased in algal symbionts of *P. damicornis* at T<sub>48h</sub> and T<sub>96h</sub> at night (Tukey HSD; one-way ANOVA,  $F(2,6) = 22.991$ ,  $p < 0.001$ ; Fig 3.3 C). The reduction in  $F_V/F_M$  when treated with lincomycin at midday and night increased with time in algal symbionts of *P. damicornis* (two-way ANOVA, interactive effect of inhibitor and sampling event;  $F(2,15) = 20.83$ ,  $p < 0.001$  and  $F(2,15) = 39.15$ ,  $p < 0.001$ , respectively).

Without the application of lincomycin,  $F_V/F_M$  remained constant in the algal symbionts in *P. decussata* for values taken at midday at  $T_{0h}$ ,  $T_{48h}$  and  $T_{96h}$ . By comparison, corals treated with lincomycin displayed a decrease in  $F_V/F_M$  levels during midday at  $T_{48h}$  and  $T_{96h}$  (Tukey HSD; one-way ANOVA,  $F(2,9) = 84.24$ ,  $p < 0.001$ , Fig 3.3 B).  $F_V/F_M$  levels increased in algal symbionts from *P. decussata* without lincomycin treatment at  $T_{96h}$  at night (Tukey HSD; one-way ANOVA,  $F(2,6) = 8.53$ ,  $p = 0.018$ ; Fig 3.3 D), and decreased with the application of lincomycin at  $T_{48h}$  and  $T_{96h}$  (Tukey HSD; one-way ANOVA,  $F(2,6) = 31.06$ ,  $p = 0.007$ ; Fig 3.3 D).

No statistical difference between species responses was detected during the decline in  $F_V/F_M$  with the application of lincomycin at midday, so that a decline of 81.3 % in *P. damicornis* and 84.5 % in *P. decussata* occurred, while untreated algal symbionts displayed unchanged  $F_V/F_M$  in both species at midday (Fig 3.3 A, B).

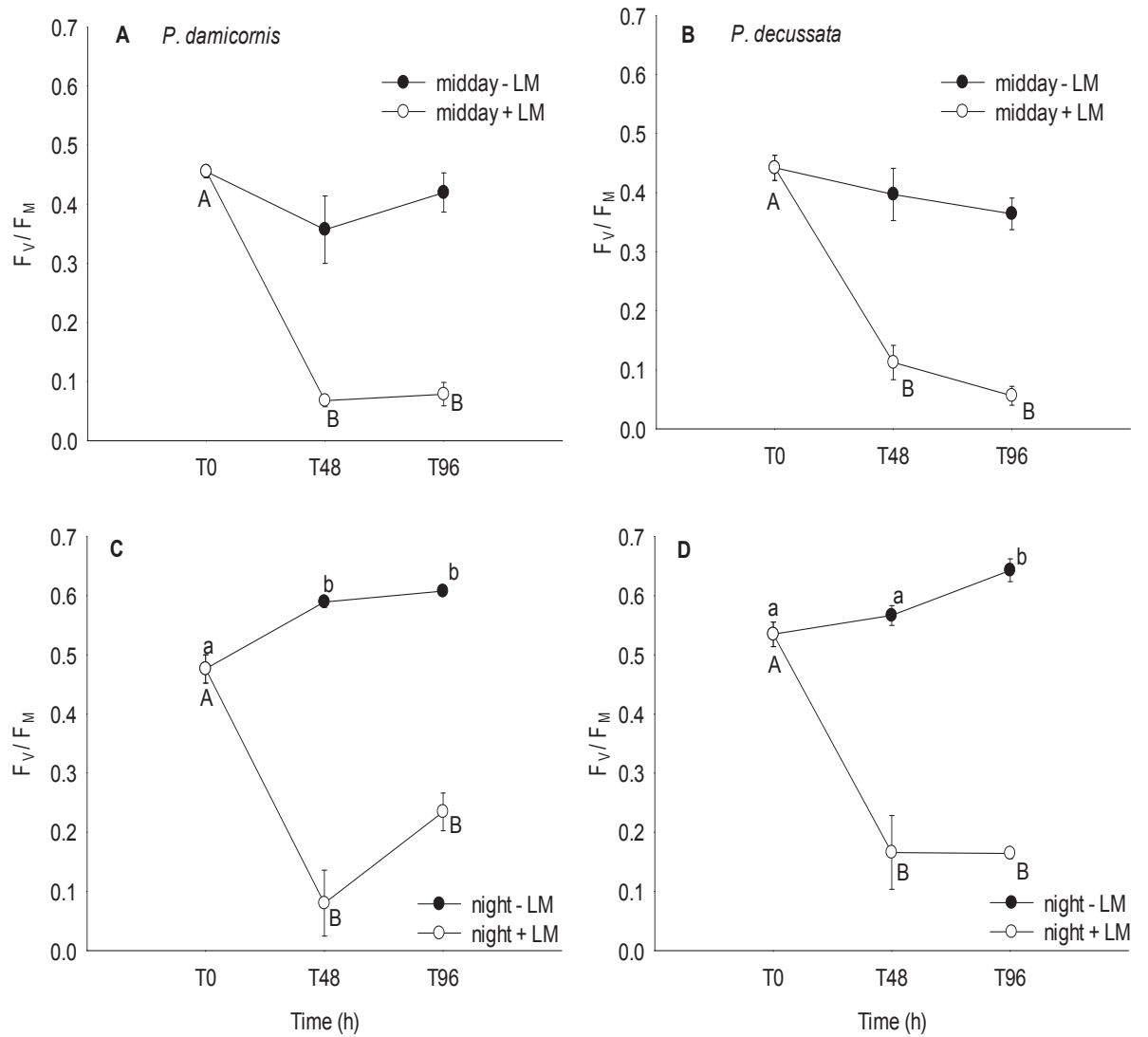


**Figure 3.3:**  $F_v/F_M$  of midday dark-adapted specimens with (+LM) and without lincomycin (-LM) treatment (panel A: *P. damicornis*, panel B: *P. decussata*) and night measurements of with (+LM) and without lincomycin (-LM) treatment (panel C: *P. damicornis*, panel D: *P. decussata*). Tukey HSD results are indicated; mean  $\pm$  SEM;  $n = 4$ .

### 3.3.2 *psbA* protein concentrations

High light exposed algal symbionts of *P. damicornis* without lincomycin did not show any changes in intact *psbA* concentrations at any sampling time throughout the experiment, where intact *psbA* concentrations were found to be higher at night compared to midday at  $T_{0\text{ h}}$  (t-test;  $t(5) = 2.73$ ,  $p = 0.041$ ). At later sampling events, *psbA* concentrations were comparable between midday and night in algal symbionts of *P. damicornis* without lincomycin treatment (Fig 3.4 A). Lincomycin treated algal symbionts significantly declined with intact *psbA* concentrations at the end of the experiment at  $T_{96\text{ h}}$  (Kruskal Wallis,  $H(2) = 7.85$ ;  $p = 0.020$ ), where *psbA* concentrations of lincomycin treated algal symbionts in *P. damicornis* remained unchanged at night.

At midday, intact *psbA* concentrations increased at  $T_{48\text{ h}}$  and decreased to initial concentrations at  $T_{96\text{ h}}$  in algal symbionts of *P. decussata* not treated with lincomycin (Tukey HSD; one-way ANOVA,  $F(2,9) = 31.63$ ,  $p < 0.001$ ; Fig 3.2 C), whereas intact *psbA* concentrations remained unchanged throughout the experimental incubation at night (Fig 3.4 C). Intact *psbA* concentrations were generally found to be higher at night in algal symbionts of *P. decussata* without lincomycin treatment and concentrations of *psbA* increased at night with time (two-way ANOVA, interactive effect sampling time and sampling event;  $F(2,15) = 5.57$ ,  $p = 0.016$ ; Fig 3.4 C). For algal symbionts of *P. decussata* treated with lincomycin, intact *psbA* concentrations decreased with exposure time and were generally lower at night with time (two-way ANOVA, interactive effect of sampling time and sampling event,  $F(2,15) = 13.31$ ,  $p < 0.001$ ; Fig 3.4 C).

*P. damicornis* and *P. decussata* displayed similar amounts of intact *psbA* concentrations at midday at the beginning of the experiment with  $4.85 \pm 0.78$  fmol *psbA*  $\mu\text{g protein}^{-1}$  and  $3.44 \pm 0.03$  fmol *psbA*  $\mu\text{g protein}^{-1}$ , respectively (Fig 3.4 A, C). Intact *psbA*

concentrations of high light exposed specimens at T<sub>96 h</sub> were significantly different between these species, where *P. damicornis* displayed much higher concentrations (t-test,  $t(6) = 5.36$ ,  $p = 0.002$ ; Fig 3.4 A, C). The intact psbA concentrations significantly decreased in both species once lincomycin was applied, where *P. damicornis* displayed a decrease to  $1.29 \pm 0.64$  fmol psbA  $\mu\text{g protein}^{-1}$  and *P. decussata* decreased concentrations to  $0.89 \pm 0.12$  fmol psbA  $\mu\text{g protein}^{-1}$  at T<sub>96h</sub> (Kruskal Wallis,  $H(2) = 7.85$ ,  $p = 0.020$ ; and Tukey HSD, one-way ANOVA,  $F(2,7) = 11.39$ ,  $p = 0.006$ , respectively; Fig 3.4 A, C).

The ratio of fragmented psbA to intact psbA ( $\text{psbA}_{\text{frag}}/\text{psbA}_{\text{intact}}$ ) increased in algal symbionts of *P. damicornis* without lincomycin for T<sub>48 h</sub> and T<sub>96 h</sub> relative to T<sub>0 h</sub> at midday (Kruskal Wallis,  $H(2) = 7.54$ ,  $p = 0.023$ ; Fig 3.2 B). The  $\text{psbA}_{\text{frag}}/\text{psbA}_{\text{intact}}$  ratios of lincomycin untreated algal symbionts of *P. damicornis* increased at T<sub>48 h</sub> relative to T<sub>0 h</sub> at night and then decreased relative to the initial T<sub>0 h</sub> levels at T<sub>96 h</sub> (Kruskal Wallis,  $H(2) = 6.48$ ,  $p = 0.039$ ; Fig 3.4 B). The application of lincomycin did not have a significant effect upon  $\text{psbA}_{\text{frag}}/\text{psbA}_{\text{intact}}$  ratios in algal symbionts associated with *P. damicornis*.

Ratios of  $\text{psbA}_{\text{frag}}/\text{psbA}_{\text{intact}}$  remained unchanged in high light exposed algal symbionts of *P. decussata* without lincomycin treatment at midday and night (Fig 3.4 D). Algal symbionts of *P. decussata* with lincomycin treatment displayed an increase in  $\text{psbA}_{\text{frag}}/\text{psbA}_{\text{intact}}$  ratios at night at T<sub>48 h</sub> and T<sub>96 h</sub> compared to initial ratios at T<sub>0 h</sub> (Tukey HSD; one-way ANOVA,  $F(2,6) = 10.08$ ,  $p = 0.012$ ; Fig 3.4 D).

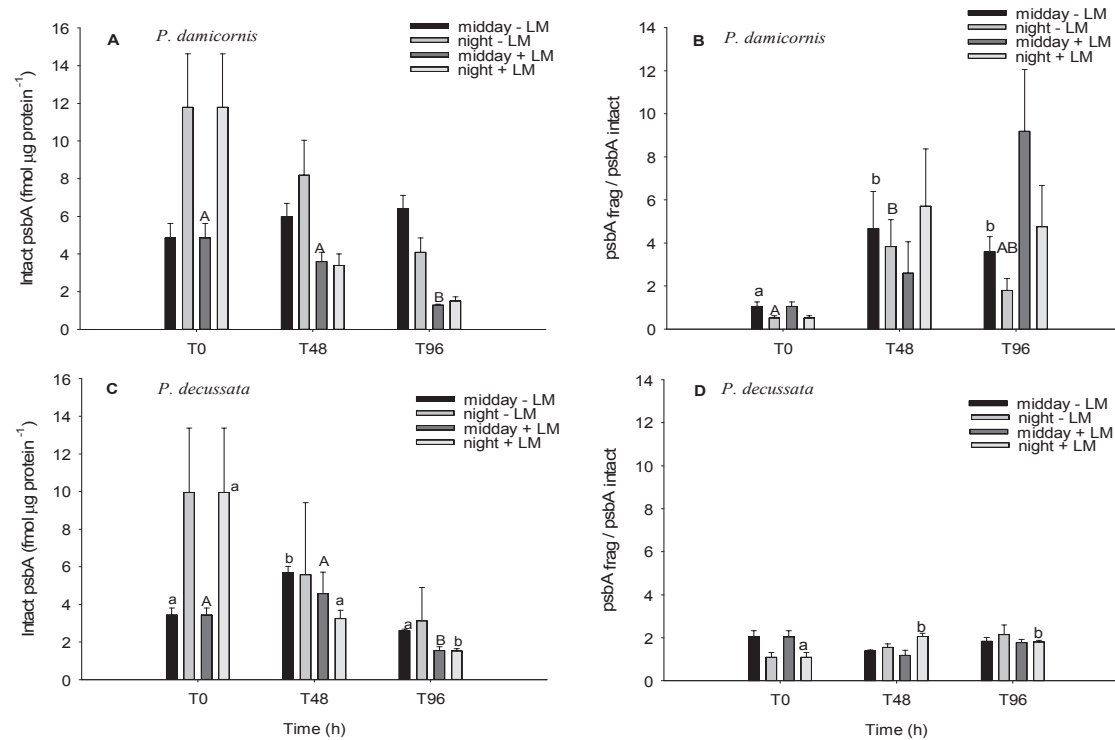


**Figure 3.4:** Intact psbA concentrations A) *P. damicornis*, C) *P. decussata*; fragmented psbA to intact psbA ratios B) *P. damicornis*, D) *P. decussata* as well as are displayed for all experimental sampling events (days) for treatments of high light exposure without lincomycin at midday (midday – LM) and night time (night – LM), as well as high light exposure with lincomycin at midday (midday + LM) and night time (night + LM). T0 measurements were taken n=4 at midday and night representative for both treatment conditions. Tukey HSD results are indicated; mean  $\pm$  SEM; n = 4.

### 3.3.3 Results of the two independent photorepair estimates

Using the measurement of Chl *a* fluorescence comparing lincomycin treated and untreated specimens (equation 7) of T<sub>0 h</sub> and T<sub>96 h</sub> demonstrated that  $70.6 \pm 11.4\%$  and  $71.51 \pm 11.4\%$  of photorepair was required to sustain  $F_V/F_M$  levels under high light exposure (Fig 3.5) in algal symbionts of *P. damicornis* and *P. decussata*, respectively.

Changes of intact psbA concentrations in algal symbionts after T<sub>96 h</sub> of high light exposure during the day, with and without lincomycin allowed for quantification of the photorepair of *de novo* synthesised psbA protein (see equation 10). Based on intact psbA concentration changes, algal symbionts in *P. damicornis* displayed greater rates of photorepair with  $142.5 \pm 28.0 \%$ , whereas algal symbionts in *P. decussata* showed significantly lower photorepair with  $39.9 \pm 16.3 \%$  (t-test;  $t(4) = 3.63$ ,  $p = 0.022$ ; Fig 3.5).

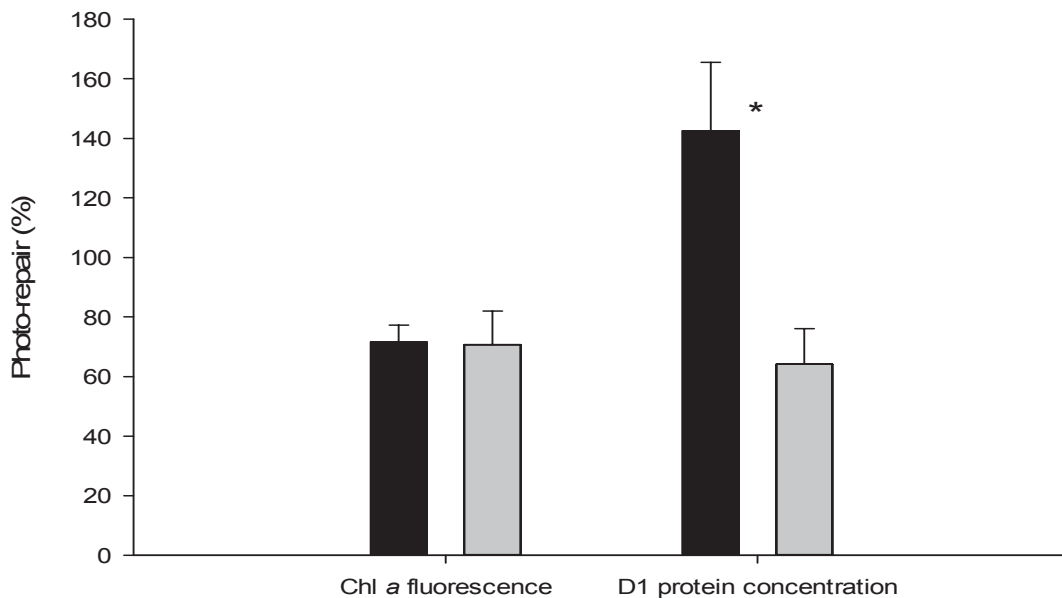


**Figure 3.5:** Photorepair (%) derived through Chl *a* fluorescence ( $F_V/F_M$  levels) and from intact psbA concentration changes for *P. damicornis* (black) and *P. decussata* (grey) Between species differences are indicated with an asterisk; mean  $\pm$  SEM;  $n = 4$ .



### 3.3.4 Chlorophyll *a* fluorescence quenching analysis

Quenching parameters of midday high light exposed algal symbionts in *P. damicornis* without lincomycin displayed an increase in Y(II) and a paralleled decrease in Y(NPQ) relative to T<sub>0 h</sub> at T<sub>96 h</sub> (Tukey HSD; one-way ANOVA,  $F(2,9) = 4.30$ ,  $p = 0.049$ ; Kruskal Wallis,  $H(2) = 7.39$ ,  $p = 0.025$ , respectively; Fig 3.6 A). Y(NO) levels remained unchanged from T<sub>0 h</sub> to T<sub>96 h</sub> and reached 0.21 to 0.31. In algal symbionts with lincomycin a decrease in Y(II) and Y(NPQ) was found at T<sub>48 h</sub> and T<sub>96 h</sub> compared to initial T<sub>0 h</sub> levels (Kruskal Wallis,  $H(2) = 6.50$ ,  $p = 0.039$ ; one-way ANOVA  $F(2,9) = 104.90$ ,  $p < 0.001$ , respectively; Fig 3.6 C), and an up-regulation of Y(NO) (Tukey HSD; one-way ANOVA,  $F(2,9) = 153.38$ ,  $p < 0.001$ ). Application of lincomycin significantly decreased Y(II) and Y(NPQ) levels in algal symbionts of *P. damicornis* (two-way ANOVA, interactive effect of inhibitor and sampling event  $F(2,15) = 6.64$   $p = 0.007$  and  $F(2) = 6.36$ ,  $p = 0.008$ , respectively; Fig 3.6 C).

Quenching parameters of algal symbionts in *P. decussata* without lincomycin displayed an increase in Y(II) and a simultaneous decrease in Y(NPQ) at T<sub>96 h</sub> (Tukey HSD; one-way ANOVA,  $F(2,9) = 4.98$ ,  $p = 0.035$  and  $F(2,9) = 7.96$ ,  $p = 0.010$ , respectively; Fig 3.6 B), where Y(NO) levels remained unchanged and reached 0.39 to 0.47. In algal symbionts of *P. decussata* treated with lincomycin, Y(II) and Y(NPQ) decreased at T<sub>96 h</sub> (Tukey HSD; one-way ANOVA,  $F(2,9) = 7.09$ ,  $p = 0.014$ ; Kruskal Wallis,  $H(2) = 8.77$ ,  $p = 0.012$ ; Fig 3.6 D) with a concomitant increase of Y(NO) T<sub>96 h</sub> (Kruskal Wallis,  $H(2) = 9.27$ ,  $p = 0.010$ ; Fig 3.6 D).

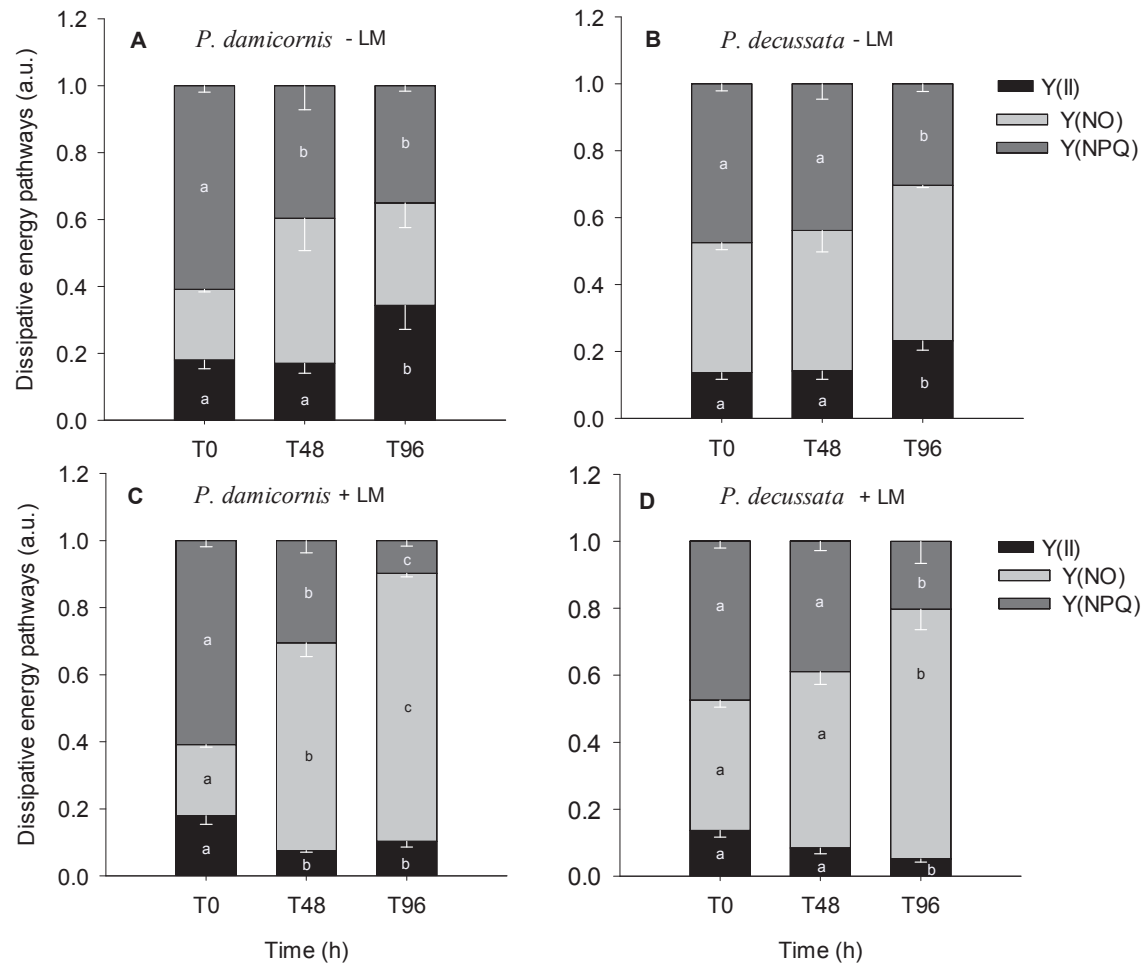


**Figure 3.6:** Quenching parameters of *P. damicornis* and *P. decussata* for all experimental sampling times (h) for midday high light exposure without lincomycin A) *P. damicornis*, b) *P. decussata* and for midday high light exposure with lincomycin treatment C) *P. damicornis*, D) *P. decussata*; Tukey HSD results are indicated; mean  $\pm$  SEM; n = 4.

### 3.3.5 *Photosynthetic productivity*

Net and gross photosynthetic productivity rates remained unchanged in algal symbionts of *P. damicornis* with and without lincomycin, where respiratory oxygen exchange increased at T<sub>48 h</sub> and T<sub>96 h</sub> resulting in a positive oxygen efflux compared to initial T<sub>0 h</sub> oxygen uptake rates in lincomycin treated and high light exposed coral specimens (Tukey HSD; one-way ANOVA,  $F(2,9) = 7.74$ ,  $p = 0.011$  and  $F(2,9) = 5.80$ ,  $p = 0.024$ , respectively; Fig 3.7 A, C).

Net, gross and respiratory oxygen exchange of *P. decussata* with and without lincomycin remained unchanged throughout the length of the experiment (Fig 3.7 B, D).

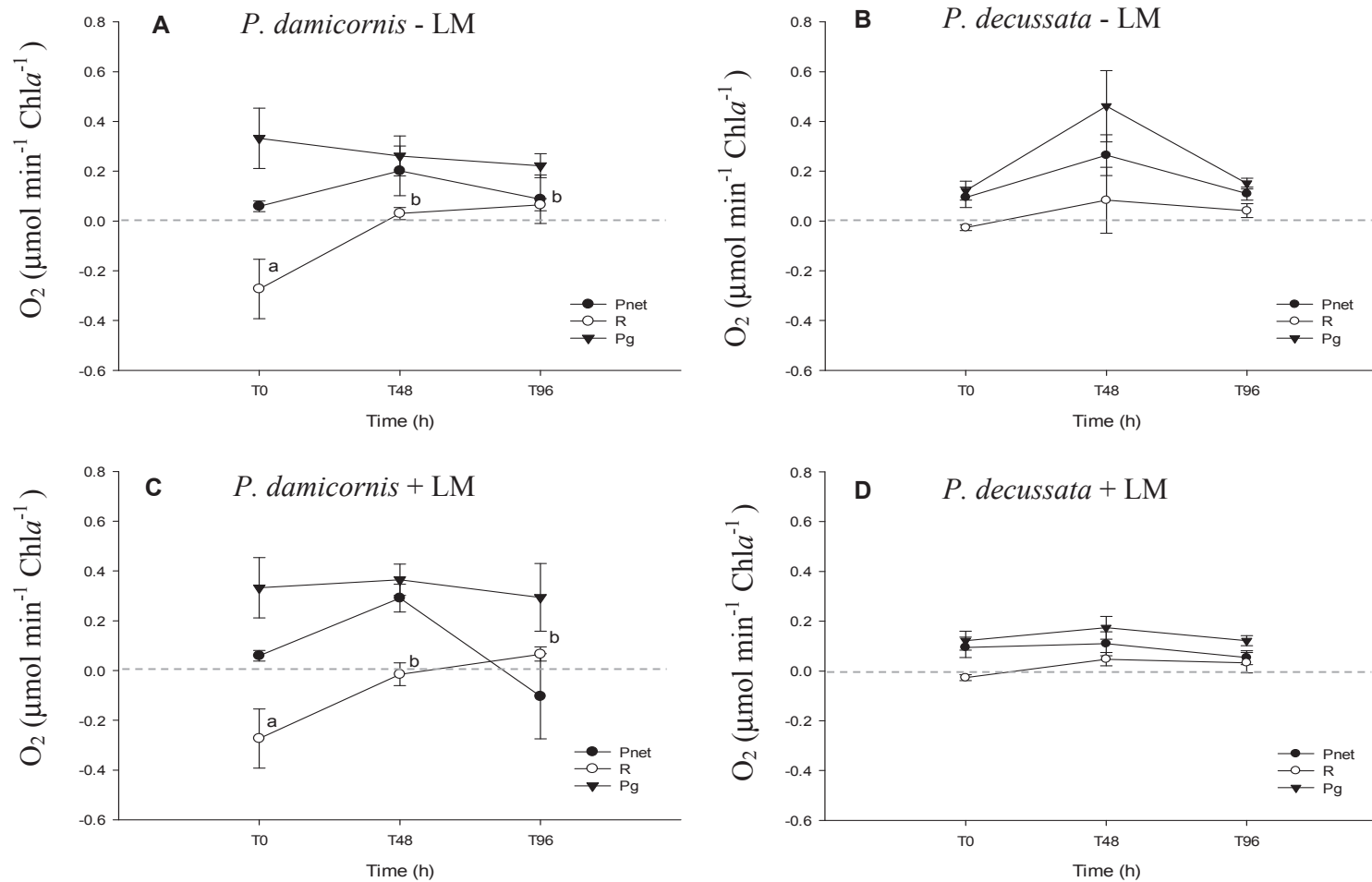


**Figure 3.7:** Gross (black circles) and net photosynthesis (black triangles) and respiration (clear circles) of for midday high light exposure without lincomycin; A) *P. damicornis* and B) *P. decussata*; as well as high light exposure with lincomycin treatment C) *P. damicornis* and B) *P. decussata* for all sampling times (h); zero is indicated as dashed grey line; Tukey HSD results are indicated; mean  $\pm$  SEM; n = 4.

### 3.3.6 Pigment analyses

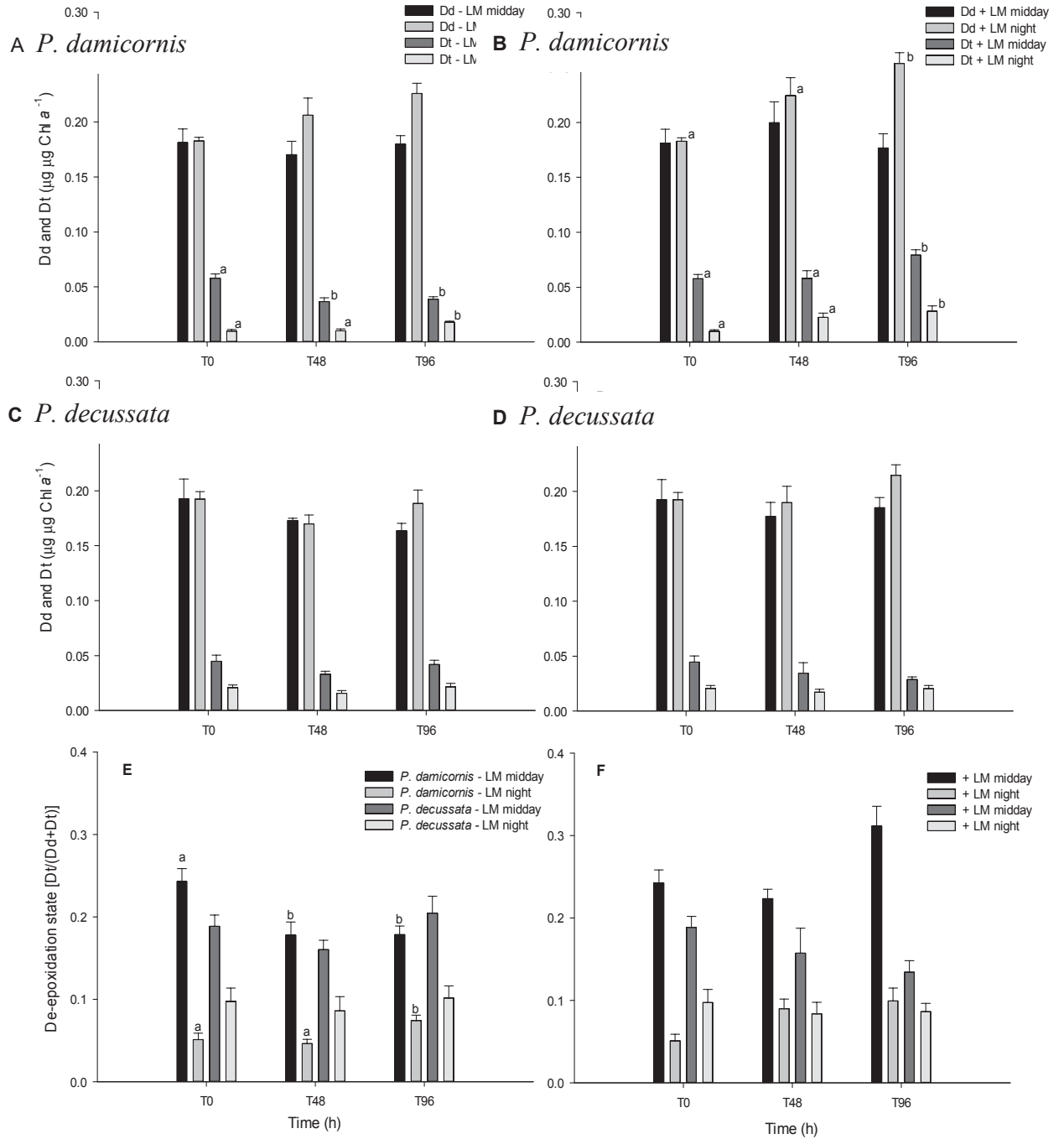
In algal symbionts of *P. damicornis* exposed to high light without lincomycin, the concentration of diadinoxanthin (Dd) normalised to Chl *a* remained unchanged for midday and night measurements throughout the experiment (Chl *a* concentrations also did not change for either of the two species), where Dd concentrations were higher at night throughout the experimental incubation (two-way ANOVA, interactive effect between sampling time and sampling event,  $F(1,15) = 8.40$ ,  $p = 0.011$ ; Fig 3.8 A). Dd concentrations normalised to Chl *a* in algal symbionts of this species treated with lincomycin displayed constant concentrations at midday throughout the experiment, whereas Dd normalised to Chl *a* increased in concentrations at T<sub>96 h</sub> at night (Tukey HSD; one-way ANOVA,  $F(2,6) = 7.71$ ,  $p = 0.012$ ; Fig 3.8 B).

Dt concentrations normalised to Chl *a* of high light exposed algal symbionts of *P. damicornis* without lincomycin application were lower throughout the experiment (T48h and T96h) compared to initial T<sub>0 h</sub> concentrations at midday (Tukey HSD; one-way ANOVA,  $F(2,9) = 12.39$ ,  $p = 0.003$ ; Fig 3.8 A). Dt concentrations normalised to Chl *a* during the night remained unchanged and peaked at the final sampling point T<sub>96 h</sub> (one-way ANOVA,  $F(2,9) = 7.71$ ,  $p = 0.012$ ; Fig 3.8 A). Lincomycin treated algal symbionts of *P. damicornis* showed increased Dt concentrations normalised to Chl *a* at the final sampling point T<sub>96 h</sub> at midday and night (Tukey HSD; one-way ANOVA,  $F(2,8) = 5.30$ ,  $p = 0.034$  and  $F(2,6) = 3.10$ ,  $p = 0.05$ , respectively; Fig 3.8 B). Dt concentrations normalised to Chl *a* were lower at night compared to midday concentrations in algal symbionts of both treatments (two-way ANOVA,  $F(1) = 115.4$ ,  $p < 0.001$ ).

A decrease in de-epoxidation status (DPS) at T<sub>48 h</sub> and T<sub>96 h</sub> relative to the initial T<sub>0 h</sub> levels occurred in algal symbionts of *P. damicornis* without lincomycin at midday (Tukey HSD; one-way ANOVA,  $F(2,9) = 6.83$ ,  $p = 0.016$ ; Fig 3.8 E), where DPS significantly increased at T<sub>96 h</sub> at night (Tukey HSD; one-way ANOVA,  $F(2,6) = 5.09$ ,  $p = 0.050$ ; Fig 3.8 E). DPS increased in lincomycin treated algal symbionts of *P. damicornis* during midday at T<sub>96 h</sub> (Tukey HSD; one-way ANOVA,  $F(2,8) = 5.68$ ,  $p = 0.029$ ; Fig 3.8 F). No changes in DPS levels were found in lincomycin treated algal symbionts of *P. damicornis* at night, but DPS levels were statistically lower at night compared to midday levels throughout (two-way ANOVA, sampling time effect:  $F(1) = 160.56$ ,  $p < 0.001$ ; Fig 3.8 F).

Dd concentrations normalised to Chl *a* in algal symbionts in *P. decussata* with or without lincomycin did not change throughout the experiment at midday or night (Fig 3.8 C, D). Where Dt concentrations normalised to Chl *a* in algal symbionts of *P. decussata* with and without lincomycin were lower at night compared to concentrations at midday throughout (two-way ANOVA,  $F(1,15) = 11.98$ ,  $p = 0.003$  and  $F(1,15) = 39.10$ ,  $p < 0.001$ , respectively; Fig 3.8 C, D).

DPS levels in algal symbionts of *P. decussata* incubated with and without lincomycin at midday and at night did not change throughout the experiment; where DPS levels were lower at night compared to midday levels throughout (two-way ANOVA,  $F(1) = 43.15$ ,  $p < 0.001$ ; Fig 3.8 E, F).



### 3.3.7 Cell density

Algal symbiont density did not change in either of the treatments for either of the species. *P. decussata* harboured a greater number of algal symbionts with  $2.05 \times 10^6 \pm 0.19 \times 10^6$  cells  $\text{cm}^{-2}$  compared to *P. damicornis* with  $0.70 \times 10^6 \pm 0.07 \times 10^6$  cells  $\text{cm}^{-2}$  (two-way ANOVA, species effect:  $F(1) = 37.01$ ,  $p < 0.001$ ).



### 3.4 Discussion

In this study, two hard coral species were examined for their algal symbionts' photoprotective response, photosynthetic productivity and efficiency, as well as photorepair requirements, when exposed to 4 days of natural high light stress during the day. Lincomycin was applied to simulate gross photoinhibitory conditions, as a result of chemically inhibited *de novo* synthesis of the central PSII core protein D1 (Bachmann et al. 2004). Recent studies suggested that the two hard coral species examined here differ in their activity of photoprotective pathways (Hill et al. 2012) and *in hospite* light levels (light levels within the tissue) (Krämer et al. 2013; Wangpraseurt et al. 2012). Here it was shown that the symbionts of the two morphologically distinct coral species also differ in their photorepair activity of the PSII core protein (D1 protein) under high light stress and demonstrate that photoprotective pathways differ once gross photoinhibitory conditions were simulated (Fig 3.5).

#### 3.4.1 Dissipative energy quenching

Lincomycin treated algal symbionts of both species showed a decrease in Y(II) and Y(NPQ) (light-induced excess energy dissipation; (Kramer et al. 2004)) along with up-regulated Y(NO). Interpretations for Y(NO) are scarce in the literature and some of the interpretations are contradictory, where a detailed review and discussion can be found in Klughammer and Schreiber (2008). It has been suggested that Y(NO) is non-light induced and that an up-regulation could be a consequence of PSII reaction center closure (Hoogenboom et al. 2012) or alternatively could be understood as non-regulatory heat dissipation indicating photoinhibition (Hill et al. 2012). Yet Y(NO) has also been described to be the fraction of energy that is passively dissipated in the form of heat and fluorescence, as a result of closed PSII reaction centers (Schreiber 2004).

Here, gross photoinhibition has been simulated with the application of lincomycin, which resulted in the significant downregulation of Y(II) and therefore progressive deterioration of electron transport through PSII. However, algal symbionts of *P. decussata* significantly up-regulated Y(NO) with time, whilst xanthophyll cycling remained unchanged throughout the experiment. In contrast to this, *P. damicornis* showed an up-regulation of Y(NO) with length of experimental exposure, along with increased xanthophyll cycling after 4 days of experimental exposure under gross photoinhibitory conditions (Fig. 3.6 C, 3.8 F). Dissipative energy pathways as analysed here have previously been reported for the two species examined here, when incubated under bleaching conditions for 2 days, where only *P. damicornis* up-regulated Y(NO) and *P. decussata* displayed unchanged Y(NO) levels (Hill et al. 2012). Furthermore, results presented here show that under high light stress algal symbionts of *P. decussata* displayed greater levels of Y(NO) compared to *P. damicornis*, indicating greater fraction of passive excess energy dissipation and points towards differential photoprotective pathways acting in the two coral symbioses examined here under high light stress.

#### ***3.4.2 Differential photorepair in the two species examined***

Algal symbionts in both species displayed similar levels of maximum quantum yield of PSII ( $F_V/F_M$ ) at midday, which gradually declined with the application of lincomycin. Both species therefore displayed comparable levels of photorepair ~ 80% to sustain  $F_V/F_M$  levels under high light exposure according to Chl *a* fluorescence measurements (Fig 3.5). Photorepair was also expressed based on the loss of D1 protein concentrations of lincomycin treated and untreated *in hospite* algal symbionts. The photorepair expressed through changes of intact D1 protein concentrations, which differed quite

substantially from photorepair derived through Chl *a* fluorescence measurements and also between the two coral species. Algal symbionts harboured in *P. damicornis* displayed ~ 143% of photorepair, where algal symbionts of *P. decussata* demonstrated only ~ 40% of photorepair to sustain intact D1 protein and unchanged  $F_V/F_M$ . *P. damicornis* has been described previously to be able to substantially up-regulate D1 photorepair rate when incubated under bleaching conditions, where under prolonged incubation of thermal and high light stress, photo-inactivation of PSII exceeds the photorepair rate resulting in photoinhibitory conditions in this species (Hill et al. 2011). Here the influence of high light stress only was examined and it was found that *P. damicornis* was experiencing a greater amount of photodamage (displayed as fragmented to intact D1 ratios, Fig 3.4 B, D) compared to *P. decussata* and consequently required greater photorepair. Algal symbionts have to invest energy into photorepair processes such as proteolysis of damaged D1 protein biomass, as well as for *de novo* synthesis of D1 (Six et al. 2007).

### ***3.4.3 Inference about photorepair***

Our results showed that *P. damicornis*, a bleaching sensitive coral species (Hill et al. 2012), experienced greater amounts of photorepair compared to *P. decussata*, a bleaching resilient coral species (Hill et al. 2012). This was indicated through changes in D1 protein concentration changes, whilst sustaining  $F_V/F_M$  after 4 days of high light stress during daytime. Previous studies used Chl *a* fluorescence-based assays indirectly probing photodamage and photorepair of the D1 protein state (Hennige et al. 2011; Krämer et al. 2013; Ragni et al. 2010). From those studies greater photorepair capacity has been related to the ability of a species to withstand greater amounts of photodamage and has been associated with bleaching resilient coral species under the combined

impact of thermal and high light stress (Hennige et al. 2011; Ragni et al. 2010). The results presented here for the bleaching resilient species *P. decussata* agree with this hypothesis, as *de novo* synthesis of D1 was found to be up-regulated when incubated under high light stress conditions (Fig 3.4 c). Photorepair rates have been demonstrated to increase for *in hospite Symbiodinium* with increasing irradiance (Hennige et al. 2011), as well as under bleaching conditions of combined thermal and high light stress (Hill et al. 2011).

However, with the application of PAM fluorometry, Chl *a* fluorescence allows inference about the state of PSII reaction centers (RCs). The greater the derived fluorescence signal, the greater the amount of closed RCs, so that under photoinhibitory conditions great fluorescence signals are measured. The photorepair of *P. damicornis*, here directly estimated through D1 protein concentration changes, did not compare to Chl *a* fluorescence derived photorepair (Fig 3.5). As the application of lincomycin inhibits the *de novo* synthesis of PSII core protein D1, photodamaged D1 protein accumulates relative to intact D1 protein concentrations. Consequently, progressive photo-inactivation of PSII causes great amounts of PSII related Chl *a* fluorescence, which was demonstrated here through the great loss in maximum quantum yield once lincomycin was applied (Fig 3.3). Without lincomycin application, *P. damicornis* experienced increased photodamage (Fig 3.4 B) simultaneous with photorepair of D1 through *de novo* synthesis (Fig 3.4 A; Fig 3.5). The dynamic regulation of D1 photodamage and *de novo* synthesis demonstrated here for *P. damicornis* was so efficient that no variability was detected by means of Chl *a* fluorescence and mirrored in the unchanged intact D1 concentrations when incubated under high light only (Fig 3.4 a).

Furthermore, the unaccounted ~ 60% distinguishing the photorepair expressed through Chl *a* fluorescence and D1 protein concentration in *P. damicornis* can be explained by 1) up-regulated D1 protein synthesis, 2) Chl *a* fluorescence signals resolved from lincomycin treated samples may have been greater through the increase in photoinactivated photosynthetic units (PSU) (Matsubara and Chow 2004) relative to intact PSUs. As a result, the two techniques used here to express photorepair are essentially expressing different characteristics of the PSII state. Chl *a* fluorescence measurements only describe PSII functionality based on efficient sustaining of PSII integrity through photorepair and photodamage dynamics, which could also be accomplished through re-organisation of the PSUs (Hoogenboom et al. 2012; Robison and Warner 2006), so that no information about either of these processes can be independently assessed. Thus, inferences of photorepair through Chl *a* fluorescence assays needs to be treated with caution and interpreted as a combined measure of stress adjustments taking place to yield integrity of PSII PSUs. With the examination of changes in D1 concentration, on the other hand, the actual D1 photorepair can be determined along with the capacity of possible preventive *de novo* D1 synthesis under high light conditions.

#### ***3.4.4 Energy expenditure for photorepair***

Metabolic processes put in place to prevent photodamage by repairing damaged PSII centres are energy dependent and have been reported to result in enhanced dark respiration (Hoogenboom et al. 2006). The results presented here for *P. damicornis*, instead demonstrated unusual oxygen evolution during dark incubation for specimens with and without lincomycin (Fig 3.5 A, C) paired with high levels of D1 photodamage. As no increase in net photosynthetic oxygen production was detected for *P. damicornis*,

high respiratory oxygen uptake during the light could have masked the potential high levels of oxygen production; upon transition from light to dark oxygen then leaked into the surrounding media and therefore masked dark respiratory processes in the incubation time chosen here. These unusual oxygen exchange rates were accompanied by an increase in effective quantum yield (Y(II)) found after T<sub>96 h</sub> of experimental incubation for algal symbionts of *P. damicornis* (Fig 3.6) and support the interpretation of the possibly increased net photosynthetic oxygen production. During high light conditions enhanced respiratory processes are active (Chapter 5, Kühl et al. 1995) and therefore consume much of the oxygen produced, so that upon transition to the dark, oxygen is leaking out into the external media. Here a longer dark incubation would have been necessary to further investigate this phenomenon, as light dependent increased respiratory activity diminishes with acclimation to the dark (Cooper et al. 2011). However, the magnitude of such an effect was not anticipated and hasn't been reported before, so that the sampling and experimental design did not account for this. In contrast to this, the photosynthetic productivity in terms of oxygen exchange dynamics for *P. decussata* remained unchanged throughout the experiment. Light-driven oxygen consumption pathways can be in place for photoprotection in order to support antioxidative system and/or utilise excess energy (see Chapter 5) i.e. photorespiration (Crawley et al. 2010), chlororespiration (Cruz et al. 2011) and also the Mehler-ascorbate peroxidase (MAP) cycle (Schreiber et al. 1995a). Under high light stress *P. damicornis* displayed an exhaustion of xanthophyll cycling (Fig. 3.8 E), as well as greater photodamage and photorepair all in contrast to *P. decussata* (Fig. 3.4). Therefore, it seems likely that light-driven oxygen consuming processes are triggered by the higher stress levels and possibly higher ROS levels generated in *P. damicornis*.

### 3.4.5 Conclusion

The two coral species examined here are known to harbor the same symbiont subclade C1, where the coral host has been suggested to modulate their algal symbionts photosynthetic operation (Hill et al. 2012; Krämer et al. 2013). This could be confirmed here and it was further demonstrated, that *Symbiodinium* differs in their utilisation of photoprotective pathways depending on the coral host.

It was demonstrated in a new finding, that the two coral species examined here differ in their photorepair capacity and preventive *de novo* D1 synthesis. *P. damicornis* displayed great expenditure on photorepair necessary to counter the much greater photodamage experienced compared to *P. decussata*. Unusual oxygen evolution during the dark along with exhaustion of xanthophyll cycling is pointing towards extensive energy requirements to sustain the symbiosis of *P. damicornis* under high light stress. *P. decussata* demonstrated low photorepair requirements and a dynamic up-regulation of D1 synthesis in response to high light conditions, as well as unchanged xanthophyll cycling activity along with up-regulation of Y(NO); together these findings are indicating differential photoprotective strategies acting in *Symbiodinium* when harboured in this species. The results are conclusively pointing towards algal symbiont/coral host effect, where *Symbiodinium* utilises differential photoprotective pathways under high light stress. Clearly coral host characteristics such as tissue thickness, light channelling, build-up of ROS, ratio of symbionts to host tissue can all play a role in the response of the holobiont to stress conditions.

### 3.5 References

- Aro, E.-M., I. Virgin, and B. Andersson. 1993. Photoinhibition of Photosystem II. Inactivation, protein damage and turnover. *Biochimica et Biophysica Acta (BBA) - Bioenergetics* **1143**: 113-134.
- Bachmann, K., V. Ebbert, W. I. Adams, A. Verhoeven, B. Logan, and B. Demmig-Adams. 2004. Effects of lincomycin on PSII efficiency, non-photochemical quenching, D1 protein and xanthophyll cycle during photoinhibition and recovery. *Functional Plant Biology* **31**: 803-813.
- Baird, A. H., R. Bhagooli, P. J. Ralph, and S. Takahashi. 2009. Coral bleaching: the role of the host. *Trends in Ecology & Evolution* **24**: 16-20.
- Bongaerts, P., T. Ridgway, E. M. Sampayo, and O. Hoegh-Guldberg. 2010. Assessing the 'deep reef refugia' hypothesis: focus on Caribbean reefs. *Coral Reefs* **29**: 309-327.
- Brown, B. E., I. Ambarsari, M. Warner, W. Fitt, R. P. Dunne, S. W. Gibb, and D. G. Cummings. 1999a. Diurnal changes in photochemical efficiency and xanthophyll concentrations in shallow water reef corals: evidence for photoinhibition and photoprotection. *Coral Reefs* **18**: 99-105.
- Brown, C. M., D. A. Campbell, and J. E. Lawrence. 2007. Resource dynamics during infections of *Micromonas pusilla* by virus MpV-Sp1. *Environmental Microbiology* **9**: 2720-2727.
- Brown, E. M., J. D. Mackinnon, A. M. Cockshutt, T. A. Villareal, and D. A. Campbell. 2008. Flux capacities and acclimation costs in *Trichodesmium* from the Gulf of Mexico. *Marine Biology* **151**.
- Burriesci, M. S., T. K. Raab, and J. R. Pringle. 2012. Evidence that glucose is the major transferred metabolite in dinoflagellate - cnidarian symbiosis. *Journal of Experimental Biology* **215**: 3467-3477.
- Burton, G. W. 1990. Antioxidant properties of carotenoids. *Journal of Nutrition* **119**: 109-111.
- Cooper, T. F., K. E. Ulstrup, S. S. Dandan, A. J. Heyward, M. Kühl, A. Muirhead, R. A. O'leary, B. E. F. Ziersen, and M. J. H. Van Oppen. 2011. Niche specialization of reef-building corals in the mesophotic zone: metabolic trade-offs between divergent *Symbiodinium* types. *Proceedings of the Royal Society B* **278**: 1840-1850.



- Crawley, A., D. I. Kline, S. Dunn, K. R. N. Anthony, and S. Dove. 2010. The effect of ocean acidification on symbiont photorespiration and productivity in *Acropora formosa*. *Global Change Biology* **16**: 851-863.
- Cruz, S., R. Goss, C. Wilhelm, R. Leegood, P. Horton, and T. Jakob. 2011. Impact of chlororespiration on non-photochemical quenching of chlorophyll fluorescence and on the regulation of the diadinoxanthin cycle in the diatom *Thalassiosira pseudonana*. *Journal of Experimental Botany* **62**: 509-519.
- Davies, P. S. 1991. Effect of daylight variations on the energy budgets of shallow-water corals. *Marine Biology* **108**: 137-144.
- Demmig-Adams, B., and W. W. Adams. 1996. The role of xanthophyll cycle carotenoids in the photoprotection of photosynthesis. *Trends in Biochemical Sciences* **1**: 21-26.
- Demmig-Adams, B., and W. W. Adams. 2006. Photoprotection in an ecological context: the remarkable complexity of thermal energy dissipation. *New Phytologist* **172**: 11-21.
- Demmig-Adams, B., C. M. CoHu, O. Muller, and W. W. R. Adams. 2012. Modulation of photosynthetic energy conversion efficiency in nature: from seconds to seasons. *Photosynthesis Research* **113**: 75-88.
- Dunn, S. R., J. R. Thomason, M. D. A. Le Tissier, and J. C. Bythell. 2004. Heat stress induces different forms of cell death in sea anemones and their endosymbiotic algae depending on temperature and duration. *Cell Death and Differentiation* **11**: 1-10.
- Edelman, M., and A. K. Mattoo. 2008. D1-protein dynamics in photosystem II: The lingering enigma. *Photosynthesis Research* **98**: 609-620.
- Edge, R., and G. T. Truscott. 1999. Carotenoid radicals and the interaction of carotenoids with active oxygen species, p. 223-234. *In* H. A. Frank, A. J. Yound, G. Britton and R. J. Cogdell [eds.], *The photochemistry of carotenoids, advances in photosynthesis*. Kluwer Academic Publishers.
- Edmunds, P. J., and R. D. Gates. 2002. Normalizing physiological data for scleractinian corals. *Coral Reefs* **21**: 193-197.
- Frank, H. A., A. Cua, V. Chynwat, A. Young, D. Gosztola, and Wasielewski. 1996. The lifetimes and energies of the first excited singlet states of diadinoxanthin and diatoxanthin: the role of these molecules in excess energy dissipation in algae. *Biochimica et Biophysica Acta* **1277**: 243-252.

- Genty, B., J.-M. Briantais, and N. R. Baker. 1989. The relationship between the quantum yield of photosynthetic electron transport and quenching of chlorophyll fluorescence. *Biochimica et Biophysica Acta* **990**: 87-92.
- Glynn, P. W., J. L. Mate, A. C. Baker, and M. O. Calderon. 2001. Coral bleaching and mortality in Panama and Ecuador during the 1997-1998 El Niño-Southern Oscillation event: spatial/temporal patterns and comparisons with the 1982-1983 event. *Bulletin of Marine Science* **69**: 79-109.
- Gorbunov, M. Y., Z. S. Kolber, M. P. Lesser, and P. G. Falkowski. 2001. Photosynthesis and photoprotection in symbiotic corals. *Limnology and Oceanography* **46**: 75-85.
- Grimsditch, G., J. Mwaura, J. Kilonzo, N. Amiyo, and D. Obura. 2008. High zooxanthellae densities and turnover correlate with low bleaching tolerance in Kenyan corals, p. 235-236. *In* D. O. Obura, J. Tamelander and O. Linden [eds.], Ten years after bleaching- facing the consequences of climate change in the Indian Ocean. CORDIO Status Report 2008. Coastal Oceans Research and Development in the Indian Ocean/Sida-SAREC.
- Hennige, S. J., M. P. Mcginley, A. G. Grottoli, and M. E. Warner. 2011. Photoinhibition of *Symbiodinium* spp. within the reef corals *Montastraea faveolata* and *Porites astreoides*: implications for coral bleaching. *Marine Biology* **158**: 2515-2526.
- Hill, R., C. M. Brown, K. Dezeew, D. A. Campbell, and P. J. Ralph. 2011. Increased rate of D1 repair in coral symbionts during bleaching is insufficient to counter accelerated photoinactivation. *Limnology and Oceanography* **56**: 139-146.
- Hill, R., C. Frankart, and P. J. Ralph. 2005. Impact of bleaching conditions on the components of non-photochemical quenching in the zooxanthellae of a coral. *Journal of Experimental Marine Biology and Ecology* **322**: 83-92.
- Hill, R., A. W. D. Larkum, C. Frankart, M. Kühl, and P. J. Ralph. 2004. Loss of functional photosystem II reaction centers in zooxanthellae of corals exposed to bleaching conditions: using fluorescence rise kinetics. *Photosynthesis Research* **82**: 59-72.
- Hill, R., A. W. D. Larkum, O. Prášil, D. M. Kramer, V. Kumar, and P. J. Ralph. 2012. Light-induced redistribution of antenna complexes in the symbionts of scleractinian corals correlates with sensitivity to coral bleaching. *Coral Reefs* **31**: 963-975.

- Hill, R. W., C. Li, A. D. Jones, J. P. Gunn, and P. R. Farade. 2010. Abundant betaines in reef-building corals and ecological indicators of a photoprotective role. *Coral Reefs* **29**: 869-880.
- Hoegh-Guldberg, O. 1999. Climate change, coral bleaching and the future of the world's coral reefs. *Marine & Freshwater Research* **50**: 839-866.
- Hoegh-Guldberg, O., and R. J. Jones. 1999. Photoinhibition and photoprotection in symbiotic dinoflagellates from reef-building corals. *Marine Ecology Progress Series* **183**: 73-86.
- Hoogenboom, M. O., K. R. N. Anthony, and S. R. Connolly. 2006. Energetic cost of photoinhibition in corals. *Marine Ecology Progress Series* **313**: 1-12.
- Hoogenboom, M. O., D. A. Campbell, E. Beraud, K. Dezeew, and C. Ferrier-Pagès. 2012. Effects of light, food availability and temperature stress on the function of photosystem II and photosystem I of coral symbionts. *Plos One* **7**: e30167.
- Hoogenboom, M. O., S. R. Connolly, and K. R. N. Anthony. 2009. Effects of photoacclimation on the light niche of corals: a process-based approach. *Marine Biology* **156**: 2493-2503.
- Jones, R. J. 2004. Testing the 'photoinhibition' model of coral bleaching using chemical inhibitors. *Marine Ecology Progress Series* **284**: 133-145.
- Jones, R. J., and O. Hoegh-Guldberg. 2001. Diurnal changes in the photochemical efficiency of the symbiotic dinoflagellates (Dinophyceae) of corals: photoprotection, photoinactivation and the relationship to coral bleaching. *Plant Cell & Environment* **24**: 89-99.
- Klughhammer, C., and U. Schreiber. 2008. Complementary PS II quantum yields calculated from simple fluorescence parameters measured by PAM fluorometry and the saturation pulse method. *PAM Application Notes* **1**: 27-35.
- Kramer, D. M., G. Johnson, O. Kiirats, and G. E. Edwards. 2004. New fluorescence parameters for the determination of  $Q_A$  redox state and excitation energy fluxes. *Photosynthesis Research* **79**: 209-218.
- Krämer, W., V. Schrameyer, R. Hill, P. J. Ralph, and K. Bischof. 2013. PSII activity and pigment dynamics of *Symbiodinium* in two Indo-Pacific corals exposed to short-term high-light stress. *Marine Biology* **160**: 563-577.
- Kühl, M., Y. Cohen, T. Dalsgaard, B. B. Jorgensen, and N. P. Revsbech. 1995. Microenvironment and photosynthesis of zooxanthellae in scleractinian corals

- studies with microsensors for O<sub>2</sub>, pH and light. *Marine Ecology Progress Series* **117**: 159-172.
- Lesser, M. P. 1997. Oxidative stress causes coral bleaching during exposure to elevated temperatures. *Coral Reefs* **16**: 187-192.
- Lesser, M. P. 2006. Oxidative stress in marine environments: biochemistry and physiological ecology. *Annual Review of Physiology* **68**: 253-278.
- Lesser, M. P., and J. H. Farrell. 2004. Exposure to solar radiation increases damage to both host tissues and algal symbionts of corals during thermal stress. *Coral Reefs* **23**: 367-377.
- Levy, O., Z. Dubinsky, K. Schneider, Y. Achituv, D. Zakai, and M. Y. Gorbunov. 2004. Diurnal hysteresis in coral photosynthesis. *Marine Ecology Progress Series* **268**: 105-117.
- Macintyre, H. L., T. Kana, and R. J. Geider. 2000. The effect of water motion on short-term rates of photosynthesis by marine phytoplankton. *Trends in Plant Science* **5**: 12-17.
- Matsubara, S., and W. S. Chow. 2004. Populations of photoinactivated photosystem II reaction centers characterized by chlorophyll *a* fluorescence lifetime *in vivo*. *PNAS* **101**: 18234-18239.
- Mattoo, A. K., H. Hoffman-Falk, J. B. Marder, and M. Edelman. 1984. Regulation of protein metabolism coupling of photosynthetic electron transport to *in vivo* degradation of the rapidly metabolized 32-kilodalton protein of the chloroplast membranes. *Proceedings of the National Academy of Sciences U.S.A.* **81**: 1380-1384.
- Muscatine, L. 1990. The role of symbiotic algae in carbon and energy flux in reef corals, p. 75-87. *In* Z. Dubinsky [ed.], *Ecosystems of the World: Coral reefs*. Elsevier.
- Nishiyama, Y., S. I. Allakhverdiev, H. Yamamoto, H. Hayashi, and N. Murata. 2004. Singlet oxygen inhibits the repair of photosystem II by suppressing translation elongation of the D1 protein in *Synechocystis* sp. PCC 6803. *Biochemistry* **43**: 11321-11330.
- Ragni, M., R. L. Airs, S. J. Hennige, D. J. Suggett, M. E. Warner, and R. J. Geider. 2010. PSII photoinhibition and photorepair in *Symbiodinium* (Pyrrhophyta) differs between thermally tolerant sensitive phylotypes. *Marine Ecology Progress Series* **406**: 57-70.

- Reynolds, M. J., B. U. Bruns, W. K. Fitt, and G. W. Schmidt. 2008. Enhanced photoprotection pathways in symbiotic dinoflagellates of shallow-water corals and other cnidarians. *Proceedings of the National Academy of Sciences U.S.A.* **105**: 13674-13678.
- Richardson, M. J., W. D. Gardner, S. P. Chung, and D. Walsh. 1993. Source of beam attenuation signal as a function of particle size. *The Oceanography Society Meeting Abstracts, Seattle, Washington* **71**.
- Robison, J. D., and M. E. Warner. 2006. Differential impacts of photacclimation and thermal stress on the photobiology of four different phylotypes of *Symbiodinium* (Pyrrhophyta). *Journal of Phycology* **42**: 568-579.
- Schreiber, U. 2004. Pulse-amplitude-modulation (PAM) fluorometry and saturation pulse method: an overview, p. 279-319. *In* G. C. Papageorgiou and Govindjee [eds.], *Chlorophyll a fluorescence: a signature of photosynthesis*. *Advances in Photosynthesis and Respiration*. Springer.
- Schreiber, U., H. Hormann, K. Asada, and C. Neubauer. 1995. O<sub>2</sub>-dependent electron flow in intact spinach chloroplasts: properties and possible regulation of the Mehler-Ascorbate-Peroxidase cycle, p. 813-818. *In* P. Mathis [ed.], *Photosynthesis: from Light to Biosphere*. Kluwer Academic Publishers.
- Shipton, C. A., and J. Barber. 1991. Photoinduced degradation of the D1 polypeptide in isolated reaction centers of photosystem II: Evidence for an autoproteolytic process triggered by the oxidizing of the photosystem. *Proceedings of the National Academy of Sciences U.S.A.* **88**: 6691-6695.
- Six, C., Z. V. Finkel, A. J. Irwin, and D. A. Campbell. 2007. Light variability illuminates niche-partitioning among marine picocyanobacteria. *Plos One* **2**: e1341.
- Stimson, J., and R. A. Kinzie. 1991. The temporal pattern and rate of release of zooxanthellae from the reef coral *Pocillopora damicornis* (Linnaeus) under nitrogen-enrichment and control conditions. *The Journal of Experimental Biology* **153**: 66-74.
- Suggett, D. J., H. L. Macintyre, T. M. Kana, and R. J. Geider. 2010. Comparing electron transport with gas exchange: parameterising exchange rates between alternative photosynthetic currencies for eukaryotic phytoplankton. *Aquatic Microbial Ecology* **65**: 147-162.

- Takahashi, S., T. Nakamura, M. Sakamizu, R. Van Woesik, and H. Yamasaki. 2004. Repair machinery of symbiotic photosynthesis as the primary target of heat stress for reef-building corals. *Plant Cell Physiology* **45**: 231-235.
- Takahashi, S., S. M. Whitney, and M. R. Badger. 2009. Different thermal sensitivity of the repair of photodamaged photosynthetic machinery in cultured *Symbiodinium* species. *Proceedings of the National Academy of Sciences U.S.A.* **106**: 3237-3242.
- Vass, I. 2011. Role of charge recombination processes in photodamage and photoprotection of the photosystem II complex. *Physiologia Plantarum* **142**: 6-16.
- Vass, I., S. Styring, T. Hundal, A. Koivuniemi, E.-M. Aro, and B. Andersson. 1992. Reversible and irreversible intermediates during photoinhibition of Photosystem II - stable reduced  $Q_A$  species promote chlorophyll triplet formation. *Proceedings of the National Academy of Sciences U.S.A.* **89**: 8964-8973.
- Wang, J.-T., and A. E. Douglas. 1997. Nutrients, signals, and photosynthate release by symbiotic algae - the impact of taurine on the dinoflagellate alga *Symbiodinium* from the sea anemone *Aiptasia pulchella*. *Plant Physiology* **114**: 631-636.
- Wang, J. T., and A. E. Douglas. 1999. Essential amino acid synthesis and nitrogen recycling in an alga-invertebrate symbiosis. *Marine Biology* **135**: 219-222.
- Wangpraseurt, D., A. W. D. Larkum, P. J. Ralph, and M. Kühl. 2012. Light gradients and optical microniches in coral tissues. *Frontiers in Microbiology* **3**: 316.
- Warner, M. E., and S. Berry-Lowe. 2006. Differential xanthophyll cycling and photochemical activity in symbiotic dinoflagellates in multiple locations of three species of caribbean coral. *Journal of Experimental Marine Biology and Ecology* **339**: 86-95.
- Warner, M. E., W. K. Fitt, and G. W. Schmidt. 1999. Damage to photosystem II in symbiotic dinoflagellates: a determinant of coral bleaching. *Proceedings of the National Academy of Sciences U.S.A.* **96**: 8007-8012.
- Weis, V. M. 2008. Cellular mechanisms of cnidarian bleaching: stress causes the collapse of symbiosis. *The Journal of Experimental Biology* **211**: 3059-3066.
- Whitehead, L. F., and A. E. Douglas. 2003. Metabolite comparisons and the identity of nutrients translocated from symbiotic algae to an animal host. *The Journal of Experimental Biology* **206**: 3149-3157.

Wilkinson, C. R., O. Linden, and H. Cesar. 1999. Ecological and socio-economic impacts of 1998 coral mortality in the Indian Ocean: an ENSO impact and a waning of future change? *Ambio* **28**: 188-196.

Yellowlees, D., T. A. Rees, and W. Leggat. 2008. Metabolic interactions between algal symbionts and invertebrate hosts. *Plant, Cell & Environment* **31**: 679-694.

### 3.6 Supplementary information



**Figure S 3.6.1:** Representative immunoblot for psbA immunoblots. The presented blot shows samples of the final sampling event.



Page intentionally left blank

## Chapter 4

# A closed chamber system to quantify photosynthesis, respiration and bioenergetic fluxes of aquatic phototrophs

Verena Schrameyer<sup>1</sup>, Rolf Gademann<sup>2</sup>, Ross Hill<sup>1,3</sup>, Lars Behrendt<sup>4</sup>, Michael Kühl<sup>1,4,5</sup>, Anthony W.D. Larkum<sup>1</sup>, Peter J. Ralph<sup>1\*</sup>

<sup>1</sup> Plant Functional Biology and Climate Change Cluster, School of the Environment, University of Technology, Sydney, PO Box 123, Broadway, 2007, NSW, Australia

<sup>2</sup> Gademann Instruments GmbH, Dürrbachtal 232, 97080 Würzburg, Germany

<sup>3</sup> Centre for Marine Bio-Innovation, School of Biological, Earth and Environmental Sciences, The University of New South Wales, Sydney 2052 NSW, Australia

<sup>4</sup> Marine Biology Biology Section, Department of Biology, University of Copenhagen, Strandpromenaden 5, 3000 Helsingør, Denmark

<sup>5</sup> Singapore Centre on Environmental Life Sciences Engineering, School of Biological Sciences, Nanyang Technological University, Singapore

Keywords: metabolic gas exchange, respiration, CO<sub>2</sub> light compensation point, integrated measurement, photosynthetic efficiency

The following chapter is formatted to be submitted to the *Journal of Limnology and Oceanography Methods* and is therefore structured according to its journal guidelines in atypical outline to the other chapters.

## 4.1 Introduction

Light is the driving force for photosynthesis which involves the interplay of biophysical and biochemical reactions to transform harvested light energy into organic compounds. During the light reactions, photons are captured by light harvesting complexes (LHCs) and this energy is used to excite electrons split from water molecules in the oxygen evolving complex (OEC). The OEC donates electrons to the first electron acceptor ( $Q_A$ ) at the reaction centre (RC) of photosystem (PS) II (i.e. temporarily closing the RC) which then initiates intersystem linear electron transport between PSII and PSI (Falkowski and Raven 2007). When irradiance exceeds what can be utilised for photosynthesis, non-photochemical quenching (NPQ) mechanisms are activated to provide photoprotection (Demmig-Adams and Adams 2006; Franklin and Badger 2001). Variable chlorophyll (Chl) fluorescence can be detected with the application of the saturation flash technique (Schreiber 2004) using a pulse amplitude modulated (PAM) fluorometer, which forces all ‘open’ reaction centers (oxidised state) into a ‘closed state’ (reduced state), where Chl fluorescence signal reaches a maximum ( $F_M$ ) and is thus indicative of the reduction of RCII (Schreiber 2004). PAM fluorometry provides a fast, non-invasive tool to determine the PSII effective quantum yield ( $\Phi_{PSII}$ ) under ambient irradiance (Ralph and Gademann 2005; Schreiber et al. 1995b) and can be used to estimate the electron transport rate through PSII (Genty et al. 1989), as well as NPQ levels. The measurement of chlorophyll fluorometry enables researchers to infer about wide ranging physiological aspects of phototrophs in terms of their photosynthetic competency. In conjunction with other techniques the interpretation can further be extended to address highly specific questions e.g. about energy balancing within the photosynthetic apparatus as well as within the phototroph itself.

O<sub>2</sub> production rates are a direct measure for the photosynthetic rate at OEC and can be related to electron transport rates through PSII (Longstaff et al. 2002). A close correlation of ETR and O<sub>2</sub> production has been documented for e.g. *Ulva lactuca* for sub-saturating irradiances (Beer et al. 2000). This linear relationship breaks down once irradiance becomes excessive, with rates of O<sub>2</sub> production saturating, but ETR continuing to rise (Beer et al. 2000; Dubinsky et al. 1986; Kroon et al. 1993). An alternative method to quantify photosynthetic rate is the measure of CO<sub>2</sub> (C) fixation, which is driven by ATP and NADPH, where the latter is the ‘end product’ of the linear electron transport from PSII to PSI (Falkowski and Raven 2007). C fixation rates are therefore closely related to the linear electron transport estimated photosynthetic rate and hence Chl fluorescence emission (Genty et al. 1989). With an integrated measurement approach, changes in C fixation rates could therefore be interpreted by measures of variable Chl fluorescence and O<sub>2</sub> evolution.

However, determinations of photosynthetic rates using different methodologies do not always match due to the operation of alternative electron pathways (AEPs), causing a deviation of electrons away from linear electron transport and instead can use their reducing power for the assimilation of nitrogen and sulphur (Sivak and Walker 1985). Electrons can also enter a cyclic transport pathway around PSII and PSI (Ralph et al. 2010) e.g. for the generation of ATP, but this also as a mechanism to dissipate excess energy harvested in the antenna pigment-protein complexes (Finazzi et al. 2002; Walker and Walker 1988; Walker 1981). The non-linearity of Chl fluorescence to gross O<sub>2</sub> production and to gross C assimilation at over-saturating irradiances has been reported in previous studies (for review Suggett et al. 2010b). Chl fluorometry can be used to monitor linear electron transport; however, when a range of cyclic electron processes become operational it is not possible to use Chl fluorometry to allocate energy

partitioning between the linear and non-linear electron pathways. To capture a snapshot of light utilisation, the differentiation between these processes can be accomplished by monitoring O<sub>2</sub> and CO<sub>2</sub> exchange, as well as Chl fluorometry (linear electron transport) simultaneously.

Photosynthetic processes of aquatic oxygenic phototrophs are unlikely to be limited by the availability of water like it is the case in terrestrial phototrophs; they are more likely to be limited by light and carbon supply. Boundary layers surrounding aquatic organisms are much thicker compared to terrestrial systems and limit the passive diffusion of CO<sub>2</sub> through the membranes of phototrophs' (Raven and Hurd 2012; Schlichting and Gersten 2000; Smith and Walker 1980). In response, specialised uptake mechanisms have evolved, such as carbon concentrating mechanisms (CCMs) to take up molecules such as HCO<sub>3</sub><sup>-</sup> /CO<sub>2</sub> via active transport mechanisms (Raven 2003). Considering HCO<sub>3</sub><sup>-</sup> as well as CO<sub>2</sub> for photosynthetic substrate measurements is therefore essential and has been addressed with the development of the photobioreactor (PBR) demonstrated here.

In this study, the PBR was evaluated by taking measurements on a species of scleractinian coral. For the first time, this has enabled the measure of metabolic gas exchange in conjunction with PAM fluorometry of a coral symbiosis. Light is one of the most important and variable parameters in coral reef ecosystems (Veal et al. 2010) and is of great importance for corals since they are nutritionally dependent upon photosynthetic products from their endosymbiotic algae (genus *Symbiodinium*). Exposure to over-saturating irradiances can exceed the capacity of photoprotective NPQ processes (Hill et al. 2005) and lead to photodamage which has consequences for the overall coral symbiosis (Hill et al. 2012). Under conditions where photoinhibition occurs, this impairment of photosynthesis can limit the translocation of organic carbon

(photosynthate) to the coral host which it requires to meet up to 95% of its daily energetic demands (Grottoli et al. 2006; Iglesias-Prieto et al. 2004). In a coral symbiosis, the algal symbionts are dependent on the delivery of nutrients and dissolved inorganic carbon (DIC) from the host, to use as photosynthetic substrate (Dubinsky and Jokiel 1994; Tremblay et al. 2012b). Although CCMs are mostly reported for aquatic oxygenic phototrophs (Raven 2003), host animals of photosynthetic symbionts (such as corals) can also contain CCMs to obtain DIC from the external surroundings for their photosynthetic symbionts (Goffredi et al. 1999) and additionally internal metabolically derived DIC can serve as photosynthetic substrate (Al-Horani et al. 2003a; Leggat et al. 1999). While light fuels photosynthesis, respiration and calcification of a coral host are also light driven processes as the level of photosynthetic activity drives the nutritional sustenance necessary for active processes (Al-Horani et al. 2003a; Atkin et al. 1998; Crawley et al. 2010; Edmunds and Davies 1988). Here the application of the PBR can help to distinguish between key processes occurring within a coral holobiont during exposure to light.

In the following, the measurement principle and operation of the newly developed PBR will be demonstrated and measurement applications performed on the coral species *Pocillopora damicornis* will be presented, where the impact of various light intensities on photophysiological processes and metabolic gas exchange of the coral holobiont were examined.

## 4.2 Materials and Procedures

### 4.2.1 Instrumental setup

A photobioreactor (PBR; see Fig. 4.1) setup was developed to simultaneously measure Chl fluorescence, O<sub>2</sub> and DIC (indirectly measured via CO<sub>2</sub> in the gas-phase, see 4.3.2) exchange rates. The PBR consisted of an Algae-Growth PAM, an enclosed, water jacketed perspex chamber (enabling temperature regulation, ± 0.1°C), containing a sample holder for the aquatic specimen. The chamber had a volume of 207 mL and was equipped with an external stirrer module to propel a magnetic stir bar inside the chamber, a thermocouple (± 0.1 °C; type K thermoelement, Walz, Effeltrich, Germany), a submersible 4π PAR sensor (US-SQS/L, Walz, Effeltrich, Germany), a plastic fiber optic (Ø 0.32 cm) orientated at 45° to the specimen for PAM measurements, as well as an O<sub>2</sub> sensor based on optical detection principle (REDFLASH technology, Pyroscience, Aachen, Germany; (Borisov et al. 2008)). The PAM fiber optic was freely adjustable in vertical movement, as well as the 4π PAR sensor to be positioned flexibly depending on the specimen. In front of the sample chamber a 96 single-spot warm white LED panel (NS2L123BT, Nichia, Japan) was mounted and allowed for the homogeneous delivery of white light up to 1650 μmol photons m<sup>-2</sup> s<sup>-1</sup>. The sample chamber (holding the liquid-phase and specimen) was connected to an Infrared Gas-Analyser (IRGA; MGA3000, ADC Gas Analysis; calibrated regularly with span-gas of 452 ppm CO<sub>2</sub>) detecting CO<sub>2</sub> in parts per million (ppm) (detection range: 0-1462 ppm). The built-in IRGA pump was used to circulate air within the closed gas-circuit and through the liquid-phase, effervescing at a rate of 500 mL min<sup>-1</sup> through the sample chamber.

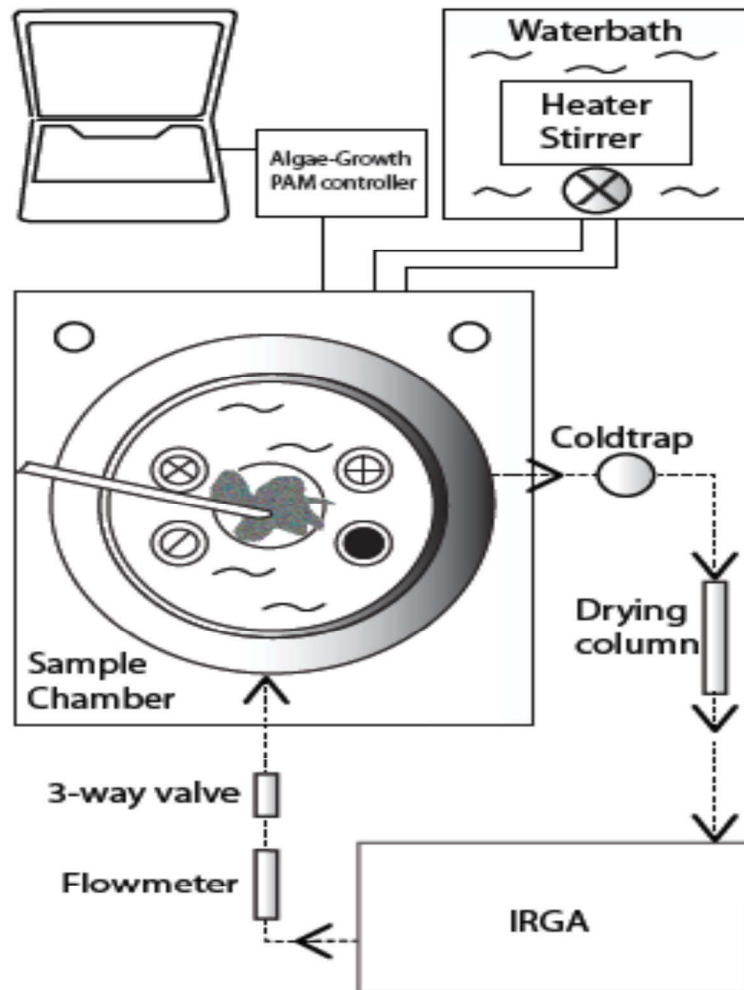


**Figure 4.1:** Schematic of the photosynthesis bioreactor (PBR); the system consists of a laptop for data management and device operation, an Algae-Growth-PAM computer interface as an optional controlling device, a temperature controlled water-bath and a pump, which feeds into the water jacket of the sample chamber. Within the sample chamber 4 sensor slots (indicated as circled symbols: pH, temperature, O<sub>2</sub> optode, 4π PAR sensor) and a PAM fiber optic (45° angle to the specimen) are recording measurements within the liquid-phase at or near the specimen surface; the mounting spots for the front-mounted LED panel are indicated as white circles on the sample chamber; the gas-phase was a closed circuit connecting a cold-trap, a drying column, an IRGA for CO<sub>2</sub> detection, flowmeter, 3-way luer-lock valve for N<sub>2</sub> purging and/or calibration. The gas flow direction is indicated by the arrows (measures are not to size).



The detection of CO<sub>2</sub> in the gas-phase therefore displayed changes in dissolved inorganic carbon (DIC) within the liquid-phase once the two aggregation phases were in equilibrium (see 4.3.2). This measurement procedure is based on the equilibrium between liquid- and gas-phase following Henry's gas law. Changes in DIC concentration, regardless of which DIC species (CO<sub>2</sub>, HCO<sub>3</sub><sup>-</sup> or CO<sub>3</sub><sup>2-</sup>), occurring in the liquid-phase can therefore be detected as fluctuations in the CO<sub>2</sub> concentration in the gas-phase (Burba et al. 2012). This consideration is important when using the PBR for certain aquatic phototrophs equipped with CCMs that are capable of taking up HCO<sub>3</sub><sup>-</sup>, as well as CO<sub>2</sub> as a DIC substrate (Leggat et al. 1999; Raven and Hurd 2012). Considering indirectly the total DIC via gaseous measurements of CO<sub>2</sub> (after passing through two drying steps, a cold-trap and a drying filter to guarantee dried air and no interference of water vapour), therefore allows defining the total net photosynthetic C substrate uptake and can be related to C fixation. The IRGA was controlled with a custom programmed LabView application (National Instruments), and the sample chamber sensors, stirrer and LED panel were controlled with the WinControl 3 program (Walz, Effeltrich, Germany) or on the Algae-Growth PAM controller interface.

#### ***4.2.2 Gaseous DIC and O<sub>2</sub> exchange measurements***

Gaseous CO<sub>2</sub> concentrations were detected in units of ppm and converted to molar units using the specific molar volume (V<sub>n</sub>) of ideal gas for carbon dioxide (55 cm<sup>3</sup> mol<sup>-1</sup>) to convert measured ppm flux rates into molar concentrations (Huang et al. 2005). O<sub>2</sub> concentrations were detected in the liquid-phase and rates were corrected for equilibration with the gas-phase by using the ideal gas law considering ambient temperature and pressure (Levine 1974) (see 4.3.5).

Net metabolic gas exchange rates for O<sub>2</sub> (P<sub>netO<sub>2</sub></sub>) and DIC (P<sub>netDIC</sub>) were obtained during light incubations, while the corresponding respiratory flux rates (R<sub>O<sub>2</sub></sub> and R<sub>CO<sub>2</sub></sub>) were obtained during dark incubation. Gross photosynthetic flux rates for O<sub>2</sub> and DIC (P<sub>gO<sub>2</sub></sub> and P<sub>gDIC</sub>) were calculated from the sum of net and respiratory flux rates (Falkowski and Raven 2007).

#### ***4.2.3 Measurement protocol***

Various light intensities were applied to establish a photosynthesis vs irradiance (P – E) curve with additional integrated PBR parameters (as outlined above). The Chl fluorescence saturation pulse technique (Schreiber 2004) using the PAM fluorometer (saturation pulses of 0.6 s and ~8,000 μmol photons m<sup>-2</sup> s<sup>-1</sup> blue excitation light with peak excitation of 450 nm), was used to measure maximum quantum yield (F<sub>v</sub>/F<sub>M</sub>; measured on dark-adapted samples) and effective quantum yield (Φ<sub>PSII</sub>) measured on light-adapted samples). These parameters were then used to determine relative electron transport rate (rETR) = Φ<sub>PSII</sub> × E, where E is the incident light intensity. Non-photochemical quenching (NPQ) was also calculated as NPQ = (F<sub>M</sub> - F<sub>M'</sub>)/F<sub>M'</sub> (Ralph and Gademann 2005). The CO<sub>2</sub>/O<sub>2</sub> light compensation point (E<sub>c</sub>) is the irradiance where net photosynthetic carbon (C) uptake/O<sub>2</sub> evolution matches respiratory C liberation/respiratory O<sub>2</sub> uptake. E<sub>c</sub> can be determined by applying a double exponent curve fit model to either P<sub>netDIC</sub> rates (to determine CO<sub>2</sub> E<sub>c</sub>) or to P<sub>netO<sub>2</sub></sub> rates (to determine O<sub>2</sub> E<sub>c</sub>) (Platt et al. 1980; Tolbert et al. 1995).

#### 4.2.4 PBR application for coral holobiont/symbioses assessment

Metabolic gas exchange rates are applied in coral physiological assessments to determine metabolic quotients of the coral holobiont, which can be estimated according to Gattuso and Jaubert (1990):

$$(1) \quad PQ_{net} = \frac{netO_2 flux}{netDIC flux}$$

$$(2) \quad RQ_c = \frac{respiratio\,nal\,CO_2\,flux}{respiratio\,nal\,O_2\,flux}$$

$$(3) \quad PQ_z = \frac{PQ_{net} * (P_c net + R_c)}{P_c net * (PQ_{net} * RQ_c * R_c)}$$

Where the  $PQ_{net}$  is the photosynthetic quotient of the coral holobiont and is estimated using net  $O_2$  and DIC gaseous exchange from light incubations. Through this parameter the relation of photosynthetic  $O_2$  evolution to respiratory  $O_2$  demand can be quantified, where the greater the value, the greater the net photosynthetic productivity in terms of  $O_2$  evolution.  $RQ_c$ , is the coral respiratory quotient and is calculated via respirational  $CO_2$  and  $O_2$  gas exchange rates (Eq. 2).  $RQ_c$  can be extremely variable when respirational gas exchange parameters are not measured simultaneously (Hatcher 1989). To avoid this problem, Quetin et al. (1980) emphasized the importance for simultaneous measurements of  $O_2$  and  $CO_2$  gas exchange rates to determine accurate ratios without introducing systematic errors. With this new PBR system, these sources of variation can be eliminated due to the simultaneous measurement of  $O_2$  and  $CO_2$ .  $PQ_z$ , is the algal symbiont photosynthetic quotient, which relates respiratory and photosynthetic productivity of the *in hospite* algal symbiont, excluding the respiratory contribution of the coral host (Eq. 3) (Gattuso and Jaubert 1990).  $P_c net$  is the net photosynthetic  $O_2$

exchange of the coral holobiont, and  $R_c$  is the coral-specific respiratory  $O_2$  uptake (for more details on metabolic quotients see Gattuso and Jaubert 1990).

### 4.3 Assessment

#### 4.3.1 *Light source capacity and resolution*

To define irradiance settings of the Algae-Growth PAM into optically meaningful units ( $\mu\text{mol photons m}^{-2} \text{ s}^{-1}$ ) all 200 possible LED intensity settings were measured with a  $4\pi$  PAR sensor in a sample chamber filled with 0.2  $\mu\text{m}$  filtered seawater (FSW; salinity 35). The LED panel light intensities were adjusted in 0.5 % intensity increments (a fixed software setting of the Algae-Growth PAM) to a maximum of 100%. Incident irradiance within the liquid-phase was measured in close proximity to the sample-holder and specimen. Light intensity readings ranged between 0 – 1650  $\mu\text{mol photons m}^{-2} \text{ s}^{-1}$  and varied between each 0.5 % LED intensity increment by  $9.83 \pm 4.25 \mu\text{mol photons m}^{-2} \text{ s}^{-1}$  up until 1280  $\mu\text{mol photons m}^{-2} \text{ s}^{-1}$  (LED intensity setting maxima: 64.5 %). For all subsequent LED intensity increments PAR irradiances linearly increased by  $5.3 \pm 0 \mu\text{mol photons m}^{-2} \text{ s}^{-1}$  increments per 0.5 % to a maximum of 1650  $\mu\text{mol photons m}^{-2} \text{ s}^{-1}$ . This information enables users of the PBR to plan experimental P – E curve intensities and allows for the creation and utilisation of batchfiles to automate the running of the PBR. For aquatic phototrophs, a hyperbolic tangent function is typically applied to the P – E curve (photosynthetic rates of either  $O_2$ , ETR or  $CO_2$ ) (Jassby and Platt 1976), for calculation of photosynthetic efficiency  $\alpha$  (the initial slope of light saturation curve),  $E_K$  (saturation irradiance),  $P_{\text{max}}$  (light saturated photosynthetic rate) and  $\beta$  (declining slope at over-saturating light irradiances) (Jassby and Platt 1976).

### ***4.3.2 Gas circuit volume***

The total gas circuit volume of the PBR was determined for calculation of metabolic gas exchange rates in units of molar concentrations (to consider metabolic O<sub>2</sub> concentration changes in the gaseous- and liquid-phase). For this, the whole PBR setup (empty incubation chamber) was partially purged with N<sub>2</sub> through an in-line 3-way luer-lock syringe port (see Fig. 4.1). A known volume of ambient air was injected (10 mL), where CO<sub>2</sub> concentrations from pre- and post-injection readings (198 and 214 ppm respectively) were recorded. CO<sub>2</sub> concentration changes ( $c_1$ ), injection volume ( $v_1$ ) and ambient CO<sub>2</sub> concentration ( $c_2$ ; 860 ppm) were calculated to determine the total volume of the setup (537.5 mL) with the equation  $c_1 \times v_1 = c_2 \times v_2$ . Further the sample chamber was filled with water to the fill-volume used during measurements and water volume was measured using a standard glass cylinder (207 mL). By subtracting chamber volume from determined total setup volume the gas-circuit volume was established (330.5 mL). This information about gas-and liquid-phase volumes must be considered for calculations of total O<sub>2</sub> exchange rates (see 4.3.5).

### ***4.3.3 Gaseous exchange in the PBR and total alkalinity of incubation seawater***

#### ***4.3.3.1 Dissolved inorganic carbon speciation at different light intensities***

During light exposure, DIC concentrations change in the surrounding medium due to uptake of DIC as a photosynthetic substrate (Leggat et al. 1999) and also through respiratory CO<sub>2</sub> release of the coral holobiont, where the latter could ultimately elevate the pH and reduce total alkalinity of the incubation FSW (Kahara and Vermaat 2005). To test if the specimen causes changes in pH and/or alkalinity in the incubation FSW, nubbins of *P. damicornis* were exposed to four light steps (78, 210, 550 and 1100  $\mu\text{mol photons m}^{-2} \text{s}^{-1}$ ) to generate P – E curves, where 15 mL samples of the incubatory FSW were taken from the chamber after 20 min light incubation (according to required sampling incubation time, see 4.3.4) and 15 mL of fresh FSW was added. We could demonstrate by using the potentiometric endpoint titration technique using an autotitrator (DL 50 Mettler Toledo, Australia) (as described in detail in Sinutok et al. 2011) that in the 207 mL of incubatory FSW no significant changes in pH, total alkalinity or DIC species (HCO<sub>3</sub><sup>-</sup>, CO<sub>3</sub><sup>-2</sup>, CO<sub>2</sub>) occurred at any of the irradiance steps applied when coral specimens were measured over 20 min (one-way ANOVA results for each DIC species along with concentrations are displayed in Table 4.1). Any respiratory derived CO<sub>2</sub> has therefore been released as a result of the vigorous stirring and bubbling of the liquid-phase, forcing respiratory CO<sub>2</sub> into the gas-phase. Titration results showed that carbon substrate availability during each irradiance step of the P – E curve was not influenced by metabolic activity of the preceding irradiance exposure, therefore photosynthetic and physiological measurements should not be affected by changes in the carbon chemistry of the incubation FSW.

**Table 4.1:** Parameters of the carbonate system each of 4 sampled light intensity incubations; pH, total dissolved inorganic carbon (DIC), total inorganic carbon speciations ( $\text{CO}_2$ ,  $\text{CO}_3^{2-}$ ,  $\text{HCO}_3^-$ ), total alkalinity (TA) (n=3; mean  $\pm$  SEM).

Light intensity ( $\mu\text{mol photons m}^{-2} \text{ s}^{-1}$ )	pH	Total DIC ( $\text{mmol kg SW}^{-1}$ )	$\text{CO}_2$ ( $\text{mmol kg SW}^{-1}$ )	$\text{HCO}_3^-$ ( $\text{mmol kg SW}^{-1}$ )	$\text{CO}_3^{2-}$ ( $\text{mmol kg SW}^{-1}$ )	TA ( $\text{mmol kg SW}^{-1}$ )
<b>78</b>	8.09 $\pm$ 0.02	2.157 $\pm$ 0.034	0.010 $\pm$ 1.18e-3	1.866 $\pm$ 0.032	0.281 $\pm$ 0.027	2.545 $\pm$ 59.75
<b>210</b>	8.18 $\pm$ 0.03	2.227 $\pm$ 0.057	0.010 $\pm$ 1.38e-3	1.927 $\pm$ 0.061	0.290 $\pm$ 0.025	2.623 $\pm$ 64.50
<b>550</b>	8.14 $\pm$ 0.06	2.410 $\pm$ 0.078	0.011 $\pm$ 1.69e-3	2.087 $\pm$ 0.091	0.312 $\pm$ 0.022	2.827 $\pm$ 61.27
<b>1100</b>	8.17 $\pm$ 0.05	2.193 $\pm$ 0.116	0.010 $\pm$ 1.80e-3	1.901 $\pm$ 0.125	0.282 $\pm$ 0.014	2.581 $\pm$ 97.33
Statistical results one-way ANOVA	n/a	F(3,12) = 2.109 p = 0.152	F(3,12) = 0.124 p = 0.944	F(3,12) = 1.343 p = 0.311	F(3,12) = 0.400 p = 0.755	F(3,12) = 4.034 p = 0.0708

#### 4.3.3.2 Dissolved inorganic carbon speciation at different salinity regimes

In the PBR applied here, a decrease in DIC concentrations within the liquid-phase due to C uptake of the phototrophic specimen is therefore modified through the prevalence of the gas-phase. To demonstrate this, specimens of *P. damicornis* were incubated in FSW with two salinity regimes and corresponding DIC concentrations. Specimens were incubated in FSW with ambient salinity (35) and DIC concentrations, as well as in FSW which was diluted with reverse-osmosis (RO) water to a salinity of 25, which decreased the DIC concentration (Fig. 4.2). The equilibrating CO<sub>2</sub> concentrations of gas- and liquid-phase relative to initial CO<sub>2</sub> concentrations were measured with the IRGA during 30 min incubation. The concentrations of each DIC species (HCO<sub>3</sub><sup>-</sup>, CO<sub>3</sub><sup>-2</sup>, CO<sub>2</sub>) for each salinity regime at the beginning of the incubation were determined by potentiometric endpoint titration using an autotitrator and are indicated in Fig. 4.2 along with the % loss of each DIC species. Total DIC concentration decreased by 35 % upon dilution to a salinity of 25 from ambient 35. Equilibration of gas- and liquid-phase was established after 10 min for both salinity regimes. Resulting equilibrating CO<sub>2</sub> concentrations in the gas-phase after 10 min deviated with a difference of 10 % between the two salinity regimes (after 10 min 103 % for salinity of 35 and 93 % for salinity of 25). The lower equilibration CO<sub>2</sub> concentration found for the salinity of 25 is a result of gaseous CO<sub>2</sub> dissolving into the liquid-phase. Lowering DIC concentrations due to processes such as CCM uptake mechanisms are therefore being controlled through the prevailing gas-phase in the PBR and allow for detection within the gas-phase.



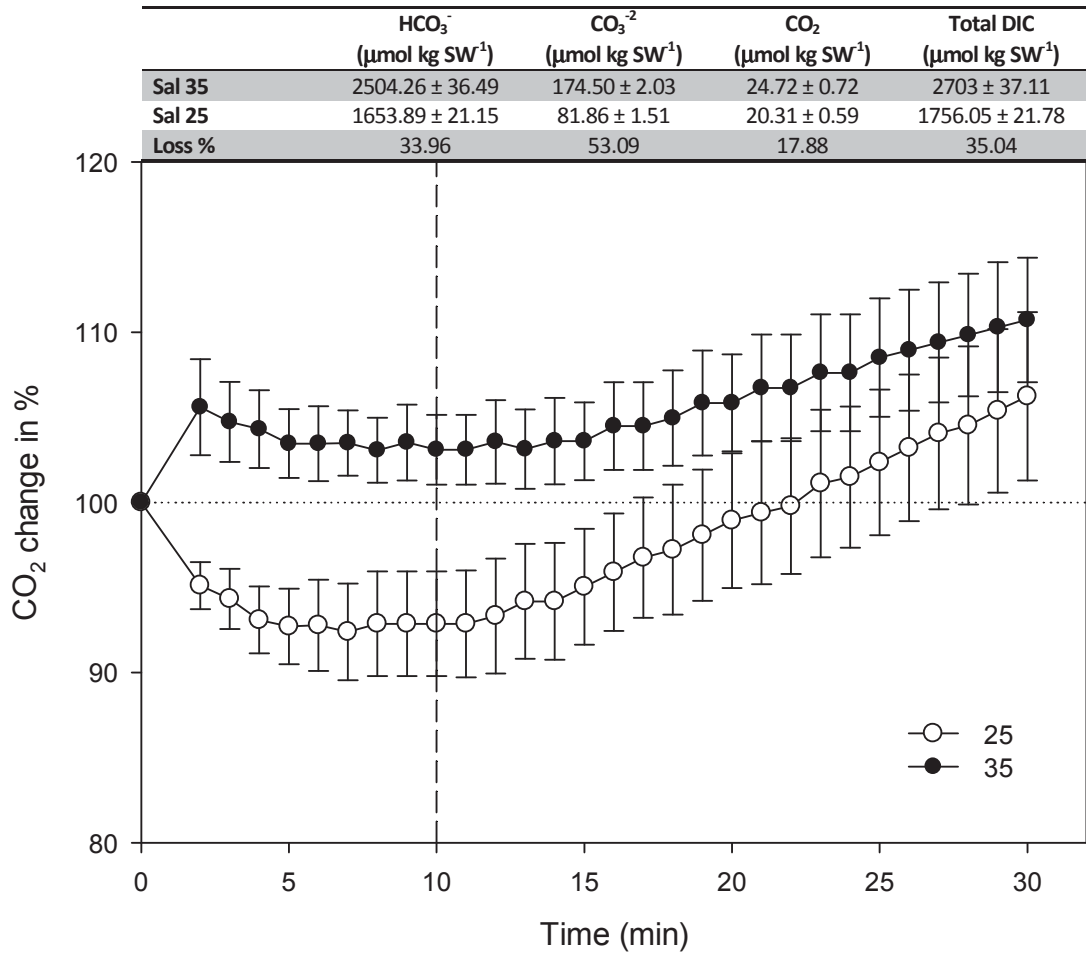


**Figure 4.2:** Relative changes (%) of CO<sub>2</sub> concentrations upon equilibration with gas- and liquid-phase (here indicated with a dashed vertical line) to initial CO<sub>2</sub> concentrations. Dark incubations of *Pocillopora damicornis* while incubating in FSW with two salinity regimes, salinity of 35 and 25 and resulting DIC species concentrations. The DIC species concentrations (HCO<sub>3</sub><sup>-</sup>, CO<sub>3</sub><sup>-2</sup>, CO<sub>2</sub> μmol kg SW<sup>-1</sup>) and total DIC (μmol kg SW<sup>-1</sup>) of salinity 35 and salinity 25, as well as the % loss in DIC species concentrations and total DIC from salinity of 35 to salinity of 25 are indicated in the table above the graph. Displayed are mean ± SEM (n = 3).

#### 4.3.4 Gas- and liquid-phase equilibration times

The DIC exchange rates measured with the PBR are based on the gas equilibration principle according to Henry's gas law (Levine 1974). As outlined above, once the system is in equilibrium, any changes which are occurring within the liquid-phase (such as metabolic gas exchange) are detected in the gas-phase. To ensure that the PBR represented a closed system, N<sub>2</sub> gas was pumped into the system for 30 min and then sealed. CO<sub>2</sub> was measured with the IRGA for 60 mins and no CO<sub>2</sub> concentration change was detected (data displayed for the first 14 min in Fig. 4.3 a).

The PBR applied here had a significantly greater gas-phase volume compared to the liquid-phase volume due to internal instrument volume of the IRGA (gas-phase 1.6 times larger compared to liquid-phase). To account for this it was necessary to determine the equilibration time between these two phases in order to plan experimental incubation times accordingly. Further, unusual non-linear changes below and above E<sub>c</sub> (O<sub>2</sub> and CO<sub>2</sub> E<sub>c</sub>) in variable Chl fluorescence signals (fluorescence quenching) as well as metabolic gas exchange rates have been described previously, due to chlororespiration formerly described as 'Kok effect' (Beardall et al. 2004; Kok 1948). These effects need to be taken into consideration for integrated measurement approaches like the ones demonstrated here. To demonstrate this, equilibration times between gas- and liquid-phase below and above E<sub>c</sub> were determined for a specimen of *P. damicornis*. The CO<sub>2</sub>E<sub>c</sub> for the coral specimen measured here was determined to be at 78 μmol photons m<sup>-2</sup> s<sup>-1</sup> (net photosynthetic DIC exchange rates were fitted with a 4 parameter exponential model). Coral specimens (n = 3) were incubated at 350 μmol photons m<sup>-2</sup> s<sup>-1</sup> (above CO<sub>2</sub>E<sub>c</sub>) and at 40 μmol photons m<sup>-2</sup> s<sup>-1</sup> (below CO<sub>2</sub>E<sub>c</sub>) until equilibration, where steady gas exchange rates were detected with the IRGA (Fig. 4.3 a,

b). Post-illumination dark incubation after exposure to above  $\text{CO}_2\text{E}_c$  ( $350 \mu\text{mol photons m}^{-2} \text{ s}^{-1}$ ) and below  $\text{CO}_2\text{E}_c$  ( $40 \mu\text{mol photons m}^{-2} \text{ s}^{-1}$ ) were used to determine equilibration times of gas and liquid-phase until steady-state respiration rates could be determined (Fig. 4.3 c, d). An equilibration period of 5 min was required to detect DIC uptake when exposed to  $350 \mu\text{mol photons m}^{-2} \text{ s}^{-1}$  and 5 mins was also required for the detection of  $\text{CO}_2$  evolution during post-illumination incubation at this irradiance (Fig. 4.3 a,c). For irradiances below  $\text{CO}_2\text{E}_c$ , all specimens displayed steady rates after an equilibration phase of  $\sim 10$  min, but displayed differing DIC exchange ( $40 \mu\text{mol photons m}^{-2} \text{ s}^{-1}$ ) (Fig. 4.3 b, rates of individual replicates are displayed). One specimen indicated DIC uptake and the other two specimens showed steady  $\text{CO}_2$  concentrations to slight respiratory  $\text{CO}_2$  evolution (Fig 4.3 b). Post-illumination dark incubations following exposure to  $40 \mu\text{mol photons m}^{-2} \text{ s}^{-1}$  yielded steady respiratory  $\text{CO}_2$  evolution rates after 10 min equilibration time (Fig. 4.3 d). DIC exchange rates for light incubations below  $\text{CO}_2\text{E}_c$  as presented here are highlighting the importance of defining  $\text{CO}_2\text{E}_c$  for the chosen specimen prior to any PBR measurement applications. This is especially important when combining gas exchange and Chl fluorescence measurements, as metabolic net gas exchange is zero at  $\text{CO}_2\text{E}_c$  ( $P_{\text{net}} = R$ ) (Tolbert et al. 1995).

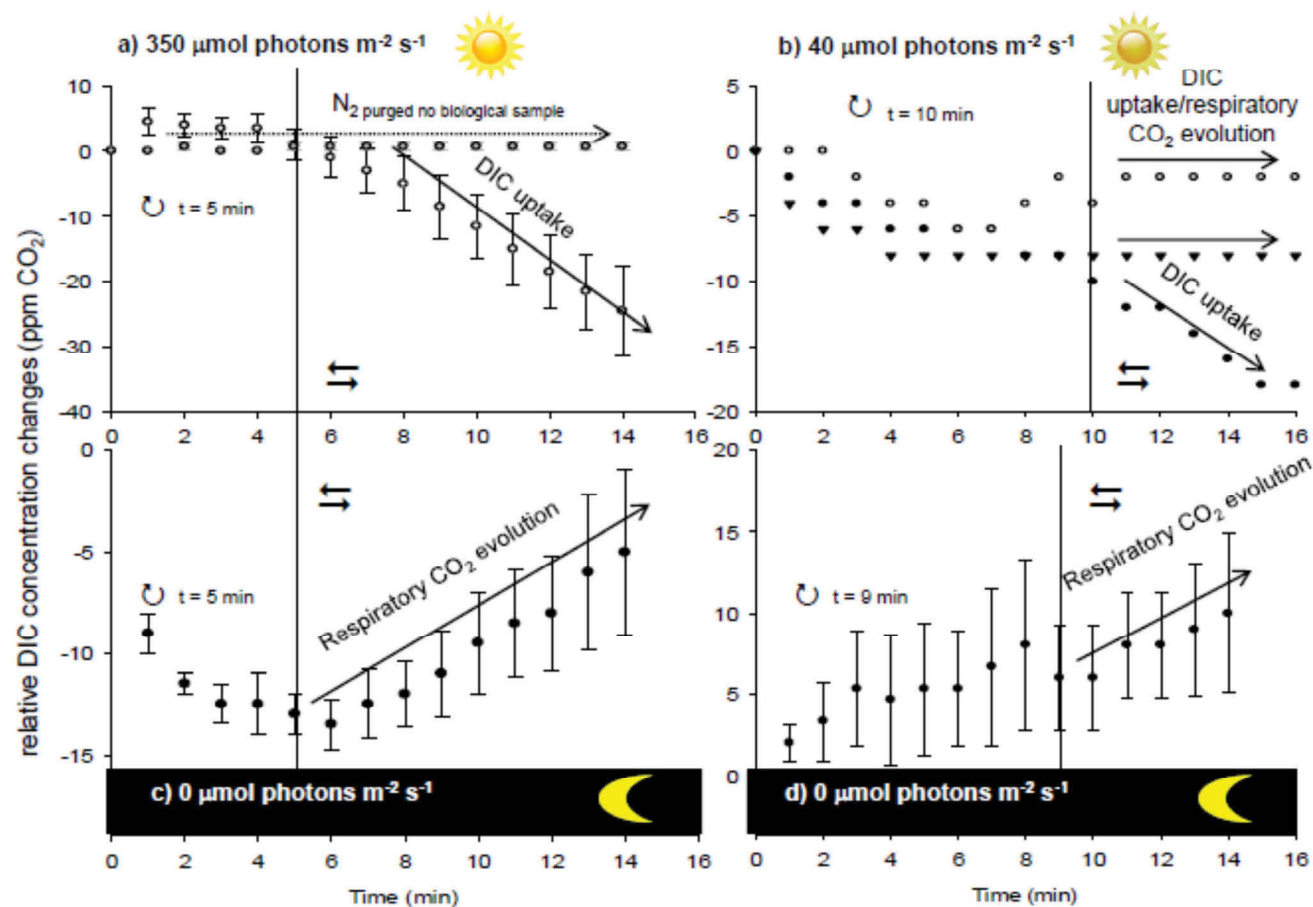


**Figure 4.3:** Results of gas- and liquid-phase equilibration times for CO<sub>2</sub> concentrations (ppm) as a function of incubation time for *Pocillopora damicornis* (n=4, standard errors are indicated) incubated at irradiances above and below O<sub>2</sub> compensation point ( $E_c$ ), (a) 350 μmol photons m<sup>-2</sup> s<sup>-1</sup> and (b) 40 μmol photons m<sup>-2</sup> s<sup>-1</sup>, respectively and post-illumination incubation of above and below  $E_c$  irradiances (c), (d) are displayed. N<sub>2</sub> purged and closed system CO<sub>2</sub> readings without biological specimen and FSW (liquid-phase) are inserted in panel a) for comparison; each panel includes information about equilibration phase time indicated with a circled arrow and equilibration time (t) next to it; pre- and post-equilibration phase are additionally indicated by separation with a dotted line in each panel. Displayed are mean ± SEM (n = 3). To highlight gas exchange variation of light incubations below  $E_c$ , replicates were plotted individually (b).

#### 4.3.5 O<sub>2</sub> concentration measurement

For correct calculations of O<sub>2</sub> exchange rates derived from PBR measurements, the physical properties of O<sub>2</sub> whether in gas- or in liquid-phase within the PBR circuit, need to be considered. Water and air are very different in their O<sub>2</sub> concentration (< 1% vs 20.9%, respectively), where dissolved O<sub>2</sub> (DO) concentrations are also temperature dependent, so that higher temperatures cause a decrease in DO (Levine 1974). During PBR operation, the strong stirring along with the effervescing of the gas-circuit through the liquid-phase of the sample chamber allowed for CO<sub>2</sub> detection in the gas-phase, but also forces DO to turn into its gaseous phase O<sub>2</sub>. To account for this, a mathematical correction of the measured DO exchange rates was applied to define the actual O<sub>2</sub> produced. Changes in DO concentrations were related to O<sub>2</sub> concentration changes in the gaseous phase as per Henry's gas law and calculated using the ideal gas law (Levine 1974). To validate these O<sub>2</sub> rate calculation corrections, a specimen of *P. damicornis* was first measured in a closed sample chamber (only stirred liquid-phase) and immediately after with the whole PBR setup (gas- and liquid-phase) for comparison. The coral was measured for 10 min in the closed sample chamber and subsequently for ~ 30 min in the whole PBR setup at a light exposure of 350 μmol photons m<sup>-2</sup> s<sup>-1</sup>. To calculate the % increase of O<sub>2</sub> in the gas-phase, the following factors were assumed: i) the gas-circuit of our PBR was 0.331 L and the liquid-phase volume was 0.207 L, ii) O<sub>2</sub> takes up 20.9 % in ambient air, iii) the ideal gas law assumes that at room temperature (293 K) 1 mol of O<sub>2</sub> occupies a volume of 24 L. Following these assumptions, the gas-circuit volume was calculated to be 0.003 mol O<sub>2</sub> at ambient conditions. During the measurements of a coral in the closed sample chamber, a production of 0.468 μmol DO min<sup>-1</sup> was detected. When incubated with the whole PBR setup Pnet<sub>O<sub>2</sub></sub> caused a DO increase of 0.4 % within the liquid-phase, resulting in an estimated increase of 11.84

$\mu\text{mol O}_2$  in the gas-phase and taking the sum of the measured  $0.19 \mu\text{mol DO}$  increase within the liquid-phase over an incubation time of  $1700 \text{ s}$  equates to an actual  $\text{Pnet}_{\text{O}_2}$  of  $0.418 \mu\text{mol O}_2 \text{ min}^{-1}$ . Our correction calculation of  $\text{Pnet}_{\text{O}_2}$  rates for algal symbionts when measured in the whole PBR setup resulted in an accuracy of  $89 \%$  relative to DO production rates of closed sample chamber (liquid-phase only) measurements. The  $11\%$  lower  $\text{O}_2$  production of the coral measured in the whole PBR setup could be a result of the three times longer incubation time at  $350 \mu\text{mol photons m}^{-2} \text{ s}^{-1}$  irradiance exposure when the coral was measured in the PBR system.

#### ***4.3.6 Coral holobiont gaseous exchange and photosynthetic efficiency***

Fragments of *P. damicornis* ( $n = 3$ ) were measured in the PBR with 6 light steps ( $78, 210, 360, 560, 860$  and  $1100 \mu\text{mol photons m}^{-2} \text{ s}^{-1}$ ) to obtain P – E curves for  $\text{O}_2$  and DIC exchange, as well as Chl fluorometry parameters ( $r\text{ETR}$ ,  $\text{NPQ}$ ,  $\Phi_{\text{PSII}}$ ). For normalisation of metabolic gas exchange parameters, coral specimen surface area was determined using single-dip waxing (Stimson and Kinzie 1991). Metabolic gas exchange rates as a function of irradiance are demonstrated in Figure 4.4.

$\text{Pg}_{\text{DIC}}$  rates were steady and remained unchanged up to  $1100 \mu\text{mol photons m}^{-2} \text{ s}^{-1}$  (one-way ANOVA,  $F(5,12) = 0.449$ ,  $p = 0.807$ ; Fig. 4.4 a). In comparison,  $\text{Pg}_{\text{O}_2}$  rates increased with increasing irradiances (one-way ANOVA,  $F(5,11) = 4.3972$ ,  $p = 0.042$ ; Fig 4 a) to a maximum at  $860 \mu\text{mol photons m}^{-2} \text{ s}^{-1}$  ( $17.29 \pm 2.87 \mu\text{mol O}_2 \text{ cm}^{-2} \text{ h}^{-1}$ , Tukey HSD,  $p < 0.05$ ) (Fig. 4.4 a).  $\text{Pg}_{\text{O}_2}$  rates as obtained here followed a classical P – E curve response, where there is typically a positive correlation with increasing irradiances at low light levels, which plateau for saturating irradiances, followed by a downturn at over-saturating irradiances (Jassby and Platt 1976; Ritchie 2008).

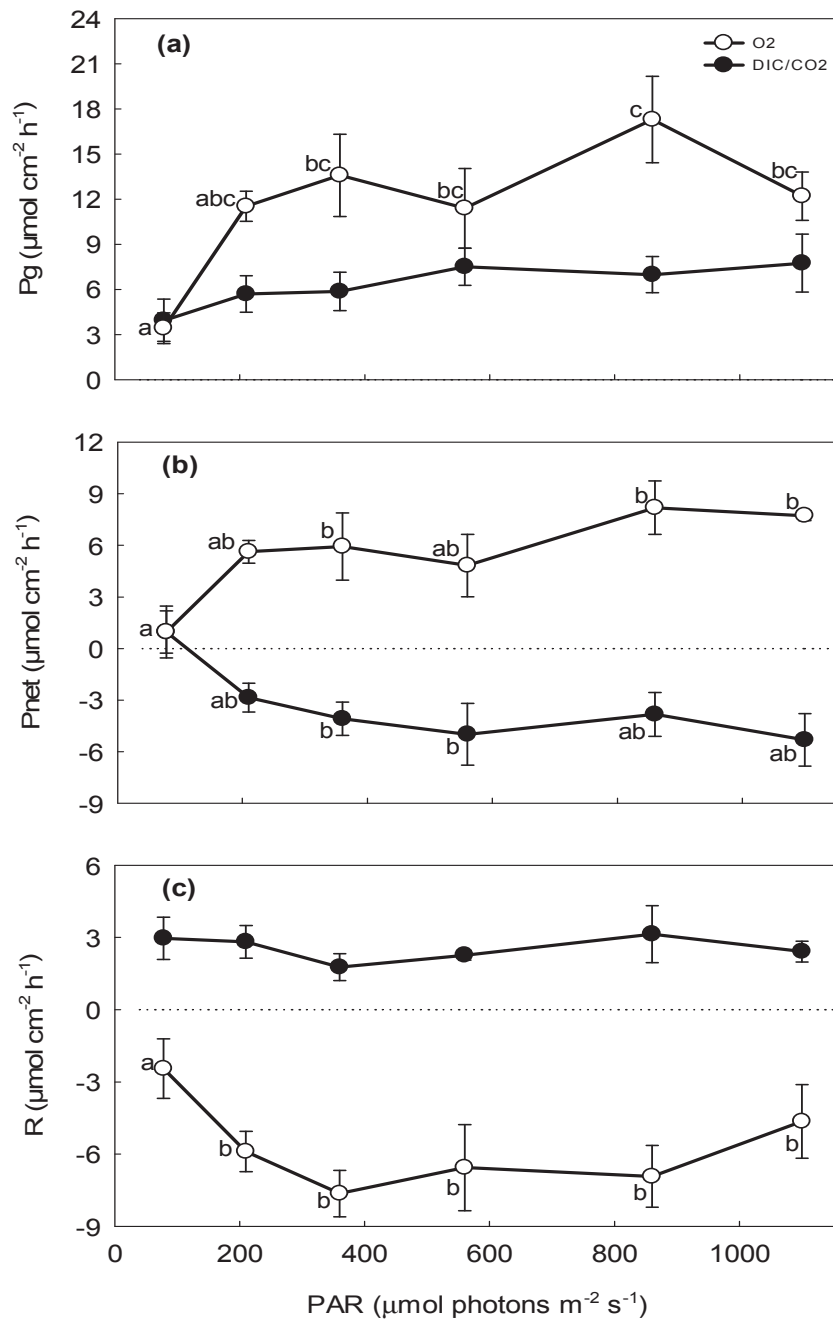


**Figure 4.4:** Gas exchange rates of  $\text{O}_2$  (open circles) and DIC ( $\text{Pg}_{\text{DIC}}$  and  $\text{Pnet}_{\text{DIC}}/\text{R}_{\text{CO}_2}$  exchange (closed circles) as a function of irradiance (78 – 1100  $\mu\text{mol photons m}^{-2} \text{s}^{-1}$ ) are displayed; (a) gross photosynthetic rates ( $\text{Pg}_{\text{O}_2}$  and  $\text{Pg}_{\text{DIC}}$ ), (b) net photosynthetic rates ( $\text{Pnet}_{\text{O}_2}$  and  $\text{Pnet}_{\text{DIC}}$ ), (c) post-illumination respiration rates ( $\text{R}_{\text{O}_2}$  and  $\text{R}_{\text{CO}_2}$ ); mean  $\pm$  SEM ( $n = 3$ ), standard errors are indicated, dotted line indicates zero (in panel b and c). Tukey HSD results are indicated.

$P_{\text{netDIC}}$  rates displayed  $\text{CO}_2$  evolution at  $78 \mu\text{mol photons m}^{-2} \text{ s}^{-1}$  (Fig. 4.4 b), which significantly switched to negative rates, where at  $360$  and  $560 \mu\text{mol photons m}^{-2} \text{ s}^{-1}$  the DIC uptake was the greatest (Tukey HSD,  $p < 0.05$ ). The internal DIC pool reportedly increases in response to light driven respiration rates, which is then directly available as a photosynthetic carbon substrate (Al-Horani et al. 2003a; Furla et al. 2000).  $P_{\text{netDIC}}$  exchange dynamics of a coral symbiosis are a useful proxy to assess the fitness of the coral holobiont. A coral holobiont is drawing on the external DIC pool to meet substrate needs for algal photosynthesis when the internal DIC pool is not sufficient. Respiratory  $\text{CO}_2$  evolution during light incubations can indicate that algal symbionts are not taking up DIC and/or the coral holobiont displays elevated respiratory activity as a result of stress impact e.g. thermal, osmotic stress.  $P_{\text{netDIC}}$  rates determined here are indicating uptake rates for irradiances  $> 210 \mu\text{mol photons m}^{-2} \text{ s}^{-1}$  with greatest uptake at  $360$  and  $560 \mu\text{mol photons m}^{-2} \text{ s}^{-1}$  and weakening towards higher irradiances. Exposure to high irradiances of  $860$  and  $1100 \mu\text{mol photons m}^{-2} \text{ s}^{-1}$  therefore cause either coral holobiont stress, or downregulation of photosynthetic C fixation (DIC consumption by the algal symbiont). To clarify, the P – E curve derived  $P_{\text{netDIC}}$  rates were fitted to the functions by Platt *et al.* (1980) to quantify descriptive parameters; initial slope ( $\alpha_{P_{\text{netDIC}}}$ ), minimum saturating scalar irradiance ( $E_{K_{P_{\text{netDIC}}}}$ ), as well as maximum net DIC uptake irradiance ( $P_{\text{netDICmax}}$ ) (Table 4.2).  $E_{K_{P_{\text{netDIC}}}}$  determined here was at  $\sim 313 \mu\text{mol photons m}^{-2} \text{ s}^{-1}$ , so that the decline in  $P_{\text{netDIC}}$  rates at irradiances  $> 860 \mu\text{mol photons m}^{-2} \text{ s}^{-1}$  could be accounted to over-saturating irradiances resulting in a downregulation of photosynthetic activity of the algal symbionts.



**Table 4.2:** Quantitative parameters derived from fitted net photosynthetic DIC uptake rates as a function of irradiances applied during P – E curves (n=3; mean  $\pm$  SEM).

<b>P-E curve parameter</b>	
$\alpha_{\text{PnetDIC}}$	$0.81 \pm 0.18$
$E_{K \text{ PnetDIC}}$ ( $\mu\text{mol photons m}^{-2} \text{ s}^{-1}$ )	$313 \pm 61.0$
$\text{Pnet}_{\text{DICmax}}$ ( $\mu\text{mol DIC m}^{-2} \text{ s}^{-1}$ )	$58.3 \pm 11.6$

PAM fluorometry results showed an inverse relationship between  $\Phi_{\text{PSII}}$  and applied irradiances where, in contrast, NPQ and rETR displayed a positive relationship with irradiance and did not saturate under irradiances applied (Fig. 4.5). Further, the decrease in  $\Phi_{\text{PSII}}$  resembled the behaviour of the respiratory activity of the coral holobiont  $RQ_c$  (Fig. 4.6 a).  $RQ_c$  was inversely related to  $PQ_{\text{net}}$  and  $PQ_z$  (Fig. 4.6 b, c), where  $RQ_c$  was negatively related to incident irradiance and  $PQ_{\text{net}}$  and  $PQ_z$  positively. As the loss in  $\Phi_{\text{PSII}}$  did not result in a loss in  $Pg_{\text{O}_2}$  output, coupled with a downturn in  $RQ_c$  and weakening of  $\text{Pnet}_{\text{DIC}}$  uptake rates, we interpret these results as a loss in fitness of the coral holobiont.

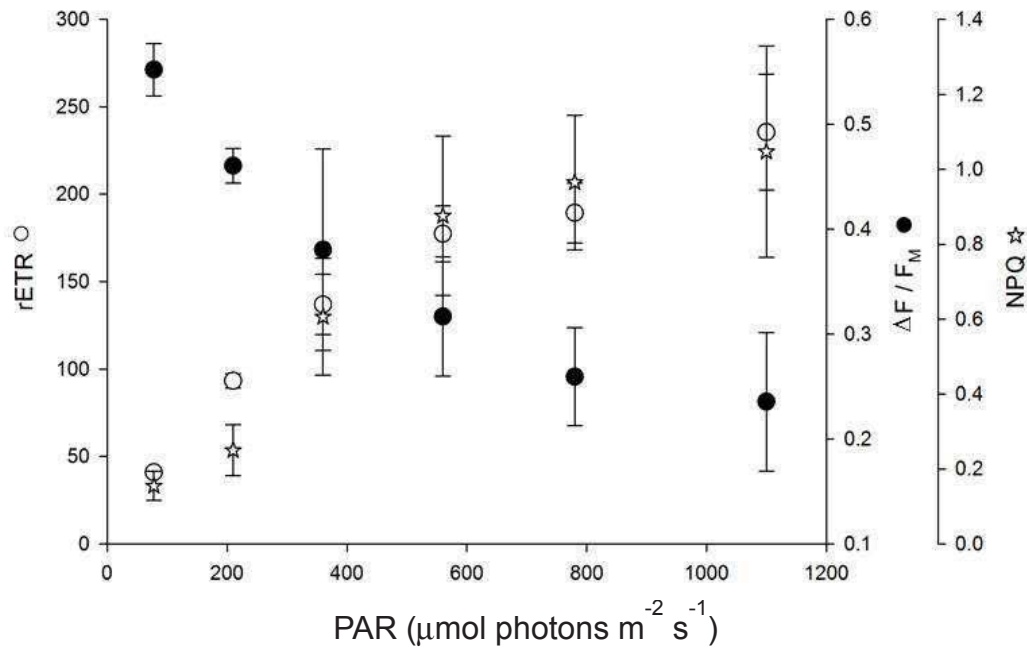


**Figure 4.5:**  $\Delta F/F_M'$  (closed circles), relative electron transport rate (rETR) (open stars) and NPQ (open circles) displayed as a function of irradiance (78 – 1100  $\mu\text{mol photons m}^{-2} \text{s}^{-1}$ );  $n=4$ , standard errors are indicated; legends are included in the axis labelling to not complicate the display of the data symbols in the graph panel.

$P_{\text{netO}_2}$  rates indicated lowest  $\text{O}_2$  production at 78  $\mu\text{mol photons m}^{-2} \text{s}^{-1}$  (Tukey HSD,  $p < 0.05$ ) and increased with increasing irradiances  $> 210 \mu\text{mol photons m}^{-2} \text{s}^{-1}$  (one-way ANOVA,  $F(5,12) = 4.296$ ,  $p = 0.018$ ; Fig 4.4 b). The  $\text{CO}_2E_c$  of the specimens examined here was determined to be  $\sim 78 \mu\text{mol photons m}^{-2} \text{s}^{-1}$ . The  $\text{CO}_2E_c$  irradiance explains the low  $P_{\text{netO}_2}$  rates, as well as  $\text{CO}_2$  evolution (indicative of respiratory activity) found at 78  $\mu\text{mol photons m}^{-2} \text{s}^{-1}$ . Generally,  $P_{\text{netO}_2}$  and  $P_{\text{netDIC}}$  exchange were found to be inversely correlated. The coral holobiont showed irradiance independent respiratory gas exchange with constant and positive  $R_{\text{CO}_2}$  rates, indicating respiratory  $\text{CO}_2$  evolution and constant negative  $R_{\text{O}_2}$  rate displaying respiratory  $\text{O}_2$  uptake (Fig. 4.4 c).

The coral respiratory quotient ( $RQ_c$ ; Fig. 4.6 a), the photosynthetic quotient of the coral ( $PQ_{net}$ ; Fig. 4.6 b) and the algal symbionts photosynthetic quotient ( $PQ_z$ ; Fig. 4.6 c) for *P. damicornis* were on average  $0.91 \pm 0.30$ ,  $1.10 \pm 0.65$  and  $1.50 \pm 0.94$  respectively ( $n=4$ ), which fit well with previously reported values (Gattuso and Jaubert 1990; Schneider et al. 2009) (Fig. 4.6). Comparable DIC exchange rates were reported for  $C^{13}$  assays of incubations at  $\sim 250 \mu\text{mol photons m}^{-2} \text{s}^{-1}$  determined for *Stylophora pistillata*, a thin-tissued branching pocilloporid coral species like *P. damicornis* as examined here (for rates obtained at  $210 \mu\text{mol photons m}^{-2} \text{s}^{-1}$ ) (Tremblay et al. 2012b).

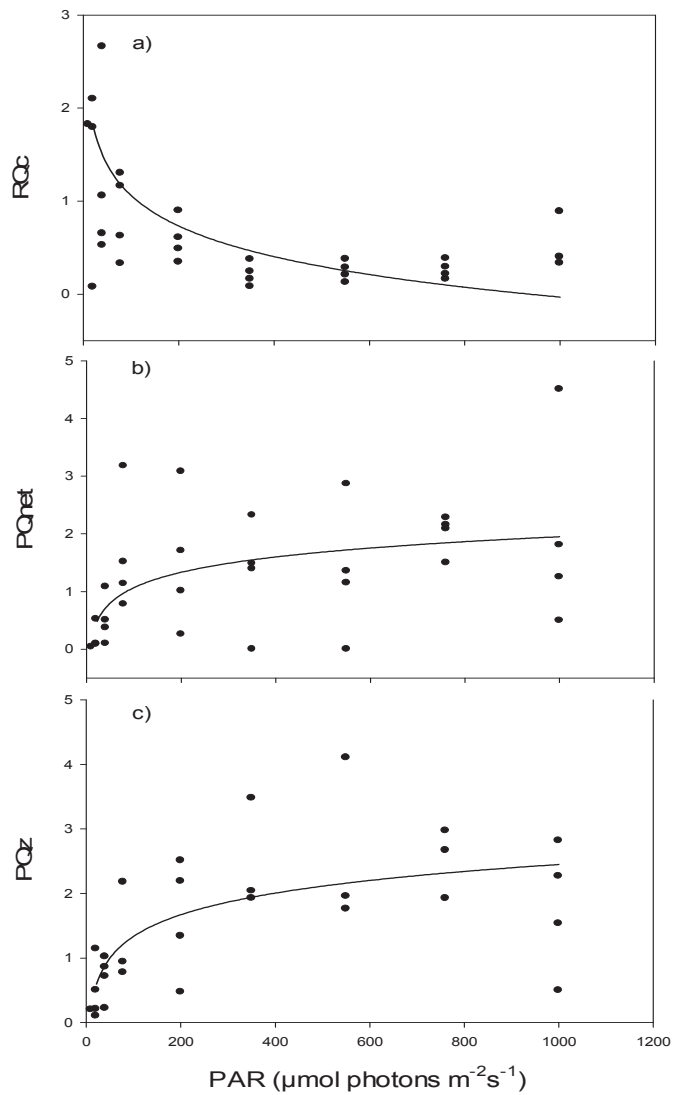


**Figure 4.6:** Replicate estimates of metabolic quotients are displayed as a function of irradiance (78 – 1100  $\mu\text{mol photons m}^{-2}\text{s}^{-1}$ ) with exponential trend lines for (a) respiratory quotient considering the holobiont (RQc), (b) photosynthetic quotient considering the holobiont (PQnet), (c) photosynthetic quotient considering the algal symbiont (PQz); replicates are indicated (n=4).

## 4.4 Discussion

### 4.4.1 Benefits of the photobioreactor setup

Previous studies investigating the photosynthetic productivity of *in hospite* coral symbionts, have analysed DIC exchange via  $^{14}\text{C}/^{13}\text{C}$  assays or used alkalinity titrations of incubation media (e.g. Fujimura et al. 2008; Higuchi et al. 2009; Tremblay et al. 2012b). However,  $^{14}\text{C}$  assays are a destructive technique and can lead to results which are difficult to interpret, since different tissue compartments may take up the radio-labelled C substrate with different affinities depending on the degree of uptake, which is related to the incubation time with the C isotope (e.g. Gilbert et al. 2000; Venn et al. 2008). Further, the application of  $^{14}\text{C}/^{13}\text{C}$  assays and alkalinity titrations only allow for the differentiation of DIC concentrations at the time of sampling and do not allow for dynamic rate detection which can be accomplished with the PBR applied here. DIC exchange rates were comparable between the PBR designed here and previous  $\text{C}^{13}$  assays (Tremblay et al. 2012b). With the application of the PBR, immediate DIC uptake and  $\text{CO}_2$  evolution rates can be measured non-destructively under various experimental abiotic conditions (e.g. variable temperature, irradiance and nutrient levels irradiance). Compared to C-isotope assays which are time-consuming, costly and in terms of  $\text{C}^{14}$  hazardous, the application of a PBR system as demonstrated here is a cost-effective and convenient alternative for DIC exchange rate measurements.

#### ***4.4.2 Dissolved inorganic carbon exchange***

The exchange of internal DIC between sources and sinks (i.e. photosynthetic processes and calcification) has been an ongoing topic of research in the field of coral physiology for the past few decades (Jokiel 2011). The most recent review about the interplay of photosynthesis and calcification by Jokiel (2011) proposed a two compartment proton flux model, which differentiates between functionally distinct layers of the coral tissue and hypothesises that the spatial separation of key processes i.e. photosynthesis and calcification could explain variability in efficiency of either of the two processes respectively. To further elucidate internal DIC exchange processes, the application of inhibitors should be considered for future assessments of hard corals with the PBR, where symbiont photosynthesis, CCM activity and host calcification could be manipulated in order to improve the interpretation of internal DIC exchange rates of a coral holobiont.

#### ***4.4.3 Gas-phase of the photobioreactor***

The prototype setup presented here in its current version is laboratory purpose build and it would need modifications for being taken in the field (e.g. on a boat for *in situ* research purposes). Modifications to high-end drying columns with less volume could decrease the gas-phase volume and would allow for quicker equilibration with the liquid-phase. But at the same time incubation time allowance would be shortened and would prevent long-term monitoring application. The 1.6 times greater gas-phase relative to liquid-phase (as demonstrated above) does fulfil a purpose as it ameliorates the altered DIC concentrations within the liquid phase by taking advantage of gas equilibration dynamics. As demonstrated with the measurements presented here, gas exchange rates of this closed circuit system consisting of a gas- and liquid-phase were

comparable with reported values of alternative measurement techniques. However, it depends on the application, whether the user is interested in fast gas exchange measurements, or long-term incubations, where the PBR setup could be tailored accordingly.

#### **4.5 Comments and recommendations**

The application of the PBR presented here will be relevant to fundamental and current photo-physiological research for a range of aquatic phototrophs (e.g. commercial algae-to-growth systems for biofuel plants). The integrated measuring approach will yield new insights into the often non-linear relationship of Chl fluorescence to O<sub>2</sub> production and C fixation parameters (Genty et al. 1989; Seaton and Walker 1990; Sivak and Walker 1985; Suggett et al. 2010b). It should be noted that the experiments presented are specimen specific and were opted to allow for short-term incubations. If long-term experiments were to be run using the PBR, one need to consider the fact that it is an enclosed system and that possible adjustments such as medium exchanges could have to be accounted for, which is subject to the specimen of choice.

In the following sections a theoretical data analysis will be presented, which should be considered for future applications of non-symbiotic aquatic phototrophs. In a symbiotic association, such as a coral, the gas exchange rates within the holobiont are not a direct result of photosynthetic processes as other metabolic processes are altering gas exchange rates. This theoretical discussion is a brief introduction to the analyses of the combined measurement approach of Chl fluorescence data with metabolic gas exchange, which aims to observe alternative electron pathways and sinks.

#### ***4.5.1 Shortfalls of utilised specimen and data analysis***

The PBR demonstrated here with its integrated measurement approach aligns three rate measures for the quantum efficiency of photosynthesis i) ETR, ii)  $P_{gO_2}$  and iii)  $P_{netDIC}$ . As reported in various previous studies and based on fundamental photosynthetic research it is generally assumed that it takes 8 photons to release 4 electrons from water, and 4 electrons are needed to produce 1 mole of  $O_2$  (Falkowski and Raven 2007). Further, there is an assumed ratio of 1:1 for the production of  $O_2$  and C fixation. Hence both rate measures can be demonstrated in electron equivalents by assuming 4 electrons per mole  $O_2$  as well as C. However, in reality, this 1:1 relationship does not occur due to processes which consume  $O_2$  (e.g. photorespiratory conditions) or deviate electrons from the linear intersystem electron transport between PSII and PSI (e.g. cyclic electron transport) (Badger et al. 2000).

Deviations in electron equivalents can therefore be used to extrapolate light energy utilisation for alternative electron pathways and linear electron transport. This approach has been taken in previous studies (Laisk and Loreto 1996; Peterson 1989; Peterson 1990; Ruuska et al. 2000; Suggett et al. 2010a), where the gas exchange and Chl fluorescence measurements were not determined simultaneously and led to potential errors in the comparative electron transport analysis. Problems arose from the use of different specimens for each measurement, different timing of each analysis and differences in light exposure (Suggett et al. 2010a). Using this PBR, all three measures can be accomplished simultaneously and on the same specimen, therefore accounting for shortfalls in previous rate measures.



#### ***4.5.2 Alternative electron pathways***

Deviations between ETR and  $P_{gO_2}$  electron equivalents can be used to quantify the loss of electrons before charge separation at PSII and the oxidation of water (termed here ‘radiative electron loss’) (Klughammer and Schreiber 2008). Further, differences between  $P_{gO_2}$  electron equivalents and  $P_{netDIC}$  electron equivalents can indicate the activity of alternative electron pathways/sinks (AEPs) deviating from the linear intersystem electron transport between PSII and PSI. This can include nitrogen (N) and sulphur (S) assimilation, and alternative oxidases (AOXs), such as the Mehler Ascorbate Peroxidase (MAP) cycle (Stirbet and Govindjee 2012; Suggett et al. 2010b), but also cyclic electron transport around PSII or PSI (Finazzi et al. 2002; Prasil et al. 1996) (intrinsic  $e^-$  sinks). It is generally assumed that ~25% of the linear electron transport between PSII and PSI is utilised for N and S assimilation in eukaryotic phytoplankton (Suggett et al. 2010a). During the MAP cycle, electrons split from water at the OEC reduce  $O_2$  through 2 intermediates ( $O_2^-$  and  $H_2O_2$ ) to water at the acceptor side of PSI (Schreiber et al. 1995a).

#### ***4.5.3. Demonstration of stoichiometric analysis of theoretical electron flow***

The stoichiometric analysis of photosynthetic rate measures in quantities of electron equivalents proposed here would allow for the identification of AEPs in operation (from charge separation at PSII, through intersystem electron transport to PSI and towards C fixation) as a function of incident irradiance. The theoretical results of this stoichiometric analysis are presented in Figure 4.7 (adapted from Wilhelm and Selmar, 2011). The theoretical quantum energy utilisation for C fixation ( $P_{netDIC}$  electron equivalents) through linear electron transport as a function of experimentally applied irradiance intensities is displayed (Fig. 4.7); where minimum saturating irradiance is

indicated as  $E_K$  (here a theoretical value is displayed, which can be calculated as described in Platt et al. 1980) (Fig. 4.7). The  $P_{net_{DIC}}$  electron equivalents are directly measured values from a P – E curve, where the fate of excess electrons not utilised for carbon fixation are displayed above  $P_{net_{DIC}}$  electron equivalents as AEPs. It was differentiated between radiative electron loss and intrinsic electron loss (see above for definition), where the former is displayed as the upper limit of the displayed AEPs and is defined as the difference between ETR and  $P_{gO_2}$  electron equivalents and the upper limit of the latter is defined as the difference between  $P_{gO_2}$  electron equivalents and  $P_{net_{DIC}}$  electron equivalents. The dotted line indicates  $E_K$ , where below  $E_K$  both theoretical AEP sinks are already in place, but greatly increase above  $E_K$ .

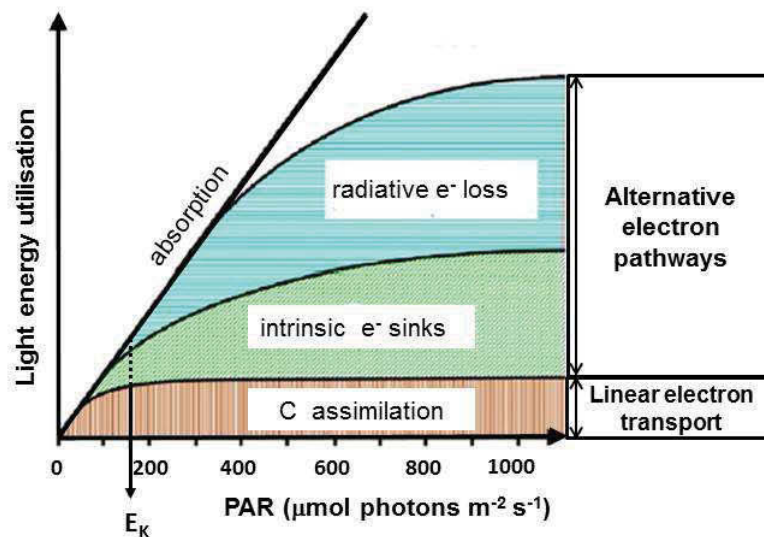


**Figure 4.7:** Conceptual display of a theoretical stoichiometric analysis of electron equivalents estimated from metabolic gas exchange rates and Chl fluorometry derived electron transport rates to describe light utilisation of aquatic phototrophs in terms of alternative electron pathways and C fixation as a function of irradiance (adapted from Wilhelm and Selmar, 2011).

With the theoretical analysis presented here AEPs acting within the photosynthetic apparatus of aquatic phototrophs can be determined for various experimental conditions (e.g. fluctuating light conditions, nutrient limitation, different salinity regimes, etc). Deviations in electron transport caused by AEPs have been described in detail for higher plants (e.g. Badger et al. 2000; Schreiber et al. 1995a; Wingler et al. 2000), but the general understanding for those processes in algae still remain limited (Wagner et al. 2005). It is desirable to define AEP regulation under various conditions as outlined above, in order to exploit this information. Such information would be useful for many applications, including the successful growth and harvest of microalgae for the use of biofuels. Furthermore, this analysis could be a practicable approach to address the ‘light to growth’ problem of phytoplankton photosynthesis, which has been raised in various studies (Jakob et al. 2007; Langner et al. 2009; Wagner et al. 2005). The fate of light energy from being harvested within the antenna pigment-protein complexes to eventually being used in C fixation in order to form biomass describes the light to growth problem (Wagner et al. 2005; Wingler et al. 2000).

This innovative PBR setup therefore represents a tool to significantly advance the field of photosynthesis research in aquatic phototrophs. The important feature of the PBR is the flexible application (e.g. for ecophysiological studies of aquatic phototrophs to assess the impact of future climate scenarios (Hughes et al. 2003)). Measurements presented here could enhance our understanding of certain physiological pathways of a coral symbiosis; the analysis allows distinguishing parameters which are characteristic to each symbiotic partner to assess their fitness and therefore aid for high-resolution physiological assessment.

#### 4.6 References

- Al-Horani, F. A., S. M. Al-Moghrabi, and D. De Beer. 2003. The mechanism of calcification and its relation to photosynthesis and respiration in the scleractinian coral *Galaxea fascicularis*. *Marine Biology* **142**: 419-426.
- Atkin, O. K., J. R. Evans, and K. Siebke. 1998. Relationship between the inhibition of leaf respiration by light and enhancement of leaf dark respiration following light treatment. *Australian Journal of Plant Physiology* **25**: 437-443.
- Badger, M. R., S. Von Caemmerer, S. Ruuska, and H. Nakano. 2000. Electron flow to oxygen in higher plants and algae: rates and control of direct photoreduction (Mehler reaction) and rubisco oxygenase. *Philosophical Transactions of the Royal Society B: Biological Sciences* **355**: 1433-1446.
- Beardall, J., A. Quigg, and J. A. Raven. 2004. Oxygen Consumption: Photorespiration and Chlororespiration, p. 157-181. *In* A. W. D. Larkum, A. E. Douglas and J. A. Raven [eds.], *Photosynthesis in Algae*. Springer Netherlands.
- Beer, S., C. Larsson, O. Poryan, and L. Axelsson. 2000. Photosynthetic rates of *Ulva* (Chlorophyta) measured by pulse amplitude modulated (PAM) fluorometry. *European Journal of Phycology* **35**: 69-74.
- Borisov, S. M., G. Nuss, and I. Klimant. 2008. Red light-excitable oxygen sensing materials based on Platinum (II) and Paladium (II) Benzoporphyrins. *Analytical Chemistry* **80**: 9435-9442.
- Burba, G., A. Schmidt, R. L. Scott, T. Nakai, J. Kathilankal, G. Fratini, C. Hanson, B. Law, D. K. Mcdermitt, R. Eckles, M. Furtaw, and M. Veldersdyk. 2012. Calculating CO<sub>2</sub> and H<sub>2</sub>O eddy covariance fluxes from an enclosed gas analyzer using an instantaneous mixing ratio. *Global Change Biology* **18**: 385-399.
- Crawley, A., D. I. Kline, S. Dunn, K. R. N. Anthony, and S. Dove. 2010. The effect of ocean acidification on symbiont photorespiration and productivity in *Acropora formosa*. *Global Change Biology* **16**: 851-863.
- Demmig-Adams, B., and W. W. Adams. 2006. Photoprotection in an ecological context: the remarkable complexity of thermal energy dissipation. *New Phytologist* **172**: 11-21.
- Dubinsky, Z., P. G. Falkowski, and K. Wyman. 1986. Light harvesting and utilization by phytoplankton. *Plant Cell and Physiology* **27**: 1335-1349.

- Dubinsky, Z., and P. L. Jokiel. 1994. Ratio of energy and nutrient fluxes regulates symbiosis between zooxanthellae and corals. *Pacific Science* **48**: 313-324.
- Edmunds, P. J., and S. P. Davies. 1988. Post-illumination stimulation of respiration rate in the coral *Porites porites*. *Coral Reefs* **7**: 7-9.
- Falkowski, P. G., and J. A. Raven. 2007. *Aquatic Photosynthesis*, 2nd ed. Princeton University Press.
- Finazzi, G., F. Rappaport, A. Furia, M. Fleischmann, J.-D. Rochaix, F. Zito, and G. Forti. 2002. Involvement of state transitions in the switch between linear and cyclic electron flow in *Chlamydomonas reinhardtii*. *EMBO reports* **3**: 280-285.
- Franklin, L. A., and M. R. Badger. 2001. A comparison of photosynthetic electron transport rates in macroalgae measured by pulse amplitude modulated chlorophyll fluorometry and mass spectrometry. *Journal of Phycology* **37**: 756-767.
- Fujimura, H., T. Higuchi, K. Shiroma, T. Arakaki, A. M. Hamdun, Y. Nakano, and T. Oomori. 2008. Continuous-flow complete-mixing system for assessing the effects of environmental factors on colony-level coral metabolism. *Journal for Biochemical and Biophysical Methods* **70**: 865-872.
- Furla, P., I. Galgani, I. Durand, and D. Allemand. 2000. Sources and mechanisms of inorganic carbon transport for coral calcification and photosynthesis. *The Journal of Experimental Biology* **203**: 3445-3457.
- Gattuso, J.-P., and J. Jaubert. 1990. Effect of light on oxygen and carbon dioxide fluxes and on metabolic quotients measured in situ in a zooxanthellate coral. *Limnology and Oceanography* **35**: 1796-1804.
- Genty, B., J.-M. Briantais, and N. R. Baker. 1989. The relationship between the quantum yield of photosynthetic electron transport and quenching of chlorophyll fluorescence. *Biochimica et Biophysica Acta* **990**: 87-92.
- Gilbert, M., A. Domin, A. Becker, and C. Wilhelm. 2000. Estimation of primary production by chlorophyll a *in vivo* fluorescence in freshwater phytoplankton. *Photosynthetica* **38**: 111-126.
- Goffredi, S. K., P. R. Girguis, J. J. Childress, and N. T. Desaulniers. 1999. Physiological functioning of carbonic anhydrase in the hydrothermal vent tubeworm *Riftia pachyptila*. *The Biological Bulletin* **196**: 257-264.
- Grottoli, A. G., L. J. Rodrigues, and J. E. Palardy. 2006. Heterotrophic plasticity and resilience in bleached corals. *Nature* **440**: 1186-1189.

- Hatcher, A. 1989. RQ of benthic marine invertebrates. *Marine Biology* **102**: 445-452.
- Higuchi, T., H. Fujimura, T. Arakaki, and T. Oomori. 2009. The synergistic effects of hydrogen peroxide and elevated seawater temperature on the metabolic activity of the coral *Galaxea fascicularis*. *Marine Biology* **156**: 580-596.
- Hill, R., C. Frankart, and P. J. Ralph. 2005. Impact of bleaching conditions on the components of non-photochemical quenching in the zooxanthellae of a coral. *Journal of Experimental Marine Biology and Ecology* **322**: 83-92.
- Hill, R., A. W. D. Larkum, O. Prášil, D. M. Kramer, V. Kumar, and P. J. Ralph. 2012. Light-induced redistribution of antenna complexes in the symbionts of scleractinian corals correlates with sensitivity to coral bleaching. *Coral Reefs* **31**: 963-975.
- Huang, X., C. J. Margulis, Y. Li, and B. J. Berne. 2005. Why is the partial molar volume of CO<sub>2</sub> so small when dissolved in a room temperature ionic liquid? Structure and dynamics of CO<sub>2</sub> dissolved in [Bmim<sup>+</sup>] [PF<sub>6</sub><sup>-</sup>]. *Journal of the American Chemistry Society* **127**: 17842-17851.
- Hughes, T. P., A. H. Baird, D. R. Bellwood, M. Card, S. R. Connolly, C. Folke, R. Grosberg, O. Hoegh-Guldber, J. B. C. Jackson, J. Kleypas, J. M. Lough, P. Marshall, M. Nystroem, S. R. Palumbi, J. M. Pandolfi, B. Rosen, and J. Roughgarden. 2003. Climate change, human impacts, and the resilience of coral reefs. *Science* **301**: 929-933.
- Iglesias-Prieto, R., V. H. Beltran, T. C. Lajeunesse, H. Reyes-Bonilla, and P. E. Thome. 2004. Different algal symbionts explain the vertical distribution of dominant reef corals in the eastern pacific. *Proceedings of the Royal Society B* **271**: 1757-1763.
- Jakob, T., H. Wagner, K. Stehfest, and C. Wilhelm. 2007. A complete energy balance from photons to new biomass reveals a light- and nutrient-dependent variability in the metabolic costs of carbon assimilation. *Journal of Experimental Botany* **58**: 2101-2112.
- Jassby, A. D., and T. Platt. 1976. Mathematical formulation of the relationship between photosynthesis and light for phytoplankton. *Limnology and Oceanography* **21**: 540-547.
- Jokiel, P. L. 2011. The reef coral two compartment proton flux model: A new approach relating tissue-level physiological processes to gross corallum morphology. *Journal of Experimental Marine Biology and Ecology* **409**: 1-12.

- Kahara, S. N., and J. E. Vermaat. 2005. The effect of alkalinity on photosynthesis-light curves and inorganic carbon extraction capacity of freshwater macrophytes. *Aquatic Botany* **75**: 217-227.
- Klughammer, C., and U. Schreiber. 2008. Complementary PS II quantum yields calculated from simple fluorescence parameters measured by PAM fluorometry and the saturation pulse method. *PAM Application Notes* **1**: 27-35.
- Kok, B. 1948. On the interrelation between respiration and photosynthesis in green plants. *Biochimica et Biophysica Acta (BBA)* **3**: 625-631.
- Kroon, B., B. B. Prezelin, and O. Schofield. 1993. Chromatic regulation of quantum yields for photosystem II charge separation, oxygen evolution and carbon fixation in *Heterocapsa pygmaea* (Pyrrophyta). *Journal of Phycology* **29**: 453-462.
- Laisk, A., and F. Loreto. 1996. Determining photosynthetic parameters from leaf CO<sub>2</sub> exchange and chlorophyll fluorescence - ribulose-1,5- biphosphate carboxylase oxygenase specificity factor, dark respiration in the light, excitation distribution between photosystems, alternative electron transport rate, and mesophyll diffusion resistance. *Plant Physiology* **110**: 903-912.
- Langner, U., T. Jakob, K. Stehfest, and C. Wilhelm. 2009. An energy balance from absorbed photons to new biomass for *Chlamydomonas reinhardtii* and *Chlamydomonas acidophila* under neutral and extremely acidic growth conditions. *Plant, Cell & Environment* **32**: 250-258.
- Leggat, W., M. R. Badger, and D. Yellowlees. 1999. Evidence for an inorganic carbon-concentrating mechanism in the symbiotic dinoflagellate *Symbiodinium* sp. *Plant Physiology* **121**: 1247-1255.
- Levine, I. N. 1974. *Physical chemistry*. McGraw-Hill.
- Longstaff, B. J., T. Kildea, J. W. Runcie, A. Cheshire, W. C. Dennison, C. Hurd, T. Kana, J. A. Raven, and L. A. W.D. 2002. An *in situ* study of photosynthetic oxygen exchange and electron transport rate in the marine macroalgae *Ulva lactuca* (Chlorophyta). *Photosynthesis Research* **74**: 281-293.
- Peterson, R. B. 1989. Partitioning of non-cyclic photosynthetic electron transport to O<sub>2</sub>-dependent dissipative processes as probed by fluorescence and CO<sub>2</sub> exchange. *Plant Physiology* **90**: 1322-1328.



- Peterson, R. B. 1990. Effects of irradiance on the *in vivo* CO<sub>2</sub>:O<sub>2</sub> specificity factor in tobacco using simultaneous gas exchange and fluorescence techniques. *Plant Physiology* **95**: 892-898.
- Platt, T., C. L. Gallegos, and W. G. Harrison. 1980. Photoinhibition of photosynthesis in natural assemblages of marine phytoplankton. *Journal of Marine Research* **38**: 687-701.
- Prasil, O., Z. Kolber, J. A. Berry, and P. G. Falkowski. 1996. Cyclic electron flow around photosystem II *in vivo*. *Photosynthesis Research* **48**: 395-410.
- Quetin, L. B., R. M. Ross, and K. Uchio. 1980. Metabolic characteristics of midwater zooplankton: ammonia excretion, O:N ratios, and the effect of starvation. *Marine Biology* **59**: 201-209.
- Ralph, P. J., and R. Gademann. 2005. Rapid light curves: a powerful tool to assess photosynthetic activity. *Aquatic Botany* **82**: 222-237.
- Ralph, P. J., C. Wilhelm, J. Lavaud, T. Jakob, K. Petrou, and S. Kranz. 2010. Fluorescence as a tool to understand changes in photosynthetic electron flow regulation, p. 75-89. *In* D. J. Suggett, M. A. Borowitzka and O. Prasil [eds.], *Chlorophyll a Fluorescence in Aquatic Sciences: Methods and Applications*. Springer.
- Raven, J. A. 2003. Inorganic carbon concentrating mechanisms in relation to the biology of algae. *Photosynthesis Research* **77**: 155-171.
- Raven, J. A., and C. L. Hurd. 2012. Ecophysiology of photosynthesis in macroalgae. *Photosynthesis Research* **113**: 105-125.
- Ritchie, R. J. 2008. Universal chlorophyll equations for estimating chlorophylls *a*, *b*, *c*, and *d* and total chlorophylls in natural assemblages of photosynthetic organisms using acetone, methanol or ethanol solvents. *Photosynthetica* **46**: 115-126.
- Ruuska, S. A., M. R. Badger, T. J. Andrews, and S. Von Caemmerer. 2000. Photosynthetic electron sinks in transgenic tobacco with reduced amounts of rubisco: little evidence for significant meyer reaction. *Journal of Experimental Botany* **51**: 357-368.
- Schlichting, H., and K. Gersten. 2000. *Boundary-Layer Theory*. Springer.
- Schneider, K., O. Levy, Z. Dubinsky, and J. Erez. 2009. *In situ* diel cycles of photosynthesis and calcification in hermatypic corals. *Limnology and Oceanography* **54**: 1995-2002.



- Schreiber, U. 2004. Pulse-amplitude-modulation (PAM) fluorometry and saturation pulse method: an overview, p. 279-319. *In* G. C. Papageorgiou and Govindjee [eds.], Chlorophyll a fluorescence: a signature of photosynthesis. Advances in Photosynthesis and Respiration. Springer.
- Schreiber, U., H. Hormann, K. Asada, and C. Neubauer. 1995a. O<sub>2</sub>-dependent electron flow in intact spinach chloroplasts: properties and possible regulation of the Mehler-Ascorbate-Peroxidase cycle, p. 813-818. *In* P. Mathis [ed.], Photosynthesis: from Light to Biosphere. Kluwer Academic Publishers.
- Schreiber, U., H. Hormann, C. Neubauer, and C. Klughammer. 1995b. Assessment of photosystem II photochemical quantum yield by chlorophyll fluorescence quenching analysis. Australian Journal of Plant Physiology **22**: 209-220.
- Seaton, G. G. R., and D. A. Walker. 1990. Chlorophyll fluorescence as a measure of photosynthetic carbon assimilation. Proceedings of the Royal Society B **242**: 29-35.
- Sinutok, S., R. Hill, M. A. Doblin, R. Wuhrer, and P. J. Ralph. 2011. Warmer more acidic conditions cause decreased productivity and calcification in subtropical coral reef sediment-dwelling calcifiers. Limnology and Oceanography **56**: 1200-1212.
- Sivak, M. N., and D. A. Walker. 1985. Chlorophyll a fluorescence: can it shed light on fundamental questions in photosynthetic carbon dioxide fixation? Plant, Cell & Environment **8**: 439-448.
- Smith, F. W., and N. A. Walker. 1980. Photosynthesis by aquatic plants: effects of unstirred layers in relation to assimilation of CO<sub>2</sub> and HCO<sub>3</sub><sup>-</sup> and to carbon isotopic discrimination. New Phytologist **86**: 245-259.
- Stimson, J., and R. A. Kinzie. 1991. The temporal pattern and rate of release of zooxanthellae from the reef coral *Pocillopora damicornis* (Linnaeus) under nitrogen-enrichment and control conditions. The Journal of Experimental Biology **153**: 66-74.
- Stirbet, A., and Govindjee. 2012. Chlorophyll *a* fluorescence induction: a personal perspective of the thermal phase, the J-I-P rise. Photosynthesis Research **113**: 15-61.

- Suggett, D. J., H. L. Macintyre, T. M. Kana, and R. J. Geider. 2010a. Comparing electron transport with gas exchange: parameterising exchange rates between alternative photosynthetic currencies for eukaryotic phytoplankton. *Aquatic Microbial Ecology* **65**: 147-162.
- Suggett, D. J., M. C. Moore, and R. J. Geider. 2010b. Estimating aquatic productivity from active fluorescence measurements. *In* D. J. Suggett, O. Prasil and M. A. Borowitzka [eds.], *Chlorophyll a Fluorescence in Aquatic Sciences: Methods and Applications*. Springer.
- Tolbert, N. E., C. Benker, and E. Beck. 1995. The oxygen and carbon dioxide compensation points of C<sub>3</sub> plants: possible role in regulating atmospheric oxygen. *Proceedings of the National Academy of Sciences U.S.A.* **92**: 11230-11233.
- Tremblay, P., R. Grover, J. F. Maguer, L. Legendre, and C. Ferrier-Pagès. 2012. Autotrophic carbon budget in coral tissue: a new <sup>13</sup>C-based model of photosynthate translocation. *The Journal of Experimental Biology* **215**: 1384-1393.
- Veal, C., M. Carmi, G. Dishon, Y. Sharon, K. Michael, D. Tchernov, O. Hoegh-Guldberg, and M. Fine. 2010. Shallow-water wave lensing in coral reefs: a physical and biological case study. *The Journal of Experimental Biology* **213**: 4303-4312.
- Venn, A. A., J. E. Loram, and A. E. Douglas. 2008. Photosynthetic symbioses in animals. *The Journal of Experimental Biology* **59**: 1069-1080.
- Wagner, H., T. Jakob, and C. Wilhelm. 2005. Balancing the energy flow from captured light to biomass under fluctuating light conditions. *New Phytologist* **169**: 95-108.
- Walker, D., and R. Walker. 1988. The use of the oxygen electrode and fluorescence probes in simple measurements of photosynthesis. Robert Hill Institute, University of Sheffield.
- Walker, D. A. 1981. Secondary fluorescence kinetics of spinach leaves in relation to the onset of photosynthetic carbon assimilation. *Planta* **153**: 273-278.
- Wingler, A., P. J. Lea, and W. P. Quick. 2000. Photorespiration: metabolic pathways and their role in stress protection. *Philosophical transactions of the Royal Society B* **355**: 1517-1529.

Page intentionally left blank

## Chapter 5

# Light respiration and CO<sub>2</sub> light compensation point of two distinct host corals

Verena Schrameyer<sup>a</sup>, Daniel Wangpraseurt<sup>a</sup>, Anthony W.D. Larkum<sup>a</sup>, Ross Hill<sup>a,b</sup>, Michael Kühl<sup>a,c,d</sup>, Peter J. Ralph<sup>a\*</sup>

<sup>a</sup> Plant Functional Biology and Climate Change Cluster, School of the Environment, University of Technology, Sydney, Ultimo, 2007, NSW, Australia

<sup>b</sup> Centre for Marine Bio-Innovation and Sydney Institute of Marine Science, School of Biological, Earth and Environmental Sciences, The University of New South Wales, Sydney 2052 NSW, Australia

<sup>c</sup> Marine Biological Section, Department of Biology, University of Copenhagen, Helsingør, Denmark

<sup>d</sup> Singapore Centre on Environmental Life Sciences Engineering, School of Biological Sciences, Nanyang Technological University, Singapore, Singapore

**Keywords:** DIC, CO<sub>2</sub> light compensation point, light utilisation, light respiration, dark respiration, photoprotection, non-photochemical quenching, P/R ratio.

## 5.1 Introduction

The success of scleractinian corals in low nutrient waters is based on the symbiotic relationship between coral host and the single-celled microalgae (genus *Symbiodinium*) that reside within the host's endodermal cells. The host derives up to 95% of the photosynthetically-fixed carbon (C) from its algal symbionts under optimal conditions (Muscatine 1990), whilst the symbiont receives nutrients and shelter (Muscatine and Porter 1977; Pernice et al. 2012). The degree of autotrophy of a coral is dependent on the quality and quantity of photosynthetic active radiation (PAR, 400-700 nm), which drives the photosynthesis of its algal symbionts (Dubinsky et al. 1984; Tremblay et al. 2012b).

*Symbiodinium* contains a prokaryotic-type form II RUBISCO (Ribulose-1,5-bisphosphate-carboxylase/oxygenase), which has a low affinity for CO<sub>2</sub> (Raven and Beardall 2003; Rowan et al. 1996; Whitney and Andrews, 1998; Yellowlees et al. 2008). High concentrations of CO<sub>2</sub> are therefore necessary to promote carbon assimilation (Ribulose-1,5-bisphosphate (RuBP) + CO<sub>2</sub> → 2 x 3-Phosphoglycerate (PGA)) and to meet the hosts energetic demand for photosynthetic products (Leggat et al. 2002; Lilley et al. 2010; Raven 2003); at the same time it has oxygenase activity, meaning that in the presence of oxygen it will catalyse the alternative reaction, RuBP + O<sub>2</sub> → 3PGA + P-glycolate, where P-glycollate is a toxic compound that has to be removed through photorespiration (Beardall et al. 2004).

The coral host generates a supply of CO<sub>2</sub> for the symbiont by cellular respiration (Muller-Parker and D'elia 1997; Muscatine et al. 1989; Yellowlees and Warner 2003), but some C is required from the ambient seawater medium; and as the passive diffusion of external CO<sub>2</sub> is restricted due to the multiple membranes which need to be traversed,

host mediated carbon concentrating mechanisms (CCMs) are necessary to take up dissolved inorganic carbon (DIC) (Al-Moghrabi et al. 1996; Leggat et al. 1999; Rands et al. 1993). Carbonic anhydrases are widespread, acting as active or passive CCMs and occur in both *Symbiodinium* and coral host tissue (Graham and Smillie 1976; Leggat et al. 1999) to catalyse the transport of  $\text{HCO}_3^-$  from the external medium to the chloroplasts of *Symbiodinium* (Kuile et al. 1989; Moya et al. 2008).

The delivery of DIC to the algal symbiont is primarily controlled by i) light intensity (modulating photosynthetic rate and DIC demand), and ii) the metabolism of the coral host (activity of CCMs i.e. C sequestration and respiration) (Yellowlees and Warner 2003). Hence, the interplay of host C acquisition, respiration rates and the photosynthetic DIC demand of the symbionts can have an immediate impact on the photosynthetic rate of the symbionts. When photosynthetic activity is high, the demand for DIC substrate is equally high; ultimately insufficient DIC availability can have negative implications for the coral host, as the host is dependent upon autotrophic nutrition from its algal symbionts (Muscatine 1990).

The  $\text{CO}_2$  light compensation point ( $\text{CO}_2\text{E}_c$ ) is defined as the light intensity at which the metabolic DIC pool is not sufficient to sustain photosynthesis and the coral host starts drawing on the external DIC pool (Tolbert et al. 1995). The light intensity level of the  $\text{CO}_2\text{E}_c$ , indicates primarily the respiratory activity of the coral holobiont. At irradiances below  $\text{CO}_2\text{E}_c$ , by definition more  $\text{CO}_2$  is produced in respiration than is taken up in photosynthesis. So there is the potential for some release of  $\text{CO}_2$  to the ambient medium. Above  $\text{CO}_2\text{E}_c$ , more  $\text{CO}_2$  is taken up by photosynthesis than is evolved in respiration and it will be necessary for the uptake of DIC from the ambient medium. Additionally calcification is enhanced through the exposure to light and also requires

DIC, which adds to the uptake of DIC from the ambient medium (Al-Horani et al. 2007; Levy et al. 2004).

The exchange of respiratory gases ( $O_2$  and  $CO_2$ ) has previously been difficult to study in photosynthetic organisms, and especially in endosymbiotic relationships such as corals, where several compartments of respiration can coexist. Many attempts, including those by Muscatine and Porter (1977) and Edmunds and Gates (1988), as well as Cooper (2011) have been made to make assumptions about gas exchange dynamics in the light and dark in such systems. However, since the pioneering study of Kühl et al. (1995) on corals, a method has been available to directly assess the  $O_2$  exchange rates within the coral tissue using fast  $O_2$  microelectrodes embedded in the coral tissue. With fast  $O_2$  microsensors, gross photosynthesis (GP) can be determined independently of light respiration ( $R_{light}$ ) via the light-dark shift technique (Al-Horani et al. 2003a; Kühl et al. 1995; Revsbech and Jorgensen 1983). In conjunction with measured net photosynthetic rates (Pnet), this technique therefore allows for the determination of light respiration rates ( $R_{light} = GP - Pnet$ ) (Jensen and Revsbech 1989). This approach has been applied here in this study with the application of photosynthesis-irradiance (P – E) curves on two differing coral-algal symbioses.

Enhanced post-illumination dark respiration (EPIR), upon transition from light to darkness, has commonly been used to make assumptions about light-driven respiratory processes in corals (Cooper et al. 2011; Levy et al. 2004). However, during dark incubations, there is no production of reducing agents due to the absence of photosynthetic light reactions, so that EPIR most likely underestimates light-driven conditions. Hence, EPIR is only a temporary solution, used to infer about light responses in respiratory rates (Cooper et al. 2011; Kühl et al. 1995); EPIR rates are given here for comparison with older methods.

Enhanced light respiratory activity is a result of processes and mechanisms, which are either light-dependent i.e. photosynthesis or dependent on energetic sustenance of the photosynthetic reaction (photosynthate). Photosynthesis and coral calcification are both light dependent processes (Levy et al. 2004; Moya et al. 2006), and both processes are also driven by the supply of DIC (Buxton et al. 2009; Herfort et al. 2008). There is a close interplay of internal utilisation of metabolic DIC, where carbonic anhydrase enzymes catalyse the reaction  $\text{CO}_2 + \text{H}_2\text{O} \leftrightarrow \text{HCO}_3^- + \text{H}^+$ , and generate substrate for the calcification reaction ( $\text{HCO}_3^- + \text{Ca}^{++} \leftrightarrow \text{CaCO}_3 + \text{H}^+$ ), as well as photosynthetic substrate ( $\text{CO}_2 + \text{H}_2\text{O} \leftrightarrow \text{CH}_2\text{O} + \text{O}_2$ ) (Jokiel 2011). But also  $\text{O}_2$  consuming processes are active during light exposure, which are in place to alleviate excess energy and ultimately prevent the formation of reactive oxygen species (ROS) (Lesser 2011). Chlororespiration (Hill and Ralph 2008a), photorespiration (Crawley et al. 2010) or the Mehler-Ascorbate Peroxidase (MAP) cycle (Schreiber et al. 1995a; Suggett et al. 2008) are  $\text{O}_2$  consuming processes, which account to respiratory activity during light exposure.

We examined the light driven respiratory responses of two hard coral species, *Pocillopora damicornis* (Linnaeus) and *Pavona decussata* (Dana), known to harbour the same algal symbiont type C1 (Hill et al. 2009), during light incubations and post-illumination phases. This was done combining measurements with a custom-built photobioreactor (PBR), employing an Algae-Growth-PAM setup allowing for the simultaneous measure of variable chlorophyll (Chl) fluorescence and metabolic gas exchange ( $\text{O}_2$  and  $\text{CO}_2$ ). In addition, an  $\text{O}_2$  microsensors technique was used to directly determine gross photosynthesis (GP) rates during light incubation and estimate light-enhanced dark respiration rates from rapid light-dark shifts during P – E curves. This experimental design enabled an in-depth analysis of the relationship between DIC



exchange and symbiont GP rates, as well as holobiont light and dark respiratory activity.

## 5.2 Materials and Methods

### 5.2.1 Coral collection and preparation

Specimens of *Pocillopora damicornis* (Pocilloporidae) and *Pavona decussata* (Agariciidae) were collected from Heron Island reef flat and maintained in recirculating aquaria in artificial seawater (ASW; Aquasonic) at the University of Technology, Sydney for up to 2 months (salinity: 32, carbonate 140 ppm,  $26 \pm 1$  °C and irradiance  $\sim 40 \mu\text{mol photons m}^{-2} \text{s}^{-1}$  on a 12:12 light:dark cycle). *P. damicornis* is a finely branched coral with a high sensitivity to coral bleaching (Hill et al. 2012), while *P. decussata* is a foliaceous (plate-like) coral and reportedly bleaching tolerant (Hill et al. 2012). After coral colonies were fragmented into experimental size pieces (average surface area:  $28.6 \pm 11.3 \text{ cm}^2$  and  $23.5 \pm 7.2 \text{ cm}^2$  for *P. damicornis* and *P. decussata*, respectively; mean  $\pm$  SEM) they were fixed with non-toxic epoxy (AquaKnead, Selleys) to sample holders.

### 5.2.2 Experimental setup

The photobioreactor (PBR) Algae-Growth- Pulse Amplitude Modulated (PAM) used in this study is a novel instrument setup combining three measuring techniques (Chl fluorescence, O<sub>2</sub> exchange and DIC exchange) to assess physiological parameters of aquatic phototrophs. The PBR consists of a closed gas-circuit with inclusion of a liquid-phase, by combining an integrated Algae-Growth-PAM Chl fluorometer (Gademann Instruments GmbH, Germany; measuring both O<sub>2</sub> and Chl fluorometry at 30 s sampling resolution) coupled with an Infra-red Gas Analyser (IRGA) to measure dissolved inorganic carbon (DIC) concentration in the incubation medium (MGA3000, ANRI

instruments, UK; measuring CO<sub>2</sub> exchange, 1 s measurement resolution). The measurement principle is based on Henry's gas law, which states that at a constant temperature and pressure the gas- and liquid-phase are in steady-state. Upon operation, the gas-phase is effervescing through the liquid-phase to liberate DIC into gaseous CO<sub>2</sub>, which is detected with the IRGA (hereafter gas exchanges related to light incubations will be referred to as 'DIC' and gas exchanges related to dark incubations will be referred to as 'CO<sub>2</sub>'). Each specimen was held in the Algae-Growth-PAM chamber, where dissolved O<sub>2</sub> (DO) was measured, as well as incident irradiance and temperature. For a more detailed setup description see Chapter 4.

### ***5.2.3 Experimental protocol***

Steady-state dark respiration rates ( $R_{\text{dark}}$ ) were measured prior to incubation of coral specimens at nine irradiance levels (10, 20, 40, 78, 210, 360, 560, 780 and 1100  $\mu\text{mol photons m}^{-2} \text{s}^{-1}$ ) (*P. damicornis* n = 4 and *P. decussata* n = 3). Light incubations of the steady-state P – E curves lasted 20 min followed by a 20 min post-illumination to account for light intensity specific respiratory activity. Variable Chl fluorescence, O<sub>2</sub> evolution and DIC uptake were recorded during the P – E curves. Net O<sub>2</sub> exchange and net DIC exchange ( $P_{\text{netO}_2}$  and  $P_{\text{netDIC}}$  respectively) were obtained during light incubations. Enhanced post illumination respiration ( $R_{\text{EPIR}}$ ) rates were determined for O<sub>2</sub> and CO<sub>2</sub> exchange ( $R_{\text{EPIR O}_2}$  and  $R_{\text{EPIR CO}_2}$ , respectively) for all irradiances during post-illumination dark incubations. The sum of net and respiratory gas exchange was used to determine gross exchange rates for O<sub>2</sub> ( $\text{GP}_{\text{PBR}}$ ; here called PBR as we also determined GP with microsensors;  $\text{GP}_{\text{micro}}$ ) and DIC (gross primary production; GPP).

### 5.2.4 Chlorophyll fluorescence

The saturation flash technique was applied using the PAM fluorometer with blue excitation light (peak wavelength = 450 nm; Ø=0.32 cm plastic fiber; settings: saturating intensity: > 5000  $\mu\text{mol photons m}^{-2} \text{s}^{-1}$ , saturating width: 0.8 s, gain: 2, measuring intensity: < 0.15  $\mu\text{mol photons m}^{-2} \text{s}^{-1}$ ) (Schreiber 2004). The quenching analysis applied here assumed that photosystem (PS) II and I share one pool of light-harvesting complexes (lake model), rather than having distinct light-harvesting complexes attached to exclusively one of the photosystems (puddle model) (Kramer et al. 2004). Photosynthetic parameters derived from P – E curves were used to estimate Y(NPQ), Y(NO) and Y(II) (see below; as per Kramer et al. 2004). In order to monitor these energy dissipation pathways for each irradiance level, photosynthesis was measured in ‘steady-state’ (Genty et al. 1989). The model assumes a total energy input of 1, which is the sum of Y(II), Y(NO) and Y(NPQ) (Kramer et al. 2004) (equation 1-3):

$$1) \ Y(\text{II}) = (F_M' - F') / F_M'$$

$$2) \ Y(\text{NPQ}) = 1 - \Phi_{\text{PSII}} - (1 / (\text{NPQ} + 1 + qL ((F_M / F_0) - 1)))$$

$$3) \ Y(\text{NO}) = 1 / (\text{NPQ} + 1 + qL ((F_M / F_0) - 1))$$

As described in detail in Chapter 3 and 4; 1) Y(II) is the yield of photochemistry (photochemical efficiency) and is equivalent to effective quantum yield ( $\Phi_{\text{PSII}}$ ) (Genty et al. 1989). Y(II) can be described with Chl *a* fluorescence parameters obtained upon illumination, where *F'* describes minimum Chl *a* fluorescence and upon application of a saturating flash the light intensity specific maximum fluorescence signal (*F<sub>M</sub>'*) can be measured to then calculate the term Y(II); 2) Y(NPQ) is the yield for dissipation by down regulation and described by  $\Phi_{\text{PSII}}$  (Y(II)), and non-photochemical quenching

(NPQ) =  $(F_M - F_M') / F_M$  (Ralph and Gademann 2005), as well as  $qL$ . The parameter  $qL$  displays an estimate for the redox state of  $Q_A$  and describes the fraction of closed PSII reaction centers on the basis of a lake model assumption for the photosynthetic antenna system (shared antenna pool between photosystems) (Kramer et al. 2004); 3)  $Y(NO)$  describes non-light induced energy dissipation and is described with parameters explained above. To determine  $Y(II)$ ,  $F_M'$  and  $F'$  from the last four saturating pulses of a steady-state incubation were averaged. Prior to P – E curves, the last four saturating pulses of the dark incubation were averaged to receive  $F_0$ ,  $F_M$  for determination of  $Y(NPQ)$  and  $Y(NO)$ . The dissipative pathways in this study were estimated for irradiances between 78 – 1100  $\mu\text{mol photons m}^{-2} \text{s}^{-1}$ , to display irradiances above  $E_c$  for both coral species as Chl fluorescence can be unusually enhanced at irradiances closely above and below  $E_c$  (Beardall et al. 2004).

Relative electron transport rate (rETR) was determined for each irradiance (equation 4):

$$4) \text{ rETR} = \Phi_{\text{PSII}} \times E$$

where  $E$  is the incident irradiance (Ralph and Gademann 2005).

### ***5.2.5 Curve fitting***

Quantitative parameters to describe Chl fluorescence derived rETR and  $O_2$  microsensor derived  $GP_{\text{micro}}$  rates as a function of irradiance, were fitted with the equations by Platt et al. (1980). Initial slope ( $\alpha_{\text{rETR/GP}}$ ), minimum saturating scalar irradiance ( $E_{k \text{ rETR/GP}}$ ), maximum rETR rate ( $\text{rETR}_{\text{max}}$ ) and maximum GP rate ( $GP_{\text{max}}$ ) were derived from the curves.

### 5.2.6 *CO<sub>2</sub> light compensation point (CO<sub>2</sub>E<sub>c</sub>)*

CO<sub>2</sub>E<sub>c</sub> was measured by interpolation of Pnet<sub>DIC</sub> exchange rates (mmol C mg Chl a<sup>-1</sup> cm<sup>-2</sup>) as a function of incident irradiance (Azcón-Bieto and Osmond 1983). An exponential 4 parameter model was then applied (Chalker 1980) to curves of Pnet<sub>DIC</sub> and R<sub>EPIR CO<sub>2</sub></sub> fluxes (mmol C mg Chl a<sup>-1</sup> cm<sup>-2</sup>), as well as GP<sub>PBR</sub> (mmol O<sub>2</sub> mg Chl a<sup>-1</sup> cm<sup>-2</sup>) as a function of incident irradiance to fit light intensity related concentrations. Metabolic gas exchange fluxes were modelled at 10 μmol photons m<sup>-2</sup> s<sup>-1</sup> < CO<sub>2</sub> E<sub>c</sub> to determine metabolic gas exchange at sub-saturating irradiances for both species. To avoid metabolic gas exchange variability due to the ‘Kok effect’ (Kok 1948), modelled fluxes were determined at 10 μmol photons m<sup>-2</sup> s<sup>-1</sup>. These fluxes were deemed as ‘low light’ metabolic gas exchange fluxes and used for species comparison.

### 5.2.7 *Oxygen microsensor measurements*

Corals were placed in an acrylic flow-through chamber (flow velocity was ~1 cm s<sup>-1</sup>) with aerated, artificial seawater (ASW of rearing aquaria, see above). Samples were illuminated vertically using a fiber-optic tungsten-halogen lamp (KL-2500, Schott GmbH, Germany) equipped with heat filter and collimated lens. O<sub>2</sub> microsensors were mounted on a PC-controlled motorized micromanipulator for automatic profiling (Pyro-Science GmbH, Germany) at an angle of 20° relative to the vertical incident irradiance. A more detailed description on the microsensor set-up used in this study can be found in (Wangpraseurt et al. 2012). Microenvironmental characterisation of O<sub>2</sub> exchange was done with fast Clark-type O<sub>2</sub> microsensors (tip size: 25 μm; stirring sensitivity: < 1%, 90% response time: < 0.5 s; Unisense AS, Denmark) under six downwelling irradiance levels (0, 40, 80, 210, 550, 1100 μmol photons m<sup>-2</sup> s<sup>-1</sup>). After photosynthesis became steady after 10-15 min in the light, the light was turned off and the light to dark shift in

O<sub>2</sub> exchange was measured using a conventional strip-chart recorder with a rapid time response (BD25, Kipp & Zonen, The Netherlands). Measurements were conducted on two coral fragments per species (n = 2). For each fragment, three spots were randomly chosen and measurements averaged. Measurements were exclusively conducted on the coenosarc (tissue connecting polyps) in order to minimize the influence of tissue movement (Kühl et al. 1995) and the spatial heterogeneity of photosynthesis (Al-Horani et al. 2005).

For each irradiance, net and gross photosynthesis rates were determined by measuring O<sub>2</sub> steady-state profiles and O<sub>2</sub> concentration dynamics under light-dark shifts, respectively (Revsbech and Jorgensen 1983, and see Kühl et al. 1995 for specific description for application on corals ). O<sub>2</sub> profiles were measured from the coral surface upwards into the water column in vertical steps of 40 µm. Light-dark shifts were conducted from the coral surface down to the coral skeleton, which covered a distance of ~80 µm for both species. The position of the sensor on the skeleton surface was identified as a slight bending of the microsensor. Net O<sub>2</sub> exchange fluxes were calculated from the measured steady-state profiles using Fick's first law of diffusion (diffusion coefficient= 2.241 x 10<sup>-5</sup> cm<sup>2</sup> s<sup>-1</sup> for 25°C and salinity 33, (Li and Gregory 1974)). The area-specific GP was obtained by dividing the measurements of volume specific GP with the thickness of the tissue, i.e. 80 µm (see above) (O<sub>2</sub> microsensor derived GP will be referred to GP<sub>micro</sub> hereafter). Light respiration (R<sub>light O<sub>2</sub></sub>) (the respiration occurring while the coral is incubated in the light) was then calculated by subtracting the area-specific GP<sub>micro</sub> and net photosynthesis rates (P<sub>net micro</sub>) as follows as per Revsbech and Jorgensen (1983) (equation 5):

$$5) R_{\text{light O}_2} = \text{GP}_{\text{micro}} - \text{P}_{\text{net micro}}$$

### 5.2.8 Metabolic gas exchange analyses

Relative rate changes of  $R_{\text{EPIR O}_2}$  and  $R_{\text{light O}_2}$  rates were computed relative to  $R_{\text{dark}}$  rates (derived from EPIR and microsensor measurements respectively). The sum of  $R_{\text{EPIR CO}_2}$  and  $P_{\text{netDIC}}$  was used to determine gross primary productivity (GPP) rates (Falkowski and Raven 2007) as follows (equation 6):

$$6) \text{ GPP} = R_{\text{EPIR CO}_2} + P_{\text{netDIC}}$$

and was displayed along with  $\text{O}_2$  microsensor derived  $\text{GP}_{\text{micro}}$  rates as a function of incident irradiance for both species.

$\text{CO}_2$  efflux detected at irradiances below  $\text{CO}_2\text{E}_c$  during light incubation indicate activity of light respiration ( $P_{\text{netDIC}} = R_{\text{light CO}_2}$  at  $< \text{CO}_2\text{E}_c$  irradiance), where the difference of  $R_{\text{EPIR CO}_2}$  and  $R_{\text{light CO}_2}$  was used to estimate the internal DIC usage (equation 7):

$$7) \text{ Internal DIC usage} = R_{\text{EPIR CO}_2} - R_{\text{light CO}_2}$$

$\text{GP}_{\text{micro}}$  to  $R_{\text{light O}_2}$  ratios (P/R ratios) obtained from  $\text{O}_2$  microsensor measurements were calculated as per equation of Muscatine and Porter (1977) (equation 8):

$$8) \text{ P/R} = \text{GP}_{\text{micro}} / R_{\text{light O}_2}$$

P/R ratios  $> 1$  indicate autotrophic activity of the symbionts, which meets the energetic demands of the coral holobiont, and ratios  $< 1$  indicate that autotrophy of the symbionts is below the respiratory demand of the holobiont (Coles and Jokiel, 1977).

### **5.2.9 Biometric measures**

Following the gas exchange measurements within the chamber, coral specimens were snap frozen in liquid nitrogen for subsequent determinations of symbiont density, photosynthetic pigment and protein concentration. Once removed from the liquid nitrogen, corals were transferred to a 100 mL Erlenmeyer flask kept on ice, with 15 mL of 4 °C homogenization buffer consisting of filtered seawater (FSW) and 1 mM phenylmethylsulfonyl fluoride (protease inhibitor). The flask was covered with Parafilm and shaken for 10 min by hand in a circular motion, allowing the coral tissue to tear off the skeleton. The resulting liquid was homogenized on ice (Ultra-Turrax, Ika, Guangzhou) for 30 s. The homogenate was centrifuged at 699 g for 5 min at 4 °C and the resulting algal symbiont pellet was kept aside for algal cell density counts and for photosynthetic pigment analyses. Of the supernatant containing the coral tissue, 2 mL was sampled for protein concentration determination using the Bradford assay, with bovine serum albumin standards (Bradford 1976). Assay absorbance was measured with a 96-well plate reader (Bio Rad Bench Mark Plus spectrophotometer) and analysed using the Microplate Manager Software (Bio Rad).

The algal symbiont pellet was re-suspended in 4 mL of FSW and subsamples were taken for algal symbiont counts. The algal suspension was again centrifuged at 1789 g and re-suspended in 3 mL of 90% acetone and incubated for 24 h at 4 °C to extract pigments. Pigment concentrations were measured using a spectrophotometer (Cary UV-VIS, USA) and absorbance results were analysed according to Ritchie (2006). Coral skeleton surface area was determined using single-dip paraffin wax technique (Stimson and Kinzie 1991).



### 5.2.10 Statistical analyses

Data were analysed by applying Student's t-test ( $t$ ;  $\alpha = 0.05$ ) to compare means of biometric parameters (symbiont density, chlorophyll concentration, protein biomass) as well as P-E curve parameters ( $rETR_{\max}$  (a.u.),  $GP_{\max}$  ( $\text{nmol O}_2 \text{ cm}^{-3} \text{ s}^{-1}$ ),  $E_k$   $rETR$  and  $E_k$   $GP$  ( $\mu\text{mol photons m}^{-2} \text{ s}^{-1}$ ) as well as  $\alpha$   $rETR$  and  $\alpha$   $GP$ ); univariate one-way and two-way analysis of variance (ANOVA;  $F$ ;  $\alpha = 0.05$ ) or when variance was heterogeneously distributed, the non-parametric Kruskal Wallis test ( $H$ ;  $\alpha = 0.05$ ) was used (using Statistica 10 Statsoft Inc, Tulsa, OK, USA) to analyse respiratory gas exchange and photosynthetic performance across the different light intensities. Tukey's HSD was used for post-hoc comparison of means to identify differences considering  $p = 0.05$ . ANOVA assumptions for normal distribution and homogeneity of variances were tested using Shapiro Wilk test and Levene's test, respectively. If necessary, data were transformed using logarithmic or arcsine transformation to meet statistical assumptions.

## 5.3 Results

### 5.3.1 Biometric measures

We compared two coral species from the reef flat at Heron Island both acclimated to high light conditions: *Pocillopora damicornis* and *Pavona decussata*. The species examined here differed in protein biomass, total Chl concentration, as well as symbiont cell density (Table 5.1).

**Table 5.1:** Biometric measures of the two hard coral species examined (n=4; mean  $\pm$  SEM) displaying total chlorophyll (Chl *a* + Chl *c*<sub>2</sub>), algal cell densities per coral surface area and total Chl per cell (significant differences are indicated with an asterisk).

	<i>Pocillopora damicornis</i>	<i>Pavona decussata</i>
<b>Total Chl (mg) *</b>	0.084 $\pm$ 0.013	0.196 $\pm$ 0.019
<b>Algal cell densities (cells cm<sup>-2</sup>) *</b>	5.32 x 10 <sup>5</sup> $\pm$ 1.91 x 10 <sup>5</sup>	16.7 x 10 <sup>5</sup> $\pm$ 2.00 x 10 <sup>5</sup>
<b>Total Chl (pg cell<sup>-1</sup>)</b>	9.735 $\pm$ 1.509	9.666 $\pm$ 2.463

### 5.3.2 Photosynthetic measurements

Both species presented a decline in PSII photochemical efficiency, Y(II), with increasing irradiance, where the utilisation of Y(NPQ) and Y(NO) for excess energy quenching, differed between the two species examined. Y(II) for *P. decussata* began to decrease at higher irradiances compared to *P. damicornis* (Tukey HSD,  $p < 0.05$ ; Fig 5.1 A, B). *P. decussata* showed a significant decline in Y(II) from 360  $\mu\text{mol photons m}^{-2} \text{s}^{-1}$  towards higher irradiances (one-way ANOVA,  $F(5,12) = 13.64$ ,  $p < 0.001$ ; Tukey HSD,  $p < 0.05$ ) (Fig 5.1 A). Simultaneously with the decline of Y(II), *P. decussata* displayed a significant increase of Y(NO), which occurred between 360  $\mu\text{mol photons m}^{-2} \text{s}^{-1}$  and subsequently higher irradiances (one-way ANOVA,  $F(5,12) = 8.92$ ,  $p < 0.001$ ; Tukey HSD,  $p < 0.05$ ), whereas Y(NPQ) levels remained unchanged. Y(II) of *P. damicornis* gradually declined with increasing irradiance from 78  $\mu\text{mol photons m}^{-2} \text{s}^{-1}$  onwards (one-way ANOVA,  $F(5,18) = 20.08$ ,  $p < 0.001$ , Tukey HSD,  $p < 0.05$ ; Fig 5.1 B). A simultaneous increase in Y(NPQ) occurred for the three highest irradiances (one-way ANOVA,  $F(5,18) = 7.76$ ,  $p < 0.001$ ; Tukey HSD,  $p < 0.05$ ); Fig 5.1 B). In contrast to *P. decussata*, Y(NO) levels remained unchanged for *P. damicornis*.

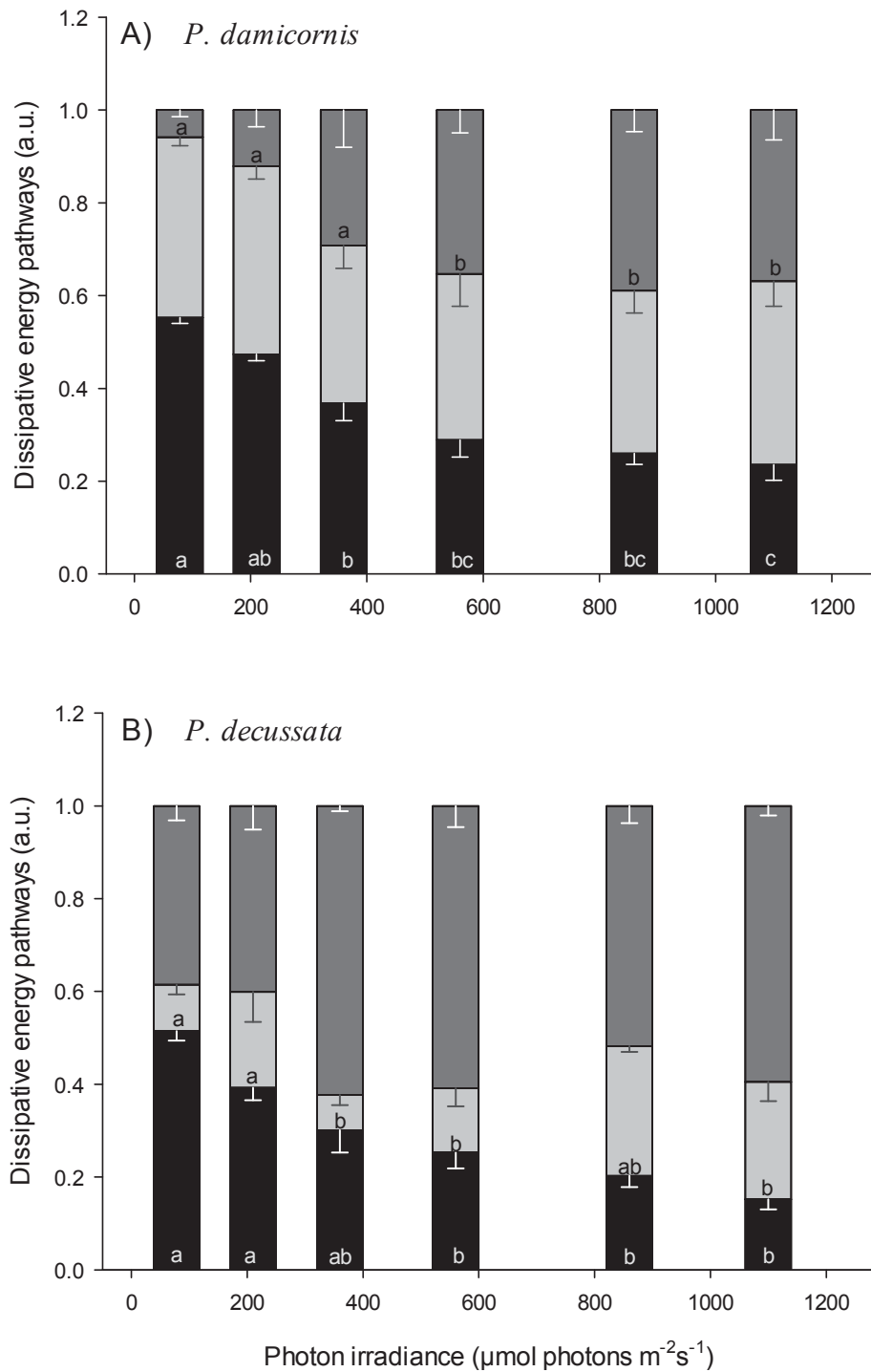


**Figure 5.1:** Dissipative energy quenching pathways displayed as the combined total light energy input of 1, at nine irradiances for (A) *P. damicornis* and (B) *P. decussata*. Photosynthetic efficiency of photosystem II indicated from bottom to top Y(II) (black bars), non-regulated non-photochemical quenching Y(NO) (light grey bars), regulated non-photochemical quenching Y(NPQ) (dark grey bars); (mean  $\pm$  SEM; *P. decussata*: n=3 and *P. damicornis*: n=4); Tukey HSD results are indicated ( $p < 0.05$ ).

### 5.3.3 Gross primary production and gross photosynthesis rates

Gross primary production (GPP) rates of *P. damicornis* were negatively related to increasing irradiance up to 78  $\mu\text{mol photons m}^{-2} \text{s}^{-1}$  (one-way ANOVA,  $F(8, 27) = 2.90$ ,  $p = 0.018$ ; Fig 5.2 A), but then increased up to 560  $\mu\text{mol photons m}^{-2} \text{s}^{-1}$  and decreased again for the two highest irradiances (Tukey HSD,  $p < 0.05$ ; Fig 5.2 A). *P. decussata*, in contrast, displayed increasing GPP rates with increasing irradiance (one-way ANOVA,  $F(8, 26) = 5.15$ ,  $p = 0.003$ ; Fig 5.2 B) to a maximum at 360  $\mu\text{mol photons m}^{-2} \text{s}^{-1}$  (Tukey HSD,  $p < 0.05$ ). The GPP rate responses at low irradiances were therefore significantly distinct in their light responses between the two species at low light intensities (pooled GPP rates for 10 - 40  $\mu\text{mol photons m}^{-2} \text{s}^{-1}$ ;  $t(22) = 3.54$ ,  $p < 0.001$ ; Fig 5.2).

$\text{GP}_{\text{micro}}$  rates, from the rapid light-dark shifts obtained from  $\text{O}_2$  microsensor measurements, were positively related to incident irradiance for both species. *P. damicornis* displayed a sharp increase to maximum  $\text{GP}_{\text{micro}}$  rates at the 3 highest irradiances applied with an average of  $0.502 \pm 0.017 \text{ nmol O}_2 \text{ cm}^{-2} \text{ s}^{-1}$  (one-way ANOVA,  $F(4,5) = 115.06$ ,  $p < 0.001$ ; Tukey HSD;  $p < 0.05$ ; Fig 5.2 A).  $\text{GP}_{\text{micro}}$  rates for *P. decussata* increased gradually to a maximum at the two highest irradiances applied with an average  $\text{GP}_{\text{micro}}$  rate of  $0.527 \pm 0.020 \text{ nmol O}_2 \text{ cm}^{-2} \text{ s}^{-1}$  at those irradiances (one-way ANOVA,  $F(4,5) = 8.9182$ ,  $p = 0.017$ ; Tukey HSD,  $p < 0.05$ ; Fig 5.2 B).

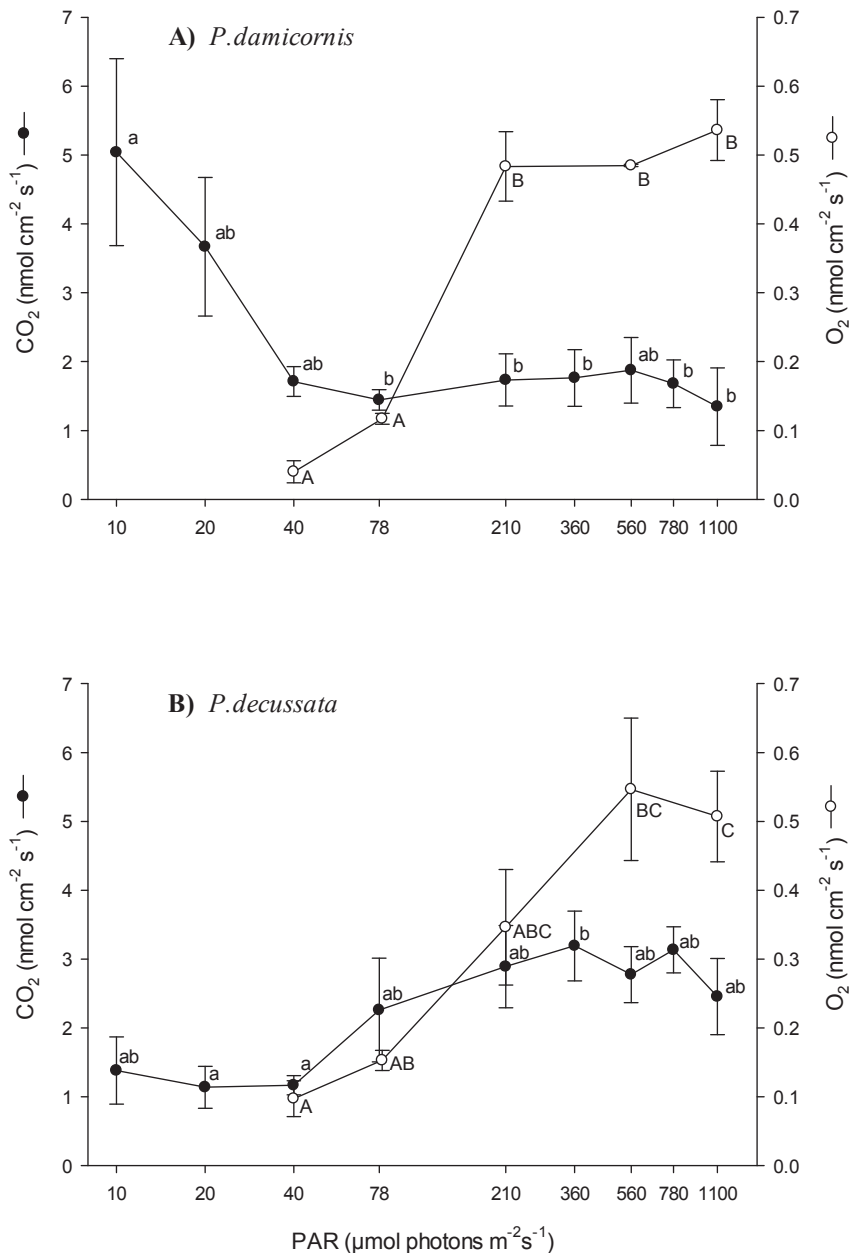


**Figure 5.2:** Gross primary production (GPP; black circles; CO<sub>2</sub> nmol cm<sup>-2</sup> s<sup>-1</sup>) and gross photosynthesis (GP; open circles; O<sub>2</sub> nmol cm<sup>-2</sup> s<sup>-1</sup>) for (A) *P. damicornis* and (B) *P. decussata* at nine irradiances; for display clarity logarithmic scale chosen for x-axis; (mean ± SEM; GPP: n=4 and GP<sub>micro</sub>: n=2); Tukey HSD results are indicated (p < 0.05).

Analysis for P – E curve parameters of rETR and GP<sub>micro</sub> rates for nine light irradiances revealed that initial slopes ( $\alpha_{\text{rETR}}$ ,  $\alpha_{\text{GP}}$ ), rETR<sub>max</sub> and GP<sub>max</sub> rates, as well as  $E_{\text{k rETR}}$  and  $E_{\text{k GP}}$  were not significantly different between the two species (Table 5.2). The rETR<sub>max</sub> rates were 6.4 times greater than GP<sub>max</sub> rates for *P. damicornis* and about 7.4 times greater than GP<sub>max</sub> rates for *P. decussata*. The initial slope of P – E curves describing the relation of rETR with incident irradiance were for both species greater than for GP<sub>max</sub> rates;  $\alpha_{\text{rETR}}$  was in both species 2.9 times greater than  $\alpha_{\text{GP}}$ . Also greater minimum saturation irradiances were found for rETR in both species, which were 2.7 times greater than  $E_{\text{k GP}}$  in *P. damicornis* and 2.1 times greater than  $E_{\text{k GP}}$  in *P. decussata*.

**Table 5.2:** Quantitative curve parameters of variable Chl fluorescence derived from fitted relative electron transport rates (rETR) and microsensor measurement derived gross photosynthesis (GP) rates as a function of incident irradiance. rETR<sub>max</sub> (a.u.), GP<sub>max</sub> (nmol O<sub>2</sub> cm<sup>-3</sup> s<sup>-1</sup>),  $E_{\text{k rETR}}$  and  $E_{\text{k GP}}$  ( $\mu\text{mol photons m}^{-2} \text{s}^{-1}$ ) as well as  $\alpha_{\text{rETR}}$  and  $\alpha_{\text{GP}}$  are presented; n=4 for *P. damicornis* and n=3 for *P. decussata* mean  $\pm$  SEM.

	<i>Pocillopora damicornis</i>	<i>Pavona decussata</i>
<b>rETR<sub>max</sub></b>	221.29 $\pm$ 45.73	240.43 $\pm$ 79.89
<b><math>\alpha_{\text{rETR}}</math></b>	0.563 $\pm$ 0.087	0.516 $\pm$ 0.027
<b><math>E_{\text{k rETR}}</math></b>	472 $\pm$ 175	421 $\pm$ 48
<b>GP<sub>max</sub></b>	35.50 $\pm$ 2.49	32.63 $\pm$ 5.48
<b><math>\alpha_{\text{GP}}</math></b>	0.197 $\pm$ 0.004	0.176 $\pm$ 0.041
<b><math>E_{\text{k GP}}</math></b>	175 $\pm$ 16	203 $\pm$ 79

### 5.3.4 Light and dark respiration

$R_{\text{light O}_2}$  rates (Fig 5.3a) as well as rate changes of  $R_{\text{light O}_2}$  and  $R_{\text{EPIR O}_2}$  relative to  $R_{\text{dark}}$  (for each measuring technique) as a response to incident irradiance were displayed (Fig 5.3 b).  $R_{\text{light O}_2}$  increased with increasing light intensities in both species (one-way ANOVA,  $F(5,6) = 10.26$ ;  $p = 0.007$  for *P. decussata* and  $F(5) = 101.08$ ;  $p < 0.001$ ).  $R_{\text{light O}_2}$  rates gradually increased for *P. decussata* with increasing light intensities to a maximum at  $780 \mu\text{mol photons m}^{-2} \text{s}^{-1}$  (Fig 5.3 a, Tukey HSD). In *P. damicornis*  $R_{\text{light O}_2}$  rates sharply increased upon exposure to  $210 \mu\text{mol photons m}^{-2} \text{s}^{-1}$  (Tukey HSD) and remained steady for all higher light intensities (Fig 5.3 a). At light intensities  $> 210 \mu\text{mol photons m}^{-2} \text{s}^{-1}$ ,  $R_{\text{light O}_2}$  rates of  $0.432 \pm 0.065 \text{ nmol O}_2 \text{ cm}^{-2} \text{s}^{-1}$  for *P. decussata* and  $0.475 \pm 0.017 \text{ nmol O}_2 \text{ cm}^{-2} \text{s}^{-1}$  for *P. damicornis* made up for 87.7 % and 96.5 % of  $\text{GP}_{\text{micro}}$ .

Both species displayed greater  $R_{\text{light O}_2}$  responses at irradiances  $> 210 \mu\text{mol photons m}^{-2} \text{s}^{-1}$  compared to  $R_{\text{EPIR O}_2}$  rates (Fig 5.3 b).  $R_{\text{light O}_2}$  rates increased compared to  $R_{\text{dark}}$  rates by  $\sim 27$  times for *P. damicornis* and  $\sim 21$  times for *P. decussata* at  $1100 \mu\text{mol photons m}^{-2} \text{s}^{-1}$ . In contrast, no light dependent changes were found for  $R_{\text{EPIR O}_2}$  rates in either of the two species (Fig 5.3 b).



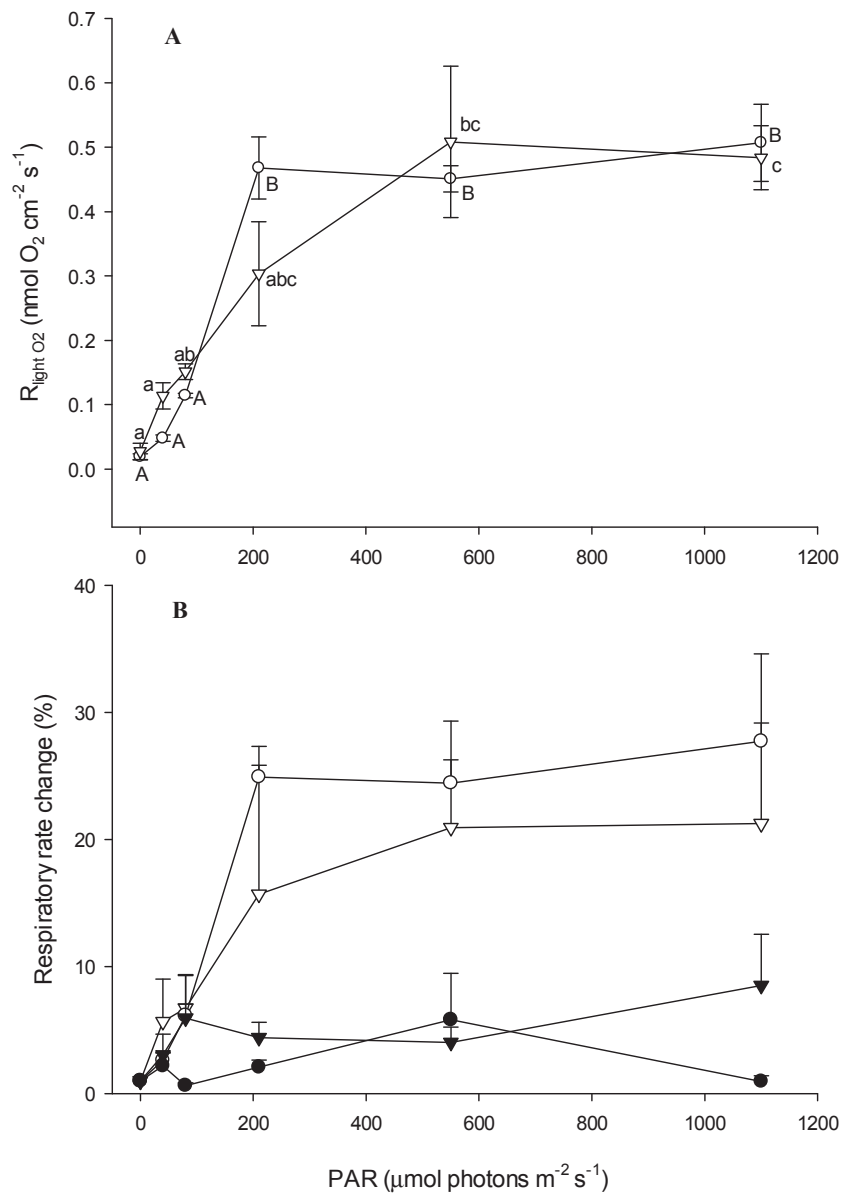


**Figure 5.3:** A)  $R_{\text{light O}_2}$  rates as a function of light intensity at 6 irradiances, *P. damicornis* (clear circle) and *P. decussata* (clear triangle); B) respiratory rate changes of  $R_{\text{light O}_2}$  (white symbols) and  $R_{\text{EPIR O}_2}$  (black symbols) relative to pre-illumination rates ( $R_{\text{dark}}$ ) for *P. damicornis* (circles) and *P. decussata* (triangles) are displayed for 6 irradiances; (mean  $\pm$  SEM;  $R_{\text{light O}_2}$ : n=2,  $R_{\text{EPIR O}_2}$ : n=4); Tukey HSD results are indicated ( $p < 0.05$ ).

### 5.3.5 CO<sub>2</sub> compensation point (E<sub>c</sub>) irradiance

The CO<sub>2</sub>E<sub>c</sub> irradiance for *P. damicornis* was determined to be at ~ 78 μmol photons m<sup>-2</sup> s<sup>-1</sup>, and for *P. decussata* at about half the photon flux density at ~ 35 μmol photons m<sup>-2</sup> s<sup>-1</sup>. To examine metabolic gas exchange rates at low light intensities, rates were determined for below CO<sub>2</sub>E<sub>c</sub> irradiance and this was chosen to be at 10 μmol photons m<sup>-2</sup> s<sup>-1</sup> < CO<sub>2</sub>E<sub>c</sub> irradiance (henceforth referred to as ‘low light intensities’; see 5.3.7). GP<sub>PBR</sub> rates were significantly lower for *P. decussata* at low light intensities compared to *P. damicornis* (0.030 ± 0.009 and 0.454 ± 0.149 mmol O<sub>2</sub> mg Chl a<sup>-1</sup> cm<sup>-2</sup>, respectively; t (6) = 2.85, p = 0.029; Table 5.3).

**Table 5.3:** Algal symbiont characteristics at CO<sub>2</sub> light compensation point (E<sub>c</sub>), metabolic gas exchange characteristics for < CO<sub>2</sub>E<sub>c</sub>: gross photosynthetic (GP) activity (mmol O<sub>2</sub> mg Chl a<sup>-1</sup> cm<sup>-2</sup>), respiratory activity measured as CO<sub>2</sub> exchange during light (R<sub>light CO2</sub>) and during dark (R<sub>EPIR CO2</sub>) (mmol C mg Chl a<sup>-1</sup> cm<sup>-2</sup>) (significant differences are indicated with an asterisk); n=4, mean ± SEM..

	<i>Pocillopora damicornis</i>	<i>Pavona decussata</i>
CO <sub>2</sub> E <sub>c</sub> (μmol photons m <sup>-2</sup> s <sup>-1</sup> )	78	35
GP (mmol O <sub>2</sub> mg Chl a <sup>-1</sup> cm <sup>-2</sup> ) *	0.454 ± 0.149	0.030 ± 0.009
R <sub>light CO2</sub> (mmol C mg Chl a <sup>-1</sup> cm <sup>-2</sup> )	5.77 ± 2.24	3.85 ± 1.35
R <sub>dark CO2</sub> (mmol C mg Chl a <sup>-1</sup> cm <sup>-2</sup> )	10.03 ± 3.75	11.56 ± 3.92

$R_{\text{light CO}_2}$  rates for *P. decussata* at low light intensities were significantly lower with  $3.85 \pm 1.35$  mmol C mg Chl  $a^{-1}$  cm $^{-2}$  compared to  $R_{\text{EPIR CO}_2}$  rates of  $11.56 \pm 3.92$  mmol C mg Chl  $a^{-1}$  cm $^{-2}$  at low light intensities ( $t(6) = 2.63$ ,  $p = 0.037$ ; data not displayed). Hence, respiration in *P. decussata* increased by  $3.9 \pm 0.9$  times upon transition from light to dark. In contrast, respiration at low light intensities in *P. damicornis* did not significantly change upon transition from light to dark; where  $R_{\text{light CO}_2}$  rates at low light intensities were  $5.77 \pm 2.24$  mmol C mg Chl  $a^{-1}$  cm $^{-2}$  and dark  $R_{\text{EPIR CO}_2}$  rates  $10.03 \pm 3.75$  mmol C mg Chl  $a^{-1}$  cm $^{-2}$ . According to the above, the internal DIC usage was  $65.02 \pm 11.84\%$  in *P. decussata* and  $69.82 \pm 7.72\%$  in *P. damicornis* (see 5.3.8).

### 5.3.6 P/R ratios

P/R ratios relating rapid light-dark shift derived  $GP_{\text{micro}}$  and  $R_{\text{light O}_2}$  rates are displayed as a function of incident irradiance (Fig 5.4). P/R ratios remained steady for *P. damicornis* displaying average ratios of  $1.01 \pm 0.05$ , where ratios retrieved for *P. decussata* significantly increased from  $40 \mu\text{mol photons m}^{-2} \text{ s}^{-1}$  to  $210 \mu\text{mol photons m}^{-2} \text{ s}^{-1}$ , when ratios reached a maximum of  $1.15 \pm 0.03$  (one-way ANOVA,  $F(4,5) = 6.39$ ,  $p = 0.033$ ; Tukey HSD,  $p < 0.05$ ).

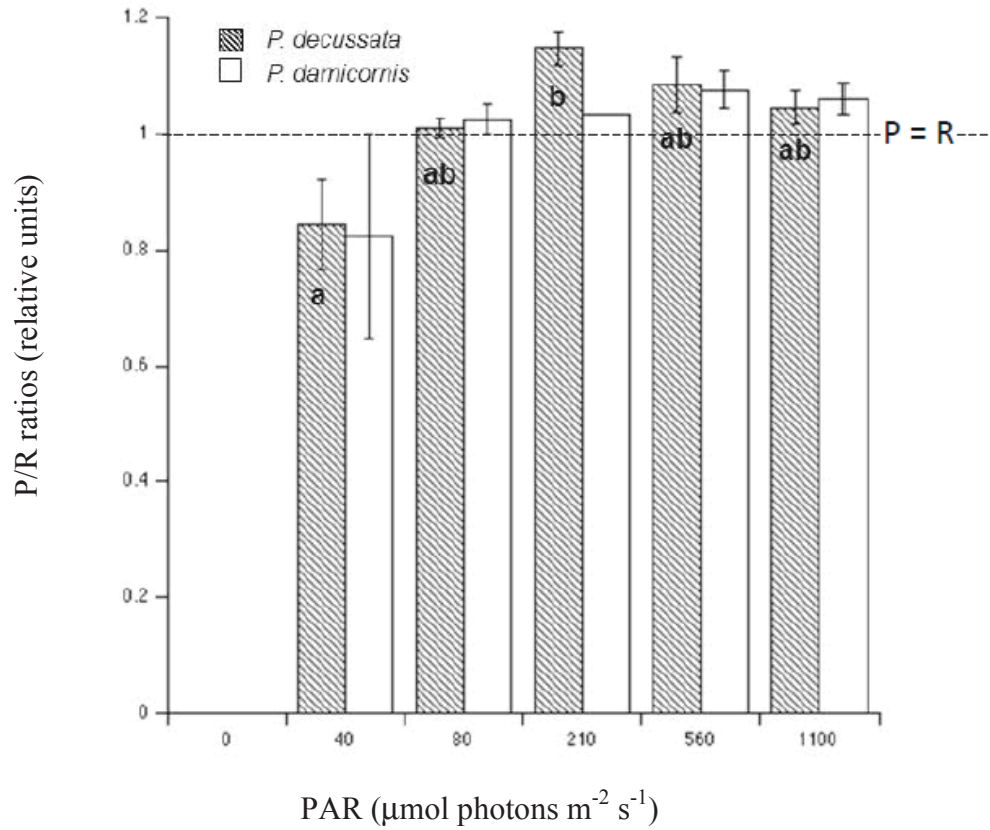


**Figure 5.4:** Photosynthesis to respiration ratios (P/R ratios) of microsensor derived gross photosynthesis ( $GP_{\text{micro}}$ ) to light respiration rates ( $R_{\text{light O}_2}$ ); *P. decussata* (streaked bars) and *P. damicornis* (clear bars) at nine irradiances; dotted line indicates  $P = R$  level where ratios  $> 1$  indicate autotrophy was efficient to meet coral holobiont respiratory demand and  $< 1$  indicate that respiratory demand of the holobiont was greater than autotrophic output; (mean  $\pm$  SEM;  $n=2$ ); Tukey HSD results are indicated for *P. decussata* ( $p < 0.05$ ), no significant differences were found for *P. damicornis*.

## 5.4 Discussion

Here, measurements of a custom-built algal photobioreactor incorporating PAM fluorometry, IRGA for CO<sub>2</sub> analysis and O<sub>2</sub> sensor were combined to gain a more complete understanding of metabolic gas exchange activity (O<sub>2</sub> and DIC/CO<sub>2</sub> fluxes) of two hard coral species and their algal symbionts when exposed to a range of irradiances. In addition, fast O<sub>2</sub> microsensor technique was used to obtain respiration rates in the light, as well as gross photosynthesis. One particular focus of this study was to assess whether host characteristics, such as host tissue protein biomass, are related to the photosynthetic output and performance of the algal symbionts. *P. damicornis* is reportedly a stress sensitive species and has been characterised as bleaching susceptible under e.g. thermal and/or high light stress, where *P. decussata* has been reported to be a more stress resilient species (Hill et al. 2012; Krämer et al. 2013). Furthermore, it was aimed to investigate these two species, in terms of respiratory responses during light and dark to draw conclusions about DIC pool utilisation, by categorising irradiances as either below or above the CO<sub>2</sub> light compensation point, CO<sub>2</sub>E<sub>c</sub>. Light respiration responses of two hard coral species during P – E curves are demonstrated here for the first time.

### 5.4.1 Light utilisation and gross primary productivity

CO<sub>2</sub>E<sub>c</sub> irradiance is directly related to the respiratory activity of the holobiont, as it is that irradiance where net photosynthesis rates are fixing C at the same rate as metabolically derived C is liberated (Sharp et al. 1984). The greater algal symbiont density found for *P. decussata* is the most likely explanation for the greater DIC exchange and the resulting comparatively low CO<sub>2</sub>E<sub>c</sub> irradiance found for this species. When *P. decussata* is exposed to low light conditions (< CO<sub>2</sub>E<sub>c</sub>), its algal symbionts

utilise the incoming light very efficiently and produce enough energetic sustenance to fuel the DIC uptake mechanisms. Gross primary production (GPP) rates for *P. decussata* were positively related to incident irradiance and 2.2 times higher at irradiances  $> 78 \mu\text{mol photons m}^{-2} \text{ s}^{-1}$  compared to *P. damicornis*. The efficient GPP demonstrated here by *P. decussata* through DIC exchange measures, is most likely a result of the efficient light utilisation to manage DIC uptake from the external media already at low light intensities. Host tissue properties, e.g. protein biomass (Krämer et al. 2013), have been suggested to create a naturally enhanced light field for algal symbionts harboured in *P. decussata* (Wangpraseurt et al. 2012). The natural diffraction of light within a tissue matrix has mostly been discussed in conjunction with microscopy techniques, where the aberration (i.e. diffusion of the light) has been explained by the different refractive indexes of the layers making up the whole tissue matrix (Wang and Smith 2012). The enhancement of incident irradiance through diffraction has been demonstrated in solar cell research (Tobías et al. 2008) and recently at the coral surface (Wangpraseurt et al. 2012). The positive enhancement of incident light reaching the algal symbionts harboured in *P. decussata* could therefore result in the greater ability to take up DIC from the external media and therefore alleviating limitations of photosynthetic substrate.

*P. damicornis* displayed a comparably high  $\text{CO}_2\text{E}_c$  irradiance indicating that much greater incident light intensities were necessary to initiate DIC uptake from the external media. Further, algal symbionts of *P. damicornis* displayed high gross photosynthetic activity just below  $\text{CO}_2\text{E}_c$  compared to rates retrieved for *P. decussata* (Table 5.3). This indicates that algal symbionts in *P. damicornis* are experiencing a high  $\text{O}_2$  relative to  $\text{CO}_2$  environment  $< \text{CO}_2\text{E}_c$ . As *Symbiodinium* is known to be equipped with a type II Rubisco (Rowan et al. 1996), high concentrations of  $\text{O}_2$  are most likely to result in

Rubisco's oxygenase functionality and therefore high rates of photorespiration (Jordan and Ogren 1981; Leggat et al. 1999). Photorespiration is a mechanism, which is energy consuming and therefore less efficient, but for this reason it can be considered as a photoprotective mechanism (Crawley et al. 2010). Photorespiration characteristically lowers the rate of carbon fixation efficiency, but does not diminish it like other photoprotective pathways (Eisenhut et al. 2006). Higher photorespiratory activity alongside the lower density of algal symbionts resulting in lower photosynthetic efficiency per unit area could be the reason for the higher susceptibility of *P. damicornis* to bleaching.

#### **5.4.2 Gross photosynthesis and light respiratory activity**

P/R ratios of O<sub>2</sub> microsensor derived GP<sub>micro</sub> and R<sub>light O<sub>2</sub></sub> rates showed that both species displayed P/R ratios > 1, indicating sufficient autotrophic productivity to meet the coral host's respiratory demands (Muscatine et al. 1981). For both species E<sub>k GP</sub> was at about half the irradiance of E<sub>k rETR</sub> and α<sub>rETR</sub>, indicated in both species a slower saturation of rETR rates compared to GP<sub>micro</sub> rates (Table 5.2). GP<sub>micro</sub> rates increased sharply and stayed steady at irradiances > E<sub>k GP</sub> (Fig 5.2) in both species, where rETR rates (not displayed) did not saturate to steady-state under irradiances applied during the P – E curves. The lack of downturn in GP rates at saturating irradiances has been reported in earlier studies from O<sub>2</sub> microsensor measurements estimating GP<sub>micro</sub> in corals (Kühl et al. 1995; Ulstrup et al. 2011; Ulstrup et al. 2006b). The results indicate that the overall GP production was being maintained with an increasing supply of electrons channeled through PSII, as rETR rates were positively related to increasing irradiances applied during P – E curve measurements. Excess electrons that did not yield greater GP rates

could therefore be attributed to the activity of alternative electron pathways (Franklin and Badger 2001; Prasil et al. 1996; Ralph et al. 2010).

Increases of  $R_{\text{light O}_2}$  rates compared to  $R_{\text{dark}}$  rates were  $\sim 20$  times higher compared to  $R_{\text{dark}}$  rates at  $> 210 \mu\text{mol photons m}^{-2} \text{ s}^{-1}$  (Fig 5.3), where no change in  $R_{\text{EPIR O}_2}$  responses could be detected in either of the two species. Pronounced light responses of  $R_{\text{light O}_2}$  have been reported for the coral species *Galaxea fascicularis* as  $\sim 12$  times greater than  $R_{\text{dark}}$  at a light intensity of  $140 \mu\text{mol photons m}^{-2} \text{ s}^{-1}$  (Al-Horani et al. 2003a) and 6 times greater than  $R_{\text{dark}}$  at  $350 \mu\text{mol photons m}^{-2} \text{ s}^{-1}$  in *Favia* sp. (Kühl et al. 1995). Further,  $R_{\text{light O}_2}$  accounted for 88% of the  $\text{GP}_{\text{micro}}$  at  $350 \mu\text{mol photons m}^{-2} \text{ s}^{-1}$  in *Favia* sp. (Kühl et al. 1995); where here  $R_{\text{light O}_2}$  rates accounted for 87.7 % in *P. decussata* and 96.5 % in *P. damicornis* of  $\text{GP}_{\text{micro}}$  at  $250 \mu\text{mol photons m}^{-2} \text{ s}^{-1}$  and are therefore comparable. Enhanced  $R_{\text{light O}_2}$  was interpreted by Al-Horani et al. (2003a) to indicate the activity of Calcium-ATPases supplying ATP for enhanced calcification processes during light incubations (for review Jokiel 2011). Further, increased  $R_{\text{light O}_2}$  has previously been attributed to greater levels of photosynthate transfer fuelling metabolic processes during light exposure (Edmunds and Davies 1986; Rink et al. 1998). However, there are a number of light-enhanced  $\text{O}_2$  consuming processes (chlororespiration, photorespiration, MAP pathway etc.) which could be responsible for the high levels of light-driven respiration found here.



### ***5.4.3 Light-driven mitochondrial processes***

A substantial part of the light-driven respiration measured here could be due to the stimulation of mitochondrial activity. Such activity would fuel calcification processes and a number of anabolic processes requiring both, direct energy source (ATP) and photosynthate, which are only readily available in the light. Recently it was shown that the main photosynthetic compound exported from the algal symbionts is glucose (Burriesci et al. 2012), rather than glycerol as had been proposed previously (Gates et al. 1995). Since glucose is a prime respiratory substrate in animal tissues of all kinds and can easily be used as a source of energy through glycolysis via the Embden-Meyerhof-Parnas (EMP) pathway, this poses no difficulty for such a respiratory mechanism (Newsholme and Crabtree 2005). What is implied, however, is a sensitive metabolic control system whereby energy and photosynthate export from the algal symbionts is switched off rapidly upon darkening and very little is known about such control systems.

#### ***5.4.3.1 Oxygen consuming pathways***

The enhanced  $R_{\text{light O}_2}$  activity observed here with increasing irradiance is a result of light-driven  $\text{O}_2$  consuming processes (Cooper et al. 2011).  $\text{O}_2$  consuming pathways include chlororespiration (Hill and Ralph 2008a; Jakob et al. 1999), photorespiration (Crawley et al. 2010; Parys and Jastz 2006) and the MAP cycle (Schreiber et al. 1995a; Suggett et al. 2008). During chlororespiration an alternative oxidase is activated, which reduces the plastoquinone pool without the necessity of a photosynthetic reaction (Hill and Ralph 2008a), the activity can make up to 10% of the mitochondrial respiration (Peltier and Schmidt 1991). However, chlororespiration is as far as is known at present a process that operates in darkness or near darkness in corals (Hill and Ralph 2008a).

Photorespiration in contrast consumes considerable amounts of O<sub>2</sub> in the light and it is also less efficient than the carboxylase driven Calvin-Benson cycle (Crawley et al. 2010), mainly through its much higher utilisation of ATP and NADPH per unit of sugar produced compared to photosynthesis (Eisenhut et al. 2006). The MAP cycle is a very efficient antioxidative pathway, which acts around PSI and takes up O<sub>2</sub> produced through the oxidation of water at the oxygen evolving complex (Schreiber et al. 1995a), and through ROS intermediates neutralize these to water again (Suggett et al. 2008). The activity of the MAP cycle is not possible to be measured under ambient O<sub>2</sub> concentrations as it does not result in any net O<sub>2</sub> concentration changes (Schreiber et al. 1995a) and is therefore not captured in GP<sub>micro</sub> rate measurements (Glud et al. 1992).

#### **5.4.3.2 Dissolved inorganic carbon as a substrate for light-driven processes**

With increasing light intensities, most studies have shown that greater amounts of photosynthate are produced and assimilated within the holobiont for processes including growth (e.g. macromolecular synthesis), protein biosynthesis (e.g. pigments) and calcification (Houldbrèque and Ferrier-Pagès 2009). The metabolic DIC pool size is dependent on the level of holobiont respiration as well as the energetically fuelled DIC uptake from the external environment, and can constitute up to 75% of the C used for calcification (at  $\sim 200 \mu\text{mol photons m}^{-2} \text{ s}^{-1}$ ) (Furla et al. 2000). Here it was demonstrated by using C exchange measurements, that 65 – 70% of the metabolically derived C was internally utilised at low light intensities in both species. It can therefore be concluded, that *P. damicornis* has a comparable respiratory activity per symbiont to *P. decussata*, but as *P. damicornis* harbours fewer symbionts per unit area, the holobiont exhibits a higher CO<sub>2</sub>E<sub>c</sub> irradiance and therefore a low internal DIC environment < CO<sub>2</sub>E<sub>c</sub>. DIC supply is a critical aspect of a coral symbiosis (Goiran et al.

1996; Muscatine et al. 1989; Weis 1993), where increased DIC supply can have positively enhancing effect upon photosynthetic rate (Buxton et al. 2009). The results presented here suggest that algal symbionts harboured in *P. decussata*, a bleaching resilient species, are not living in DIC limiting conditions. This may suggest that DIC supply can alleviate the effect of stressful conditions e.g. in terms of excessively high photosynthetic rates under high light stress and might explain the more resilient response of algal symbionts in *P. decussata* under bleaching conditions (Hill et al. 2012). Here it could be confirmed that *P. decussata* contains much greater tissue protein biomass compared to *P. damicornis*, which could be partly the cause of differing light fields created within the tissue matrix (Jacques 1998; Wang et al. 1995). This would further support the finding that much lower incident light intensities were necessary to engage DIC uptake mechanisms from the external media in *P. decussata*.

#### **5.4.4 Measuring gross photosynthesis rates**

Maximum gross photosynthesis rates measured with O<sub>2</sub> microsensors (GP<sub>micro</sub>) found here were on average  $\sim 0.53 \text{ nmol O}_2 \text{ cm}^{-2} \text{ s}^{-1}$  for both coral species at saturating irradiances ( $> E_{k \text{ GP}}$ ) and were comparable with previously reported gross photosynthesis (GP) rates derived through microsensor measurements (e.g. Ulstrup et al. 2006b). Commonly, GP rates are estimated by using the sum of light incubation derived net O<sub>2</sub> production and the amount of O<sub>2</sub> replaced from respiratory processes during dark incubation. Respiration rate dynamics in the dark, as demonstrated here, were less dependent on pre-illumination intensity compared to respiratory activity during the light (Fig 5.3). Hence, a natural underestimation can be assumed when GP rates are estimated with the common GP estimation technique ( $\text{GP} = R_{\text{EPIR}} + P_{\text{net}}$ ). The reason why enhanced post-illumination respiration ( $R_{\text{EPIR}}$ ) rates have been used to

estimate GP is simply because of limitation in technology. Unlike O<sub>2</sub> microsensors, commonly applied O<sub>2</sub> optodes do not possess the temporal resolution necessary to apply the light-dark shift technique to retrieve light respiration rates (Kühl et al. 1995; Revsbech and Jorgensen 1983). True light respiration rates have not been reported from P – E curve results to date and the results clearly highlight that R<sub>EPIR</sub> rates are not even close to mirroring the actual light respiratory activity. Previous studies focused on characteristic O<sub>2</sub> exchanges at one light intensity rather than running P – E curves (Al-Horani et al. 2003a; Kühl et al. 1995) or focused on a different aspect such as the R<sub>EPIR</sub> activity (Cooper et al. 2011). The use of fast O<sub>2</sub> microsensors (< 0.5 s resolution) to measure the light-driven respiration is a relatively new technique and the results of which need to be applied cautiously. Kühl et al. (1995) found that the placement of the microelectrode depth wise in the coral tissue made a big difference. Here the microsensors were moved through the coral tissue at equal intervals for *P. damicornis* as well as *P. decussata* and allowed for profiling to up to 80 µm. While the technique has not been applied extensively to corals (see e.g. Al-Horani et al. 2003b; Cooper et al. 2011; Kühl et al. 1995; Ulstrup et al. 2011; Ulstrup et al. 2006b) the identical technique has been tested on many other marine and terrestrial tissues and communities and has been found to give reliable results (Behrendt et al. 2012; Kühl and Fenchel 2000; Rink et al. 1998).

#### 5.4.5 Photosynthetic energy dissipation

Although both coral species showed a decline in Y(II) at increasing irradiances, *P. decussata* displayed the onset of Y(II) decline at higher irradiances ( $> 360 \mu\text{mol photons m}^{-2} \text{s}^{-1}$ ) compared to *P. damicornis*, which showed an induction of Y(II) decline at much lower irradiance intensities ( $> 78 \mu\text{mol photons m}^{-2} \text{s}^{-1}$ ). In *P. decussata*, as Y(II) began to decrease, Y(NO) was up-regulated. Y(NO) is a non-light induced energy dissipative pathway, which is releasing excess energy through heat radiation rather than active dissipative processes (Kramer et al. 2004). In contrast, *P. damicornis* up-regulated light-induced Y(NPQ) as a dissipative pathway with increasing irradiances when Y(II) declined.

Interestingly, GPP rates as well as Y(II) started to decline at irradiances  $> 360 \mu\text{mol photons m}^{-2} \text{s}^{-1}$  in *P. decussata* whereupon  $\text{GP}_{\text{micro}}$  rates and  $\text{R}_{\text{light}}$  rates were at their maximum at the two highest irradiances along with up-regulated Y(NO). As  $\text{GP}_{\text{micro}}$  rates did not decline, it can be excluded that there was any effect on the water splitting mechanism of PSII, which is supported by findings of Hill and Ralph (2008b). A downregulation of Y(II) could be a result of changes in the overall antenna size of PSII (Silva et al. 2001). The dynamic regulation of antenna size may occur in *P. decussata* and could be an explanation for the results presented here. Dynamic re-distribution of light harvesting complexes (LHC) and/or reaction center parts of PSII have been described to occur in *Symbiodinium* in order to partition harvested light energy between the two photosystems (Chapter 2.2, Hennige et al. 2009; Hill et al. 2012; Hoogenboom et al. 2012). Under these proposals, more energy would be channeled to the dissociated PSII LHCs, where the excitation energy is dissipated as heat.

Further, no up-regulated xanthophyll cycling was found in *P. decussata*, when exposed to high light stress as has been reported previously (Krämer et al. 2013). In contrast, *P. damicornis* responds with an up-regulation in xanthophyll cycling upon exposure to high light stress as reported here and in previous studies (Hill et al. 2012; Krämer et al. 2013). Overall these findings suggest that *Symbiodinium* harboured in *P. decussata* is utilising photoprotective pathways more efficiently under high light stress than *Symbiodinium* harboured in *P. damicornis*.

#### **5.4.6 Conclusion**

This is the first study reporting the measurement of light-driven respiration using fast O<sub>2</sub> microsensors embedded in coral tissue during the application of P – E curves. Respiration during the light was considerably higher than enhanced post-illumination respiration (R<sub>EPIR</sub>) activity in both species examined here and this should be taken into consideration for gross photosynthesis (GP) estimates when using R<sub>EPIR</sub> for GP rate calculations to avoid underestimation of ‘true’ photosynthetic productivity.

Rapid light-dark shift measurements revealed that GP rates were comparable for the two species examined here. At irradiances < CO<sub>2</sub>E<sub>c</sub> both coral species utilised 65 - 70% of their internal DIC pool for e.g. growth, calcification and/or photosynthetic substrate. Greater light utilisation efficiency of *P. decussata* was highlighted by the much lower CO<sub>2</sub>E<sub>c</sub> irradiance retrieved for this species, indicating that 2.2 times lower light intensities were required for higher GPP efficiency compared to *P. damicornis*. The CO<sub>2</sub>E<sub>c</sub> of *P. damicornis* at greater light intensities along with higher GP at just below < CO<sub>2</sub>E<sub>c</sub> indicated high O<sub>2</sub> to CO<sub>2</sub> tissue environment and most likely resulted in photorespiratory activity in this species. Activity of photorespiration indicates high energetic cost, which could be a clue why *P. damicornis* is characterised as a bleaching

sensitive species. Greater heat dissipation was found to occur in *P. decussata* indicating the activity of differing photoprotective mechanisms compared to *P. damicornis* in terms of Y(NPQ) and Y(NO).

The differing DIC supply as well as host tissue protein biomass have been identified here as critical governing aspects for a coral symbiosis; where DIC supply is a substrate for fundamental processes within the holobiont and protein biomass can create specific light fields within the host tissue environment effecting the photosynthesis of the algal symbiont.

Overall, the results presented here show that the photosynthetic performance of *Symbiodinium* clade C1 must depend to a great deal on the properties of associated coral host tissue, as well as the density and distribution of *Symbiodinium*. Further unexplored matters include the distribution of host pigmentation (e.g. green fluorescent pigments) and light channelling properties of the coral tissue.

## 5.5 References

- Al-Horani, F. A., S. M. Al-Moghrabi, and D. De Beer. 2003a. The mechanism of calcification and its relation to photosynthesis and respiration in the scleractinian coral *Galaxea fascicularis*. *Marine Biology* **142**: 419-426.
- Al-Horani, F. A., S. M. Al-Moghrabi, and D. De Beer. 2003b. Microsensor study of photosynthesis and calcification in the scleractinian coral *Galaxea fascicularis*: active internal carbon cycle. *Journal of Experimental Marine Biology and Ecology* **288**: 1-15.
- Al-Horani, F. A., T. Ferdelman, S. M. Al-Moghrabi, and D. De Beer. 2005. Spatial distribution of calcification and photosynthesis in the scleractinian coral *Galaxea fascicularis*. *Coral Reefs* **24**: 173-180.
- Al-Horani, F. A., E. Tambutte, and D. Allemand. 2007. Dark calcification and the daily rhythm of calcification in the scleractinian coral, *Galaxea fascicularis*. *Coral Reefs* **26**: 531-538.
- Al-Moghrabi, S., C. Goiran, D. Allemand, N. Speziale, and J. Jaubert. 1996. Inorganic carbon uptake for photosynthesis by the symbiotic coral-dinoflagellate association II. Mechanisms for bicarbonate uptake. *Journal of Experimental Marine Biology and Ecology* **199**: 227-248.
- Azcón-Bieto, J., and C. B. Osmond. 1983. Relationship between photosynthesis and respiration. *Plant Physiology* **71**: 574-581.
- Beardall, J., A. Quigg, and J. A. Raven. 2004. Oxygen Consumption: Photorespiration and Chlororespiration, p. 157-181. *In* A. W. D. Larkum, A. E. Douglas and J. A. Raven [eds.], *Photosynthesis in Algae*. Springer Netherlands.
- Behrendt, L., V. Schrammeyer, K. Qvortrup, L. Lunding, S. Sorensen, A. W. D. Larkum, and M. Kühl. 2012. Biofilm growth and near infrared radiation-driven photosynthesis of the chlorophyll-d-containing cyanobacterium *Acaryochloris marina*. *Applied Environmental Microbiology* **78**: 3896-3904.
- Bradford, M. M. 1976. A rapid and sensitive method for the quantitation of microgram quantities of protein utilizing the principle of protein-dye binding. *Analytical Biochemistry* **72**: 248-254.
- Burriesci, M. S., T. K. Raab, and J. R. Pringle. 2012. Evidence that glucose is the major transferred metabolite in dinoflagellate - cnidarian symbiosis. *Journal of Experimental Biology* **215**: 3467-3477.



- Buxton, L., M. Badger, and P. J. Ralph. 2009. Effects of moderate heat stress and dissolved inorganic carbon concentration on photosynthesis and respiration of *Symbiodinium* sp. (Dinophyceae) in culture and in symbiosis. *Journal of Phycology* **45**: 357-365.
- Chalker, B. E. 1980. Modelling light saturation curves for photosynthesis: an exponential function. *Journal of Theoretical Biology* **82**: 205-215.
- Coles, S. L., and P. L. Jokiel. 1977. Effects of temperature on photosynthesis and respiration in hermatypic corals. *Marine Biology* **43**: 209-216.
- Cooper, T. F., K. E. Ulstrup, S. S. Dandan, A. J. Heyward, M. Kühl, A. Muirhead, R. A. O'leary, B. E. F. Ziersen, and M. J. H. Van Oppen. 2011. Niche specialization of reef-building corals in the mesophotic zone: metabolic trade-offs between divergent *Symbiodinium* types. *Proceedings of the Royal Society B* **278**: 1840-1850.
- Crawley, A., D. I. Kline, S. Dunn, K. R. N. Anthony, and S. Dove. 2010. The effect of ocean acidification on symbiont photorespiration and productivity in *Acropora formosa*. *Global Change Biology* **16**: 851-863.
- Dubinsky, Z., P. G. Falkowski, J. W. Porter, and L. Muscatine. 1984. Absorption and utilization of radiant energy by light-and shade adapted colonies of the hermatypic coral *Stylophora pistillata* *Proceedings of the Royal Society B* **222**: 203-214.
- Edmunds, P. J., and P. S. Davies. 1986. An energy budget for *Porites porites* (Scleractinia). *Marine Biology* **92**: 339-347.
- Edmunds, P. J., and S. P. Davies. 1988. Post-illumination stimulation of respiration rate in the coral *Porites porites*. *Coral Reefs* **7**: 7-9.
- Eisenhut, M., S. Kahlon, and D. Hasse. 2006. The plant-like C2 glycolate cycle and the bacterial-like glycerate pathway cooperate in phosphoglycolate metabolism in cyanobacteria. *Plant Physiology* **142**: 333-342.
- Falkowski, P. G., and J. A. Raven. 2007. *Aquatic Photosynthesis*, 2nd ed. Princeton University Press.
- Franklin, L. A., and M. R. Badger. 2001. A comparison of photosynthetic electron transport rates in macroalgae measured by pulse amplitude modulated chlorophyll fluorometry and mass spectrometry. *Journal of Phycology* **37**: 756-767.

- Furla, P., I. Galgani, I. Durand, and D. Allemand. 2000. Sources and mechanisms of inorganic carbon transport for coral calcification and photosynthesis. *The Journal of Experimental Biology* **203**: 3445-3457.
- Gates, R. D., O. Hoegh-Guldberg, M. J. Mcfall-Ngai, K. Y. Bil', and L. Muscatine. 1995. Free amino acids exhibit anthozoan "host factor" activity: they induce the release of photosynthate from symbiotic dinoflagellates *in vitro*. *Proceedings of the National Academy of Sciences U.S.A.* **92**: 7430-7434.
- Genty, B., J.-M. Briantais, and N. R. Baker. 1989. The relationship between the quantum yield of photosynthetic electron transport and quenching of chlorophyll fluorescence. *Biochimica et Biophysica Acta* **990**: 87-92.
- Glud, R. N., N. B. Ramsing, and N. P. Revsbech. 1992. Photosynthesis and photosynthesis-coupled respiration in natural biofilms quantified with oxygen microsensors. *Journal of Phycology* **28**: 51-60.
- Goiran, C., S. Al-Moghabri, D. Allemand, and J. Jaubert. 1996. Inorganic carbon uptake for photosynthesis by the symbiotic coral/dinoflagellate association I. Photosynthetic performances of symbionts and dependence on sea water bicarbonate. *Journal of Experimental Marine Biology and Ecology* **199**: 207-225.
- Graham, D., and R. M. Smillie. 1976. Carbonate dehydratase in marine organisms of the Great Barrier Reef. *Australian Journal of Plant Physiology* **3**: 153-179.
- Hennige, S. J., D. J. Suggett, M. E. Warner, K. E. Mcdougall, and D. J. Smith. 2009. Photobiology of *Symbiodinium* revisited: bio-physical and bio-optical signatures. *Coral Reefs* **28**: 179-195.
- Herfort, L., B. Thake, and I. Taubner. 2008. Bicarbonate stimulation of calcification and photosynthesis in two hermatypic corals. *Journal of Phycology* **44**: 91-98.
- Hill, R., A. W. D. Larkum, O. Prášil, D. M. Kramer, V. Kumar, and P. J. Ralph. 2012. Light-induced redistribution of antenna complexes in the symbionts of scleractinian corals correlates with sensitivity to coral bleaching. *Coral Reefs* **31**: 963-975.
- Hill, R., and P. J. Ralph. 2008a. Dark-induced reduction of the plastoquinone pool in zooxanthellae of scleractinian corals and implications for measurements of chlorophyll a fluorescence. *Symbiosis* **46**: 45-56.

- Hill, R., and P. J. Ralph. 2008b. Impact of bleaching stress on the function of the oxygen evolving complex of zooxanthellae from scleractinian corals. *Journal of Phycology* **44**: 299-310.
- Hoogenboom, M. O., D. A. Campbell, E. Beraud, K. Dezeew, and C. Ferrier-Pagès. 2012. Effects of light, food availability and temperature stress on the function of photosystem II and photosystem I of coral symbionts. *Plos One* **7**: e30167.
- Houldbrèque, F., and C. Ferrier-Pagès. 2009. Heterotrophy in tropical scleractinian corals. *Biological Reviews* **84**: 1-17.
- Jacques, S. L. 1998. Light distributions from point, line and plane sources for photochemical reactions and fluorescence in turbid biological tissues. *Photochemistry and Photobiology* **67**: 23-32.
- Jakob, T., R. Goss, and C. Wilhelm. 1999. Activation of diadinoxanthin de-epoxidase due to a chlororespiratory proton gradient in the dark in the diatom *Phaeodactylum tricornutum*. *Plant Biology* **1**: 76-82.
- Jensen, J., and N. P. Revsbech. 1989. Photosynthesis and respiration of a diatom biofilm cultured in a new gradient growth chamber. *FEMS Microbiology Ecology* **62**: 29-38.
- Jokiel, P. L. 2011. The reef coral two compartment proton flux model: A new approach relating tissue-level physiological processes to gross corallum morphology. *Journal of Experimental Marine Biology and Ecology* **409**: 1-12.
- Jordan, D. B., and W. L. Ogren. 1981. Species variation in the specificity of ribulose biphosphate carboxylase/oxygenase. *Nature* **291**: 513-515.
- Kok, B. 1948. On the interrelation between respiration and photosynthesis in green plants. *Biochimica et Biophysica Acta (BBA)* **3**: 625-631.
- Kramer, D. M., G. Johnson, O. Kiirats, and G. E. Edwards. 2004. New fluorescence parameters for the determination of  $Q_A$  redox state and excitation energy fluxes. *Photosynthesis Research* **79**: 209-218.
- Krämer, W., V. Schrameyer, R. Hill, P. J. Ralph, and K. Bischof. 2013. PSII activity and pigment dynamics of *Symbiodinium* in two Indo-Pacific corals exposed to short-term high-light stress. *Marine Biology* **160**: 563-577.
- Kühl, M., Y. Cohen, T. Dalsgaard, B. B. Jorgensen, and N. P. Revsbech. 1995. Microenvironment and photosynthesis of zooxanthellae in scleractinian corals studies with microsensors for  $O_2$ , pH and light. *Marine Ecology Progress Series* **117**: 159-172.

- Kühl, M., and T. Fenchel. 2000. Bio-optical characteristics and the vertical distribution of photosynthetic pigments and photosynthesis in an artificial cyanobacterial mat. *Microbial Ecology* **40**: 94-103.
- Kuile, B., J. Erez, and E. Padan. 1989. Competition for inorganic carbon between photosynthesis and calcification in the symbiont-bearing foraminifer *Amphistegina lobifera*. *Marine Biology* **103**: 253-259.
- Leggat, W., M. R. Badger, and D. Yellowlees. 1999. Evidence for an inorganic carbon-concentrating mechanism in the symbiotic dinoflagellate *Symbiodinium* sp. *Plant Physiology* **121**: 1247-1255.
- Leggat, W., E. M. Marendy, B. Baillie, S. M. Whitney, M. Ludwig, M. R. Badger, and D. Yellowlees. 2002. Dinoflagellate symbioses: strategies and adaptations for the acquisition and fixation of inorganic carbon. *Functional Plant Biology* **29**: 309-322.
- Lesser, M. 2011. Coral Bleaching: causes and mechanisms, p. 405-419. *In* Z. Dubinsky and N. Stambler [eds.], *Coral Reefs: An Ecosystem in Transition*. Springer Netherlands.
- Levy, O., Z. Dubinsky, K. Schneider, Y. Achituv, D. Zakai, and M. Y. Gorbunov. 2004. Diurnal hysteresis in coral photosynthesis. *Marine Ecology Progress Series* **268**: 105-117.
- Li, Y. H., and S. Gregory. 1974. Diffusion of ions in sea water and in deep-sea sediments. *Geochimica Cosmochimica Acta* **38**: 703-714.
- Lilley, R. M., P. J. Ralph, and A. W. D. Larkum. 2010. The determination of activity of the enzyme Rubisco in cell extracts of the dinoflagellate alga *Symbiodinium* sp. by manganese chemiluminescence and its response to short-term stress of the alga. *Plant, Cell & Environment* **33**: 995-1004.
- Moya, A., S. Tambutte, A. Bertucci, E. Tambutte, S. Lotto, D. Vullo, C. T. Supuran, D. Allemand, and D. Zoccola. 2008. Carbonic anhydrase in the scleractinian coral *Stylophora pistillata*- Characterization, localization, and role in biomineralization. *Journal of Biological Chemistry* **283**: 25475-25484.
- Moya, A., S. Tambutte, E. Tambutte, D. Zoccola, N. Caminiti, and D. Allemand. 2006. Study of calcification during a daily cycle of the coral *Stylophora pistillata*: implications for 'light-enhanced calcification'. *The Journal of Experimental Biology* **209**: 3413-3419.

- Muller-Parker, G., and C. F. D'elia. 1997. Interactions between corals and their symbiotic algae, p. 96-113. *In* C. Birkeland [ed.], *Life and Death of Coral Reefs*. Chapman and Hall.
- Muscatine, L. 1990. The role of symbiotic algae in carbon and energy flux in reef corals, p. 75-87. *In* Z. Dubinsky [ed.], *Ecosystems of the World: Coral reefs*. Elsevier.
- Muscatine, L., L. R. McCloskey, and R. E. Marian. 1981. Estimating the daily contribution of carbon from zooxanthellae to coral animal respiration. *Limnology and Oceanography* **26**: 601-611.
- Muscatine, L., and J. W. Porter. 1977. Reef Corals: mutualistic symbioses adapted to nutrient-poor environments. *Bioscience* **27**: 454-460.
- Muscatine, L., J. W. Porter, and I. R. Kaplan. 1989. Resource partitioning by reef corals as determined from stable isotope composition: I. delta <sup>13</sup>C of zooxanthellae and animal tissue vs. depth. *Marine Biology* **100**: 185-193.
- Newsholme, E. A., and B. Crabtree. 2005. Maximum catalytic activity of some key enzymes in provision of physiologically useful information about metabolic fluxes. *Journal of Experimental Zoology* **239**: 159-167.
- Parys, E., and H. Jastz. 2006. Light-enhanced dark respiration in leaves, isolated cells and protoplasts of various types of C4 plants. *Journal of Plant Physiology* **163**: 638-647.
- Peltier, G., and G. W. Schmidt. 1991. Chlororespiration: an adaptation to nitrogen deficiency in *Chlamydomonas reinhardtii*. *Proceedings of the National Academy of Sciences U.S.A.* **88**: 4791-4795.
- Pernice, M., A. Meibom, A. Van Den Heuvel, C. Kopp, I. Domart-Coulon, O. Hoegh-Guldberg, and S. Dove. 2012. A single-cell view of ammonium assimilation in coral–dinoflagellate symbiosis. *International Society for Microbial Ecology* **6**: 1314-1324.
- Platt, T., C. L. Gallegos, and W. G. Harrison. 1980. Photoinhibition of photosynthesis in natural assemblages of marine phytoplankton. *Journal of Marine Research* **38**: 687-701.
- Prasil, O., Z. Kolber, J. A. Berry, and P. G. Falkowski. 1996. Cyclic electron flow around photosystem II *in vivo*. *Photosynthesis Research* **48**: 395-410.
- Ralph, P. J., and R. Gademann. 2005. Rapid light curves: a powerful tool to assess photosynthetic activity. *Aquatic Botany* **82**: 222-237.

- Ralph, P. J., C. Wilhelm, J. Lavaud, T. Jakob, K. Petrou, and S. Kranz. 2010. Fluorescence as a tool to understand changes in photosynthetic electron flow regulation, p. 75-89. *In* D. J. Suggett, M. A. Borowitzka and O. Prasil [eds.], Chlorophyll a Fluorescence in Aquatic Sciences: Methods and Applications. Springer.
- Rands, M. L., B. C. Loughman, and A. E. Douglas. 1993. The symbiotic interface in an alga-invertebrate symbiosis. *Proceedings of the Royal Society B* **253**: 161-165.
- Raven, J. A. 2003. Inorganic carbon concentrating mechanisms in relation to the biology of algae. *Photosynthesis Research* **77**: 155-171.
- Raven, J. A., and J. Beardall. 2003. Carbon acquisition mechanisms in algae: carbon dioxide diffusion and carbon dioxide concentrating mechanisms, p. 225-244. *In* A. W. D. Larkum, A. E. Douglas and J. A. Raven [eds.], *Photosynthesis in Algae*. Kluwer.
- Revsbech, N. P., and B. B. Jorgensen. 1983. Photosynthesis of benthic microflora measured with high spatial resolution by the oxygen microprofile method: capabilities and limitations of the method. *Limnology and Oceanography* **28**: 749-756.
- Rink, S., M. Kühl, J. Bijma, and H. J. Spero. 1998. Microsensor studies of photosynthesis and respiration in the symbiotic foraminifer *Orbulina universa*. *Marine Biology* **131**: 583-595.
- Ritchie, R. J. 2006. Consistent sets of spectrophotometric chlorophyll equations for acetone, methanol and ethanol solvents. *Photosynthesis Research* **89**: 27-41.
- Rowan, R., S. M. Whitney, A. Fowler, and D. Yellowlees. 1996. Rubisco in marine symbiotic dinoflagellates: form II enzymes in eukaryotic oxygenic phototrophs encoded by a nuclear multigene family. *The Plant Cell* **8**: 539-553.
- Schreiber, U. 2004. Pulse-amplitude-modulation (PAM) fluorometry and saturation pulse method: an overview, p. 279-319. *In* G. C. Papageorgiou and Govindjee [eds.], *Chlorophyll a fluorescence: a signature of photosynthesis*. *Advances in Photosynthesis and Respiration*. Springer.
- Schreiber, U., H. Hormann, K. Asada, and C. Neubauer. 1995. O<sub>2</sub>-dependent electron flow in intact spinach chloroplasts: properties and possible regulation of the Mehler-Ascorbate-Peroxidase cycle, p. 813-818. *In* P. Mathis [ed.], *Photosynthesis: from Light to Biosphere*. Kluwer Academic Publishers.

- Sharp, R. E., M. A. Matthews, and J. S. Boyer. 1984. Kok effect and the quantum yield of photosynthesis. *Plant Physiology* **75**: 95-101.
- Silva, L. M. T., C. P. Dos Santos, and R. M. Chaloub. 2001. Effect of the respiratory activity on photoinhibition of the cyanobacterium *Synechocystis* sp. *Photosynthesis Research* **68**: 61-69.
- Stimson, J., and R. A. Kinzie. 1991. The temporal pattern and rate of release of zooxanthellae from the reef coral *Pocillopora damicornis* (Linnaeus) under nitrogen-enrichment and control conditions. *The Journal of Experimental Biology* **153**: 66-74.
- Suggett, D. J., M. E. Warner, D. J. Smith, P. Davey, S. Hennige, and N. R. Baker. 2008. Photosynthesis and production of hydrogen peroxide by *Symbiodinium* (Pyrrophyta) phylotypes with different thermal tolerances. *Journal of Phycology* **44**: 948-956.
- Tobías, I., A. Luque, and A. Martí. 2008. Light intensity enhancement by diffracting structures in solar cells. *Journal of Applied Physics* **104**: 1-9.
- Tolbert, N. E., C. Benker, and E. Beck. 1995. The oxygen and carbon dioxide compensation points of C<sub>3</sub> plants: possible role in regulating atmospheric oxygen. *Proceedings of the National Academy of Sciences U.S.A.* **92**: 11230-11233.
- Tremblay, P., R. Grover, J. F. Maguer, L. Legendre, and C. Ferrier-Pagès. 2012. Autotrophic carbon budget in coral tissue: a new <sup>13</sup>C-based model of photosynthate translocation. *The Journal of Experimental Biology* **215**: 1384-1393.
- Ulstrup, K. E., M. Kühl, M. J. H. Van Oppen, T. F. Cooper, and P. J. Ralph. 2011. Variation in photosynthesis and respiration in geographically distinct populations of two reef-building coral species. *Aquatic Biology* **12**: 241-248.
- Ulstrup, K. E., P. J. Ralph, A. W. D. Larkum, and M. Kühl. 2006. Intra-colonial variability in light acclimation of zooxanthellae in coral tissues of *Pocillopora damicornis*. *Marine Biology* **149**: 1325-1335.
- Wang, G., and S. J. Smith. 2012. Sub-diffraction limit localization of proteins in volumetric space using bayesian restoration of fluorescence images from ultrathin specimens. *PLOS* **8**: e1002671.



- Wang, L., S. L. Jacques, and L. Zheng. 1995. MCML - Monte Carlo modeling of light transport in multi-layered tissues. *Computer Methods and Programs in Biomedicine* **47**: 131-146.
- Wangpraseurt, D., A. W. D. Larkum, P. J. Ralph, and M. Kühl. 2012. Light gradients and optical microniches in coral tissues. *Frontiers in Microbiology* **3**: 316.
- Weis, V. M. 1993. Effect of dissolved inorganic carbon concentration on the photosynthesis of the symbiotic sea anemone *Aiptasia pulchella* Carlgren: Role of carbonic anhydrase. *Journal of Experimental Marine Biology and Ecology* **174**: 209-225.
- Whitney, S. M., and T. J. Andrews. 1998. The CO<sub>2</sub>/O<sub>2</sub> specificity of single-subunit ribulose-bisphosphate carboxylase from the dinoflagellate, *Amphidinium carterae*. *Australian Journal of Plant Physiology* **25**: 131-138.
- Yellowlees, D., T. A. Rees, and W. Leggat. 2008. Metabolic interactions between algal symbionts and invertebrate hosts. *Plant, Cell & Environment* **31**: 679-694.
- Yellowlees, D., and M. Warner. 2003. Photosynthesis in Symbiotic Algae. *In* A. W. D. Larkum, S. E. Douglas and J. A. Raven [eds.], *Photosynthesis in Algae*. Kluwer Academic Publishers



This page was intentionally left blank

# **Chapter 6**

## **General Discussion**

## **6.1 Assessing *Symbiodinium*'s photoprotective capacity and bio-energetic limits**

The synergistic effect of thermal and high light stress is known to result in coral bleaching, the dissociation of the algal symbionts and the coral host. Resilience to these stress conditions has been found to be species-specific; however it is unclear whether this is algal symbiont or host related. In order to predict coral bleaching it is necessary to understand the impact of each individual stressor to describe physiological responses of *Symbiodinium* and the coral host. Presented in the thesis are new findings of *Symbiodinium*'s photoprotective strategies in culture and *in hospite*. Non-photochemical quenching (NPQ) is important for *Symbiodinium* to operate efficiently even under saturating light intensities to avoid oversaturation of photosystem (PS) II reaction centers (Demmig-Adams et al. 1996). One of the aims of this thesis was to describe the NPQ capacity of *Symbiodinium* on the molecular basis (**Chapter 2.1 and 2.2**). By examining *Symbiodinium* of the same clade when harboured in two morphologically distinct coral species (**Chapter 3, 4, 5**), the photoprotective capability of *Symbiodinium* was assessed when living *in hospite*.

## **6.2 NPQ capacity of cultured *Symbiodinium***

In this thesis, the dynamic regulation and substantial capacity of *Symbiodinium*'s NPQ pathways were explored under cultured as well as *in hospite* conditions. Under bleaching conditions, the synergistic effect of thermal and high light stress were found to be impacting upon the coral organism, which can lead to the dissociation of algal symbionts and coral host (Hill et al. 2005). Here it was demonstrated that the thermal stress is the main precursor under bleaching conditions (high light and thermal stress) to induce light harvesting complex (LHC) movement as an NPQ pathway in *Symbiodinium*

(**Chapter 2.1 and 2.2**). The significance of this newly described NPQ mechanism in dinoflagellates is the ability to dynamically distribute harvested excitation energy towards the more stable reaction center (RC) of photosystem (PS) I (Hoogenboom et al. 2012), which prevents over-excitation at RCII and consequently equilibrates excitation pressure upon PSII and PSI. Even energy distribution between RCII and RCI favours carbon fixation and allows for effective absorption by the two photosystems under any given incident light conditions (Hennige et al. 2011; Suggett et al. 2007).

Results of this thesis presented for the first time that the synergistic effect of thermal and high light stress, as well as thermal stress alone, can change the organisation of *Symbiodinium*'s thylakoid membrane (**Chapter 2.1**). The characterisation of PSII associated LHCs as heterogeneously organised and dynamically operating as a photoprotective strategy is a new finding for *Symbiodinium* and changes our understanding of *Symbiodinium*'s photosynthetic apparatus. Additionally, the presence of stressor-dependent LHC movement (**Chapter 2.2**) was presented in this thesis and is highlighting the great flexibility of cultured *Symbiodinium* to adjust its photosynthetic apparatus to improve light utilisation and therefore enhance the production of reducing agents to fix more carbon (**Chapter 2.2**).

Furthermore, through the re-organisation of LHCs *Symbiodinium* and the ability to effectively shunt excess harvested light energy away from PSII, the potential for photodamage to the PSII core protein D1 is being alleviated (Hill et al. 2011; Vass 2011). Also, especially when high light conditions saturate the electron transport chain, the strong redox potential of RCII (Rappaport et al. 2002) can result in reactive oxygen species (ROS) formation through the reaction with triplet oxygen leading to photodamage (Durrant et al. 1990) (see Fig 1.2). The capability of *Symbiodinium* to

utilise LHC movement as a NPQ mechanism can therefore be a physiological strategy to alleviate photodamage of PSII.

### 6.3 High light stress impact upon *in hospite Symbiodinium*

Photosynthetic efficiency in terms of carbon fixation is of utmost importance for a coral-*Symbiodinium* symbiosis as the coral host relies on this critical nutritional input from its algal symbionts (Grottoli et al. 2006; Lesser and Farrell 2004; Muscatine et al. 1981). Based on the findings of **Chapter 2.1 and 2.2**, it was found that *Symbiodinium* utilises NPQ pathways dynamically and stressor dependent; the next part of the thesis focussed on examining *Symbiodinium* when living *in hospite*. To account for variability in physiological stress response of *Symbiodinium* at the clade and subclade level (Fisher et al. 2012), two morphologically distinct coral host species were chosen, which are known to harbour *Symbiodinium* clade C1 at the chosen sampling location (Fig 3.1). The two species *Pocillopora damicornis* (Linnaeus) and *Pavona decussata* (Dana) were examined for their photoprotective mechanisms and photorepair requirements of *in hospite Symbiodinium*, when exposed to natural high light exposure during the day and ambient seawater temperature. Here both coral species were found to not be photosynthetically impaired during high light conditions at daytime (Fig 3.3 A and B). These findings agree with results of **Chapter 2.1 and 2.2**, where cultured *Symbiodinium* was exposed to high light stress and found to be photosynthetically viable, whilst supporting the hypothesis that detachment of PSII LHCs has occurred (**Table 2.2.1**).

However, by examining dissipative energy quenching strategies of the two coral species it was shown that *Symbiodinium* harboured in *P. damicornis* utilised xanthophyll cycling (XC) as a primary dissipative mechanism, whereas *Symbiodinium* harboured in *P. decussata* did not increase XC; however, both species up-regulated Y(NO), non-light

induced passive heat radiation (Klughammer and Schreiber 2008; Kramer et al. 2004), under simulated gross-photoinhibitory conditions (**Chapter 3**). Interestingly, under moderate light stress levels during photosynthesis – irradiance (P – E) curve measurements, only *P. decussata* up-regulated Y(NO) (**Chapter 5**). In concert the findings clearly indicate differential photoprotective responses occurring in *Symbiodinium* under high light stress depending on the coral host.

Further, by observing concentration changes of intact and fragmented PSII D1 core protein (displayed as ratios of fragmented to intact psbA concentrations; **Fig 3.4 B, D**) after 4 days of high light exposure during the day, revealed that much greater photodamage had occurred to *Symbiodinium* harboured in *P. damicornis* when compared to *Symbiodinium* harboured in *P. decussata*. Also, the bleaching-tolerant species *P. decussata* responded with up-regulated *de novo* synthesis of D1 under high light conditions (**Fig 3.4 C**) to counter photodamage. These results further indicate the differential impact of a stressor, here high light, upon *Symbiodinium* when harboured in different coral host organisms. Bleaching susceptibility of a coral species might therefore be a result of the photorepair capacity of its symbionts and the associated energetic cost to maintain the integrity its photosynthetic apparatus under high light stress conditions.

#### **6.4 Symbiotic interdependencies within the coral holobiont**

The coral-algal symbiosis is a complex interplay of substrate exchange, which allows the algal symbiont to successfully photosynthesise and the coral host to grow in nutrient poor tropical waters through the exchange of carbon products (Muscatine et al. 1981). However, the symbiosis is therefore based on the mutual exchange of essential products for fundamental physiological processes of each of the symbiotic partners, which

highlights the intricacy of this living arrangement. In order to examine the coral host, as well as algal symbiont performance as an intact holobiont, a photobioreactor was developed, which allows for the combined measurement of Chl *a* fluorescence, O<sub>2</sub>, as well as DIC exchange processes. Individual physiological performance characteristics of each symbiotic partner were extracted from the obtained parameters (**Chapter 4** and **5**). By measuring P – E curves, the symbiotic performance could be described at different irradiances.

The light intensity when carbon (C) respiratory gas exchange switches from CO<sub>2</sub> evolution to C uptake to meet photosynthetic C substrate demand is the CO<sub>2</sub> light compensation point (CO<sub>2</sub>E<sub>c</sub>). The coral host starts to draw on the external DIC pool once the respiratory DIC pool is unable to meet the algal symbionts' photosynthetic substrate requirements (Goreau 1977a; Goreau 1977b; Muscatine et al. 1989). The bleaching resilient species *P. decussata* was found to exhibit its CO<sub>2</sub>E<sub>c</sub> at about half the photon flux density compared to *P. damicornis*, the bleaching sensitive species (**Chapter 5**). Enhanced levels of dissolved inorganic carbon (DIC) supplied to the algal symbionts resulted in greater gross primary production output detected for *P. decussata* compared to *P. damicornis* (**Chapter 5**). These results therefore suggested, that greater carbon fixation at much lower light intensities than required in *P. damicornis* activated carbon concentrating mechanisms in *P. decussata*. The sufficient supply of DIC could therefore support one of the attributes that make *P. decussata* a stress resilient coral species (Hill et al. 2012; Krämer et al. 2013; Chapter 5). The positive effect of sufficient internal DIC supply prevents the shortage in photosynthetic substrate (Buxton et al. 2009) and therefore supports the efficient substrate exchange processes within the coral holobiont (**Chapter 5**).

The positive effect of increasing light intensity upon increased metabolic activity in hard corals was shown in **Chapter 5**. This enhanced respiratory activity, reported here for the first time under the application of P – E curves, was discussed as a result of photosynthate fuelled host metabolic processes e.g. calcification (Reynaud-Vaganay et al. 2001) and/or photoprotective mechanisms of the algal symbiont (e.g. chlororespiration (Jakob et al. 2001) or photorespiration (Crawley et al. 2010)). But also the activity of photorepair has been discussed to play a role in enhanced respiratory activity (Hoogenboom et al. 2006). Significant amounts of photodamage and consequently similar photorepair requirements for *P. damicornis* were caused by incubation in natural high light conditions, which also resulted in unusual oxygen exchange dynamics interpreted as high light respiratory activity (**Chapter 3**). In contrast, as mentioned above, *Symbiodinium* harboured in *P. decussata* did not experience the same amount of photodamage as when harboured in *P. damicornis* and therefore displayed normal oxygen exchange dynamics (Borell et al. 2008). The governing processes behind the substantial oxygen consumption occurring during light exposure have yet to be investigated. Here, future applications of the photobioreactor (PBR) presented in **Chapter 4**, could aid in resolving light respiratory processes in hard coral species (Chapter 5, Kühl et al. 1995). The PBR could easily be equipped with O<sub>2</sub> microsensors, which in conjunction with the use of inhibitors, would allow for examination of different ‘states’ of the photosynthetic apparatus (e.g. gross photodamaged PSII (lincomycin), reduced electron transport chain (DBMIB), reduced Q<sub>B</sub> as electron acceptor (DCMU), unlimited electron turnover at PSI (Methyl Viologen), absence of cyclic electron transport (Antimycin A), see Ralph et al. (2010) for review). This approach could aid to understand the operation of oxygen consuming processes and alternative electron pathways (see for review Ralph et al. 2010). Further, the PBR



setup would allow investigations into light-dependent respiratory activity of hard coral species as presented in **Chapter 5**.

## **6.5 Ecological significance**

Species-specific bleaching susceptibility has been widely observed (Baghooli and Hidaka 2003; Loya et al. 2001) and raised the question whether the algal symbionts or the coral host are the ‘weak link’ in the coral symbiosis (Baird et al. 2009a; Berkelmans and Van Oppen 2006; Ralph et al. 2005a). The role of the host in a bleaching situation has been a matter of discussion in the past few years (Abrego et al. 2008; Baird et al. 2009b; Fitt et al. 2009; Marshall and Baird 2000), where different physiological aspects such as host pigmentation (Dove et al. 2008), tissue lipid content (Glynn et al. 1985), skeletal structure (Enriquez et al. 2005) as well as micro-environmental light conditions (Wangpraseurt et al. 2012) have been considered.

The results presented in this thesis indicate that the bio-energetic limits of *Symbiodinium* are driven by host characteristics such as the ratio of symbiont to host tissue area, DIC supply, as well as tissue protein biomass. These host characteristics could all be key aspects involved in governing processes impacting upon *Symbiodinium*’s photosynthetic capacity. The same clade of *Symbiodinium*, but harboured in different coral host species displayed different photodamage, photorepair dynamics, as well as dissipative energy quenching pathways. Although these findings are based on high light stress only, (Fisher et al. 2012) also reported differing excitation pressure for *Symbiodinium* of the same clade, but harboured in morphologically distinct coral host organisms when exposed to bleaching conditions. Interestingly, *Symbiodinium* of the same clade but harboured in morphologically comparable host organisms did not show differences in photosynthetic viability (Fisher et al. 2012).

Furthermore, differential sites of photodamage, up- or downstream of ferredoxin, have been reported for *Symbiodinium* clade C1 in morphologically comparable species (Buxton et al. 2012). Thus, the host-specific stress responses cannot solely be explained by host morphology, other aspects will need to be considered to explain this phenomenon.

Another critical finding of the thesis presented here highlights the species-specific differences in DIC acquisition and carbon exchange dynamics (**Chapter 5**). The source of carbon required to meet the needs of DIC dependent processes such as calcification and photosynthesis have been discussed before (Buxton et al. 2009; Davy et al. 2012; Goiran et al. 1996; Leggat et al. 2002; Weis 1993; Weis et al. 1989). The acquisition of carbon is species-specific, as carbonic anhydrase activity differs depending on the morphology of the coral species (Weis et al. 1989). Surface area to volume ratio of a coral species and the resulting diffusion boundary layer characteristics (Smith and Walker 1980) can influence the inward CO<sub>2</sub> diffusion. A sufficient CO<sub>2</sub> diffusion into the holobiont is prevalent when a low surface area to volume ratio is characterising the coral species; for the contrary ratio scenario a coral species would rely on the activity of carbonic anhydrases, the carbon uptake carrier enzymes of corals (Leggat et al. 1999), to meet the internal substrate needs (Weis et al. 1989). Further, the photosynthetic efficiency of *Symbiodinium* has been demonstrated to be directly related to the external DIC concentration (Buxton et al. 2009; Herfort et al. 2008) as well as to the activity of carbonic anhydrases (Weis et al. 1989). Here the bleaching resilient species *P. decussata*, with a high surface area to volume ratio, displayed greater DIC uptake at low light intensities compared to *P. damicornis*, exhibiting a low surface area to volume (**Chapter 5**). Clearly, more investigation is required, however, based on the existing literature that shows enzyme driven carbon uptake is species-specific, these results

could hint towards host related characteristics, which need to be considered as an explanation of species-specific bleaching resilience.

## 6.6 Conclusion

The results presented in this thesis indicate that cultured *Symbiodinium* has the ability to dynamically utilise NPQ pathways (**Chapter 2.1 and 2.2**), where the utilisation of NPQ pathways when living *in hospite* differs depending on the harbouring coral host (**Chapter 3, 5**). The efficiency of a photoprotective response is therefore dependent on the host-environment. The basis of a healthy coral-algal living association even under stressful conditions is formed through sufficient DIC supply (**Chapter 5**), light environment (**Chapter 3,5**), low symbiont density (**Chapter 3,5**). Upon exposure to high light and/or thermal stress a limited supply of either of the base requirements for DIC and light, or greater algal symbiont density can result in greater susceptibility to photodamage and resulting requirements for photorepair, where the efficiency of photorepair mechanisms is crucial for maintaining the integrity of PSII. A sustained PSII integrity prevents excess light energy and thus the magnitude of ROS formation. Further, the overall energy capacity (ATP, lipids, nutrient supply) governs the capacity of sustaining PSII integrity under prolonged stress exposure. A shift in energy resources to counter photodamage could therefore possibly result in a loss of photosynthate translocation to the coral host.

## 6.7 Remarks about instruments and methodologies used

### 6.7.1 77K and ultrafast fluorescence

Algae exposed to both thermal and high light stress displayed an immediate re-distribution of acpPC towards PSI along with active xanthophyll cycling. Algae experiencing high light stress at control temperature displayed an enhanced fluorescence emission at 675 nm which is interpreted as a detachment of LHCs away from PSII. Further a DCMU treatment was also measured during the experiment presented in Chapter 2.2 (not presented), where the results displayed energy distribution towards PSI. The latter finding in particular, was in disagreement with the results of Chapter 2.1, which demonstrated that no LHC re-distribution occurred without the impact of thermal stress. One possible explanation to why these results differ could be due to the normalising procedure of 77K fluorescence emission spectra. The fluorescence emission spectra are commonly normalised to the main PSII fluorescence band at 686 nm (Hill et al. 2012).

This approach of normalising emission spectra from experiments investigating high light stress effects, does not take into account that PSII quenching under high light conditions decreases the peak at the 686 nm wavelength band (red region of low temperature fluorescence emission spectra) (Lambrev et al. 2010). As a result, component bands normalised to the quenched 686 nm wavelength band of samples from high light exposure experiments therefore can result in the appearance of misleading elevations in the PSI region ( $> 700$  nm), as well as in wavelengths regions  $< 688$  nm.

Ultrafast fluorescence derived and low temperature (77K) fluorescence derived methodologies displayed a mismatch in outcomes for DCMU-treated algae, which

resulted in an exclusion of the  $F_{\max}$  treatment from Chapter 2.2. This baseline issue will need to be addressed in future applications of 77K fluorescence measurements. One possible approach could be the usage of the 686 nm peak of T0 measurements as a fixed value for standardised normalisation of 77K fluorescence emission spectra. This would assume that photosynthetic pigment concentrations do not change over time (an assumption which is likely not to be realistic under coral bleaching conditions). For treatment conditions, where pigment concentrations are likely to have changed, a different normalising procedure will have to be found. Further investigations to establish a commonly accepted normalisation technique will need to be undertaken. Nevertheless, both methodologies (**Chapter 2.1 and 2.2**) were in agreement that the operation of LHC movement as a photoprotective mechanism in *Symbiodinium* which requires thermal stress as a precursor to allow for energy distribution towards PSI, which was demonstrated for the first time through the work presented in **Chapter 2.1**.

### ***6.7.2 Application of the photobioreactor***

In **Chapter 4** a newly developed PBR was presented, which allows for the acquisition of a unique dataset, combining three different measures for photosynthetic efficiency. The PBR developed here is equipped with a pulse-amplitude modulated fluorometer measuring through a simple fiber-optic with a diameter of 0.32 cm. The Chl *a* fluorescence data obtained with from measurements using this fiber-optic are therefore considering only a small fraction compared to the total surface area of  $\sim 25$  cm of a hard coral specimen for PBR cuvette measurements. Gas exchange measurements of  $O_2$  and  $CO_2$  are usually normalised to surface area ( $cm^2$ ) but could nevertheless lead to a mismatch in data output alignment as the spatial heterogeneity of the total coral surface is not considered by the PAM fiber-optic. Here a fluorometer with broader detection

field, comparable to an Imaging PAM (Ralph et al. 2005b), and operating like a fast repetition rate fluorometer (Gorbunov et al. 2001) could aid for higher resolution of Chl *a* fluorescence detection. Spatial heterogeneity of photosynthetic efficiency (Kühl et al. 1995) on the coral surface could therefore be accounted for.

## 6.8 Key findings

- *Symbiodinium* (strain CS-156) contains heterogeneously organised light harvesting complexes associated with PSII allowing for energy distribution towards PSI under thermal and/or high light stress conditions
- *Symbiodinium*'s heterogeneously organised photosynthetic apparatus operates dynamically through shifts of LHCs; where thermal stress displayed the main precursor for LHC re-distribution towards PSI
- *Symbiodinium* of the same clade displayed differential photoprotection and photodamage when harboured in morphologically and physiologically distinct coral species, where DIC supply, symbiont density and light micro-environment have been identified to possibly govern the energy levels required for photorepair
- light respiratory activity is positively related to incident light intensity, which is much greater than enhanced post-illumination respiration and therefore indicates ongoing light-driven processes
- the developed photobioreactor allows for measurements of key integrated exchange processes relevant to photophysiological assessments of aquatic phototrophs and analysis of critical electron pathways

## 6.9 Future research objectives

The findings presented here raise several critical questions, where further research is needed to further elucidate key pathways of *Symbiodinium*'s photoprotection. Ideas for future research activities:

- The potential for thylakoid re-organisation needs to be validated using a visual approach to further evaluate the presented findings in terms of thylakoid stacking characteristics under thermal and high light stress; this could be done with commonly applied electron microscopy techniques (**Chapter 2.1**)
- The role of acpPC and PCP in photoprotection needs to be elucidated, extracts and/or mutants would allow for in-depth examination of *Symbiodinium*'s photoprotective mechanisms; this approach would allow for functional separation of acpPC and PCP and could aid to further describe *Symbiodinium*'s photosynthetic apparatus (**Chapter 2.2**)
- Applying photobioreactor (PBR) measurements to different *Symbiodinium* clades would allow for description of electron pathways, linear and alternative, under various light intensities and temperature regimes and could extend our understanding clade-specific physiological stress responses (**Chapter 2.1 and 3**)
- Pharmacological approaches in conjunction with microsensor technique and PBR measurements could help to further examine the role of DIC acquisition under bleaching conditions and the influence upon key physiological processes of the holobiont. Although this wouldn't be a new approach *per se*, a new assessment of the holobiont has been made possible with measurements performed using the newly developed PBR, which allows to define the physiological fitness of the coral symbiosis with all its intricate interdependencies (**Chapter 5**).



## General References

- Abrego, D., K. E. Ulstrup, B. L. Willis, and M. J. H. Van Oppen. 2008. Species-specific interactions between algal endosymbionts and coral hosts define their bleaching response to heat and light stress. *Proceedings of the Royal Society B* **275**: 2273-2282.
- Acevedo, R., and C. Goenaga. 1986. Note on coral bleaching after a chronic flooding in southwestern Puerto Rico. *Caribbean Journal of Science* **22**: 225.
- Al-Horani, F. A., S. M. Al-Moghrabi, and D. De Beer. 2003a. The mechanism of calcification and its relation to photosynthesis and respiration in the scleractinian coral *Galaxea fascicularis*. *Marine Biology* **142**: 419-426.
- Al-Horani, F. A., S. M. Al-Moghrabi, and D. De Beer. 2003b. Microsensor study of photosynthesis and calcification in the scleractinian coral *Galaxea fascicularis*: active internal carbon cycle. *Journal of Experimental Marine Biology and Ecology* **288**: 1-15.
- Al-Horani, F. A., T. Ferdelman, S. M. Al-Moghrabi, and D. De Beer. 2005. Spatial distribution of calcification and photosynthesis in the scleractinian coral *Galaxea fascicularis*. *Coral Reefs* **24**: 173-180.
- Al-Horani, F. A., E. Tambutte, and D. Allemand. 2007. Dark calcification and the daily rhythm of calcification in the scleractinian coral, *Galaxea fascicularis*. *Coral Reefs* **26**: 531-538.
- Al-Moghrabi, S., C. Goiran, D. Allemand, N. Speziale, and J. Jaubert. 1996. Inorganic carbon uptake for photosynthesis by the symbiotic coral-dinoflagellate association II. Mechanisms for bicarbonate uptake. *Journal of Experimental Marine Biology and Ecology* **199**: 227-248.
- Alexandre, M. T. A., D. C. Lührs, I. H. M. Van Stokkum, R. G. Hiller, M.-L. Groot, J. T. M. Kennis, and R. Van Grondelle. 2007. Triplet state dynamics in peridinin-chlorophyll-*a*-protein: a new pathway of photoprotection in LHCs? *Biophysical Journal* **93**: 2118-2128.
- Allahverdiyeva, Y., and E.-M. Aro. 2012. Photosynthetic responses of plants to excess light: mechanisms and conditions for photoinhibition, excess energy dissipation and repair, p. 276-291. *In* J. J. Eaton-Rye, B. C. Tripathy and T. D. Sharkey [eds.], *Advances in Photosynthesis and Respiration*. Springer.

- Allemand, D., E. Tambutte, J. P. Girard, and J. Jaubert. 1998. Organic matrix synthesis in the scleractinian coral *Stylophora pistillata*: role in biomineralization and potential target of the organotin tributyltin. *J Exp Biol* **201**: 2001-2009.
- Allen, J. F. 1992. Chloroplast protein phosphorylation couples plastoquinone redox state to distribution of excitation energy between photosystems. *Nature* **291**: 25-29.
- Ambarsari, I., B. E. Brown, R. G. Barlow, G. Britton, and D. Cummings. 1997. Fluctuations in algal chlorophyll and carotenoid pigments during solar bleaching in the coral *Goniastrea aspera* at Phuket, Thailand. *Marine Ecology Progress Series* **159**: 303-307.
- Anthony, K. R. N., S. R. Connolly, and B. L. Willis. 2002. Comparative analysis of energy allocation to tissue and skeletal growth in corals. *Limnology and Oceanography* **47**: 1417-1429.
- Anthony, K. R. N., and K. E. Fabricius. 2000. Shifting roles in heterotrophy and autotrophy in coral energetics under varying turbidity. *Journal of Experimental Marine Biology and Ecology* **252**: 221-253.
- Anthony, K. R. N., and O. Hoegh-Guldberg. 2003. Kinetics of photoacclimation in corals *Oecologia* **134**: 23-31.
- Aro, E.-M., I. Virgin, and B. Andersson. 1993. Photoinhibition of Photosystem II. Inactivation, protein damage and turnover. *Biochimica et Biophysica Acta (BBA) - Bioenergetics* **1143**: 113-134.
- Arrhenius, S. 1896. On the influence of carbonic acid in the air upon the temperature of the ground. *Philosophical Magazine* **41**: 237-276.
- Asada, K. 1999. The water-water cycle in chloroplasts: scavenging of active oxygens and dissipation of excess photons. *Annual Review of Plant Physiology and Plant Molecular Biology* **50**: 601-639.
- Atkin, O. K., J. R. Evans, and K. Siebke. 1998. Relationship between the inhibition of leaf respiration by light and enhancement of leaf dark respiration following light treatment. *Australian Journal of Plant Physiology* **25**: 437-443.
- Azcón-Bieto, J., and C. B. Osmond. 1983. Relationship between photosynthesis and respiration. *Plant Physiology* **71**: 574-581.

- Bachmann, K., V. Ebbert, W. I. Adams, A. Verhoeven, B. Logan, and B. Demmig-Adams. 2004. Effects of lincomycin on PSII efficiency, non-photochemical quenching, D1 protein and xanthophyll cycle during photoinhibition and recovery. *Functional Plant Biology* **31**: 803-813.
- Badger, M. R., S. Von Caemmerer, S. Ruuska, and H. Nakano. 2000. Electron flow to oxygen in higher plants and algae: rates and control of direct photoreduction (Mehler reaction) and rubisco oxygenase. *Philosophical Transactions of the Royal Society B: Biological Sciences* **355**: 1433-1446.
- Baghooli, R., and M. Hidaka. 2003. Comparison of stress susceptibility of in hospite isolated zooxanthellae among five coral species. *Journal for Experimental Marine Biology and Ecology* **291**: 181-197.
- Bailey, S., A. Melis, K. R. M. Mackey, P. Cardol, G. Finazzi, G. Van Dijken, G. M. Berg, K. Arrigo, J. Shrager, and A. Grossman. 2008. Alternative photosynthetic electron flow to oxygen in marine *Synechococcus*. *Biochimica et Biophysica Acta* **1777**: 269-276.
- Baird, A. H., R. Bhagooli, P. J. Ralph, and S. Takahashi. 2009a. Coral bleaching: the role of the host. *Trends in Ecology & Evolution* **24**: 16-20.
- Baird, A. H., J. R. Guest, and B. L. Willis. 2009b. Systematic and Biogeographical patterns in the reproductive biology of scleractinian corals. *Annual Review of Ecology, Evolution and Systematics* **40**: 551-571.
- Baker, A. 2008. Chlorophyll Fluorescence: A probe of photosynthesis *in vivo*. *Annual Review of Plant Biology* **59**: 89-113.
- Baker, A. 2011. Z - Zooxanthellae, p. 1188-1192. *In* D. Hopley [ed.], *Encyclopedia of modern coral reefs - Structure, Form and Process*. Encyclopedia of earth sciences series. Springer Science and Business Media.
- Baker, A. C. 2003. Flexibility and specificity in coral-algal symbiosis: diversity, ecology, and biogeography of Symbiodinium. *Annual Review of Ecology, Evolution and Systematics* **34**: 661-689.
- Barnes, D. J., R. B. Taylor, and J. M. Lough. 2003. Measurement of luminescence in coral skeletons. *Journal of Experimental Marine Biology and Ecology* **295**: 91-106.
- Beardall, J., A. Quigg, and J. A. Raven. 2004. Oxygen Consumption: Photorespiration and Chlororespiration, p. 157-181. *In* A. W. D. Larkum, A. E. Douglas and J. A. Raven [eds.], *Photosynthesis in Algae*. Springer Netherlands.

- Beer, S., C. Larsson, O. Poryan, and L. Axelsson. 2000. Photosynthetic rates of *Ulva* (Chlorophyta) measured by pulse amplitude modulated (PAM) fluorometry. *European Journal of Phycology* **35**: 69-74.
- Behrendt, L., V. Schrameyer, K. Qvortrup, L. Lunding, S. Sorensen, A. W. D. Larkum, and M. Kühl. 2012. Biofilm growth and near infrared radiation-driven photosynthesis of the chlorophyll-d-containing cyanobacterium *Acaryochloris marina*. *Applied Environmental Microbiology* **78**: 3896-3904.
- Bellwood, D. R., T. Hughes, P., C. Folke, and M. Nystroem. 2004. Confronting the coral reef crisis. *Nature* **429**: 827-833.
- Beltran, V. H., W. C. Dunlap, and P. F. Long. 2012. Comparison of the photosynthetic bleaching response of four coral species common to the central GBR. *Proceedings of the 12th International Coral Reef Symposium, Cairns, Australia* **9A Coral bleaching and climate change**.
- Berkelmans, R. 2002. Time-integrated thermal bleaching thresholds of reefs and their variation on the Great Barrier Reef. *Marine Ecology Progress Series* **229**: 73-82.
- Berkelmans, R., G. De'ath, S. Kininmonth, and W. J. Skirving. 2004. A comparison of the 1998 and 2002 coral bleaching events on the Great Barrier Reef: spatial correlation, patterns, and predictions. *Coral Reefs* **23**: 74-83.
- Berkelmans, R., and J. K. Oliver. 1999. Large-scale bleaching of corals on the Great Barrier Reef. *Coral Reefs* **18**: 55-60.
- Berkelmans, R., and M. J. H. Van Oppen. 2006. The role of zooxanthellae in the thermal tolerance of corals: a 'nugget of hope' for coral reefs in an era of climate change. *Proceedings of the Royal Society B* **273**: 2305-2312.
- Bertos, N. R., and S. P. Gibbs. 1998. Evidence for a lack of photosystem segregation in *Chlamydomonas reinhardtii* (Chlorophyceae). *Journal of Phycology* **34**: 1009-1016.
- Bom, and Government. 2005. *El Niño, La Niña and Australia's Climate*.
- Bongaerts, P., T. Ridgway, E. M. Sampayo, and O. Hoegh-Guldberg. 2010. Assessing the 'deep reef refugia' hypothesis: focus on Caribbean reefs. *Coral Reefs* **29**: 309-327.
- Bongaerts, P., C. Riginos, K. B. Hay, M. J. H. Van Oppen, O. Hoegh-Guldberg, and S. Dove. 2011. Adaptive divergence in a scleractinian coral: physiological adaptation of *Seriatopora hystrix* to shallow and deep reef habitats. *BMC Evolutionary Biology* **11**: 1471-2148.

- Borell, E. M., A. R. Yuliantri, K. Bischof, and C. Richter. 2008. The effect of heterotrophy on photosynthesis and tissue composition of two scleractinian corals under elevated temperature. *Journal of Experimental Marine Biology and Ecology* **364**: 116-123.
- Borisov, S. M., G. Nuss, and I. Klimant. 2008. Red light-excitable oxygen sensing materials based on Platinum (II) and Paladium (II) Benzoporphyrins. *Analytical Chemistry* **80**: 9435-9442.
- Bradford, M. M. 1976. A rapid and sensitive method for the quantitation of microgram quantities of protein utilizing the principle of protein-dye binding. *Analytical Biochemistry* **72**: 248-254.
- Brown, B. E., I. Ambarsari, M. Warner, W. Fitt, R. P. Dunne, S. W. Gibb, and D. G. Cummings. 1999a. Diurnal changes in photochemical efficiency and xanthophyll concentrations in shallow water reef corals: evidence for photoinhibition and photoprotection. *Coral Reefs* **18**: 99-105.
- Brown, B. E., J. H. S. Blaxter, and A. J. Southward. 1997. *Adaptations of Reef Corals to Physical Environmental Stress*. Academic Press.
- Brown, B. E., R. P. Dunne, I. Ambarsari, M. D. A. Le Tissier, and U. Satapoomin. 1999b. Seasonal fluctuations in environmental factors and variations in symbiotic algae and chlorophyll pigments in four Indo-Pacific coral species. *Marine Ecology Progress Series* **191**: 53-69.
- Brown, C. M., D. A. Campbell, and J. E. Lawrence. 2007. Resource dynamics during infections of *Micromonas pusilla* by virus MpV-Sp1. *Environmental Microbiology* **9**: 2720-2727.
- Brown, E. M., J. D. Mackinnon, A. M. Cockshutt, T. A. Villareal, and D. A. Campbell. 2008. Flux capacities and acclimation costs in *Trichodesmium* from the Gulf of Mexico. *Marine Biology* **151**.
- Buddemeier, R. W., J. A. Kleypas, and R. B. Aronson. 2004. Potential Contributions of Climate Change to Stresses on Coral Reef Ecosystems, p. 1-56. *In* P. Center [ed.], *Coral reefs & Global Climate Change*.
- Burba, G., A. Schmidt, R. L. Scott, T. Nakai, J. Kathilankal, G. Fratini, C. Hanson, B. Law, D. K. Mcdermitt, R. Eckles, M. Furtaw, and M. Veldersdyk. 2012. Calculating CO<sub>2</sub> and H<sub>2</sub>O eddy covariance fluxes from an enclosed gas analyzer using an instantaneous mixing ratio. *Global Change Biology* **18**: 385-399.

- Burriesci, M. S., T. K. Raab, and J. R. Pringle. 2012. Evidence that glucose is the major transferred metabolite in dinoflagellate - cnidarian symbiosis. *Journal of Experimental Biology* **215**: 3467-3477.
- Burton, G. W. 1990. Antioxidant properties of carotenoids. *Journal of Nutrition* **119**: 109-111.
- Buxton, L., M. Badger, and P. J. Ralph. 2009. Effects of moderate heat stress and dissolved inorganic carbon concentration on photosynthesis and respiration of *Symbiodinium* sp. (Dinophyceae) in culture and in symbiosis. *Journal of Phycology* **45**: 357-365.
- Buxton, L., S. Takahashi, R. Hill, and P. J. Ralph. 2012. Variability in the primary site of photosynthetic damage in *Symbiodinium* sp. (Dinophyceae) exposed to thermal stress. *Journal of Phycology*.
- Campbell, D. A., V. Hurry, A. K. Clarke, P. Gustafsson, and G. Öquist. 1998. Chlorophyll fluorescence analysis of cyanobacterial photosynthesis and acclimation. *Microbiology and molecular biology reviews* **6**: 667-683.
- Campbell, D. A., and G. Öquist. 1996. Predicting light acclimation in cyanobacteria from non-photochemical quenching of photosystem II fluorescence, which reflects state transitions in these organisms. *Plant Physiology* **111**: 1293-1298.
- Campbell, N. A., and J. B. Reece. 2011. *Biology*. Pearson/Benjamin Cummings
- Carbonera, D., G. Giacometti, and U. Segre. 1996. Carotenoid interactions in peridinin chlorophyll *a* proteins from dinoflagellates. *Journal of Chemistry Society, Faraday Transactions* **92**: 989-993.
- Chalker, B. E. 1980. Modelling light saturation curves for photosynthesis: an exponential function. *Journal of theoretical biology* **82**: 205-215.
- Cohen, A. L., and T. A. McConnaughey. 2003. Geochemical perspectives on coral mineralization, p. 151-187. *Reviews in Mineralogy and Geochemistry*.
- Cole, A. J., M. S. Pratchett, and G. P. Jones. 2009. Effects of coral bleaching on the feeding response of two species of coral-feeding fish. *Journal of Experimental Marine Biology and Ecology* **373**: 11-15.
- Coles, S. L., and B. E. Brown. 2003. Coral bleaching - capacity for acclimatization and adaptation, p. 183-223. *Advances in Marine Biology*. Academic Press.
- Coles, S. L., and P. L. Jokiel. 1977. Effects of temperature on photosynthesis and respiration in hermatypic corals. *Marine Biology* **43**: 209-216.

- Cooper, T. F., K. E. Ulstrup, S. S. Dandan, A. J. Heyward, M. Kühl, A. Muirhead, R. A. O'leary, B. E. F. Ziersen, and M. J. H. Van Oppen. 2011. Niche specialization of reef-building corals in the mesophotic zone: metabolic trade-offs between divergent *Symbiodinium* types. *Proceedings of the Royal Society B* **278**: 1840-1850.
- Coral, T. C. R. A. 2006. *Coral Reefs and Sustainable Marine Recreation, A Resource Guide for Marine Tourism Professionals*.
- Costanza, R., R. D'arge, R. De Groot, S. Farberk, M. Grasso, B. Hannon, K. Limburg, S. Naeem, R. V. O'Neill, J. Paruelo, R. G. Raskin, P. Suttonkk, and M. Van Den Belt. 1997. The value of the world's ecosystem services and natural capital. *Nature* **387**: 253-260.
- Crawley, A., D. I. Kline, S. Dunn, K. R. N. Anthony, and S. Dove. 2010. The effect of ocean acidification on symbiont photorespiration and productivity in *Acropora formosa*. *Global Change Biology* **16**: 851-863.
- Cruz, S., R. Goss, C. Wilhelm, R. Leegood, P. Horton, and T. Jakob. 2011. Impact of chlororespiration on non-photochemical quenching of chlorophyll fluorescence and on the regulation of the diadinoxanthin cycle in the diatom *Thalassiosira pseudonana*. *Journal of Experimental Botany* **62**: 509-519.
- Cunning, R., and A. C. Baker. 2013. Excess algal symbionts increase the susceptibility of reef corals to bleaching. *Nature Climate Change* **3**: 259-262.
- Davies, P. S. 1991. Effect of daylight variations on the energy budgets of shallow-water corals. *Marine Biology* **108**: 137-144.
- Davy, S. K., D. Allemand, and V. M. Weis. 2012. Cell biology of cnidarian-dinoflagellate symbiosis. *Microbiology and molecular biology reviews* **76**: 229-261.
- Dawson, T. L. 2007. Light-harvesting and light-protecting pigments in simple life forms. *Coloration Technology* **123**: 129-142.
- De Bianchi, S., M. Ballottari, L. Dall'osto, and R. Bassi. 2010. Regulation of plant light harvesting by thermal dissipation of excess energy. *Biochemical society transactions* **38**: 651-660.
- Demmig-Adams, B. 1990. Carotenoids and photoprotection in plants: a role for the xanthophyll zeaxanthin. *Biochimica et Biophysica Acta* **1020**: 1-24.



- Demmig-Adams, B., and W. W. Adams. 1996. The role of xanthophyll cycle carotenoids in the photoprotection of photosynthesis. *Trends in Biochemical Sciences* **1**: 21-26.
- Demmig-Adams, B., and W. W. Adams. 2006. Photoprotection in an ecological context: the remarkable complexity of thermal energy dissipation. *New Phytologist* **172**: 11-21.
- Demmig-Adams, B., W. W. I. Adams, D. H. Barker, B. A. Logan, A. S. Verhoeven, and D. R. Bowling. 1996. Using chlorophyll fluorescence to assess the allocation of absorbed light to thermal dissipation or excess excitation. *Physiologia Plantarum* **98**: 253-264.
- Demmig-Adams, B., C. M. Cohu, O. Muller, and W. W. R. Adams. 2012. Modulation of photosynthetic energy conversion efficiency in nature: from seconds to seasons. *Photosynthesis Research* **113**: 75-88.
- Díaz-Almeyda, E., P. E. Thomé, M. E. Hafidi, and R. Iglesias-Prieto. 2011. Differential stability of photosynthetic membranes and fatty acid composition at elevated temperature in *Symbiodinium*. *Coral Reefs* **30**: 217-225.
- Done, T. J. 1992. Phase shifts in coral reef communities and their ecological significance. *Hydrobiologia* **247**: 121-132.
- Dove, S., J. C. Ortiz, S. Enriquez, M. Fine, P. Fisher, R. Iglesias-Prieto, D. Thornhill, and O. Hoegh-Guldberg. 2006. Response of holosymbiont pigments from the scleractinian coral *Montipora monasteriata* to short-term heat stress. *Limnology and Oceanography* **51**: 1149-1158.
- Dove, S. G., C. Lovell, M. Fine, J. Deckenback, O. Hoegh-Guldberg, R. Iglesias-Prieto, and K. R. N. Anthony. 2008. Host pigments: potential facilitators of photosynthesis in coral symbioses. *Plant, Cell & Environment* **31**: 1532-1533.
- Dubinsky, Z., P. G. Falkowski, J. W. Porter, and L. Muscatine. 1984. Absorption and utilization of radiant energy by light-and shade adapted colonies of the hermatypic coral *Stylophora pistillata* *Proceedings of the Royal Society B* **222**: 203-214.
- Dubinsky, Z., P. G. Falkowski, and K. Wyman. 1986. Light harvesting and utilization by phytoplankton. *Plant Cell and Physiology* **27**: 1335-1349.
- Dubinsky, Z., and P. L. Jokiel. 1994. Ratio of energy and nutrient fluxes regulates symbiosis between zooxanthellae and corals. *Pacific Science* **48**: 313-324.



- Dunn, S. R., J. R. Thomason, M. D. A. Le Tissier, and J. C. Bythell. 2004. Heat stress induces different forms of cell death in sea anemones and their endosymbiotic algae depending on temperature and duration. *Cell Death and Differentiation* **11**: 1-10.
- Durchan, M., F. Vacha, and A. Krieger-Liszkay. 2001. Effects of severe CO<sub>2</sub> starvation on the photosynthetic electron transport chain in tobacco plants. *Photosynthesis Research* **68**: 203-213.
- Durrant, J. R., L. B. Giorgi, J. Barber, D. R. Klug, and G. Porter. 1990. Characterisation of triplet states in isolated photosystem II reaction centres: oxygen quenching as a mechanism for photodamage. *Biochimica et Biophysica Acta - Bioenergetics* **1017**.
- Edelman, M., and A. K. Mattoo. 2008. D1-protein dynamics in photosystem II: The lingering enigma. *Photosynthesis Research* **98**: 609-620.
- Edge, R., and G. T. Truscott. 1999. Carotenoid radicals and the interaction of carotenoids with active oxygen species, p. 223-234. *In* H. A. Frank, A. J. Yound, G. Britton and R. J. Cogdell [eds.], *The photochemistry of carotenoids, advances in photosynthesis*. Kluwer Academic Publishers.
- Edmunds, P. J., and P. S. Davies. 1986. An energy budget for *Porites porites* (Scleractinia). *Marine Biology* **92**: 339-347.
- Edmunds, P. J., and S. P. Davies. 1988. Post-illumination stimulation of respiration rate in the coral *Porites porites*. *Coral Reefs* **7**: 7-9.
- Edmunds, P. J., and R. D. Gates. 2002. Normalizing physiological data for scleractinian corals. *Coral Reefs* **21**: 193-197.
- Eisenhut, M., S. Kahlon, and D. Hasse. 2006. The plant-like C<sub>2</sub> glycolate cycle and the bacterial-like glycerate pathway cooperate in phosphoglycolate metabolism in cyanobacteria. *Plant Physiology* **142**: 333-342.
- Enriquez, S., E. R. Mendez, and R. Iglesias-Prieto. 2005. Multiple scattering on coral skeletons enhances light absorption by symbiotic algae. *Limnology and Oceanography* **50**: 1025-1032.
- Fabricius, K. E. 2006. Effects of irradiance, flow and colony pigmentation on the temperature microenvironment around corals: IMplications for coral bleaching? *Limnology and Oceanography* **51**: 30-37.
- Fabricius, K. E., Y. Benayahu, and A. Genin. 1995. Herbivory in asymbiotic soft corals. *Science* **268**: 90-92.

- Falkowski, P. G., and J. A. Raven. 2007. *Aquatic Photosynthesis*, 2nd ed. Princeton University Press.
- Finazzi, G., F. Rappaport, A. Furia, M. Fleischmann, J.-D. Rochaix, F. Zito, and G. Forti. 2002. Involvement of state transitions in the switch between linear and cyclic electron flow in *Chlamydomonas reinhardtii*. *EMBO reports* **3**: 280-285.
- Fisher, P. L., M. K. Malme, and S. Dove. 2012. The effect of temperature stress on coral-*Symbiodinium* associations containing distinct symbiont types. *Coral Reefs* **31**: 473-485.
- Fitt, W., F. McFarland, M. Warner, and G. Chilcoat. 2000. Seasonal patterns of tissue biomass and density of symbiotic dinoflagellates in reef corals and relation to coral bleaching. *Limnology and Oceanography* **45**: 667-687.
- Fitt, W. K., B. E. Brown, M. E. Warner, and R. P. Dunne. 2001. Coral bleaching: interpretation of thermal tolerance limits and thermal thresholds in tropical corals. *Coral Reefs* **20**: 51-65.
- Fitt, W. K., O. Hoegh-Guldberg, J. C. Bythell, A. Jatkar, A. G. Grottoli, M. Gomez, P. L. Fisher, T. C. Lajeunesse, O. Pantos, R. Iglesias-Prieto, D. J. Franklin, L. J. Rodrigues, J. M. Torregiani, R. Van Woesik, and M. P. Lesser. 2009. Response of two species of Indo-Pacific corals, *Porites cylindrica* and *Stylophora pistillata*, to short-term thermal stress: the host does matter in determining the tolerance of corals to bleaching. *Journal of Experimental Marine Biology and Ecology* **373**: 102-110.
- Flores-Ramírez, L. A., and M. A. Liñán-Cabello. 2007. Relationships among thermal stress, bleaching and oxidative damage in the hermatypic coral, *Pocillopora capitata*. *Comparative Biochemistry and Physiology - Part C: Toxicology and Endocrinology* **146**: 194-202.
- Frank, H. A., A. Cua, V. Chynwat, A. Young, D. Gosztola, and Wasielewski. 1996. The lifetimes and energies of the first excited singlet states of diadinoxanthin and diatoxanthin: the role of these molecules in excess energy dissipation in algae. *Biochimica et Biophysica Acta* **1277**: 243-252.
- Franklin, D. J., O. Hoegh-Guldberg, R. J. Jones, and J. A. Berges. 2004. Cell death and degeneration in the symbiotic dinoflagellates of the coral *Stylophora pistillata* during bleaching. *Marine Ecology Progress Series* **272**: 117-130.

- Franklin, L. A., and M. R. Badger. 2001. A comparison of photosynthetic electron transport rates in macroalgae measured by pulse amplitude modulated chlorophyll fluorometry and mass spectrometry. *Journal of Phycology* **37**: 756-767.
- Freudenthal, H. D. 1962. *Symbiodinium* gen. nov. and *Symbiodinium microadriaticum* sp. nov., a zooxanthella: taxonomy, life cycle and morphology. *Journal of Protozoology* **9**: 45-52.
- Fujimura, H., T. Higuchi, K. Shiroma, T. Arakaki, A. M. Hamdun, Y. Nakano, and T. Oomori. 2008. Continuous-flow complete-mixing system for assessing the effects of environmental factors on colony-level coral metabolism. *Journal for Biochemical and Biophysical Methods* **70**: 865-872.
- Furla, P., I. Galgani, I. Durand, and D. Allemand. 2000. Sources and mechanisms of inorganic carbon transport for coral calcification and photosynthesis. *The Journal of Experimental Biology* **203**: 3445-3457.
- Garcia-Mendoza, E., H. C. P. Matthijs, H. Schubert, and L. R. Mur. 2002. Non-photochemical quenching of chlorophyll fluorescence in *Chlorella fusca* acclimated to constant and dynamic light conditions. *Photosynthesis Research* **74**: 303-315.
- Gates, R. D., and P. J. Edmunds. 1999. The physiological mechanisms of acclimatization in tropical reef corals. *American Zoologist* **39**: 30-43.
- Gates, R. D., O. Hoegh-Guldberg, M. J. Mcfall-Ngai, K. Y. Bil', and L. Muscatine. 1995. Free amino acids exhibit anthozoan "host factor" activity: they induce the release of photosynthate from symbiotic dinoflagellates *in vitro*. *Proceedings of the National Academy of Sciences U.S.A.* **92**: 7430-7434.
- Gattuso, J.-P., D. Allemand, and M. Frankignoulle. 1999. Photosynthesis and calcification at cellular, organismal and community levels in coral reefs: a review on interactions and control by carbonate chemistry. *American Zoologist* **39**: 160-183.
- Gattuso, J.-P., and J. Jaubert. 1990. Effect of light on oxygen and carbon dioxide fluxes and on metabolic quotients measured in situ in a zooxanthellate coral. *Limnology and Oceanography* **35**: 1796-1804.

- Gattuso, J.-P., S. Reynaud-Vaganay, P. Furla, S. Romaine-Lioud, J. Jaubert, I. Bourge, and M. Frankignoulle. 2000. Calcification does not stimulate photosynthesis in the zooxanthellate scleractinian coral *Stylophora pistillata*. *Limnology and Oceanography* **45**: 246-250.
- Geider, R. J., B. A. Osborne, and J. A. Raven. 1985. Light dependence of growth and photosynthesis in *Phaeodactylum tricornerutum*. *Journal of Phycology* **21**: 609-619.
- Genty, B., J.-M. Briantais, and N. R. Baker. 1989. The relationship between the quantum yield of photosynthetic electron transport and quenching of chlorophyll fluorescence. *Biochimica et Biophysica Acta* **990**: 87-92.
- Gilbert, M., A. Domin, A. Becker, and C. Wilhelm. 2000. Estimation of primary production by chlorophyll a *in vivo* fluorescence in freshwater phytoplankton. *Photosynthetica* **38**: 111-126.
- Giordano, M., J. Beardall, and J. A. Raven. 2005. Mechanisms, environmental modulation, and evolution. *Annual Review of Plant Biology* **56**: 99-131.
- Gleason, D. F., and G. M. Wellington. 1993. Ultraviolet radiation and coral bleaching. *Nature* **365**: 836-838.
- Glud, R. N., N. B. Ramsing, and N. P. Revsbech. 1992. Photosynthesis and photosynthesis-coupled respiration in natural biofilms quantified with oxygen microsensors. *Journal of Phycology* **28**: 51-60.
- Glynn, P. W. 1993. Coral reef bleaching: ecological perspectives. *Coral Reefs* **12**: 1-17.
- Glynn, P. W., J. L. Mate, A. C. Baker, and M. O. Calderon. 2001. coral bleaching and mortality in Panama and Ecuador during the 1997-1998 El Niño-Southern Oscillation event: spatial/temporal patterns and comparisons with the 1982-1983 event. *Bulletin of Marine Science* **69**: 79-109.
- Glynn, P. W., M. Perez, and S. L. Gilchrist. 1985. Lipid decline in stressed corals and their crustacean symbionts. *Biological Bulletin* **168**: 276-284.
- Goffredi, S. K., P. R. Girguis, J. J. Childress, and N. T. Desaulniers. 1999. Physiological functioning of carbonic anhydrase in the hydrothermal vent tubeworm *Riftia pachyptila*. *The Biological Bulletin* **196**: 257-264.

- Goiran, C., S. Al-Moghabri, D. Allemand, and J. Jaubert. 1996. Inorganic carbon uptake for photosynthesis by the symbiotic coral/dinoflagellate association I. Photosynthetic performances of symbionts and dependence on sea water bicarbonate. *Journal of Experimental Marine Biology and Ecology* **199**: 207-225.
- Gorbunov, M. Y., Z. S. Kolber, M. P. Lesser, and P. G. Falkowski. 2001. Photosynthesis and photoprotection in symbiotic corals. *Limnology and Oceanography* **46**: 75-85.
- Goreau, T. F. 1959. The physiology of skeleton formation in corals. I. A method for measuring the rate of calcium deposition by corals under different conditions. *Biological Bulletin (Woods Hole)* **116**: 59-75.
- Goreau, T. F. 1977a. Carbon metabolism in calcifying and photosynthetic organisms: theoretical models based on stable isotope data. *Proceedings 3rd international Symposium Coral Reefs* **2**: 395-401.
- Goreau, T. F. 1977b. Coral skeletal chemistry: physiological and environmental regulation of stable isotopes and trace metals in *Montastrea annularis*. *Proceedings of the Royal Society B* **196**: 291-315.
- Goreau, T. F. 1994. Coral Reefs, Rain Forests of the Ocean. *In* R. A. Eble and W. R. Eble [eds.], *The Encyclopedia of the Environment*. Houghton Mifflin Co.
- Goulet, T. L., T. C. Lajeunesse, and K. E. Fabricius. 2008. Symbiont specificity and bleaching susceptibility among soft corals in the 1998 Great Barrier Reef mass coral bleaching event. *Marine Biology* **154**: 795-804.
- Govindje, W. D., B. B. Prézelin, and B. M. Sweeney. 1979. Chlorophyll *a* fluorescence of *Gonyaulax polyedra* grown on a light-dark cycle and after transfer to constant light. *Photochemistry and Photobiology* **30**: 405-411.
- Graham, D., and R. M. Smillie. 1976. Carbonate dehydratase in marine organisms of the Great Barrier Reef. *Australian Journal of Plant Physiology* **3**: 153-179.
- Green, E. P., and D. G. Durnford. 1996. The chlorophyll-carotenoid proteins of oxygenic photosynthesis. *Annual Review in Plant Physiology and Plant Molecular Biology* **47**: 685-714.

- Grimsditch, G., J. Mwaura, J. Kilonzo, N. Amiyo, and D. Obura. 2008. High zooxanthellae densities and turnover correlate with low bleaching tolerance in Kenyan corals, p. 235-236. *In* D. O. Obura, J. Tamelander and O. Linden [eds.], Ten years after bleaching- facing the consequences of climate change in the Indian Ocean. CORDIO Status Report 2008. Coastal Oceans Research and Development in the Indian Ocean/Sida-SAREC.
- Grottoli, A. G., L. J. Rodrigues, and J. E. Palardy. 2006. Heterotrophic plasticity and resilience in bleached corals. *Nature* **440**: 1186-1189.
- Guillard, R. R. L., and J. H. Ryther. 1962. Studies of marine planktonic diatoms. I. *Cyclotella nana* Hustedt, and *Detonula confervacea* (Cleve) Gran. *Canadian Journal for Microbiology* **8**: 229-239.
- Hatcher, A. 1989. RQ of benthic marine invertebrates. *Marine Biology* **102**: 445-452.
- Hennige, S. J., M. P. Mcginley, A. G. Grottoli, and M. E. Warner. 2011. Photoinhibition of *Symbiodinium* spp. within the reef corals *Montastraea faveolata* and *Porites astreoides*: implications for coral bleaching. *Marine Biology* **158**: 2515-2526.
- Hennige, S. J., D. J. Suggett, M. E. Warner, K. E. McDougall, and D. J. Smith. 2009. Photobiology of *Symbiodinium* revisited: bio-physical and bio-optical signatures. *Coral Reefs* **28**: 179-195.
- Herfort, L., B. Thake, and I. Taubner. 2008. Bicarbonate stimulation of calcification and photosynthesis in two hermatypic corals. *Journal of Phycology* **44**: 91-98.
- Higuchi, T., H. Fujimura, T. Arakaki, and T. Oomori. 2009. The synergistic effects of hydrogen peroxide and elevated seawater temperature on the metabolic activity of the coral *Galaxea fascicularis* *Marine Biology* **156**: 580-596.
- Hill, R., C. M. Brown, K. Dezeew, D. A. Campbell, and P. J. Ralph. 2011. Increased rate of D1 repair in coral symbionts during bleaching is insufficient to counter accelerated photoinactivation. *Limnology and Oceanography* **56**: 139-146.
- Hill, R., C. Frankart, and P. J. Ralph. 2005. Impact of bleaching conditions on the components of non-photochemical quenching in the zooxanthellae of a coral. *Journal of Experimental Marine Biology and Ecology* **322**: 83-92.
- Hill, R., A. W. D. Larkum, C. Frankart, M. Kühl, and P. J. Ralph. 2004a. Loss of functional photosystem II reaction centers in zooxanthellae of corals exposed to bleaching conditions: Using fluorescence rise kinetics. *Photosynthesis Research* **82**: 59-72.

- Hill, R., A. W. D. Larkum, O. Prášil, D. M. Kramer, V. Kumar, and P. J. Ralph. 2012. Light-induced redistribution of antenna complexes in the symbionts of scleractinian corals correlates with sensitivity to coral bleaching. *Coral Reefs* **31**: 963-975.
- Hill, R., and P. J. Ralph. 2006. Photosystem II heterogeneity of *in hospite* zooxanthellae in scleractinian corals exposed to bleaching conditions. *Photochemistry and Photobiology* **82**: 1577-1585.
- Hill, R., and P. J. Ralph. 2007. Post-bleaching viability of expelled zooxanthellae from the scleractinian coral *Pocillopora damicornis*. *Marine Ecology Progress Series* **352**: 137-144.
- Hill, R., and P. J. Ralph. 2008a. Dark-induced reduction of the plastoquinone pool in zooxanthellae of scleractinian corals and implications for measurements of chlorophyll a fluorescence. *Symbiosis* **46**: 45-56.
- Hill, R., and P. J. Ralph. 2008b. Impact of bleaching stress on the function of the oxygen evolving complex of zooxanthellae from scleractinian corals. *Journal of Phycology* **44**: 299-310.
- Hill, R., U. Schreiber, R. Gademann, A. W. D. Larkum, M. Kuehl, and P. J. Ralph. 2004b. Spatial heterogeneity of photosynthesis and the effect of temperature-induced bleaching conditions in three species of corals. *Marine Biology* **144**: 633-640.
- Hill, R., K. E. Ulstrup, and P. J. Ralph. 2009. Temperature induced changes in thylakoid membrane thermostability of cultured, freshly isolated, and expelled zooxanthellae from scleractinian corals. *Bulletin of Marine Science* **85**: 223-244.
- Hill, R. W., C. Li, A. D. Jones, J. P. Gunn, and P. R. Farade. 2010. Abundant betaines in reef-building corals and ecological indicators of a photoprotective role. *Coral Reefs* **29**: 869-880.
- Hiller, R. G., P. M. Wrench, A. P. Gooley, G. Shoebridge, and J. Breton. 1993. The major intrinsic light-harvesting protein of Amphidinium: characterization and relation to other light-harvesting proteins. *Photochemistry and Photobiology* **57**: 125-131.
- Hiller, R. G., P. M. Wrench, and F. P. Sharples. 1995. The light-harvesting chlorophyll *a-c* binding protein of dinoflagellates: a putative polyprotein. *FEBS Letters* **363**: 175-178.



- Hoegh-Guldberg, O. 1999. Climate change, coral bleaching and the future of the world's coral reefs. *Marine & Freshwater Research* **50**: 839-866.
- Hoegh-Guldberg, O. 2009. Climate change and coral reefs: Trojan horse or false prophecy? *Coral Reefs* **28**: 569-575.
- Hoegh-Guldberg, O. 2010. The impact of climate change on the world's marine ecosystems. *Science* **328**: 1523-1528.
- Hoegh-Guldberg, O., M. Fine, W. Skirving, R. Johnstone, S. Dove, and A. Strong. 2005. Coral bleaching following wintry weather. *Limnology and Oceanography* **50**: 265-271.
- Hoegh-Guldberg, O., and R. J. Jones. 1999. Photoinhibition and photoprotection in symbiotic dinoflagellates from reef-building corals. *Marine Ecology Progress Series* **183**: 73-86.
- Hoegh-Guldberg, O., P. J. Mumby, H. A.J., R. S. Steneck, P. Greenfield, E. Gomez, C. D. Harvell, P. F. Sale, A. J. Edwards, K. Caldeira, N. Knowlton, C. M. Eakin, R. Iglesias-Prieto, N. Muthiga, R. H. Bradbury, A. Dubi, and M. E. Hatziolos. 2007. Coral reefs under rapid climate change and ocean acidification. *Science* **318**: 1737-1742.
- Hoegh-Guldberg, O., and G. J. Smith. 1989. The effect of sudden changes in temperature, light and salinity on the population density and export of zooxanthellae from the reef corals *Stylophora hystrix* Dana. *Journal of Experimental Marine Biology and Ecology* **129**: 279-303.
- Hofmann, E., P. M. Wrench, F. P. Sharples, R. G. Hiller, W. Welte, and K. Diederichs. 1996. Structural basis of light harvesting by carotenoids: peridinin-chlorophyll-protein from *Amphidinium carterae*. *Science* **272**: 1788-1791.
- Holzwarth, A. R. 1996. Data analysis of time-resolved measurements, p. 75-92. *In* J. Amez and A. J. Hoff [eds.], *Biophysical Techniques in Photosynthesis. Advances in Photosynthesis Research*. Kluwer Academic Publishers.
- Holzwarth, A. R. 2004. p. 43-115. *In* M. D. Archer and J. Barber [eds.], *Molecular to global photosynthesis*. Imperial college press.
- Holzwarth, A. R. 2008a. Primary reactions-from isolated complexes to intact plants, p. 77-83. *In* J. F. Allen, E. Gantt, J. H. Golbeck and B. Osmond [eds.], *Photosynthesis: Energy from the Sun*.



- Holzwarth, A. R. 2008b. Ultrafast primary reactions in the photosystems of oxygen-evolving organisms, p. 141-164. *In* M. Braun, P. Gilch and W. Zinth [eds.], *Ultrashort laser pulses in biology and medicine*. Springer.
- Holzwarth, A. R., Y. Miloslavina, M. Nilkens, and P. Jahns. 2009. Identification of two quenching sites active in the regulation of photosynthetic light-harvesting studied by time-resolved fluorescence. *Chemical Physics Letters* **483**: 262-267.
- Holzwarth, A. R., M. G. Mueller, J. Niklas, and J. Lubitz. 2005. Charge Recombination Fluorescence in Photosystem I Reaction Centers from *Chlamydomonas reinhardtii*. *Journal of Physical Chemistry* **109**: 5903-5911.
- Hoogenboom, M. O., K. R. N. Anthony, and S. R. Connolly. 2006. Energetic cost of photoinhibition in corals. *Marine Ecology Progress Series* **313**: 1-12.
- Hoogenboom, M. O., D. A. Campbell, E. Beraud, K. Dezeeuw, and C. Ferrier-Pagès. 2012. Effects of Light, Food Availability and Temperature Stress on the Function of Photosystem II and Photosystem I of Coral Symbionts. *Plos One* **7**: e30167.
- Hoogenboom, M. O., S. R. Connolly, and K. R. N. Anthony. 2009. Effects of photoacclimation on the light niche of corals: a process-based approach. *Marine Biology* **156**: 2493-2503.
- Houldbrèque, F., and C. Ferrier-Pagès. 2009. Heterotrophy in tropical scleractinian corals. *Biological Reviews* **84**: 1-17.
- Huang, X., C. J. Margulis, Y. Li, and B. J. Berne. 2005. Why is the partial molar volume of CO<sub>2</sub> so small when dissolved in a room temperature ionic liquid? Structure and dynamics of CO<sub>2</sub> dissolved in [Bmim<sup>+</sup>] [PF<sub>6</sub><sup>-</sup>]. *Journal of the American Chemistry Society* **127**: 17842-17851.
- Hughes, T. P., and J. H. Connell. 1999. Multiple stressors on coral reefs: A long-term perspective. *Limnology and Oceanography* **44**: 932-940.
- Hughes, T. P., A. H. Baird, D. R. Bellwood, M. Card, S. R. Connolly, C. Folke, R. Grosberg, O. Hoegh-Guldberg, J. B. C. Jackson, J. Kleypas, J. M. Lough, P. Marshall, M. Nystroem, S. R. Palumbi, J. M. Pandolfi, B. Rosen, and J. Roughgarden. 2003. Climate change, human impacts, and the resilience of coral reefs. *Science* **301**: 929-933.

- Iglesias-Prieto, R., V. H. Beltran, T. C. Lajeunesse, H. Reyes-Bonilla, and P. E. Thome. 2004. Different algal symbionts explain the vertical distribution of dominant reef corals in the eastern pacific. *Proceedings of the Royal Society B* **271**: 1757-1763.
- Iglesias-Prieto, R., N. S. Govind, and R. K. Trench. 1991. Apoprotein composition and spectroscopic characterization of the water-soluble peridinin chlorophyll alpha-proteins from 3 symbiotic dinoflagellates. *Proceedings of the Royal Society B* **246**: 275-283.
- Iglesias-Prieto, R., N. S. Govind, and R. K. Trench. 1993. Isolation and characterization of three membrane-bound chlorophyll-protein complexes from four dinoflagellate species. *Philosophical Transactions of the Royal Society B* **340**: 381-392.
- Iglesias-Prieto, R., J. L. Matta, W. A. Robins, and R. K. Trench. 1992. Photosynthetic response to elevated temperature in the symbiotic dinoflagellate *Symbiodinium microadriaticum* in culture. *Proceedings of the National Academy of Sciences U.S.A.* **89**: 10302-10305.
- Iglesias-Prieto, R., and R. K. Trench. 1996. Spectroscopic properties of chlorophyll *a* in the water-soluble peridinin-chlorophyll *a*-protein complexes (PCP) from the symbiotic dinoflagellate *Symbiodinium microadriaticum*. *Journal of Plant Physiology* **149**: 510-516.
- Iglesias-Prieto, R., and R. K. Trench. 1997. Acclimation and adaptation to irradiance in symbiotic dinoflagellates. II. Response of chlorophyll-protein complexes to different photon flux densities. *Marine Biology* **130**: 23-30.
- IPCC. 2007. *Climate Change 2007: The Physical Science Basis. Contribution of Working Group I to the Fourth Assessment Report of the Intergovernmental Panel on Climate Change.* Cambridge University Press.
- Jacques, S. L. 1998. Light distributions from point, line and plane sources for photochemical reactions and fluorescence in turbid biological tissues. *Photochemistry and Photobiology* **67**: 23-32.
- Jakob, T., R. Goss, and C. Wilhelm. 1999. Activation of diadinoxanthin de-epoxidase due to a chlororespiratory proton gradient in the dark in the diatom *Phaeodactylum tricornutum*. *Plant Biology* **1**: 76-82.

- Jakob, T., R. Goss, and C. Wilhelm. 2001. Unusual pH-dependence of diadinoxanthin de-epoxidase activation causes chlororespiratory induced accumulation of diatoxanthin in the diatom *Phaeodactylum tricoratum*. *Journal of Plant Physiology* **158**: 383-390.
- Jakob, T., H. Wagner, K. Stehfest, and C. Wilhelm. 2007. A complete energy balance from photons to new biomass reveals a light- and nutrient-dependent variability in the metabolic costs of carbon assimilation. *Journal of Experimental Botany* **58**: 2101-2112.
- Jassby, A. D., and T. Platt. 1976. Mathematical formulation of the relationship between photosynthesis and light for phytoplankton. *Limnology and Oceanography* **21**: 540-547.
- Jeffrey, S. W., and F. T. Haxo. 1968. Photosynthetic pigments of dinoflagellates (Zooxanthellae) from corals and clams. *Biological Bulletin* **135**: 149-165.
- Jensen, J., and N. P. Revsbech. 1989. Photosynthesis and respiration of a diatom biofilm cultured in a new gradient growth chamber. *FEMS Microbiology Ecology* **62**: 29-38.
- Jiang, J., H. Zhang, Y. Kang, D. Bina, C. S. Lo, and R. E. Blankenship. 2012. Characterization of the peridinin-chlorophyll *a*-protein complex in the dinoflagellate *Symbiodinium*. *Biochimica et Biophysica Acta (BBA)* **1817**: 983-989.
- Jimenez, I. M., M. Kühl, A. W. D. Larkum, and P. J. Ralph. 2008. Heat budget and thermal microenvironment of shallow-water corals: Do massive corals get warmer than branching corals? *Limnology and Oceanography* **53**: 1548-1561.
- Johnston, I. S. 1980. The ultrastructure of skeletogenesis in hermatypic corals. *International Review of Cytology* **67**: 171-214.
- Jokiel, P. L. 2011. The reef coral two compartment proton flux model: A new approach relating tissue-level physiological processes to gross corallum morphology. *Journal of Experimental Marine Biology and Ecology* **409**: 1-12.
- Jones, R. J. 2004. Testing the 'photoinhibition' model of coral bleaching using chemical inhibitors. *Marine Ecology Progress Series* **284**: 133-145.
- Jones, R. J., and O. Hoegh-Guldberg. 2001. Diurnal changes in the photochemical efficiency of the symbiotic dinoflagellates (Dinophyceae) of corals: photoprotection, photoinactivation and the relationship to coral bleaching. *Plant Cell & Environment* **24**: 89-99.

- Jones, R. J., O. Hoegh-Guldberg, A. W. D. Larkum, and U. Schreiber. 1998. Temperature-induced bleaching of corals begins with impairment of the CO<sub>2</sub> fixation mechanism in zooxanthellae. *Plant, Cell & Environment* **21**: 1219-1230.
- Jordan, D. B., and W. L. Ogren. 1981. Species variation in the specificity of ribulose biphosphate carboxylase/oxygenase. *Nature* **291**: 513-515.
- Kahara, S. N., and J. E. Vermaat. 2005. The effect of alkalinity on photosynthesis-light curves and inorganic carbon extraction capacity of freshwater macrophytes. *Aquatic Botany* **75**: 217-227.
- Kawaguti, S., and D. Sakumoto. 1948. The effects of light on the calcium deposition of corals. *Bulletin of Oceanography in Taiwan Strait/ Tai Wan Hai Xia* **4**: 65-70.
- Kerswell, A. P., and R. J. Jones. 2003. Effects of hypo-osmosis on the coral *Stylophora pistillata*: nature and cause of 'low-salinity bleaching'. *Marine Ecology Progress Series* **253**: 145-154.
- Kleppel, G., R. E. Dodge, and C. J. Reese. 1989. Changes in pigmentation associated with the bleaching of stony corals. *Limnology and Oceanography* **34**: 1331-1335.
- Klughammer, C., and U. Schreiber. 2008. Complementary PS II quantum yields calculated from simple fluorescence parameters measured by PAM fluorometry and the Saturation Pulse method. *PAM Application Notes* **1**: 27-35.
- Kok, B. 1948. On the interrelation between respiration and photosynthesis in green plants. *Biochimica et Biophysica Acta (BBA)* **3**: 625-631.
- Kramer, D. M., G. Johnson, O. Kiirats, and G. E. Edwards. 2004. New fluorescence parameters for the determination of Q<sub>A</sub> redox state and excitation energy fluxes. *Photosynthesis Research* **79**: 209-218.
- Krämer, W., I. Caamaño-Ricken, C. Richter, and K. Bischof. 2012. Dynamic Regulation of Photoprotection Determines Thermal Tolerance of Two Phylotypes of Symbiodinium Clade A at Two Photon Fluence Rates. *Photochemistry and Photobiology* **88**: 398-413.
- Krämer, W., V. Schrameyer, R. Hill, P. J. Ralph, and K. Bischof. 2013. PSII activity and pigment dynamics of *Symbiodinium* in two Indo-Pacific corals exposed to short-term high-light stress. *Marine Biology* **160**: 563-577.

- Kroon, B., B. B. Prezelin, and O. Schofield. 1993. Chromatic regulation of quantum yields for photosystem II charge separation, oxygen evolution and carbon fixation in *Heterocapsa pygmaea* (Pyrrophyta). *Journal of Phycology* **29**: 453-462.
- Kühl, M., Y. Cohen, T. Dalsgaard, B. B. Jorgensen, and N. P. Revsbech. 1995. Microenvironment and photosynthesis of zooxanthellae in scleractinian corals studies with microsensors for O<sub>2</sub>, pH and light. *Marine Ecology Progress Series* **117**: 159-172.
- Kühl, M., and T. Fenchel. 2000. Bio-optical characteristics and the vertical distribution of photosynthetic pigments and photosynthesis in an artificial cyanobacterial mat. *Microbial Ecology* **40**: 94-103.
- Kühlbrandt, W., and D. N. Wang. 1991. Three-dimensional structure of plant light-harvesting complex determined by electron crystallography. *Nature* **350**: 130-134.
- Kuile, B., J. Erez, and E. Padan. 1989. Competition for inorganic carbon between photosynthesis and calcification in the symbiont-bearing foraminifer *Amphistegina lobifera*. *Marine Biology* **103**: 253-259.
- Laisk, A., and F. Loreto. 1996. Determining photosynthetic parameters from leaf CO<sub>2</sub> exchange and chlorophyll fluorescence - ribulose-1,5- biphosphate carboxylase oxygenase specificity factor, dark respiration in the light, excitation distribution between photosystems, alternative electron transport rate, and mesophyll diffusion resistance. *Plant Physiology* **110**: 903-912.
- Lajeunesse, T. C., R. Bhagooli, M. Hidaka, L. De Vantier, T. Done, G. Schmidt, W., W. K. Fitt, and O. Hoegh-Guldberg. 2004. Closely related *Symbiodinium* spp. differ in relative dominance in coral reef host communities across environmental, latitudinal and biogeographic gradients. *Marine Ecology Progress Series* **284**: 147-161.
- Lajeunesse, T. C., R. Smith, M. Walther, J. Pinzón, D. T. Pettay, M. Mcginley, M. Aschaffenburg, P. Medina-Rosas, A. L. Cupul-Magaña, A. L. Pérez, H. Reyes-Bonilla, and M. E. Warner. 2010. Host-symbiont recombination versus natural selection in the response of coral-dinoflagellate symbioses to environmental disturbance. *Proceedings of the Royal Society B* **277**: 2925-2934.

- Lambrev, P. H., M. Nilkens, Y. Miloslavina, P. Jahns, and A. R. Holzwarth. 2010. Kinetic and spectral resolution of multiple nonphotochemical quenching components in *Arabidopsis* leaves. *Plant Physiology* **152**: 1611-1624.
- Langner, U., T. Jakob, K. Stehfest, and C. Wilhelm. 2009. An energy balance from absorbed photons to new biomass for *Chlamydomonas reinhardtii* and *Chlamydomonas acidophila* under neutral and extremely acidic growth conditions. *Plant, Cell & Environment* **32**: 250-258.
- Larkum, A. W. D. 2003. Light-harvesting systems in algae, p. 277-304. *In* A. W. D. Larkum, Douglas, S.E., Raven, J.A. [ed.], *Photosynthesis in Algae*. Kluwer Academic Publishers.
- Larkum, A. W. D., and J. Barrett. 1983. Light-harvesting processes in algae. *Advances in Botanical Research* **10**: 1-219.
- Larkum, A. W. D., and C. J. Howe. 1997. Molecular aspects of light-harvesting processes in algae. *Advances in Botanical Research* **27**: 257-330.
- Larkum, A. W. D., P. J. Lockhart, and C. J. Howe. 2007. Shopping for plastids. *Trends in Plant Science* **12**: 189-195.
- Leggat, W., M. R. Badger, and D. Yellowlees. 1999. Evidence for an inorganic carbon-concentrating mechanism in the symbiotic dinoflagellate *Symbiodinium* sp. *Plant Physiology* **121**: 1247-1255.
- Leggat, W., E. M. Marendy, B. Baillie, S. M. Whitney, M. Ludwig, M. R. Badger, and D. Yellowlees. 2002. Dinoflagellate symbioses: strategies and adaptations for the acquisition and fixation of inorganic carbon. *Functional Plant Biology* **29**: 309-322.
- Lemeille, S., and J.-D. Rochaix. 2010. State transitions at the crossroad of thylakoid signalling pathways. *Photosynthesis Research* **106**: 33-46.
- Lesser, M. 2011. Coral Bleaching: Causes and Mechanisms, p. 405-419. *In* Z. Dubinsky and N. Stambler [eds.], *Coral Reefs: An Ecosystem in Transition*. Springer Netherlands.
- Lesser, M. P. 1996. Elevated temperatures and ultraviolet radiation cause oxidative stress and inhibit photosynthesis in symbiotic dinoflagellates. *Limnology and Oceanography* **41**: 271-283.

- Lesser, M. P. 1997. Oxidative stress causes coral bleaching during exposure to elevated temperatures. *Coral Reefs* **16**: 187-192.
- Lesser, M. P. 2006. Oxidative stress in Marine Environments: Biochemistry and Physiological Ecology. *Annual Review of Physiology* **68**: 253-278.
- Lesser, M. P., and J. H. Farrell. 2004. Exposure to solar radiation increases damage to both host tissues and algal symbionts of corals during thermal stress. *Coral Reefs* **23**: 367-377.
- Lesser, M. P., W. R. Stochaj, D. W. Tapley, and J. M. Shick. 1990. Bleaching in coral reef anthozoans: effects of irradiance, ultraviolet radiation, and temperature on the activities of protective enzymes against active oxygen. *Coral Reefs* **8**: 225-232.
- Levine, I. N. 1974. *Physical chemistry*. McGraw-Hill.
- Levy, O., Z. Dubinsky, K. Schneider, Y. Aчитuv, D. Zakai, and M. Y. Gorbunov. 2004. Diurnal hysteresis in coral photosynthesis. *Marine Ecology Progress Series* **268**: 105-117.
- Li, Y. H., and S. Gregory. 1974. Diffusion of ions in sea water and in deep-sea sediments. *Geochimica Cosmochimica Acta* **38**: 703-714.
- Li, Z., S. Wakao, B. B. Fischer, and K. K. Niyogi. 2009. Sensing and responding to excess light. *Annual review of plant biology* **60**: 239-260.
- Lilley, R. M., P. J. Ralph, and A. W. D. Larkum. 2010. The determination of activity of the enzyme Rubisco in cell extracts of the dinoflagellate alga *Symbiodinium* sp. by manganese chemiluminescence and its response to short-term stress of the alga. *Plant, Cell & Environment* **33**: 995-1004.
- Loeblich, A. R. I., and J. L. Sherley. 1979. Observations on the theca of the motile phase of free-living and symbiotic isolates of *Zooxanthella microadriatica* (Freudenthal) comb.nov. *Journal of the Marine Biological Association of the United Kingdom* **59**: 195-205.
- Long, S. P., S. Humphries, and P. G. Falkowski. 1994. Photoinhibition of photosynthesis in nature. *Annual Review of Plant Physiology and Plant Molecular Biology* **45**: 633-662.
- Longstaff, B. J., T. Kildea, J. W. Runcie, A. Cheshire, W. C. Dennison, C. Hurd, T. Kana, J. A. Raven, and L. A. W.D. 2002. An *in situ* study of photosynthetic oxygen exchange and electron transport rate in the marine macroalgae *Ulva lactuca* (Chlorophyta). *Photosynthesis Research* **74**: 281-293.



- Lough, J. M. 2004. A strategy to improve the contribution of coral data to high-resolution paleoclimatology. *Paleogeography, Paleoclimatology, Palaeoecology* **204**: 115-143.
- Lough, J. M. 2007. Climate and climate change on the Great Barrier Reef, p. 15-50. *In* J. Johnson and P. Marshall [eds.], *Climate Change and the Great Barrier Reef. A Vulnerability Assessment*. GBRMPA/AGO.
- Loya, Y., K. Sakai, K. Yamazato, Y. Nakano, H. Sambali, and R. Van Woesik. 2001. Coral bleaching: the winners and the losers. *Ecology Letters* **4**: 122-131.
- Lunde, C., P. E. Jensen, A. Haldrup, J. Knoetzel, and H. V. Scheller. 2000. The PSI-H subunit of photosystem I is essential for state transitions in plant photosynthesis. *Nature* **408**: 613-615.
- Macintyre, H. L., T. Kana, and R. J. Geider. 2000. The effect of water motion on short-term rates of photosynthesis by marine phytoplankton. *Trends in Plant Science* **5**: 12-17.
- Marshall, P. A., and A. H. Baird. 2000. Bleaching of corals on the Great Barrier Reef: differential susceptibilities among taxa. *Coral Reefs* **19**: 155-163.
- Matsubara, S., and W. S. Chow. 2004. Populations of photoinactivated photosystem II reaction centers characterized by chlorophyll *a* fluorescence lifetime *in vivo*. *PNAS* **101**: 18234-18239.
- Mattoo, A. K., H. Hoffman-Falk, J. B. Marder, and M. Edelman. 1984. Regulation of protein metabolism coupling of photosynthetic electron transport to *in vivo* degradation of the rapidly metabolized 32-kilodalton protein of the chloroplast membranes. *Proceedings of the National Academy of Sciences U.S.A.* **81**: 1380-1384.
- McClanahan, T. R. 2002. The near future of coral reefs. *Environmental Conservation* **29**: 1-24.
- McCloskey, L. R., and L. Muscatine. 1984. Production and respiration in the Red Sea coral *Stylophora pistillata* as a function of depth. *Proceedings of the Royal Society B* **222**: 215-230.
- Mendes, J. M., and J. D. Woodley. 2002. Effect of the 1995-1996 bleaching event on polyp tissue depth, growth, reproduction and skeletal band formation in *Montastrea annularis*. *Marine Ecology Progress Series* **235**: 93-102.



- Middlebrook, R., K. R. N. Anthony, O. Hoegh-Guldberg, and S. Dove. 2010. Heating rate and symbiont productivity are key factors determining thermal stress in the reef-building coral *Acropora formosa*. *The Journal of Experimental Biology* **213**: 1026-1034.
- Mills, L. S., M. E. Soulé, and D. F. Doak. 1993. The Keystone-Species Concept in Ecology and Conservation. *BioScience* **43**: 219-224.
- Miloslavina, Y., I. Grouneva, P. H. Lambrev, B. Lepetit, R. Goss, C. Wilhelm, and A. R. Holzwarth. 2009. Ultrafast fluorescence study on the location and mechanism of non-photochemical quenching in diatoms. *Biochimica et Biophysica Acta* **1787**: 1189-1197.
- Morse, D. 1995. A culear-encoded form II Rubisco in dinoflagellates. *Science* **268**: 1622-1624.
- Moya, A., S. Tambutte, A. Bertucci, E. Tambutte, S. Lotto, D. Vullo, C. T. Supuran, D. Allemand, and D. Zoccola. 2008. Carbonic anhydrase in the scleractinian coral *Stylophora pistillata*- Characerization, localization, and role in biomineralization. *Journal of Biological Chemistry* **283**: 25475-25484.
- Moya, A., S. Tambutte, E. Tambutte, D. Zoccola, N. Caminiti, and D. Allemand. 2006. Study of calcification during a daily cycle of the coral *Stylophora pistillata*: implications for 'light-enhanced calcification'. *The Journal of Experimental Biology* **209**: 3413-3419.
- Muller-Parker, G., and C. F. D'elia. 1997. Interactions between corals and their symbiotic algae, p. 96-113. *In* C. Birkeland [ed.], *Life and Death of Coral Reefs*. Chapman and Hall.
- Munge, B., S. K. Das, R. Ilagan, Z. Pendon, J. Yang, H. A. Frank, and J. F. Rusling. 2003. Electron transfer reactions of redox cofactors in spinach photosystem I reaction center protein in lipid films on electrodes. *Journal of the American Chemical Society* **125**: 12457-12463.
- Muscatine, L. 1990. The role of symbiotic algae in carbon and energy flux in reef corals, p. 75-87. *In* Z. Dubinsky [ed.], *Ecosystems of the World: Coral reefs*. Elsevier.
- Muscatine, L. 1991. Release of symbiotic algae by tropical sea anemones and corals after cold shock. *Marine Ecology Progress Series* **77**: 233-243.

- Muscatine, L., and E. Cernichiari. 1969. Assimilation of photosynthetic products of zooxanthellae by a reef coral. *Biological Bulletin* **137**: 506-523.
- Muscatine, L., L. R. McCloskey, and R. E. Marian. 1981. Estimating the daily contribution of carbon from zooxanthellae to coral animal respiration. *Limnology and Oceanography* **26**: 601-611.
- Muscatine, L., and J. W. Porter. 1977. Reef Corals: Mutualistic symbioses adapted to nutrient-poor environments. *BioScience* **27**: 454-460.
- Muscatine, L., J. W. Porter, and I. R. Kaplan. 1989. Resource partitioning by reef corals as determined from stable isotope composition: I. delta <sup>13</sup>C of zooxanthellae and animal tissue vs. depth. *marine Biology* **100**: 185-193.
- Nagelkerken, I., C. M. Roberts, G. Van Der Velde, M. Dorenbosch, M. C. Van Riel, E. Cocheret De La Moriniere, and P. H. Nienhuis. 2002. How important are mangroves and seagrass beds for coral-reef fish? The nursery hypothesis tested on an island scale. *Marine Ecology Progress Series* **244**: 299-305.
- Newsholme, E. A., and B. Crabtree. 2005. Maximum catalytic activity of some key enzymes in provision of physiologically useful information about metabolic fluxes. *Journal of experimental zoology* **239**: 159-167.
- Nishiyama, Y., S. I. Allakhverdiev, H. Yamamoto, H. Hayashi, and N. Murata. 2004. Singlet oxygen inhibits the repair of photosystem II by suppressing translation elongation of the D1 protein in *Synechocystis* sp. PCC 6803. *Biochemistry* **43**: 11321-11330.
- Niyogi, K. 1999. Photoprotection revisited: genetic and molecular approaches. *Annual Review of Plant Physiology and Plant Molecular Biology* **50**: 333-359.
- Norris, B., and D. Miller. 1994. Nucleotide sequence of a cDNA clone encoding the precursor of the peridinin-chlorophyll a-binding protein from the dinoflagellate *Symbiodinium* sp. *Plant Molecular Biology* **24**: 673-677.
- Ochoa De Alda, J. a. G., M. I. Tapia, F. Franck, M. J. Llama, and J. L. Serra. 1996. Changes in nitrogen source modify distribution of excitation energy in the cyanobacterium *Phormidium laminosum*. *Physiologia plantarum* **97**: 69-78.
- Paine, R. T. 1969. The *Pisaster-Tegula* interaction: prey patches, predator food preferences and intertidal community structure. *Ecology* **50**: 950-961.
- Parys, E., and H. Jastz. 2006. Light-enhanced dark respiration in leaves, isolated cells and protoplasts of various types of C4 plants. *Journal of Plant Physiology* **163**: 638-647.

- Pearse, V. B., and L. Muscatine. 1971. Role of symbiotic algae (zooxanthellae) in coral calcification. *Biological Bulletin (Woods Hole)* **141**: 350-363.
- Peltier, G., and G. W. Schmidt. 1991. Chlororespiration: an adaptation to nitrogen deficiency in *Chlamydomonas reinhardtii*. *Proceedings of the National Academy of Sciences U.S.A.* **88**: 4791-4795.
- Pernice, M., A. Meibom, A. Van Den Heuvel, C. Kopp, I. Domart-Coulon, O. Hoegh-Guldberg, and S. Dove. 2012. A single-cell view of ammonium assimilation in coral–dinoflagellate symbiosis. *International Society for Microbial Ecology* **6**: 1314-1324.
- Peterson, R. B. 1989. Partitioning of non-cyclic photosynthetic electron transport to O<sub>2</sub>-dependent dissipative processes as probed by fluorescence and CO<sub>2</sub> exchange. *Plant Physiology* **90**: 1322-1328.
- Peterson, R. B. 1990. Effects of irradiance on the *in vivo* CO<sub>2</sub>:O<sub>2</sub> specificity factor in tobacco using simultaneous gas exchange and fluorescence techniques. *Plant Physiology* **95**: 892-898.
- Platt, T., C. L. Gallegos, and W. G. Harrison. 1980. Photoinhibition of photosynthesis in natural assemblages of marine phytoplankton. *Journal of Marine Research* **38**: 687-701.
- Prasil, O., Z. Kolber, J. A. Berry, and P. G. Falkowski. 1996. Cyclic electron flow around photosystem II *in vivo*. *Photosynthesis Research* **48**: 395-410.
- Putnam, H. M., M. Stat, X. Pochon, and R. D. Gates. 2012. Endosymbiotic flexibility associates with environmental sensitivity in scleractinian corals. *Proceedings of the Royal Society B* **279**: 4352-4361.
- Pysznik, A. M., and S. P. Gibbs. 1992. Immunocytochemical localization of photosystem I and the fucoxanthin-chlorophyll a/c light-harvesting complex in the diatom *Phaeodactylum tricorutum*. *Protoplasma* **166**: 208-217.
- Quetin, L. B., R. M. Ross, and K. Uchio. 1980. Metabolic characteristics of midwater zooplankton: ammonia excretion, O:N ratios, and the effect of starvation. *Marine Biology* **59**: 201-209.
- Ragni, M., R. L. Airs, S. J. Hennige, D. J. Suggett, M. E. Warner, and R. J. Geider. 2010. PSII photoinhibition and photorepair in *Symbiodinium* (Pyrrophyta) differs between thermally tolerant sensitive phylotypes. *Marine Ecology Progress Series* **406**: 57-70.

- Ralph, P. J., and R. Gademann. 2005. Rapid light curves: A powerful tool to assess photosynthetic activity. *Aquatic Botany* **82**: 222-237.
- Ralph, P. J., R. Gademann, and A. W. D. Larkum. 2001. Zooxanthellae expelled from bleached corals at 33°C are photosynthetically competent. *Marine Ecology Progress Series* **220**: 163-168.
- Ralph, P. J., A. W. D. Larkum, and M. Kühl. 2005a. Temporal patterns in effective quantum yield of individual zooxanthellae expelled during bleaching. *Journal of Experimental Marine Biology and Ecology* **316**: 17-28.
- Ralph, P. J., U. Schreiber, R. Gademann, M. Kühl, and A. W. D. Larkum. 2005b. Coral photobiology studied with a new imaging pulse amplitude modulated fluorometer. *Journal of Phycology* **41**: 335-342.
- Ralph, P. J., C. Wilhelm, J. Lavaud, T. Jakob, K. Petrou, and S. Kranz. 2010. Fluorescence as a tool to understand changes in photosynthetic electron flow regulation, p. 75-89. *In* D. J. Suggett, M. A. Borowitzka and O. Prasil [eds.], *Chlorophyll a Fluorescence in Aquatic Sciences: Methods and Applications*. Springer.
- Rands, M. L., B. C. Loughman, and A. E. Douglas. 1993. The symbiotic interface in an alga-invertebrate symbiosis. *Proceedings of the Royal Society B* **253**: 161-165.
- Rappaport, F., M. Guergova-Kuras, P. J. Nixon, B. A. Diner, and J. Lavergne. 2002. Kinetics and pathways of charge recombination in Photosystem II. *Biochemistry* **41**: 8518-8527.
- Raven, J. A. 1992. *Biology of Plants*, 5th ed. Worth Publisher Inc.
- Raven, J. A. 2003. Inorganic carbon concentrating mechanisms in relation to the biology of algae. *Photosynthesis Research* **77**: 155-171.
- Raven, J. A., and J. Beardall. 2003. Carbon acquisition mechanisms in algae: carbon dioxide diffusion and carbon dioxide concentrating mechanisms, p. 225-244. *In* A. W. D. Larkum, A. E. Douglas and J. A. Raven [eds.], *Photosynthesis in Algae*. Kluwer.
- Raven, J. A., and C. L. Hurd. 2012. Ecophysiology of photosynthesis in macroalgae. *Photosynthesis Research* **113**: 105-125.
- Revsbech, N. P., and B. B. Jorgensen. 1983. Photosynthesis of benthic microflora measured with high spatial resolution by the oxygen microprofile method: capabilities and limitations of the method. *Limnology and Oceanography* **28**: 749-756.

- Reynaud-Vaganay, S., A. Juillet-Leclerc, J. Jaubert, and J. P. Gatusso. 2001. Effect of light on skeletal  $^{13}\text{C}$  and  $^{18}\text{O}$  and interaction with photosynthesis, respiration and calcification in 2 zooxanthellate scleractinian corals. *Paleogeography, Paleoclimatology, Paleoecology* **175**: 393-404.
- Reynolds, M. J., B. U. Bruns, W. K. Fitt, and G. W. Schmidt. 2008. Enhanced photoprotection pathways in symbiotic dinoflagellates of shallow-water corals and other cnidarians. *Proceedings of the National Academy of Sciences U.S.A.* **105**: 13674-13678.
- Richardson, M. J., W. D. Gardner, S. P. Chung, and D. Walsh. 1993. Source of beam attenuation signal as a function of particle size. *The Oceanography Society Meeting Abstracts, Seattle, Washington* **71**.
- Rink, S., M. Kühl, J. Bijma, and H. J. Spero. 1998. Microsensor studies of photosynthesis and respiration in the symbiotic foraminifer *Orbulina universa*. *Marine Biology* **131**: 583-595.
- Ritchie, R. J. 2006. Consistent sets of spectrophotometric chlorophyll equations for acetone, methanol and ethanol solvents. *Photosynthesis Research* **89**: 27-41.
- Ritchie, R. J. 2008. Universal chlorophyll equations for estimating chlorophylls *a*, *b*, *c*, and *d* and total chlorophylls in natural assemblages of photosynthetic organisms using acetone, methanol or ethanol solvents. *Photosynthetica* **46**: 115-126.
- Robison, J. D., and M. E. Warner. 2006. Differential impacts of photacclimation and thermal stress on the photobiology of four different phylotypes of *Symbiodinium* (Pyrrhophyta). *Journal of Phycology* **42**: 568-579.
- Roff, G., and P. J. Mumby. 2012. Global disparity in the resilience of coral reefs. *Trends in Ecology & Evolution* **27**: 404-413.
- Roth, K. E., K. Jeon, and G. Stacey. 1988. Homology in endosymbiotic systems: the term "Symbiosome", p. 220-225. *In* R. Palacios and D. P. S. Verma [eds.], *Molecular Genetics of Plant-Microbe Interactions*. APS Press.
- Rowan, R., S. M. Whitney, A. Fowler, and D. Yellowlees. 1996. Rubisco in marine symbiotic dinoflagellates: form II enzymes in eukaryotic oxygenic phototrophs encoded by a nuclear multigene family. *The Plant Cell* **8**: 539-553.
- Ruuska, S. A., M. R. Badger, T. J. Andrews, and S. Von Caemmerer. 2000. Photosynthetic electron sinks in transgenic tobacco with reduced amounts of Rubisco: little evidence for significant Mehler reaction. *Journal of Experimental Botany* **51**: 357-368.

- Sabine, C. L., R. A. Feely, N. Gruber, R. M. Key, K. M. Lee, J. L. Bullister, R. Wanninkhof, C. S. Wong, D. W. R. Wallace, B. Tilbrok, F. J. Millero, T.-H. Peng, A. Kozyr, T. Ono, and A. F. Rios. 2004. The ocean sink for anthropogenic CO<sub>2</sub>. *Science* **305**: 367-371.
- Satoh, K., and D. C. Fork. 1983a. A new mechanism for adaptation to changes in light intensity and quality in the red alga, *Porphyra perforata*. I. relation to state 1 - state 2 transitions. *Biochimica et Biophysica Acta (BBA) - Bioenergetics* **722**: 190-196.
- Satoh, K., and D. C. Fork. 1983b. State I - state II transitions in the green alga *Scenedesmus obliquus*. *Photochemistry and Photobiology* **37**: 429-434.
- Schlichting, H., and K. Gersten. 2000. *Boundary-Layer Theory*. Springer.
- Schneider, K., O. Levy, Z. Dubinsky, and J. Erez. 2009. *In situ* diel cycles of photosynthesis and calcification in hermatypic corals. *Limnology and Oceanography* **54**: 1995-2002.
- Schreiber, U. 2004. Pulse-amplitude-modulation (PAM) fluorometry and saturation pulse method: an overview, p. 279-319. *In* G. C. Papageorgiou and Govindjee [eds.], *Chlorophyll a fluorescence: a signature of photosynthesis*. *Advances in Photosynthesis and Respiration*. Springer.
- Schreiber, U., H. Hormann, K. Asada, and C. Neubauer. 1995a. O<sub>2</sub>-dependent electron flow in intact spinach chloroplasts: properties and possible regulation of the Mehler-Ascorbate-Peroxidase cycle, p. 813-818. *In* P. Mathis [ed.], *Photosynthesis: from Light to Biosphere*. Kluwer Academic Publishers.
- Schreiber, U., H. Hormann, C. Neubauer, and C. Klughammer. 1995b. Assessment of photosystem II photochemical quantum yield by chlorophyll fluorescence quenching analysis. *Australian Journal of Plant Physiology* **22**: 209-220.
- Seaton, G. G. R., and D. A. Walker. 1990. Chlorophyll fluorescence as a measure of photosynthetic carbon assimilation. *Proceedings of the Royal Society B* **242**: 29-35.
- Seibt, C., and D. Schlichter. 2001. Compatible intracellular ion composition of the host improves carbon assimilation by zooxanthellae in mutualistic symbioses. *Naturwissenschaften* **88**: 382-386.
- Sharp, R. E., M. A. Matthews, and J. S. Boyer. 1984. Kok effect and the quantum yield of photosynthesis. *Plant Physiology* **75**: 95-101.

- Shick, J. M., and M. P. Lesser. 1996. Effects of ultraviolet radiation on corals and other coral reef organisms. *Global Change Biology* **2**: 527-545.
- Shipton, C. A., and J. Barber. 1991. Photoinduced degradation of the D1 polypeptide in isolated reaction centers of photosystem II: Evidence for an autoprolytic process triggered by the oxidizing of the photosystem. *Proceedings of the National Academy of Sciences U.S.A.* **88**: 6691-6695.
- Silva, L. M. T., C. P. Dos Santos, and R. M. Chaloub. 2001. Effect of the respiratory activity on photoinhibition of the cyanobacterium *Synechocystis* sp. *Photosynthesis Research* **68**: 61-69.
- Sinutok, S., R. Hill, M. A. Doblin, R. Wuhrer, and P. J. Ralph. 2011. Warmer more acidic conditions cause decreased productivity and calcification in subtropical coral reef sediment-dwelling calcifiers. *Limnology and Oceanography* **56**: 1200-1212.
- Sivak, M. N., and D. A. Walker. 1985. Chlorophyll a fluorescence: can it shed light on fundamental questions in photosynthetic carbon dioxide fixation? . *Plant, Cell & Environment* **8**: 439-448.
- Six, C., Z. V. Finkel, A. J. Irwin, and D. A. Campbell. 2007. Light variability illuminates niche-partitioning among marine picocyanobacteria. *Plos One* **2**: e1341.
- Smith, F. W., and N. A. Walker. 1980. Photosynthesis by aquatic plants: effects of unstirred layers in relation to assimilation of CO<sub>2</sub> and HCO<sub>3</sub><sup>-</sup> and to carbon isotopic discrimination *New Phytologist* **86**: 245-259.
- Spalding, M. D., C. Ravilious, and E. P. Green. 2001. *World atlas of coral reefs*. University of California Press.
- Stat, M., D. Carter, and O. Hoegh-Guldberg. 2006. The evolutionary history of *Symbiodinium* and scleractinian hosts - symbiosis, diversity, and the effect of climate change. *Perspectives in Plant Ecology, Evolution and Systematics* **8**: 23-43.
- Stimson, J., and R. A. Kinzie. 1991. The temporal pattern and rate of release of zooxanthellae from the reef coral *Pocillopora damicornis* (Linnaeus) under nitrogen-enrichment and control conditions. *The Journal of Experimental Biology* **153**: 66-74.



- Stirbet, A., and Govindjee. 2012. Chlorophyll *a* fluorescence induction: a personal perspective of the thermal phase, the J-I-P rise. *Photosynthesis Research* **113**: 15-61.
- Strychar, K. B., M. Coates, and P. W. Sammarco. 2005. Loss of *Symbiodinium* from bleached soft corals *Sarcophyton ehrenbergi*, *Sinularia sp.* and *Xenia sp.* *Journal of Experimental Marine Biology and Ecology* **320**: 159-177.
- Suggett, D. J., E. Le Floch, G. N. Harris, N. Leonardos, and P. J. Geider. 2007. Different strategies of photoacclimation by two strains of *Emiliana huxleyi* (Haptophyta). *Journal of Phycology* **43**: 1209-1222.
- Suggett, D. J., H. L. Macintyre, T. M. Kana, and R. J. Geider. 2010a. Comparing electron transport with gas exchange: parameterising exchange rates between alternative photosynthetic currencies for eukaryotic phytoplankton. *Aquatic Microbial Ecology* **65**: 147-162.
- Suggett, D. J., M. C. Moore, and R. J. Geider. 2010b. Estimating Aquatic Productivity from Active Fluorescence Measurements. In D. J. Suggett, O. Prasil and M. A. Borowitzka [eds.], *Chlorophyll a Fluorescence in Aquatic Sciences: Methods and Applications*. Springer.
- Suggett, D. J., M. E. Warner, D. J. Smith, P. Davey, S. Hennige, and N. R. Baker. 2008. Photosynthesis and production of hydrogen peroxide by *Symbiodinium* (Pyrrophyta) phylotypes with different thermal tolerances. *Journal of Phycology* **44**: 948-956.
- Szmant, A. M., and N. J. Gassman. 1990. The effects of prolonged "bleaching" on the tissue biomass and reproduction of the reef coral *Montastrea annularis*. *Coral Reefs* **8**: 217-224.
- Takahashi, S., and M. R. Badger. 2011. Photoprotection in plants: a new light on photosystem II damage. *Trends in Plant Science* **16**: 53-60.
- Takahashi, S., T. Nakamura, M. Sakamizu, R. Van Woesik, and H. Yamasaki. 2004. Repair machinery of symbiotic photosynthesis as the primary target of heat stress for reef-building corals. *Plant Cell Physiology* **45**: 231-235.
- Takahashi, S., S. M. Whitney, and M. R. Badger. 2009. Different thermal sensitivity of the repair of photodamaged photosynthetic machinery in cultured *Symbiodinium* species. *Proceedings of the National Academy of Sciences U.S.A.* **106**: 3237-3242.



- Taylor, F. J. R. 1990. Dinoflagellata (Dinomastigota), p. 419-437. *In* L. Margulis, C. C. Corliss, M. Melkonian and D. J. Chapman [eds.], Handbook of Protoctista. Jones and Bartlett Publishers.
- Tchernov, D., M. Y. Gorbunov, C. De Vargas, S. N. Yadav, A. J. Milligan, M. Haegglom, and P. G. Falkowski. 2004a. Membrane lipids of symbiotic algae are diagnostic of sensitivity to thermal bleaching in corals. Proceedings of the National Academy of Sciences U.S.A. **101**: 13531-13535.
- Tchernov, D., M. Y. Gorbunov, C. De Vargas, S. N. Yadav, A. J. Milligan, M. Haegglom, and P. G. Falkowski. 2004b. Membrane lipids of symbiotic algae are diagnostic of sensitivity to thermal bleaching in corals. Proceedings of the National Academy of Sciences U.S.A. **101**: 13531-13535.
- Telfer, A., S. M. Bishop, D. Phillips, and J. Barber. 1994. Isolated photosynthetic reaction center of photosystem II as a sensitizer for the formation of singlet oxygen. the Journal of Biological Chemistry **269**: 13244-13253.
- Ten Lohuis, M. R., and D. J. Miller. 1998. Light-regulated transcription of genes encoding peridinin chlorophyll a proteins and the major intrinsic light-harvesting complex proteins in the dinoflagellate *Amphidinium carterae* Hulbert (Dinophyceae) - changes in cytosine methylation accompany photoadaptation. Plant Physiology **117**: 189-196.
- Tikkanen, M., M. Grieco, and E.-M. Aro. 2011. Novel insights into plant light-harvesting complex II phosphorylation and 'state transitions'. Trends in Plant Science **16**: 126-131.
- Timasheff, S. N. 1992. A physicochemical basis for the selection of osmolytes by nature. Springer-Verlag.
- Timmermann, A., J. Oberhuber, A. Bacher, M. Esch, M. Latif, and E. Roeckner. 1999. Increased El Niño frequency in a climate model forced by future greenhouse warming. Nature **398**: 694-697.
- Tobías, I., A. Luque, and A. Martí. 2008. Light intensity enhancement by diffracting structures in solar cells. Journal of applied physics **104**: 1-9.
- Tolbert, N. E., C. Benker, and E. Beck. 1995. The oxygen and carbon dioxide compensation points of C<sub>3</sub> plants: Possible role in regulating atmospheric oxygen. Proceedings of the National Academy of Sciences U.S.A. **92**: 11230-11233.

- Tremblay, P., C. Ferrier-Pagès, J. F. Maguer, C. Rottier, L. Legendre, and R. Grover. 2012a. Controlling effects of irradiance and heterotrophy on carbon translocation in the temperate coral *Cladocora caespitosa*. *Plos One* **7**: E44672.
- Tremblay, P., R. Grover, J. F. Maguer, L. Legendre, and C. Ferrier-Pagès. 2012b. Autotrophic carbon budget in coral tissue: a new  $^{13}\text{C}$ -based model of photosynthate translocation. *The Journal of Experimental Biology* **215**: 1384-1393.
- Trench, R. K. 1979. The Cell Biology of Plant-Animal Symbiosis. *Annual Review of Plant Physiology* **30**.
- Ulstrup, K. E., R. Berkelmans, P. J. Ralph, and M. J. H. Van Oppen. 2006a. Variation in bleaching susceptibility of two coral species along a latitudinal gradient on the Great Barrier Reef: the role of zooxanthellae. *Marine Ecology Progress Series* **314**: 135-148.
- Ulstrup, K. E., R. Hill, M. J. H. Van Oppen, A. W. D. Larkum, and P. J. Ralph. 2008. Seasonal variation in the photo-physiology of homogeneous and heterogeneous *Symbiodinium* consortia in two scleractinian corals. *Marine Ecology Progress Series* **361**: 139-150.
- Ulstrup, K. E., M. Kühl, M. J. H. Van Oppen, T. F. Cooper, and P. J. Ralph. 2011. Variation in photosynthesis and respiration in geographically distinct populations of two reef-building coral species. *Aquatic Biology* **12**: 241-248.
- Ulstrup, K. E., P. J. Ralph, A. W. D. Larkum, and M. Kühl. 2006b. Intra-colonial variability in light acclimation of zooxanthellae in coral tissues of *Pocillopora damicornis*. *Marine Biology* **149**: 1325-1335.
- Van Amerongen, H., L. Valkunas, and R. Van Grondelle. 1996. Photosynthetic excitons, p. 1-590. World scientific.
- Van Heukelem, L., and C. Thomas. 2001. Computer-assisted high-performance liquid chromatography method development with applications to the isolation and analysis of phytoplankton pigments. *Journal of Chromatography A* **910**: 31-49.
- Van Stokkum, I. H. M., D. S. Larsen, and R. Van Grondelle. 2004. Global and target analysis of time-resolved spectra. *Biochimica et Biophysica Acta* **1657**: 82-104.
- Vass, I. 2011. Role of charge recombination processes in photodamage and photoprotection of the photosystem II complex. *Physiologia Plantarum* **142**: 6-16.

- Vass, I. 2012. Molecular mechanisms of photodamage in the photosystem II complex. *Biochimica et Biophysica Acta* **1817**: 209-217.
- Vass, I., S. Styring, T. Hundal, A. Koivuniemi, E.-M. Aro, and B. Andersson. 1992. Reversible and irreversible intermediates during photoinhibition of Photosystem II - stable reduced Q<sub>A</sub> species promote chlorophyll triplet formation. *Proceedings of the National Academy of Sciences U.S.A.* **89**: 8964-8973.
- Veal, C., M. Carmi, G. Dishon, Y. Sharon, K. Michael, D. Tchernov, O. Hoegh-Guldberg, and M. Fine. 2010. Shallow-water wave lensing in coral reefs: a physical and biological case study. *The Journal of Experimental Biology* **213**: 4303-4312.
- Veit, W., and R. Govindje. 2000. The Z-scheme diagram of photosynthesis.
- Venn, A. A., J. E. Loram, and A. E. Douglas. 2008. Photosynthetic symbioses in animals. *The Journal of Experimental Biology* **59**: 1069-1080.
- Venn, A. A., M. A. Wilson, H. G. Trapido-Rosenthal, B. J. Keely, and A. E. Douglas. 2006. The impact of coral bleaching on the pigment profile of the symbiotic alga, *Symbiodinium*. *Plant, Cell & Environment* **29**: 2133-2142.
- Wagner, H., T. Jakob, and C. Wilhelm. 2005. Balancing the energy flow from captured light to biomass under fluctuating light conditions. *New Phytologist* **169**: 95-108.
- Wakefield, T. S., and S. C. Kempf. 2001. Development of host- and symbiont - specific monoclonal antibodies and confirmation of the origin of the symbiosome membrane in a cnidarian-dinoflagellate symbiosis. *Biological Bulletin* **200**: 127-143.
- Walker, D., and R. Walker. 1988. The use of the oxygen electrode and fluorescence probes in simple measurements of photosynthesis. Robert Hill Institute, University of Sheffield.
- Walker, D. A. 1981. Secondary fluorescence kinetics of spinach leaves in relation to the onset of photosynthetic carbon assimilation. *Planta* **153**: 273-278.
- Wang, G., and S. J. Smith. 2012. Sub-diffraction limit localization of proteins in volumetric space using bayesian restoration of fluorescence images from ultrathin specimens. *PLOS computational biology* **8**: e1002671.
- Wang, J.-T., and A. E. Douglas. 1997. Nutrients, signals, and photosynthate release by symbiotic algae - the impact of taurine on the dinoflagellate alga *Symbiodinium* from the sea anemone *Aiptasia pulchella*. *Plant Physiology* **114**: 631-636.

- Wang, J. T., and A. E. Douglas. 1999. Essential amino acid synthesis and nitrogen recycling in an alga-invertebrate symbiosis. *Marine Biology* **135**: 219-222.
- Wang, L., S. L. Jacques, and L. Zheng. 1995. MCML - Monte Carlo modeling of light transport in multi-layered tissues. *Computer Methods and Programs in Biomedicine* **47**: 131-146.
- Wangpraseurt, D., A. W. D. Larkum, P. J. Ralph, and M. Kühl. 2012. Light gradients and optical microniches in coral tissues. *Frontiers in Microbiology* **3**: 316.
- Warner, M. E., and S. Berry-Lowe. 2006. Differential xanthophyll cycling and photochemical activity in symbiotic dinoflagellates in multiple locations of three species of Caribbean coral. *Journal of Experimental Marine Biology and Ecology* **339**: 86-95.
- Warner, M. E., G. C. Chilcoat, F. K. Mcfarland, and W. K. Fitt. 2002. Seasonal fluctuations in the photosynthetic capacity of photosystem II in symbiotic dinoflagellates in the Caribbean reef-building coral *Montastrea*. *Marine Biology* **141**: 31-38.
- Warner, M. E., W. K. Fitt, and G. W. Schmidt. 1996. The effects of elevated temperature on the photosynthetic efficiency of zooxanthellae *in hospite* from four different species of reef coral: a novel approach. *Plant, Cell & Environment* **19**: 291-299.
- Warner, M. E., W. K. Fitt, and G. W. Schmidt. 1999. Damage to photosystem II in symbiotic dinoflagellates: a determinant of coral bleaching. *Proceedings of the National Academy of Sciences U.S.A.* **96**: 8007-8012.
- Weis, V. M. 1993. Effect of dissolved inorganic carbon concentration on the photosynthesis of the symbiotic sea anemone *Aiptasia pulchella* Carlgren: Role of carbonic anhydrase. *Journal of Experimental Marine Biology and Ecology* **174**: 209-225.
- Weis, V. M. 2008. Cellular mechanisms of cnidarian bleaching: stress causes the collapse of symbiosis. *The Journal of Experimental Biology* **211**: 3059-3066.
- Weis, V. M., G. J. Smith, and L. Muscatine. 1989. A "CO<sub>2</sub> supply" mechanism in zooxanthellate cnidarians: role of carbonic anhydrase. *Marine Biology* **100**: 195-202.
- Whitehead, L. F., and A. E. Douglas. 2003. Metabolite comparisons and the identity of nutrients translocated from symbiotic algae to an animal host. *The Journal of Experimental Biology* **206**: 3149-3157.

- Wilkinson, C. 2002. Status of Coral Reefs of the World: 2002. Australian Institute of Marine Science.
- Wilkinson, C. R., O. Linden, and H. Cesar. 1999. Ecological and socio-economic impacts of 1998 coral mortality in the Indian Ocean: an ENSO impact and a waning of future change? *Ambio* **28**: 188-196.
- Wingler, A., P. J. Lea, and W. P. Quick. 2000. Photorespiration: metabolic pathways and their role in stress protection. *Philosophical transactions of the Royal Society B* **355**: 1517-1529.
- Whitney, S. M., and T. J. Andrews. 1998. The CO<sub>2</sub>/O<sub>2</sub> specificity of single-subunit ribulose-bisphosphate carboxylase from the dinoflagellate, *Amphidinium carterae*. *Australian Journal of Plant Physiology* **25**: 131-138.
- Wollman, F.-A. 2001. State transitions reveal the dynamics and flexibility of the photosynthetic apparatus. *The EMBO Journal* **20**: 3623-3630.
- Woodger, F. J., M. R. Badger, and G. D. Price. 2005. Sensing of inorganic carbon limitation in *Synechococcus* PCC7942 is correlated with the size of the internal inorganic carbon pool and involves oxygen. *Plant Physiology* **139**: 1959-1969.
- Wydrzynski, T. J. 2008. Water splitting by photosystem II - where do we go from here? *Photosynthesis Research* **98**: 43-51.
- Yamashiro, H. 1995. The effect of HEBP, an inhibitor of mineral deposition, upon photosynthesis and calcification in the scleractinian coral, *Stylophora pistillata*. *Journal of Experimental Marine Biology and Ecology* **191**: 57-63.
- Yellowlees, D., T. A. Rees, and W. Leggat. 2008. Metabolic interactions between algal symbionts and invertebrate hosts. *Plant, Cell & Environment* **31**: 679-694.
- Yellowlees, D., and M. Warner. 2003. Photosynthesis in Symbiotic Algae. In A. W. D. Larkum, S. E. Douglas and J. A. Raven [eds.], *Photosynthesis in Algae*. Kluwer Academic Publishers.
- Yonge, C. M., and A. G. Nicholls. 1931. Studies on the physiology of corals. IV. The structure, distribution, and physiology of the zooxanthellae. *Scientific Report of the Great Barrier Reef Expedition 1928* **29**: 135-176.

This page was intentionally left blank

‘The sea, once it casts its spell, holds one in its net of wonder forever’

- Jacques Yves Cousteau -

